Final

Fiscal Year 2012 Water Modelling Analysis Report, Faro Mine Remediation Project

Prepared for

Government of Canada as represented by Aboriginal Affairs and Northern Development Canada and the Government of Yukon

March 8, 2013

CH2MHILL®

309 Strickland Street, Suite 301
Whitehorse, Yukon Y1A 2J9

The document contained herein should be considered Final as approved by the Government of Yukon on August 27, 2014 with no changes made since the draft submission.

Contents

Section **Page**

Appendices

Tables **Page**

Figures

Acronyms and Abbreviations

°C	degree Celsius
3D	three-dimensional
AECOM	AECOM Canada Ltd
AMP	adaptive management plan
ATI	antecedent temperature index
BGC	BGC Engineering Inc.
$CaCO_3$	calcite
CGVD28	Canadian Geodetic Vertical Datum of 1928
CHSP	Crusher Stockpile
cm	centimetre
cm/sec	centimetre per second
CSM	conceptual site model
CSM Report	*Draft Conceptual Site Model, Faro Mine Remediation Project*
CVD	Cross Valley Dam
DEM	digital elevation model
DES	Denison Environmental Services
EQuIS	Environmental Quality Information System
ESI	Environmental Simulations, Inc.
ET	evapotranspiration
ETA	Emergency Tailings Area
FCD	Faro Creek Diversion
$Fe(OH)_3$	ferric iron hydroxide
FMC	Faro Mine Complex
FMRP	Faro Mine Remediation Project
FTE	Fuel Tank Dump E
FTW	Fuel Tank Dump W
FVN	Faro Valley North
FVS	Faro Valley South
FWL	fracture well
FWMT	Faro Water Modelling Team
FY12	Fiscal Year 2012
GEEC	Gomm Environmental Engineering and Consulting
GHB	general head boundary

GHL	Lower Guardhouse Creek catchment
GHU	Upper Guardhouse Creek catchment
GIS	geographic information system
GLL	Gartner Lee Limited
Golder	Golder Associates Ltd.
GoldSim model	site-wide water quality model
GW	groundwater
GW_{ppn}	groundwater recharge from precipitation
ha	hectare
HEC-HMS	Hydrologic Engineering Center-Hydrologic Modeling System
HGL	HydroGeoLogic, Inc.
ID	Intermediate Dump
IDSC	Intermediate Dump Sulphide Cell
K_h	horizontal hydraulic conductivity
km	kilometre
km^2	square kilometre
K_v	vertical hydraulic conductivity
L/sec	litre per second
Laberge	Laberge Environmental Services
LGSP A	low-grade stockpile “A”
LGSP C	low-grade stockpile “C”
LiDAR	light detection and ranging
LPL	Lower Parking Lot Dump
m	metre
m/day	metre per day
m/m	metre per metre
m^2	square metre
m^3	cubic metre
m^3/day	cubic metre per day
m^3/sec	cubic metre per second
mbgs	metre below ground surface
MDE	Main Dump East
MDW	Main Dump West
ME	mean error
MESC	Main East Sulphide Cell

mg/L	milligram per litre
MGSP	Medium Grade Stockpile
mm	millimetre
mm/hr	millimetre per hour
mm/yr	millimetre per year
MME	Mt. Mungly East
MMW	Mt. Mungly West
mol/L	moles per litre
MP	Main Pit (Faro) catchment
NEL	Lower Northeast Dump
NELS	Lower Northeast sulphide cell
NEO	Outer Northeast Dump
NEU	Upper Northeast Dump
NFRC	North Fork Rose Creek
NFRC Subarea	North Fork of Rose Creek, Zone 2 Pit and Outwash, and S-Wells Subarea
NWID	North Wall Interceptor Ditch
NWL	Lower Northwest Dump
NWM	Middle Northwest Dump
NWU	Upper Northwest Dump
O_2	oxygen
OHRE	Outer Haul Road East
OHRW	Outer Haul Road West
OXSP	Oxide Fines Stockpile
PMF	probable maximum flood
R^2	coefficient of determination; square of the correlation coefficient
RCAA	Rose Creek Alluvial Aquifer
RCAA Subarea	Rose Creek Alluvial Aquifer and Cross Valley Dam Subarea
RCD	Rose Creek Diversion
RCDC	Rose Creek Diversion Channel
RCTA	Rose Creek Tailings Area
RCV	Rose Creek Valley catchment
RD	Ranch Dump
RGC	Robertson GeoConsultants, Inc.
RMSE	root mean squared error
RMSE/range	root mean squared error divided by the range of target head values

RZD	Ramp Zone Dump
SCS	Soil Conservation Service
SI	saturation index
SIS	subsurface interception system
SPB	Stock Piles Base
SRK	SRK Consulting Engineers and Scientists
SW	surface water
SWPWD	Southwest Pit Wall Dump
TDS	total dissolved solids
tonne/yr	tonne per year
UPL	Upper Parking Lot Dump
USACE	United States Army Corps of Engineers
USGS	United States Geological Survey
WRD	waste rock dump
WTP	water treatment plant
X2	Catchment draining near stream monitoring location X2
X23	Catchment draining near seep monitoring location X23
YESAB	Yukon Environmental and Socio-economic Assessment Board
YG	Government of Yukon
YT	Yukon Territory
Z2	Catchment draining near Zone 2 drainage area
Z2E	Zone 2 East
Z2W	Zone 2 West

SECTION 1

Introduction

The CH2M HILL Canada Limited (CH2M HILL) Faro Water Modelling Team (FWMT) has developed computer models for the Government of Yukon (YG), Canada, that simulate hydrological, geochemical, and operational processes of interest in the Faro Mine Complex (FMC) and surrounding area. Figures 1-1 through 1-3 (figures are located at the end of their respective sections) show the location of the FMC at three different scales to orient the reader both regionally and locally. Figure 1-4 shows the locations of interest in the Vangorda/Grum area. This report documents the development, calibration, and application of these computer models, which were constructed to support the ongoing development, refinement, and implementation of the Faro Mine Remediation Project (FMRP). These computer models are subdivided into three classifications: surface water (SW) flow models, groundwater (GW) flow models, and geochemical models. For each type of model, this report documents objectives, approaches, data sources, construction, calibrations, applications, and recommendations.

The level of complexity varies among these computer models, reflecting the intent of the initial modelling exercise and the availability of data to define the particular aspects of the conceptual site model (CSM) that each computer model attempts to simulate. As such, these computer models were developed to the extent practical given the site data, time, intent, and resources available for this effort during Fiscal Year 2012 (FY12), which runs from April 1, 2012 until March 31, 2013. The computer models described herein will continue to evolve in response to changes associated with the dynamic natural environment and the collection of additional information during the implementation of site engineering activities. As a result, information presented herein should be considered work in progress when this report was submitted. Improvements to these computer models will continue as additional site characterization, monitoring, and operational data become available; as knowledge of the FMC evolves; and as necessitated by the FMRP. These models will provide a foundation to support future enhancements.

This report is closely integrated with other FMRP documents that have been developed or are currently in production. The underlying CSM that was used as the foundation for the computer models described herein is documented in the draft *Conceptual Site Model, Faro Mine Remediation Project* (CSM Report) (CH2M HILL, 2012). Selected aspects of the SW flow, GW flow, and geochemical computer models will be incorporated into the site-wide water quality model (GoldSim model) (SRK Consulting Engineers and Scientists [SRK], 2004a, 2006a; Gomm Environmental Engineering and Consulting [GEEC], 2010), which has been and will be used to forecast water quality at locations of interest within and downstream from the FMC. The construction, calibration, and application of the GoldSim model and the integration of information from the computer models described herein will be presented in the draft *Fiscal Year 2012 Site-wide Water Quality Modelling Report, Faro Mine Remediation Project* (CH2M HILL, in preparation).

The computer modelling files serve as companion files to this report and include additional details not addressed in this report; these files are available upon request.

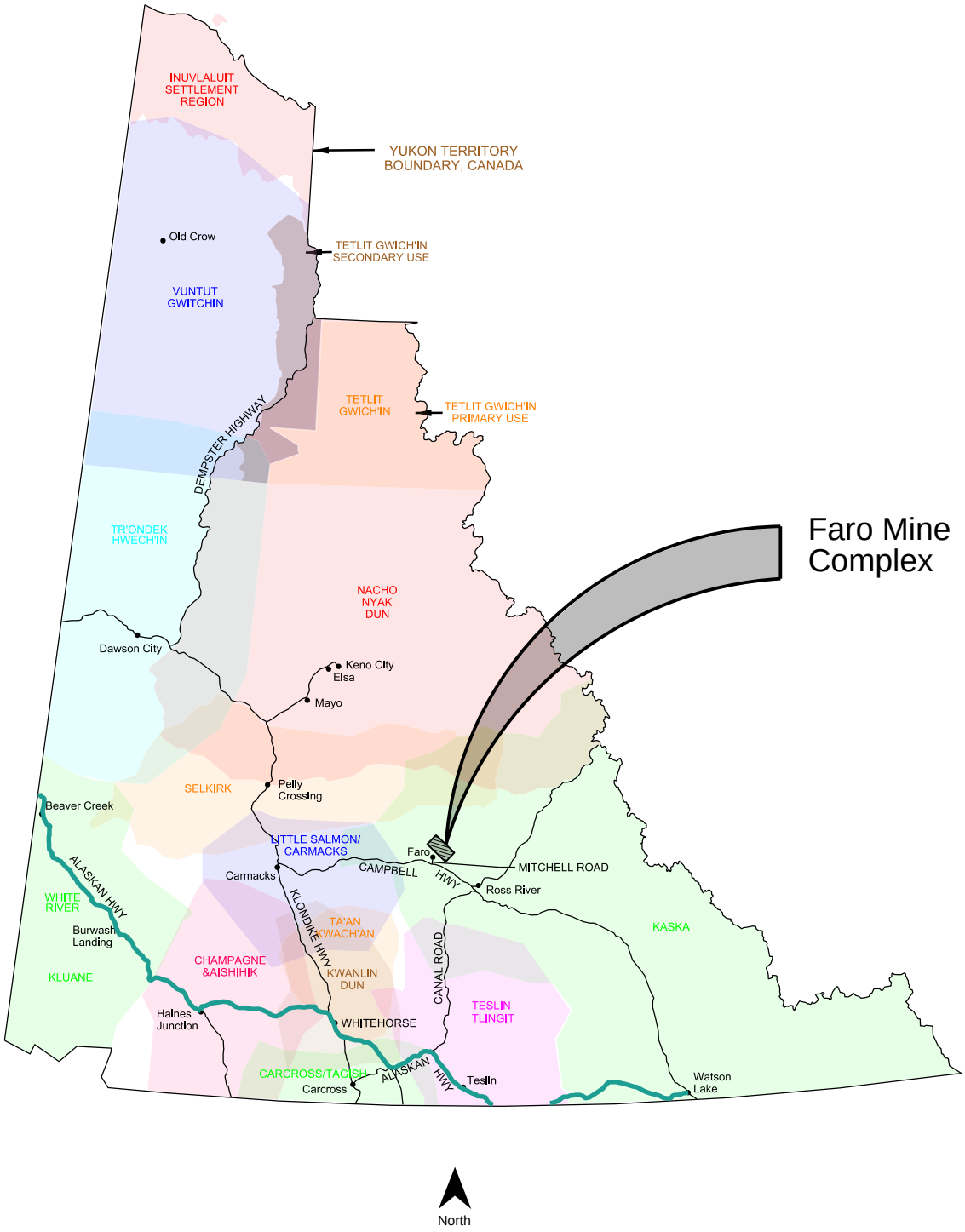

FIGURE 1-1
Regional Location Map
Faro Mine Remediation Project

FIGURE 1-2
Faro Mine Complex
Faro Mine Remediation Project

RU:\FNAKR RO:M\FIANREO_2M0I0N0E0_324020\0M0A3P4F2INLMEASP\CFIOLENSC\ECPOTNUCAELP_TSUITAEL__MSOITDEE_LM\FOIDGEULR\FEI_G1U-2R_EF_A1R-O2__FSAITREO.M_SXIDTE E.MCLXADR EKC 8L/A13R/K2 081/123 1/2:5011:22 31 :P5M1:23 PM

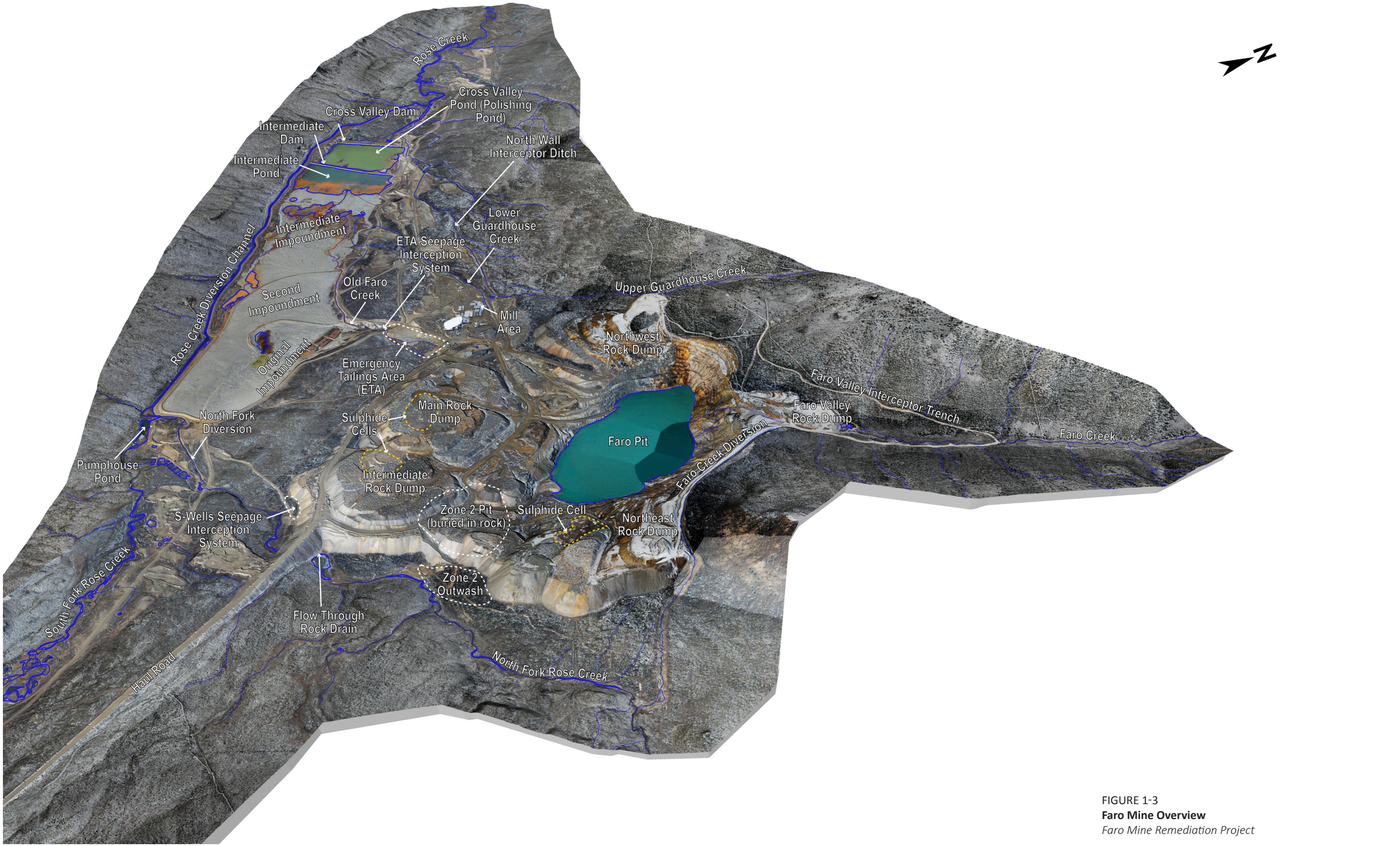

FIGURE 1-3
Faro Mine Overview
Faro Mine Remediation Project

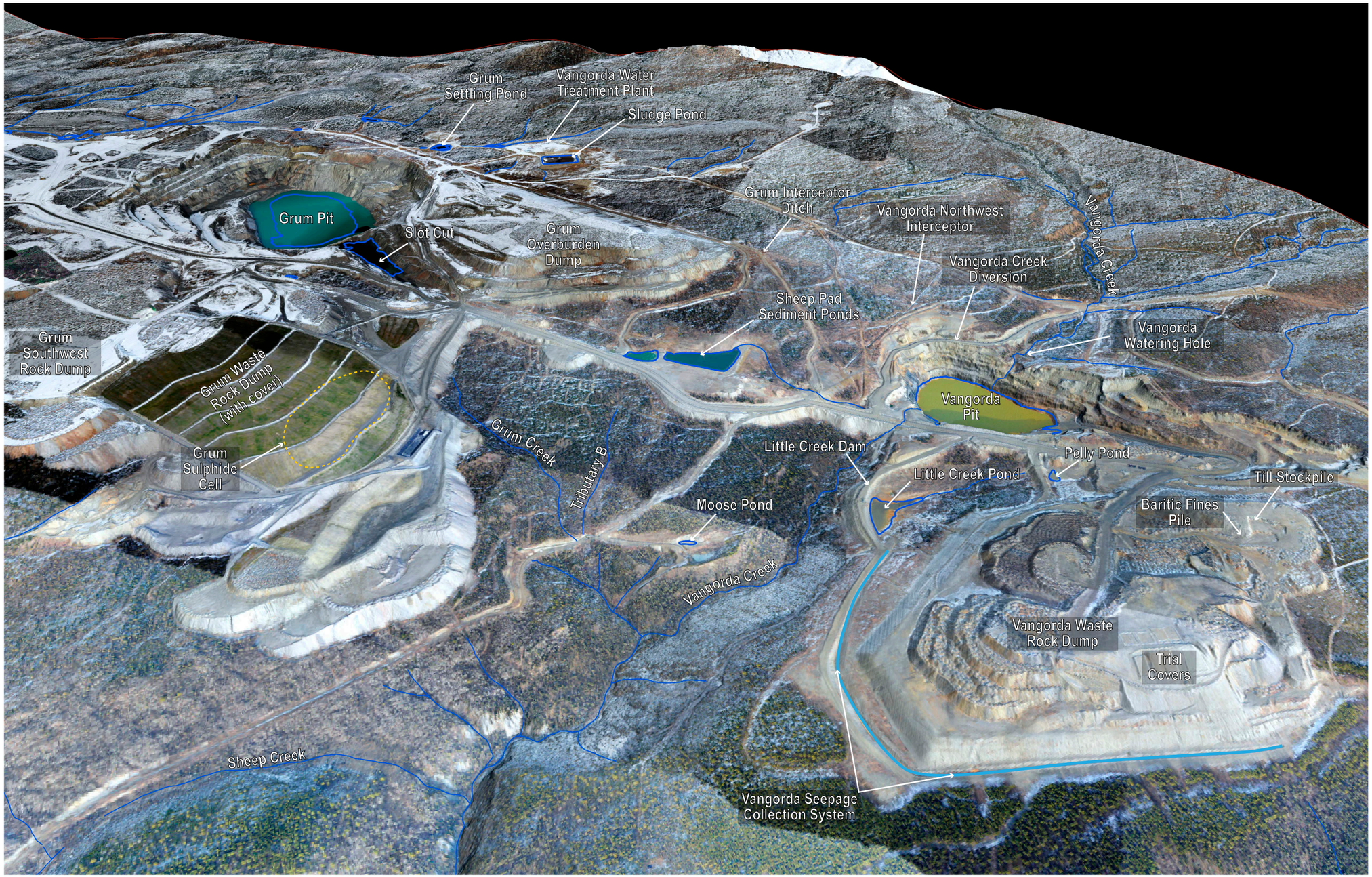

FIGURE 1-4
Vangorda/Grum Area Overview
Faro Mine Remediation Project

SECTION 2

Surface Water Flow Modelling

2.1 Surface Water Modelling Objectives

The FY12 objective of the SW flow modelling task was to develop a dynamic hydrological model of the FMC that would be used to provide a better understanding of the FMC hydrological characteristics and support FMC future design and investigation activities. A number of FMC design and investigative activities will be supported by the SW modelling efforts including, but not limited to:

- Stream channel diversion designs
- Regulatory-related information for the Yukon Environmental and Socio-economic Assessment Board (YESAB) project proposal
- Geochemistry and water quality evaluations
- Hydrogeology and GW interceptor designs
- Waste piles and tailings hydrology evaluations
- Water treatment evaluations
- Dam design and other major structures evaluations
- Environmental monitoring and reporting
- Revegetation and reclamation evaluations

Building on the CSM Report (CH2M HILL, 2012), the SW flow models have been used to define precipitation-runoff processes throughout the FMC. Existing physical site characteristics, meteorological data, and SW flow monitoring data were used to develop and calibrate the models. The models were then used to assist in characterizing the occurrence, conveyance, and management of SW within the FMC under varying assumptions of land use and meteorological conditions.

The main objective of the current SW flow modelling effort is to develop a calibrated tool that can be used to simulate precipitation-runoff processes from the FMC on a continuous, multiyear simulation basis. The focus of this model is to simulate the timing and magnitude of runoff events throughout the year, ranging from low-flow (i.e., base flow) conditions to peak flow conditions that occur during the spring freshet.

In addition to development of the hydrological model, the FWMT team is also currently completing hydraulic analyses of portions of the FMC, including the Rose Creek Diversion (RCD) and Cross Valley Dam (CVD). These analyses, including details related to hydraulic model development and results, are included in separate documents.

2.2 Surface Water Modelling Approach

The following tasks summarize the overall approach used to develop continuous SW flow models for the FMC:

1. Gathering and processing available information
2. Delineating regional and local FMC SW catchments
3. Developing SW flow models
4. Calibrating SW flow models

The following sections provide details regarding each of the modelling approach tasks.

2.3 Surface Water Data Sources and Review

2.3.1 Available Data and Sources

The development of a hydrological model involves three main categories of data. The first category consists of meteorological data, which are used to characterize precipitation processes including rainfall distribution and intensity, snow accumulation, and snowmelt. The second category consists of input data related to the definition of the catchment's physical characteristics, and the third category consists of flow data, which are used to calibrate precipitation-runoff processes that are derived from the first two categories of data.

Development and calibration of a hydrological model requires coincident meteorological and SW flow data. A preliminary review of available SW flow and meteorological data for the FMC indicated that the most suitable record of coincident data was available from approximately 2000 to present; therefore, compilation and analysis of data for the current SW flow model development effort focused on this timeframe, as described herein.

2.3.1.1 Meteorological Data

Meteorological data are available for two FMC stations that are operated by the site care and maintenance contractor. These stations are referred to as the Faro and Grum Dump stations, both of which were installed in 2003 and record the following parameters:

- Air temperature
- Relative humidity
- Incoming, outgoing, and net radiation
- Wind speed and direction
- Rainfall
- Snow depth
- Soil moisture
- Soil temperature and heat flux

In February 2008, instrumentation to record total precipitation (i.e., rainfall and snowfall) was added to each FMC meteorological station. Processed hourly data for the two stations; however, substantial gaps were identified in the data sets, as later sections of this report describe.

In addition to the Faro and Grum Dump stations, data were compiled from a station operated by Environment Canada at the nearby Faro Airport. Precipitation and air temperature were key parameters from this station that were used to develop the hydrological model. Figure 2-1 illustrates the locations for each of the aforementioned meteorological stations.

2.3.1.2 Surface Water Catchment Physical Data

Definition of physical catchment parameters includes data related to subcatchment area, vegetation cover, and subsurface soil conditions. These data are used to support the simulation of water cycle processes, including evapotranspiration (ET), evaporation, and infiltration. General geological mapping is available for the regional area; however, detailed information on vegetation and soil conditions for the FMC is limited, especially for the upper reaches of the regional catchment area. Available data were incorporated into the initial catchment parameterization, which formed the basis from which the calibration process was completed. Subsequent sections of this report provide details about physical catchment parameters.

2.3.1.3 Flow Monitoring Data

The following locations, shown on Figure 2-2, provide continuous flow monitoring within the Rose Creek drainage basin:

- FCD-1 at the head of the Faro Creek Diversion (FCD)
- R7 in the North Fork Rose Creek (NFRC) upstream from the FMC
- X2 in the NFRC upstream from the tailings facility

- X14 in Rose Creek, downstream from the tailings facility
- X23/FCS-1 below the Faro Valley waste rock dump (WRD)

The following locations, shown on Figure 2-2, provide continuous flow monitoring within the Vangorda Creek drainage basin:

- V1 in Vangorda Creek, upstream from the Vangorda Pit
- V8 in Lower Vangorda Creek at the footbridge
- V27 in Vangorda Creek, upstream from the confluence with Shrimp Creek

In addition to operating continuous SW flow monitoring stations, the care and maintenance staff have implemented a field program that includes collecting spot-flow measurements at various locations throughout the FMC monthly during the ice-free season. Data from this monitoring program were also incorporated into the development and calibration of the FMC hydrological models.

2.3.2 Data Review

Available physical catchment, meteorological, and flow data were reviewed in detail to determine the quality and suitability of this information for the development of the hydrological models. Observations and conclusions from this review are detailed in this subsection.

2.3.2.1 Faro Mine Complex Meteorological Station Data Review

The review of the FMC meteorological station data focused on the reported air temperature, rainfall, snow depth, and precipitation records.

Air Temperature Record

The air temperature records were reviewed from a data quality perspective, primarily to identify significant data gaps and to identify potential data errors through comparison with concurrent data recorded at the Faro Airport station. Based on this review, the air temperature data record for the Faro Dump and Grum Dump meteorological climate stations was determined to be stable and within climate normals for the region. Several significant gaps in the air temperature record were identified during this data review, primarily in the fall of 2008 and fall of 2009.

Rainfall Record

Both the Faro Dump and Grum Dump meteorological stations record rainfall. The rainfall record provided for these stations was reviewed for significant data gaps and extreme events significantly (i.e., greater than 30 percent) outside of climate normals. Outliers identified within the two records were compared with measurements recorded at the Faro Airport Station, regional climate normals, extreme events of record onsite, and records from the FMC continuous flow monitoring stations. Outliers were also compared to available reports that document extreme events at the FMC for the purposes of design work. Previous work indicates that the FMC can experience precipitation events greater than those recorded at the Faro Airport. For this analysis, events that were 30 percent greater than regional climate normals (as reported by Environment Canada at the Faro Airport Station) were flagged for further investigation. A decision was made whether to remove an outlier from the record only after further investigation and comparison with available data. This approach was deemed to be a reasonable approach for the purposes of constructing input data sets for the hydrological model. This review identified several data gaps and outliers requiring additional investigation.

Snow Depth Record

The Faro Dump and Grum Dump meteorological stations do not record snowfall in water equivalents but do record the total snow depth using an ultrasonic sensor. This record was reviewed to determine whether it was sufficient to estimate the contribution of snow to the total precipitation record at the FMC. The snow depth sensor record reports the depth of the snow pack hourly but does not report accumulated snowfall values. When processed to determine the hourly and daily accumulation of snowfall, negative values in snow depth accumulation are frequently reported. The negative values in the snow depth accumulation record were compared with the station's air temperature record to determine whether these events were potentially associated with melt events (i.e., when air temperature is greater than 0 degrees Celsius [°C]). In many cases, it

was determined that negative snow depth was not likely to have accumulated based on greater than zero temperature events. Therefore, the FWMT determined that this record contained too much variability and "noise" in the recorded data to accurately estimate the daily contribution of snow to the precipitation record.

Total Precipitation Record

Total precipitation (i.e., rain and snow) was not recorded at the FMC meteorological stations until February 2008. Total precipitation data, collected hourly between February 2008 and 2010, were obtained and reviewed. These data were processed to determine hourly and daily variations in total precipitation. Similar to the snow depth record, it was determined that negative hourly and daily precipitation totals were often included within the data set. Unlike the snow pack data, which could be influenced by melting conditions and therefore have negative values, total daily precipitation cannot be less than zero; therefore, the FWMT determined that this record could not be used for the development of the meteorological data input record.

In addition to reviewing the unprocessed meteorological data, the 2010 and 2011 FMC annual reports prepared by Denison Environmental Services (DES) were reviewed (DES, 2011, 2012a). These reports include daily total precipitation data and figures that illustrate hourly cumulative precipitation. These annual reports confirm the findings of the data review. The 2010 annual report identified that it is likely that the reported precipitation record is underestimating the total precipitation occurring at the FMC (DES, 2011).

2.3.2.2 Environment Canada Climate Database (Faro Airport Station)

A meteorological station is operated by Environment Canada at the Faro Airport. The location of this station is included on Figure 2-1. This station is located at elevation 717 metres (m), which is 508 m and 503 m below the Faro Dump and Grum Dump meteorological stations, respectively. Data from this station are available over a period between 1978 to present. To correspond with the period in which flow monitoring and meteorological data are available at the FMC, air temperature, rainfall, snowfall, and total precipitation data from the Faro Airport record, as well typical climate normals, were downloaded from Environment Canada. The data downloaded from this database are considered to be reliable because Environment Canada subjects field data to a quality control program prior to making the data available for download. The level of Environment Canada's quality review is documented within the data package.

The Faro Airport Station data set was reviewed for significant data gaps, as well as the station's suitability for filling data gaps in the FMC meteorological station data records. A large data gap in the FMC meteorological station data records was identified from 2002 to 2003, in addition to several month-long gaps. The Faro Airport record was compared to the Faro Dump and Grum Dump meteorological stations and was determined to be a suitable source for filling large data gaps within the FMC records.

2.3.2.3 Continuous Flow Monitoring Data

Continuous SW flow monitoring data were reviewed to determine their suitability for use in the hydrological model calibration. The location of the continuous flow monitoring stations is included on Figure 2-2. Table 2-1 summarizes the continuous SW flow monitoring data available and indicates years where significant data gaps exist during critical periods (e.g., spring freshet and significant precipitation events). The X marks that are highlighted in orange indicate years when gaps within the spring freshet and summer period exist, whereas rows that do not have an X mark indicate that no data are available at the given station in the given year. Rows with plain X marks indicate data that are adequate for model calibration.

TABLE 2-1
Continuous Flow Monitoring Data Available for the Surface Water Modelling Task
Faro Mine Remediation Project

Year	R7	X2	X14	X23/FCS-1	V1	V8
2011	X	X	X		X	X
2010	X		X		X	X
2009	X		X		X	X
2008			X	X	X	X
2007	X		X	X		
2006	X		X	X		
2005	X		X	X		
2004	X		X			
2003	X					
2002	X		X			
2001	X		X			
2000						

2.3.2.4 Summary of Available Data

As discussed, developing and calibrating a hydrological model requires coincident records of meteorological and flow data. Based on the review of various data sources described, Figure 2-3 summarizes available coincident data.

2.4 Surface Water Model Construction

2.4.1 Surface Water Model Code Selection

Hydrological models of the FMC were developed using the United States Army Corps of Engineers (USACE) Hydrologic Engineering Center-Hydrologic Modeling System (HEC-HMS) Version 3.5 (USACE, 2010). This is a publicly available code that is widely used and is designed to simulate the precipitation-runoff processes of dendritic drainage basins. HEC-HMS is designed to apply to a wide range of geomorphic conditions and to solve a wide range of surface routing scenarios. The hydrological models were used to estimate SW runoff from the Rose Creek and Vangorda Creek drainage basins and from smaller subbasins within the FMC. Hydrographs produced by HEC-HMS will be used to forecast SW availability at downgradient locations of interest within the modelling domain.

2.4.2 Surface Water Model Domain

When developing hydrological models, the domain is defined by the overall catchment area tributary to the receiving point of interest. For the FMC, the domain is defined by flow monitoring station X14 in the Rose Creek drainage basin and by V8 in the Vangorda Creek drainage basin, as shown on Figure 2-4. Some catchment areas downstream from these monitoring stations were also delineated to account for all SW generated from the FMC. These regional basin delineations define the lateral boundaries for the SW flow models.

2.4.3 Surface Water Model Parameters

Using HEC-HMS, the FWMT developed a continuous hydrological model to simulate rainfall-runoff and snowmelt processes in both the Rose Creek and Vangorda Creek drainage basins under the existing FMC operational

conditions. The model was set up to compare runoff hydrographs at key locations in the system with available SW flow data. The calibration process involved adjusting subbasin parameters to best match the magnitude and duration of runoff events observed in the field.

The development of an HEC-HMS model includes selecting one or more meteorological models and one or more basin models. A meteorological model includes the air temperature and precipitation data, monthly ET, and snowmelt parameters that apply to a specific basin. A basin model is a physical representation of the watershed and may include elements such as: subbasins, channel reaches, storage elements, junctions, diversions, sources, and sinks. Subbasin elements are further defined by the various parameters that will affect runoff generation such as: surface and canopy losses, infiltration losses, precipitation-to-runoff transform methods, and base flow contributions. Channel reaches can be described using various geometries and hydraulic routing methods.

To analyze the FMC, two meteorological models were created: one for Rose Creek drainage basin and one for Vangorda Creek drainage basin. Four basin models were also created: one each for the Rose Creek and Vangorda Creek drainage basins during the winter period and one each for the Rose Creek and Vangorda Creek drainage basins during the summer period. The difference between the two meteorological models is reflected in the precipitation and melt-rate functions, whereas the difference between the two basin models for each mine site is related to the soil infiltration parameter.

The following subsections describe the processes applied to develop the input parameters for the HEC-HMS models. These parameters include the catchment area development, the meteorological record development (including air temperature, precipitation, evaporation and snowmelt data), and the physical catchment parameter development (including the precipitation loss parameters, runoff transform parameters, and base flow inputs).

2.4.3.1 Surface Water Catchment Development

The first step in the basin model development process was to delineate local FMC and regional catchments within the surface water model domain. Detailed light detection and ranging (LiDAR) data were available for the FMC, while only standard topographic information was available for the surrounding regional area. The elevation data for the FMC were collected at a resolution of 1 square metre (m^2) per pixel. The regional elevation data were not available at a similar resolution; therefore, the catchment development process was conducted in two stages.

LiDAR data were collected for the FMC on two separate occasions in 2012. These data provided a high-resolution data set of the FMC (1 m^2 per pixel). These data were used to develop a raster elevation data set, which was processed using the Flow Direction Spatial Analyst algorithm in ArcGIS Version 10.0. This resulted in a gridded data set that represents the flow direction from each raster cell to its steepest downslope neighbour. The flow direction data set was then processed using a Flow Accumulation Spatial Analyst algorithm to obtain a data set containing the accumulated flow in each raster cell. This process identifies likely SW drainage paths.

“Pour points,” representing known SW flow monitoring locations, were applied to the raster grid of SW flow paths. The ArcGIS tool calculated the boundaries for the area that is tributary to each pour point. The catchments were refined by repeating this process and adding or relocating pour points to reflect the known site conditions. Additional pour points were used to account for onsite conditions that may not have been reflected in the elevation data (e.g., culverts between catchments). This resulted in the delineation of a number of subdivided catchments to define onsite conditions. These were grouped together to form subcatchments reflecting the known site conditions. An attempt was made to select pour point locations and catchment boundaries that best fit the locations of continuous SW flow monitoring locations. This was done to better enable the calibration of the hydrological models using the existing SW flow records. The local catchments for the Faro and Vangorda/Grum areas are illustrated on Figures 2-5 and 2-6, respectively.

The most recent elevation model for the region surrounding the FMC predates the mining activity and is a lower resolution than the LiDAR data for the FMC. For this reason, the local FMC catchments were delineated first. The local FMC LiDAR data were merged into the regional elevation data to produce a hybrid elevation data set. This data set was processed as described in the previous section, resulting in a flow accumulation data set for the regional area, as well as the local catchments.

Pour points were selected in similar locations to those selected for the local catchment delineation exercise. In some cases, the same pour locations could not be used because of the differences in the pre- and post-mining elevations. The regional catchments were overlaid with those delineated for the FMC, and several iterations were performed until the regional catchment boundaries were optimized against the local catchment boundaries delineated earlier.

Where exact boundary matches were not made using the geographic information system (GIS) algorithms, manual adjustments were made using available topographic information and aerial photography. When combined with the catchments delineated earlier for the FMC, the final catchments represent the areas draining to pour points; these, in turn, represent continuous SW flow monitoring locations. Figure 2-7 shows the final catchments used to develop the hydrological model.

Figure 2-8 and 2-9 depict node diagrams illustrating the conceptual hydrological model development for both the Rose Creek and Vangorda Creek drainage basin model, respectively. These node diagrams illustrate the interconnection of various subbasins, as well as key routing elements included in the model.

The basin models developed for the analysis only included subbasins and channel reaches. Attenuation provided by overland storage has not been explicitly modelled by a distinct storage element. Section 2.5.4 provides a discussion supporting this decision, specifically for the Rose Creek drainage basin.

The Rose Creek model consists of eight unique subbasins covering an overall catchment area of 23,163 hectares (ha). Note that nine subbasins are included on Figure 2-5, but that Subbasin RC9 is downstream of continuous flow station X14 and is therefore not included in the current model domain. Subbasin RC1, which at 9,874 ha is the largest subbasin, was used as the main calibration subbasin for the Rose Creek model because continuous SW flow data are available at station R7. R7 is located at the downstream point of this subbasin. The discharge from the Faro Water Treatment Plant (WTP), which is a tributary to the CVD Polishing Pond, was included in the form of a constant monthly hydrograph and represents the input for Subbasins RC8a and RC8b.

The Vangorda Creek models consist of five unique subbasins covering an overall catchment area of 8,737 ha. Subbasin VC1, which is 2,007 ha, was used as the main calibration subbasin for the Vangorda Creek model because continuous SW flow data are available at station V1. V1 is located at the downstream point of the subbasin.

2.4.3.2 Surface Water Routing

A simplified approach to routing was applied to the development of the hydrological model. The following reaches were simulated in the Rose Creek model, as illustrated in Figure 2-8:

- NFRC between Station R7 and the Haul Road
- NFRC between Station X2 and the confluence with the South Fork
- Rose Creek Diversion Channel (RCDC)/Rose Creek between the confluence of the North and South Forks and Station X14

The following reaches were simulated in the Vangorda Creek model, as illustrated in Figure 2-9:

- Vangorda Creek Diversion Channel
- Vangorda Creek downstream of the Diversion Channel to Station V27
- Vangorda Creek between Station V27 and Station V8

For each reach, several cross sections were generated based on LiDAR data. From these reaches, a representative, or average cross section was developed. LiDAR is unable to penetrate water; therefore, for channels that had standing water, cross sections were extrapolated by a depth of 0.3 m below the constant plane that represents the water surface elevation. The longitudinal slope of the reach was also calculated based on LiDAR data. Cross sections are coarsely represented in HEC-HMS via eight points (i.e., distance-elevation coordinates) to include both the channel and the adjacent floodplain. A Manning's roughness coefficient of 0.03 was applied to all sections in the model.

The simplified routing approach applied to development of the HEC-HMS model is considered suitable for the current analysis because a more detailed hydraulic model will be developed in subsequent stages of the FMC project to which hydrographs generated from the hydrological model will be routed.

2.4.3.3 Air Temperature Record

Two temperature records were developed for the FMC: one based on data collected at the Faro Dump Station and another for data collected at the Grum Dump Station. The temperature record for input to the hydrological model must represent a continuous daily record for an entire calendar year. Data gaps identified during the review process were filled using several methods and a number of steps, depending on the type of data gap.

The first step was to fill gaps in the Faro and Grum Dump stations air temperature records with the air temperature recorded at the Faro Airport Station. Where there were gaps in the FMC meteorological station records, for which there was no coincident data recorded at the Faro Airport Station, data gaps were filled as follows:

1. Data gaps consisting of 1 week to 1 month of consecutive missing data were patched using average daily air temperature from the period immediately before and after the data gap period.
2. Data gaps consisting of no more than 6 consecutive days of missing data were patched using the air temperature from adjacent days keeping the trend before and after the missing data point(s). For example, if the air temperature trend is increasing before and after the missing data point, the higher of the two adjacent data points was used to fill the data gap.

Work completed by Lewkowicz and Bonnaventure (2009) investigated the influence of topography on permafrost distribution and ground surface lapse rates at various sites throughout the Yukon Territory (YT), including Faro. They found that, although summer air temperatures shows normal lapse rates close to the standard environmental lapse rate of -6.5 °C per kilometre (km), winter lapse rates were found to be inverted by as much as +11 °C per km. They concluded that air temperature trends in the YT are influenced by topography at a variety of scales, with significant seasonal differences. Given the lack of temperature data at various locations throughout the regional catchment area, combined with potential temperature lapse rate inversions, the proposed methodology of temperature record development is considered appropriate for the current model development. Figures 2-10 and 2-11 show the complete air temperature records for input to the hydrological model, indicating the data points from each source for the Faro and Grum Dump stations, respectively.

2.4.3.4 Precipitation Record

This section describes the methodology applied to the development of the precipitation data set. As with the air temperature record, the precipitation input to the hydrological model must be on a continuous daily basis for a calendar year. Because of the limitations of the rainfall and snowfall records discussed in Section 2.3.2, various methods were applied to construct a complete precipitation record for input into the hydrological model. The precipitation record consists of the rainfall and snowfall (as rainfall water equivalent) records which, when combined, represent the total precipitation on site. Two precipitation data sets were developed, one for each area of the site (Faro Dump and Grum Dump stations).

Rainfall Record

The preferred data source is data collected at the FMC meteorological stations. The data collected at the Faro and Grum stations were converted to daily rainfall totals and reviewed for data gaps, as discussed in Section 2.3.2. These gaps were filled using the daily rainfall record from the Faro Airport Station. In the *Faro Mine Complex Closure and Reclamation–Project Proposal, Current Environmental Conditions Supporting Document* (AECOM Canada Ltd [AECOM], 2009), relationships were developed between the Faro Airport Station and the Faro Dump and Grum Dump stations. These correlations indicate that the Faro Dump and Grum Dump stations receive 6.79 percent and 10.01 percent more rainfall, respectively, than the Faro Airport Station. These correlations are limited to rainfall occurring between May and September; as such, they were only applied to fill gaps in the FMC rainfall records for that timeframe. If rainfall occurred at the Faro Airport Station between October and April, the correlation was not applied, and the unchanged Faro Airport rainfall record was used to fill data gaps occurring during that timeframe. This was compared with the air temperature record to confirm that rainfall was plausible during this period based on air temperature. Figures 2-12 and 2-13 show the rainfall records developed for the Faro Dump and Grum Dump stations, respectively.

Snowfall Record

As discussed in Section 2.3.2, the Faro and Grum Dump stations do not record snowfall. AECOM (2009) compares snowpack water content at the Faro and Grum Dump stations with accumulated snowfall at the Faro Airport Station. This analysis indicated that the dumps receive about 25 percent more snowfall (as a water equivalent) than the Faro Airport. It is recognized that orographic effects and impacts of blowing snow influence snow accumulation at the FMC; however, information beyond that provided in the 2009 AECOM report is not available to better estimate such effects. Therefore, to construct a snow record at the Faro and Grump Dump stations, snow depth recorded at the Faro Airport was increased by 25 percent and applied to both stations.

The following assumptions were made while developing the snowfall (as water equivalent) record:

1. To convert the snowfall (reported in centimetres [cm]) recorded at the Faro Airport Station to water equivalents, it is reasonable to assume a snow density of 1 cm equals 1 millimetre (mm) of water equivalent.
2. Where snowfall data are missing for winter months, it is reasonable to patch the data with average-day snowfall from the period of record for the missing dates.
3. It is reasonable to assume that, when snowfall data are missing during summer months (i.e., June to September), no snowfall occurred.

Where gaps exist in the Faro Airport Station records, the average day snowfall was used to patch data gaps. Figure 2-14 illustrates the snowfall record developed for the FMC.

Total Precipitation Estimate

The rainfall and snowfall data sets developed, using the described methodology, were used to compile complete precipitation data sets for each of the two FMC meteorological stations. The precipitation data for the Faro and Grum stations at the FMC are shown on Figures 2-15 and 2-16, respectively. When these data sets were reviewed, several outliers were identified and are shown on these figures.

Outliers were identified through comparison with climate normals reported by Environment Canada for the Faro Airport Station. If an extreme event occurred that was not documented in the available site records, it was determined to be a likely outlier. Where possible, these events were compared with the available continuous flow monitoring data collected on the FMC. If a similar increase in SW flow was not reflected in the data, the event was corrected using rainfall and snowfall data from one of the nearby stations.

Table 2-2 compares daily precipitation estimates, developed as described, for the Faro and Grum areas of the FMC, with climate normals for the region as reported by Environment Canada. This table also presents the percent difference from the Faro Airport Station for each area of the FMC.

TABLE 2-2
Comparison to Climate Normals
Faro Mine Remediation Project

		FMC – Faro Area		FMC – Grum Area	
Description	**Faro Airport**	**Estimate**	**% Difference**	**Estimate**	**% Difference**
Average Yearly Rainfall (mm)	214	215	0	225	5
Average Yearly Snowfall (cm)	112	162	37	162	37
Average Total Precipitation (mm)	316	377	17	387	20
Extreme Daily Rainfall (mm)	24.8	28	11	29	14
Extreme Daily Snowfall (cm)	12.8	17	27	17	27

Notes:
Faro Airport climate normals are for 1971 to 2000.
FMC Area comparison values are for the data available between January 2000 and December 2011 (excluding 2001 and 2002).

Some differences between the Faro Airport and FMC are expected due to elevation and orographic effects. The precipitation record is considered a reasonable estimate for this modelling exercise if the total annual precipitation is within 20 percent of climate normals recorded at the Faro Airport Station. The average total precipitation is 17 percent for the Faro Dump Station and 20 percent for the Grum Dump Station. The average yearly rainfall depths for all three locations are consistent. The key difference between the Faro Airport and the FMC data sets is related to the snowfall estimate. Snowfall is expected to be approximately 25 percent greater at the FMC as water equivalent; however, because of the procedures used to patch data gaps, the total snowfall in units of cm is approximately 37 percent greater. Because the total annual precipitation numbers are within 20 percent of the climate normals, this was determined to be acceptable.

The extreme daily rainfall and extreme daily snowfall climate normals were used to determine the outliers, as previously discussed. The comparison to climate normals shown in Table 2-2 does not include the data points identified as outliers. The extreme daily rainfall for both the Faro Dump and Grum Dump stations are between 10 and 15 percent greater than those reported at the Faro Airport Station. The FMC extreme daily snowfall is approximately 27 percent greater than those reported at the Faro Airport Station.

2.4.3.5 Evapotranspiration Data

ET, expressed in terms of total depth per month, is a combination of evaporation from the ground surface and transpiration by vegetation. The monthly ET data used in the model were obtained from AECOM (2009), as summarized in Table 2-3 for the Rose Creek Model and the Vangorda Creek Model.

TABLE 2-3
Monthly Evapotranspiration Data
Faro Mine Remediation Project

Month	Rose Creek Model ET (mm)	Vangorda Creek Model ET (mm)
January	0	0
February	0	0
March	10	10
April	30	32
May	48	47
June	50	56
July	48	57
August	26	30
September	20	20
October	5	4
November	0	0
December	0	0

2.4.3.6 Snowmelt Parameters

A variety of parameters are required to define the snowpack accumulation and snowmelt processes that can be simulated by HEC-HMS. In response to the atmospheric conditions, this accumulation and melt is simulated, and the resulting liquid water available at the soil surface is available as a hyetograph for the subbasin.

The Temperature-Index method was used for snowpack simulation within HEC-HMS, which is an extension of the degree-day modelling approach. The degree-day approach typically applies a fixed amount of snowmelt for each degree above freezing. The Temperature-Index method instead allows for a dynamic computation of the melt rate based on current atmospheric conditions and past conditions of the snow pack, which improves the

representation of the ripening of the snow pack. Through use of a cold-content parameter, this method also allows for liquid water to potentially freeze as it enters the snow pack, a result of the snow pack's existing cold content. The following points describe the snowmelt model parameters according to HEC-HMS User's Manual:

- **Px Temperature (°C) = 1 °C.** The Px temperature is used to discriminate between precipitation falling as rain or snow. The discrimination temperature is usually 1 to 2 degrees above freezing.
- **Base Temperature (°C) = 0 °C.** The difference between the base temperature and the air temperature defines the temperature index used in calculating snowmelt. The melt rate is multiplied by the difference between the base temperature and the air temperature to estimate the snowmelt amount. If the air temperature is less than the base temperature, then the snowmelt is zero. Typically, the base temperature should be 0 °C or close to it.
- **Wet Melt Rate (mm/°C-day) = 4.2 mm/°C-day.** The wet melt rate is used during times of precipitation when the precipitation is falling as rain at rates greater than the rain rate limit. It represents the rate at which the snow pack melts when it is raining on the snow pack.
- **Rain Rate Limit (mm/day) = 1 mm/day.** The rain rate limit discriminates between dry melt and wet melt. The wet melt rate is applied as the melt rate when it is raining at rates greater than the rain rate limit. If the rain rate is less than the rain rate limit, the melt rate is computed as if there were no precipitation.
- **Antecedent Temperature Index (ATI) Melt Rate Coefficient = 0.98.** The ATI melt rate coefficient is used to update the ATI melt rate index from one time interval to the next. A typical coefficient value is 0.98.
- **ATI Melt Rate Function.** The ATI melt rate function defines the melt rate values to use over the range of melt rate indexes that will be encountered during the simulation. Table 2-4 presents the ATI melt rate functions used in this analysis for the Rose Creek and Vangorda Creek models. The melt rate was found to have a significant impact on the shape of the hydrograph and therefore was used as a main calibration parameter.

TABLE 2-4
Meteorological Model ATI Melt Rate Functions
Faro Mine Remediation Project

ATI (°C-day)	Rose Creek Model Melt Rate (mm/°C-day)	Vangorda Creek Model Melt Rate (mm/°C-day)
0	0.80	0.80
50	0.80	0.80
100	0.65	0.50
150	0.65	0.50
500	0.65	0.50

Cold Limit (mm/day) = 20 mm/day. The cold limit accounts for rapid changes in temperature that the snow pack undergoes during high precipitation rates. When the precipitation rate exceeds the specified cold limit, the antecedent cold content index is set to the temperature of the precipitation. If the temperature is above the base temperature, the cold content index is set to the base temperature. If the temperature is below the base temperature, the cold content index is set to the actual temperature. If the precipitation rate is less than the cold limit, the cold content index is computed as an antecedent index. A typical cold limit value is 20 mm per day.

ATI Cold Rate Coefficient = 0.84. The cold content antecedent temperature index coefficient is used to update the antecedent cold content index from one time interval to the next. A typical coefficient is 0.84.

ATI Cold Rate Function. This function defines appropriate cold contents to use over the range of cold content index values that will be encountered in a simulation. The function used was provided as a default starting point from USACE personnel (Scharffenberg, 2011, personal communication). Unlike the melt rate function, the cold

rate function was not used as a significant calibration parameter. Table 2-5 summarizes the ATI cold rate function used for the Rose Creek and Vangorda Creek models.

TABLE 2-5
Rose Creek and Vangorda Creek Meteorological Model ATI Cold Rate Functions
Faro Mine Remediation Project

ATI (°C-day)	Cold Rate (mm/°C-day)
0	1.32
50	1.32
100	1.32
150	1.32
500	1.32

Water Capacity (%) = 5 percent. The maximum liquid water capacity specifies the amount of melted water that must accumulate in the snowpack before the liquid water becomes available at the soil surface for infiltration or runoff. Typically, the maximum liquid water held in the snow pack is on the order of 3 to 5 percent of the snow water equivalent, although it can be higher.

Ground Melt (mm/day) = 0 mm/day. Heat from the ground can cause snow melt, especially if the snow pack accumulates on ground that is only partially frozen or completely unfrozen. In these cases, the warm ground is insulated by the snow pack, and heat from the warm ground will cause the snow pack to melt. It was assumed that zero ground melt occurs at the FMC.

Published literature reflects uncertainty in winter sublimation in northern environments, with estimates ranging from 10 to 45 percent (Scenarios Network for Alaska and Arctic Planning, 2011). Water balance work completed on the FMC waste dumps indicated that sublimation was insignificant (Janowicz et al., 2006, 2008). In general, sublimation is more significant in areas where snow is intercepted by canopy. Snow depth information and data required to estimate sublimation are not available for much of the overall FMC catchment area. The HEC-HMS model does not quantify sublimation specifically. However, effects of sublimation have been accounted for in the model calibration process, as discussed in Section 2.5. During the calibration process, input parameters were varied, and resultant modelled runoff hydrographs were compared to observed data. Certain parameters had a more significant effect on the calibration processes than others. Any losses due to sublimation are accounted for via “overcompensation” of one or a combination of the various calibration parameters.

2.4.3.7 Canopy Storage

Canopy storage represents intercepted precipitation that is stored in the vegetation layer, which will evaporate during storm events. The canopy storage will first consume the potential ET, and unused ET will then be transferred to the surface and soil components. Once the canopy storage is filled, the remainder of the precipitation falls to the surface storage. If there is no representation of surface storage, or if the surface storage is filled up, it falls directly to the soil.

A final effective canopy storage value of 10 mm was applied to all subbasins within the models. This was determined through a calibration process that examined values higher and lower than 10 mm. There was considered to be no initial storage percentage already used at the beginning of the simulation.

2.4.3.8 Surface Storage

The surface storage parameter represents the depression ground surface volume where water can accumulate. Precipitation fall-through from the canopy layer or direct precipitation will accumulate in the surface storage and infiltrate up to the soil capacity. Runoff occurs when the precipitation rate exceeds the soil infiltration rate and the surface storage is fully used. Precipitation residing in the surface storage can infiltrate after the precipitation stops and is subject to potential ET after the ET from the canopy layer is used.

A final effective surface storage value of 10 mm was applied to all subbasins within the models. This was determined through a calibration process that examined values higher and lower than 10 mm. There was considered to be no initial storage percentage already used at the beginning of the simulation.

2.4.3.9 Soil Infiltration Loss Method

HEC-HMS provides 12 different methods describing soil infiltration losses. Some of the loss methods are more suitable for continuous simulations (e.g., Deficit and Constant and Soil Moisture Accounting methods), whereas others are more suitable for event based simulations (e.g., Soil Conservation Service [SCS] Nurve Number and Green and Ampt methods). By design, certain loss methods require a more detailed level of information in regard to the subbasin characteristics. The absence of this information can introduce a great deal of uncertainty into the calibration and can complicate the model calibration process. For this model, the Deficit and Constant Loss method was used. The Deficit and Constant loss method is suitable for continuous simulations and requires four input parameters. The parameters required in the Deficit and Constant Loss method are the initial and maximum deficits, the constant rate, and the percent imperviousness. The initial and maximum deficits are the initial and maximum amount of water the soil can hold; both are specified as depths. The constant rate (mm per hour [mm/hr]) defines the infiltration rate when the soil layer is saturated and can be approximated by the hydraulic conductivity of the soil as a starting point. Lastly, the percent of directly connected imperviousness area is required because no loss calculations are carried out on the impervious area. A final, directly connected impervious value of 10 percent was applied to all subbasins within the models. This was determined through a calibration process that examined impervious values from 0 to 10 percent. The final soil loss parameters that were developed through calibration for each subbasin are listed in Table 2-6.

TABLE 2-6
Rose Creek and Vangorda Creek Models Deficit and Constant Soil Loss Parameters
Faro Mine Remediation Project

Model	Initial Deficit (mm)	Maximum Deficit (mm)	Constant Infiltration Rate (mm/hr)	Imperviousness (percent)
Rose Creek Model (Winter)	0	10	0.1	10
Rose Creek Model (Summer)	0	10	0.35	10
Vangorda Creek Model (Winter)	0	10	0.02	10
Vangorda Creek Model (Summer)	0	10	0.35	10

2.4.3.10 Precipitation-runoff Transform

HEC-HMS provides seven different runoff transform methods. The runoff transform methods describe how excess precipitation is transformed into point runoff in the subbasin. The available runoff transform method choices include various unit hydrograph transformations, a kinematic wave transformation, and a linear quasi-distributed method. Again, the requirement of subbasin specific parameters influenced the decision to employ the most simplified runoff transform method possible—the SCS Unit Hydrograph—because the only parameter required was a hydrograph lag time. There is discussion around the suitability of each transform method for the type of expected simulation and nature of hydrograph in the HEC-HMS User's Manual (USACE, 2010). The application of SCS Unit Hydrograph may not be entirely supported for this case; however, the model results were found to be well calibrated to the observed results. The runoff transform method and parameters also did not prove to be a very powerful calibration parameter when compared to the precipitation loss parameters discussed previously. The SCS hydrograph lag time used for all subbasins was 50 minutes.

2.4.3.11 Base Flow

There are five different options for accounting for base flow into the model. Constant monthly base flow was chosen because the availability of continuous flow data provided an opportunity to observe the actual base flow in certain subbasins. Tables 2-7 and 2-8 summarize the base flow values applied to each of the subbasins in the Rose Creek and Vangorda Creek models, respectively. The continuous flow data sets for R7 and V1 were

examined, and representative base flow values were then applied to subbasins Rose Creek RC1 and Vangorda Creek VC1. These patterns were then factored to the other subbasins according to their relative areas compared to RC1 and VC1. Note that base flow rates and monthly distributions were selected based on analysis of multiple years of low-flow data at various flow monitoring stations. These values are not adjusted annually, which could result in a potential over- or underestimation of base flow contribution during dry or wet years, respectively.

TABLE 2-7
Rose Creek Model Monthly Base Flow Estimates
Faro Mine Remediation Project

Rose Creek Model Catchments	Area (ha)	Constant Monthly Base Flow (m^3/sec)
RC1	9,874	Dec-Apr: 0.3 May-Nov: 1.0
RC2	1,589	Dec-Apr: 0.05 May-Nov: 0.16
RC3	992	Dec-Apr: 0.03 May-Nov: 0.1
RC4	7,253	Dec-Apr: 0.22 May-Nov: 0.73
RC5	124	Dec-Apr: 0.003 May-Nov: 0.0125
RC6	1,842	Dec-Apr: 0.06 May-Nov: 0.18
RC7	637	Dec-Apr: 0.02 May-Nov: 0.06
RC8a and RC8b (Siphon)	852	0.4 (monthly)

Note:
m^3/sec = cubic metre per second

TABLE 2-8
Vangorda Creek Model Monthly Base Flow Estimates
Faro Mine Remediation Project

Vangorda Creek Model Catchments	Area (ha)	Constant Monthly Base Flow (m^3/sec)
VC1	2,007	Sept-Apr: 0.30 May-Aug: 0.40
VC2	742	Sept-Apr: 0.11 May-Aug: 0.15
VC3	276	Sept-Apr: 0.04 May-Aug: 0.05
VC4	1,360	Sept-Apr: 0.20 May-Aug: 0.27
VC5	4,352	Sept-Apr: 0.65 May-Aug: 0.87

2.4.4 Surface Water Model Initial Conditions

Initial parameter conditions were chosen as a starting point in the model prior to calibration. The sensitivity of basin model loss parameters (i.e., canopy storage, surface storage, soil loss method) and snowmelt parameters was evaluated, and if a given parameter proved to be a useful calibration parameter, it was modified during the

calibration process to a final optimized value. If a parameter did not prove to be a useful calibration parameter, it was returned to its default, or initial, condition. The final parameter values used in the Rose Creek and Vangorda Creek models were listed in Section 2.4.3. The initial conditions of the parameters that were used in the calibration process are described in this subsection.

Because limited information is available for the catchment area, the initial conditions for canopy storage and surface storage were taken as 200 mm each as an arbitrary starting point. The calibration process ultimately led to the use of canopy and surface storage depths of 10 mm each.

The soil information available for the study area (Robertson GeoConsultants Inc. [RGC], 1996) describes a mix of both well-drained and poorly drained soils. As a starting point in the calibration process for the constant soil infiltration parameter, a typical value for the hydraulic conductivity of soils was used based on a soil type that lies between the classification of a good aquifer and a poor aquifer. A good aquifer is described by clean sands and a mixture of clean sands and gravel with hydraulic conductivity ranging from approximately 16.8 to 1,697 mm/hr (5×10^{-4} to 5×10^{-2} centimetres per second [cm/sec]). A poor aquifer is described by very fine sands and mixture of sand, silt and clay, glacial till, and stratified clays, with hydraulic conductivity ranging from slightly lower than 0.01 to 16.8 mm/hr (2×10^{-4} to 5×10^{-2} cm/sec) (Chow, 1964). The calibration process ultimately led to the use of constant infiltration parameters that fall within the classification of poor aquifers (0.02 to 0.35 mm/hr or 6×10^{-7} to 1×10^{-5} cm/sec).

The initial condition for the percent imperviousness was set to 0 percent. The calibration process ultimately led to the use of a percent imperviousness of 10 percent.

It is recognized that the final calibrated values for the canopy, surface, and soil loss parameters may not be consistent with theoretical or expected values based on existing physical characteristics of the subcatchments. However, the specific combination of values derived during the calibration process produced the best match of observed versus modelled runoff hydrographs for the duration of the simulation.

The initial condition for the ATI melt rate function was used from a reference document provided by USACE personnel (Scharffenberg, 2011, personal communication). This initial melt rate function is summarized in Table 2-9.

TABLE 2-9
Rose Creek Meteorological Model Initial Conditions ATI Melt Rate Function
Faro Mine Remediation Project

ATI (°C-day)	Melt Rate (mm/°C-day)
0	1.09
50	1.32
100	2.23
150	1.77
500	1.77

The ATI melt rate function was a powerful calibration parameter, and the final calibrated values were provided in Section 2.4.3.6.

As mentioned in Section 2.4.3.1, runoff from subbasins RC8a and RC8b are represented in the form of a constant monthly hydrograph. Runoff and seepage from catchment area RC8a is tributary to the Faro Pit, whereas runoff and seepage from catchment area RC8b is ultimately captured above the Intermediate Dam. This runoff and seepage is ultimately stored in the Faro Pit or in the Intermediate Dam Pond for subsequent treatment at the Faro WTP. Discharge from the WTP is tributary to the CVD Polishing Pond. Water is discharged from the CVD Polishing Pond via a siphon equipped with a control valve. As such, direct runoff from these catchment areas was not

routed through the hydrological model. Rather, a manual hydrograph with monthly time steps was developed to represent controlled discharge through the siphon. Review of available discharge data indicates that flow through the siphon occurs through most months of the year and ranges from 0.0 to approximately 0.4 m^3/sec. For model development, an average monthly discharge estimate of 0.4 m^3/sec was applied and is considered to be a conservative (i.e., high) value for the purposes of model development. Given the relatively low flow rate associated with discharge from the CVD compared with flows coincident at the next downstream model node (i.e., the 23,163 ha X14 catchment area), it is not anticipated that the assumed siphon flow will significantly impact downstream flows from a volume perspective during peak flow events. It would be necessary to further refine this hydrograph, based on additional field data, to better estimate impacts of controlled releases on the receiving watercourse flow regime during low-flow, interevent periods.

2.4.5 Surface Water Model Boundary Conditions

The catchment delineation, described in Section 2.4.3.1 and illustrated in Figures 2-5 and 2-6, provides a no-flow boundary condition for the Rose Creek and Vangorda Creek SW flow models.

When developing hydrological models, the domain is defined by the overall catchment area tributary to the receiving point of interest. For the FMC, the domain is defined by flow monitoring station X14 in the Rose Creek drainage basin and by V8 in the Vangorda Creek drainage basin, shown on Figure 2-4.

Time series and paired data also define boundary conditions in the development of hydrological and meteorological models. For the current model development, time-series data for meteorological parameters (including precipitation and air temperature) were developed. Similarly, time-series data for base flow contribution and flow monitoring data were used. The model was run from January 1, 2004 until December 31, 2011. This period corresponds with the time when the most flow and meteorological data were available for model development and calibration.

2.4.6 Surface Water Model Time Discretization

The SW flow models were discretized to run daily time steps from January 1, 2004 until December 31, 2011. Although certain meteorological data are available hourly, some of it is only available over a 1-day period. HEC-HMS can process time-series data with time steps ranging from 1 minute to 1 day. Given that the models are developed to run continuously for multiple years, a time step of 1 day was selected for run definition. As well, given the relative times of concentrations for the catchments of the Rose Creek and Vangorda Creek models, runoff processes are better represented in terms of days rather than hours.

2.5 Surface Water Model Calibration

The intent of the calibration process was to match the simulated hydrograph peak flows and volumes as closely as possible to the observed data from the various flow monitoring locations over the years of recorded data available.

2.5.1 Surface Water Model Calibration Approach

The flow monitoring stations that were used in the calibration process, and the locations at which they are compared in the model, are summarized herein. Refer to Figure 2-2 for monitoring locations and Figures 2-8 and 2-9 for node and junction definitions, respectively.

Rose Creek Model

- **R7 NFRC above FCD:** Compared to output from node RC1 (total of 9,874 ha contributing catchment area)
- **X2 NFRC Upstream from Mine Access Road:** Compared to output from node Junction RC3, which includes flows from RC1, RC2, and RC3 (total of 12,455 ha contributing catchment area).
- **X14 Rose Creek Downstream from the RCDC:** Compared to output from node Junction RC5, which is the most downstream point in the model that includes flow from the entire catchment area (total of 23,163 ha contributing catchment area)

Vangorda Creek Model

- **V1 Vangorda Creek Upstream from the FMC and Blind Creek Road:** Compared to output from node Vangorda VC1 (total of 2,007 ha contributing catchment area)
- **V27 Vangorda Creek, Just Upstream from Shrimp Creek (DES, 2011):** Compared to output from node Junction VC1 (total of 3,025 ha catchment area)
- **V8 Lower Vangorda Creek at the Footbridge:** Compared to output from Junction VC3 (total of 8,737 ha contributing catchment area)

The calibration process started with the most upstream subbasins from each model (i.e., Rose Creek RC1 and Vangorda VC1). For each of these subbasins, continuous flow data were available at the respective discharge points. This allowed for the comparison and subsequent calibration of the subbasin-specific models. Once the subbasin parameters were appropriately calibrated for these catchments, subsequent downstream catchments were added to the models, with results compared to available continuous and spot flow data.

2.5.2 Surface Water Model Calibration Targets

For the winter models, the magnitude and duration of spring freshet was the key calibration target because this is the event that defines peak annual runoff hydrographs for the system. For the summer models, the frequency and magnitude of runoff events was the key calibration target because runoff hydrographs, in this case, are not influenced by longer-duration melt periods, as is the case with the winter models, but rather shorter duration runoff events with a more frequent return period. The shape of the hydrograph, in terms of the lag during the spring freshet, as well as during more frequent summer runoff events, was a particularly important calibration target because it dictated the volume of SW being simulated by the model annually.

2.5.3 Surface Water Model Calibration Process

After an initial sensitivity analysis was performed on parameters, those that exhibited the most influence on model results were selected for further analysis. These parameters included the ATI melt rate index function, the constant infiltration parameter, the surface storage depth, and the canopy storage depth.

The most significant effect on the hydrograph volume during the spring freshet resulted from calibrating the ATI melt rate index function value. Adjusting the melt rate values higher or lower and varying the melt rate value within the range of the ATI function itself either increased or decreased the extent of the hydrograph lag during the melt. Table 2-4 lists the final ATI melt rate index functions that best suited the simulations. The melt rate function was calibrated in conjunction with the calibration of the precipitation loss parameters because, although these parameters govern different aspects of the simulation, they interact with one other.

The most significant effect on the magnitude of peak flows resulted from varying the constant soil infiltration parameter. As mentioned earlier, two separate basin models were developed, one with the soil infiltration parameter calibrated for the snowmelt peak (which is typically the largest peak in the annual record) and one with the soil infiltration parameter calibrated to the later summer peaks. The soil infiltration parameters are presented in Table 2-6. The results of the snowmelt-calibrated model were used from the beginning of November until the end of June, and the results from the summer-calibrated model were used from the end of June until the end of October. The difference in soil infiltration parameter is intended to reflect the fact that during the snowmelt calibration period, the ground is frozen and the infiltration parameter can be expected to be lower than during nonfrozen periods of the year. During the summer calibration period, the ground has thawed, and the infiltration parameter can be expected to be slightly higher than during the frozen periods of the year. The modelling results support this reasoning; when the snowmelt-calibrated infiltration loss parameter was used, the peaks during the spring freshet were well-matched to the observed data; however, the simulated peaks in the later summer months (July through September) were much higher than those observed. Likewise, when the summer-calibrated infiltration loss parameter was used, the summer peaks were better calibrated to the observed data; however, the snowmelt peaks during the spring freshet (May through June) were much lower compared to those observed. As such, a two-model approach was developed to simulate the change in soil infiltration resulting from the change in temperature over the course of the different hydrological events. A difference was also found in the Rose Creek

model- and Vangorda Creek model-calibrated winter soil infiltration parameters, which could reflect different soil and land cover conditions between the two sites during the winter months (0.02 mm/hr versus 0.1 mm/hr [6×10^{-7} cm/sec versus 3×10^{-6} cm/sec]). The same summer-calibrated soil infiltration parameter was used for both areas (0.35 mm/hr [1×10^{-5} cm/sec]).

The modelled hydrographs at each flow station, provided in Section 2.5.4, are an amalgamation of the results from both of these models. The simulated behaviour during the potential overlap periods (end of June until early July and end of October until early November) was examined for each subbasin to determine whether the soil infiltration parameter for the snowmelt or summer period would be better suited for specific portions of this transition period. As a starting point, July 1 was initially taken as the date when the change in soil infiltration rates would occur. This remained as such for most of the years simulated, except for 2007 and 2011, where, upon examination, it appeared that there were precipitation events toward the end of June (June 25, 2007 and June 20, 2011) that were better simulated with the summer-calibrated soil infiltration parameter for these years.

Because certain years of continuous flow monitoring data are more complete than others (e.g., at times snowmelt period flow data were missing), the calibration process sometimes favoured certain years more than others. This was particularly true for the Vangorda Creek model at flow monitoring station V1. Although there are flow monitoring station V1 data available for 4 years (2008 through 2011), only the data from 2009 contains the snowmelt period of May and June; therefore, this year was relied on for the calibration process. Likewise, further downstream at station V8, although there are data available for 2008, 2010, and 2011, it is suspected that the data from 2010 and 2011 are inaccurate. As a result, only the 2008 data were used for the calibration process. The continuous 2010 and 2011 flow monitoring readings appear to be abnormally low. For verification, they were first compared to the spot-flow measurements from the 2010 and 2011 environmental monitoring reports (DES, 2011, 2012a) at the same station locations, and the values were found to agree fairly well with each other. However, the fact that the peak flow recorded at monitoring station V27 in 2011, which is located upstream of station V8, is slightly higher than that recorded at V8 (both are approximately 3 m^3/sec for the spring snowmelt peak) supports the hypothesis that the flow data in 2010 and 2011 at V8 may be compromised. Compared to V27, V8 would be expected to receive an additional 5,712 ha of catchment area; therefore, the peak flows at V8 would be expected to be higher than at V27. The model results at the location of V27 (Junction VC1) agree well with the observed data from the 2011 flow monitoring report (approximately 3 m^3/sec), whereas the modelled peak flows at the V8 location (Junction VC3) are approximately 7.5 m^3/sec.

2.5.4 Surface Water Model Calibration Results

Figures 2-17 through 2-21 compare the observed versus modelled hydrographs at flow monitoring stations R7, X2, and X14 (for the Rose Creek Model) and V1 and V8 (for the Vangorda Creek model), respectively, spanning the years of continuous flow data available for each station. Appendix A includes a separate figure for each flow monitoring station. In Appendix A, the continuous flow monitoring data are shown in black, whereas the modelled data from the winter-calibrated model are shown in green and the summer-calibrated model data are shown in orange.

As discussed, the models have been calibrated to generally match the peak flows and hydrograph volume across all years of available data. However, there are certain years where the modelled results better match the observed data as compared to others. For the Rose Creek model, years 2005, 2009, and 2011 are better calibrated to the observed hydrographs than in other years at both flow monitoring stations R7 and X14. For the Vangorda Creek model, 2009 is the best-calibrated year for V1, and 2008 is the best-calibrated year for V8.

Considering the fairly coarse resolution of the models, in terms of catchment delineation size and parameter estimation, the calibrated model appears to be adequate because it tends to achieve similar results to flow monitoring data at the most downstream end of both systems (X14 and V8, for Rose Creek and Vangorda Creek models, respectively). Nonetheless, model weaknesses include the fact that it does not succeed in replicating every event that was recorded in the continuous flow monitoring data (e.g., November 2005 and 2006 events). Further, the time lag in the spring freshet portion of the simulated hydrograph remains in general briefer than was observed. This remains true even after pushing the limits of calibration to extend it as much as possible without adversely affecting other aspects of the hydrograph. The timing of the simulated hydrograph is generally

coincident with the observed data, with the spring melt occurring on average within a few days of observed melt; however certain years match better than others. For 2005, the modelled and observed spring freshet peaks coincide well with each other around May 17. However, in 2007, the continuous flow monitoring data and spot-flow measurement data (Laberge Environmental Services [Laberge], 2007) show two peaks within the freshet period: one at the end of May (coinciding around the time of the main modelled peak) and another greater peak in early June. The model does simulate these two peaks; however, the first one is the largest, while the second peak is dampened.

It is acknowledged that base flow will vary both seasonally and annually; however, to develop a calibrated model that can be used in subsequent analyses, an average monthly base flow was applied. Because base flow varies by year, the average monthly base flow succeeded in better representing the observed base flow for certain years compared to others. For 2010, the estimated base flow is approximately double the observed base flow because this year was significantly drier than the others and experienced a smaller spring freshet. The implication of this is that, along with the base flow, the modelled events during the summer and autumn period in particular were higher than those observed.

As mentioned previously, a manual hydrograph with monthly time step was developed to represent controlled discharge from the CVD Polishing Pond. Peak flow rates from the siphon are relatively small compared with cumulative flows directly downstream in Rose Creek. Therefore, assumed discharges from the CVD Polishing Pond do not significantly impact downstream flows from a volume perspective during peak flow events. It is necessary to further refine this hydrograph, based on additional field data, to better estimate impacts of controlled releases on the flow regime of the receiving watercourse during low-flow, interevent periods.

The modelling results were calibrated against the continuous flow monitoring results and, whenever possible, the results were also compared to spot flow measurements available from other sources such as DES (2011, 2012a), Gartner Lee Limited (GLL) (2007, 2008), and Laberge (2005a, 2007). Figure 2-2 illustrates the location of the flow monitoring sites where spot readings were evaluated.

Of particular importance in the Rose Creek model was an analysis of potential attenuation effects upstream of the Haul Road Rock Drain. Based on anecdotal information, runoff appears to pool behind the rock drain during significant runoff events. Hydrographs generated from the calibrated model both upstream and downstream of the rock drain were compared to available continuous field data, as well as spot-flow measurements recorded by FMC care and maintenance operators. Based on the similarity in peak flows recorded by the continuous flow data and spot-flow measurements upstream and downstream of the Haul Road Rock Drain, as well as the general agreement between modelled and observed hydrographs from locations upstream and downstream of the rock drain, the Haul Road Rock Drain does not provide significant peak flow attenuation for events that were simulated between 2004 and 2011. To further corroborate this conclusion, the water surface elevations provided immediately upstream and downstream from the rock drain at locations NF1 and NF2 in DES (2012a) exhibit the same fluctuation over time. This suggests that the flow rates are the same over this period. In light of these observations, the model has been developed without specifically including the Haul Road Rock Drain as a separate hydraulic element. The increase in head that develops as water pools upstream of the rock drain may sufficiently maintain a constant peak flow through the structure. However, for events exceeding those that have been simulated in this modelled exercise, the rock drain would likely provide peak flow attenuation once the capacity through the porous structure was exceeded.

The spot-flow measurements in DES (2011, 2012a) typically did not coincide with significant hydrological events (such as a spring freshet or a peak summer storm). Therefore, the general comparison of these data sets to the model results was not always very telling but was nonetheless carried out. Laberge (2005a) provides more significant data because the spot-flow measurements were taken on May 11 and 12, 2005, which nearly coincides with the peak of the spring freshet (May 17, 2005). Measurements were taken at various locations along the NFRC and the RCD (at R7, X2, X14), and these were compared to both the model results and the observed continuous data, as summarized in Tables 2-10 and 2-11, respectively. Note that the nearest continuous flow monitoring station to Station RCDC4 that includes runoff from both the north and south forks of Rose Creek is X14. Although

the catchment area tributary to Station X14 is larger than that tributary to Station RCDC4, it is the most representative station to which peak flows reported by Laberge (2005a) can be compared.

TABLE 2-10
Comparison of May 12, 2005 Flow Rates
Faro Mine Remediation Project

Flow Monitoring Station	Location	Laberge (2005a)[a] (m^3/sec)	Continuous Flow Data (m^3/sec)	HEC-HMS Model (m^3/sec)
R7	NFRC	4.1	4.6	5.2
X2	NFRC Downstream from Tailings Facility	6.3	n/a	6.3
X14	Rose Creek Downstream from Tailing Facility	13.1	14.3	11.9
RCDC4	Entrance of RCDC	11.1	14.3[b]	11.9[b]

Notes:
n/a = not applicable
[a] instantaneous (i.e., spot) flow measurement
[b] based on data from continuous station X14

TABLE 2-11
Comparison of 2007 Spring Freshet Peak Flows
Faro Mine Remediation Project

Flow Monitoring Station	Location	Laberge (2007)[a] (m^3/sec)	Continuous Flow Data (m^3/sec)	HEC-HMS Model (m^3/sec)
R7	NFRC	13 (June 6)	6.5 (June 7)	6.3 (May 25)
X14	Rose Creek Downstream from Tailing Facility	30 (June 6)	17.6 (June 6)	14.3 (May 25)
V8	Lower Vangorda Creek at the Footbridge	10 (June 6)	n/a	7.5 (May 25)

Notes:
n/a = not applicable
[a] instantaneous (i.e., spot) flow measurement

2.6 Surface Water Model Application

As defined earlier in this report, the FY12 objective of the SW flow modelling task was to develop a dynamic hydrological model of the FMC that can be used to provide a better understanding of the hydrological characteristics of the FMC and support future FMC design and investigative activities. Building on the CSM Report (CH2M HILL, 2012), the SW flow models are used to define precipitation-runoff processes throughout the FMC and to assist in characterizing the occurrence, conveyance, and management of SW within the FMC under varying assumptions of land use and meteorological conditions.

The SW flow models described herein have been used to simulate rainfall-runoff processes from the FMC on a continuous, multiyear simulation basis to simulate the timing and magnitude of runoff events throughout the year ranging from low-flow (i.e., base flow) conditions up to the peak flows occurring during the spring freshet. To establish flow rates for diversion designs that exceed those produced by the freshet, a regional analysis will be used. This involves transposing flood data from regional flow gauging stations to the outlets of the respective diversion.

The SW flow models detailed in this report require further development to support the design of the SW diversion structures planned at the FMC and to support various other design activities at the FMC. The models also require further refinement to address YESAB requirements, as well as to analyze climate change scenarios. During these

efforts, the existing models will be revised to facilitate the evaluation of potential future hydrological and hydraulic stream diversion behaviour under a variety of flow conditions up to and including the probable maximum flood event (PMF). The SW flow models will be used primarily to develop stream diversion designs but will also be further integrated with the GW flow and water quality modelling efforts to support the FMRP. The following are key remedial design areas including the objective for each area:

- **FCD (East Valley).** Direct clean water around the Faro Pit and minimize seepage losses that could impact the stability of the Faro Pit walls and add to water treatment volumes.
- **North Wall Interceptor Ditch (NWID).** Remediate the existing NWID and discharge to a location below the CVD (instead of the Rose Creek Tailings Area [RCTA]).
- **Guardhouse Creek Water Management.** Intercept seepage from the mill pad and associated stockpiles and redirect this water to the Faro Pit.
- **Upgrade NFRC.** Protect the NFRC from potential sources of contamination.
- **Upgrade RCD Upstream from the Fuse Plug to PMF.** Enable the RCDC to accommodate an excess of the current 1-in-500-year flood event.
- **Breach North Fork Rock Drain.** Protect the NFRC from potential sources of contamination and restore channel.
- **Down Valley Interim Hydraulic Upgrades.** Increase the Intermediate Dam spillway capacity to pass PMF flows.
- **RCDC Fuse Plug Upgrades.** Design an RCD hydraulic structure to divert flows exceeding the 1-in-500-year flood event.
- **Upgrade of RCD Downstream of Existing Fuse Plug.** Address the freeboard inadequacy issues to enable the RCDC to pass the flow of Rose Creek on a year-round basis for all flows up to the 1-in-500-year flood event.
- **Construct New Vangorda Diversion.** Permanently realign Vangorda Creek around the Vangorda Pit to minimize leakage into Vangorda Pit and safely convey the PMF.
- **Upgrade Runoff Interceptor Ditch to Dixon Creek.** Divert uncontaminated surface runoff from the northeast side of the Vangorda to the south and into Dixon Creek via the Dixon Creek Diversion.

Associated efforts in future GW analysis and hydraulic/hydrological dam structure design tasks across the FMC will be integrated with the future SW flow modelling efforts to develop comprehensive remedial designs.

2.6.1 Surface Water Model Use and Limitations

As detailed earlier in this report, the hydrological models were developed and calibrated based on available meteorological and flow data collected at the FMC over a number of years and from additional data collected at offsite stations such as the Faro Airport Station. Modelled hydrographs compare well with those observed at the continuous monitoring stations for the duration of the analysis. However, continuous flow data were available at a relatively small number of stations, which resulted in the need to lump large catchment areas. The current SW flow models for the FMC are not sufficiently detailed to accurately develop the diversion design and stream channel upgrades. The deficiencies in the current models are based on the quality and quantity of the available data records and physical site data to adequately support model development and the current level of discretization applied to some critical basins. The proposed efforts, defined in this report, to collect additional data will facilitate further refinement and enhancement of the SW flow models. Additional flow data and site characteristics data will also allow for additional discretization of drainage catchment areas at the FMC. This additional detail will also allow for the models to be refined and the required diversion designs and stream upgrades to be better facilitated.

REGIONAL MAP

LEGEND

- Meteorological Station
- National Road Network Major Road

Notes:

1. Aerial photography acquired by Peregrine Aerial Surveyors Inc. and Eagle Mapping in August 2012.
2. Orthophotography prepared by Critigen Canada Corp.

N

0 1,000 2,000 3,000 4,000

Metres

Created by: CRITIGEN

FIGURE 2-1

Site Area Meteorological Stations

Faro Mine Remediation Project

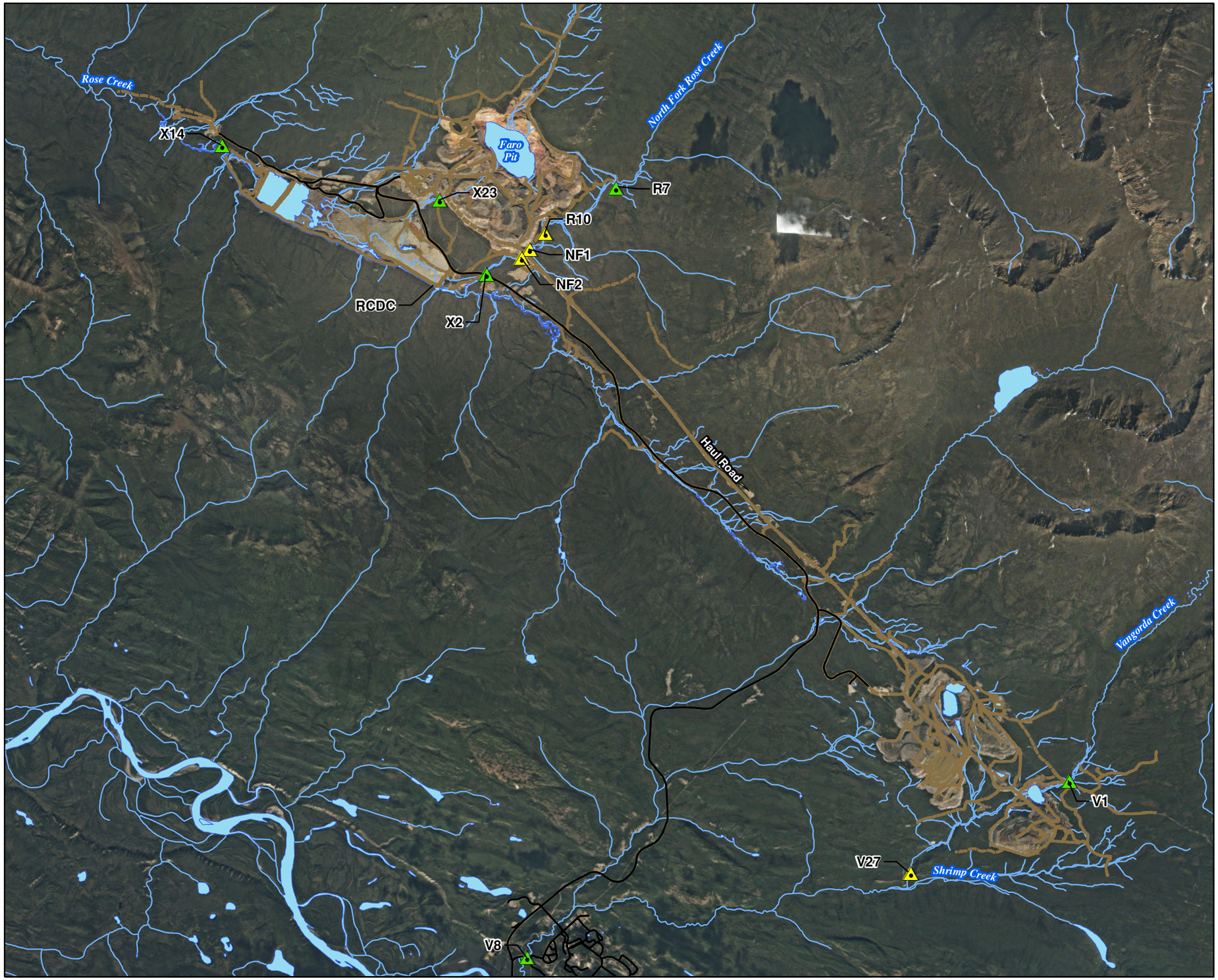

REGIONAL MAP

LEGEND

- Continuous Flow Monitoring Location
- Spot Monitoring Location
- National Road Network Major Road
- Faro Site Watercourse
- Roads Unpaved
- Faro Site Waterbody

Notes:

1. Aerial photography acquired by Peregrine Aerial Surveyors Inc. and Eagle Mapping in August 2012.
2. Orthophotography prepared by Critigen Canada Corp.

N

0 700 1,400 2,100 2,800

Metres

Created by: CRITIGEN

FIGURE 2-2

Continuous Flow Monitoring Stations

Faro Mine Remediation Project

CH2MHILL

R:\FAROMINE_20000342\MAPFILES\WATERMODELANALYSISRPT\FIG02_02.MXD ECLARK 2/26/2013 3:32:49 PM

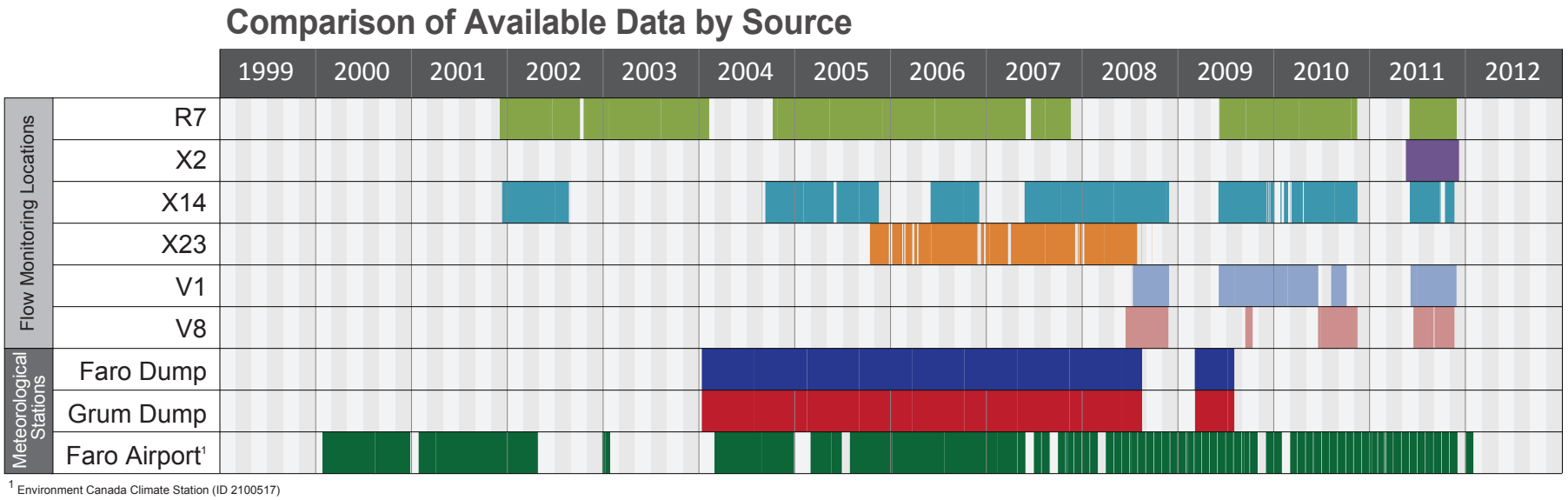

[1] Environment Canada Climate Station (ID 2100517)

FIGURE 2-3
Comparison of Available Data by Source
Faro Mine Remediation Project

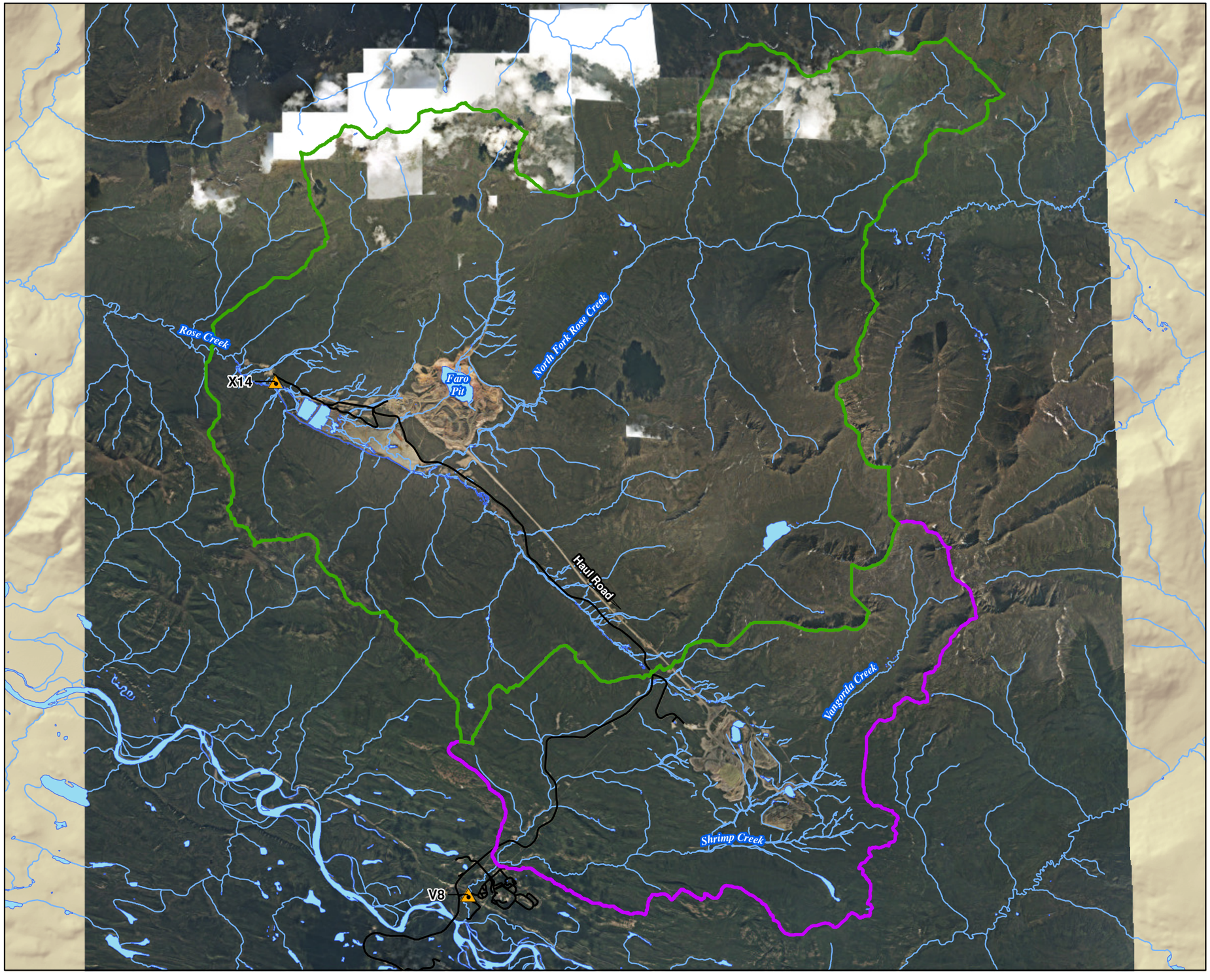

LEGEND

- Flow Monitoring Location
- National Road Network Major Road
- Faro Site Watercourse
- Faro Site Waterbody
- Rose Creek Regional Catchment
- Vangorda Creek Regional Catchment

Notes:

1. Aerial photography acquired by Peregrine Aerial Surveyors Inc. and Eagle Mapping in August 2012.
2. Orthophotography prepared by Critigen Canada Corp.

N

0 1,100 2,200 3,300 4,400

Metres

Created by: CRITIGEN

FIGURE 2-4

FMC Surface Water Catchment Boundary

Faro Mine Remediation Project

CH2MHILL

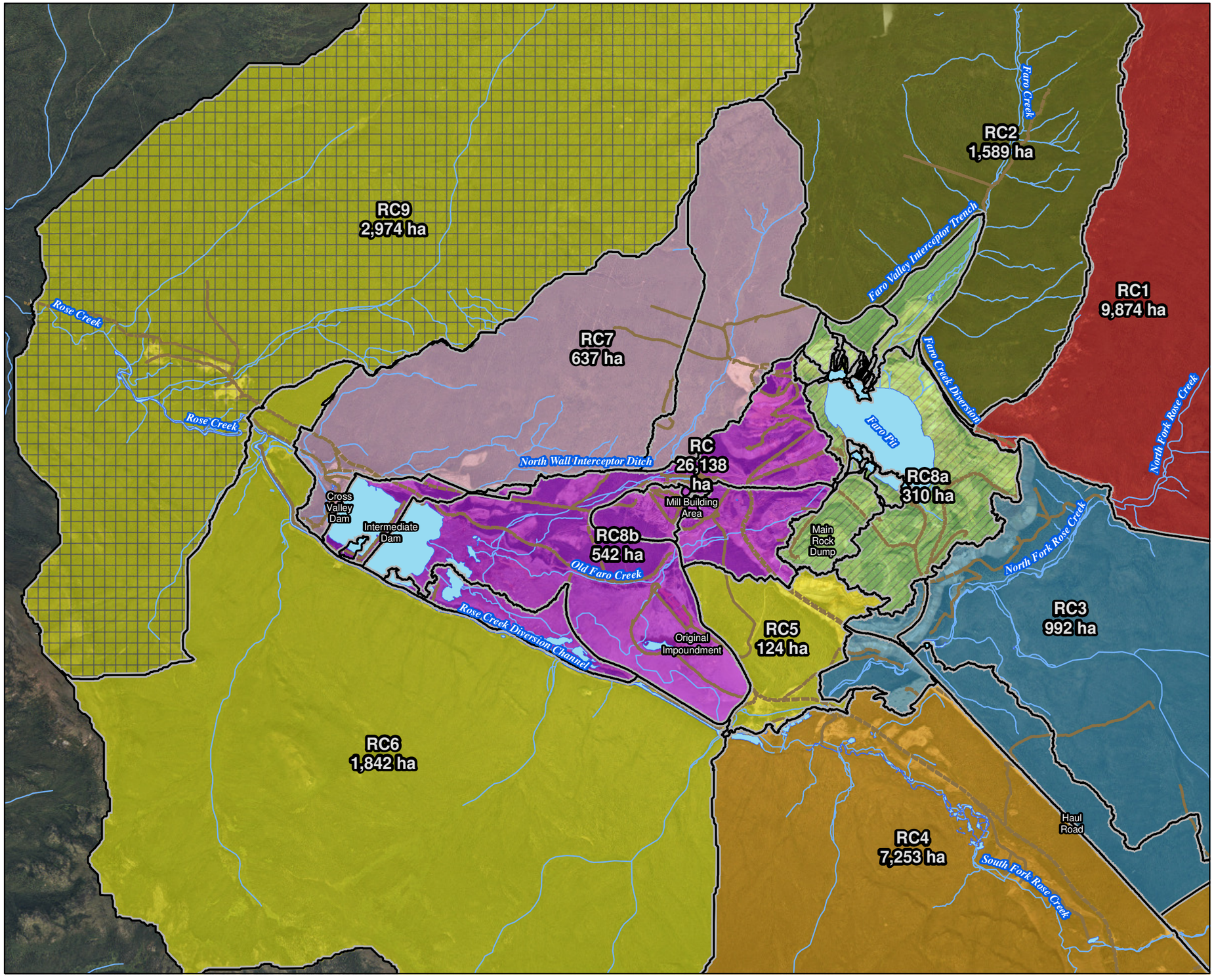

VICINITY MAP

LEGEND

- Roads Unpaved
- Faro Site Watercourse
- Faro Site Waterbody
- Catchment Boundary

Catchment Name

- North Fork Rose Creek (Upper) (RC1)
- Faro Creek & Faro Creek Diversion (RC2)
- North Fork Rose Creek (Lower) (RC3)
- South Fork Rose Creek (RC4)
- Rose Creek Diversion (RC5 + RC6)
- Upper Guardhouse Creek/North Wall Interceptor (RC7)
- Faro Pit (RC8a)
- Tailings Area (RC8b)
- Rose Creek (RC9)

Notes:

1. Aerial photography acquired by Peregrine Aerial Surveyors Inc. and Eagle Mapping in August 2012.
2. Orthophotography prepared by Critigen Canada Corp.

N

0 320 640 960 1,280

Metres

Created by: CRITIGEN

FIGURE 2-5

Faro Dump Area: Local Surface Water Catchments

Faro Mine Remediation Project

RC4
7,253 ha

Haul Road

VC3
276 ha

Grum Pit

Grum Interceptor Ditch

VC1
2,007 ha

Vangorda Creek

VC5
4,352 ha

VC2
742 ha

Grum Creek

VC
8,737 ha

Vangorda Creek

Sheep Creek

Vangorda Waste Rock Dump

Shrimp Creek

VC4
1,360 ha

VICINITY MAP

LEGEND

- Roads Unpaved
- Faro Site Watercourse
- Faro Site Waterbody
- Catchment Boundary

Catchment Name

- South Fork Rose Creek (RC4)
- Vangorda Creek & Vangorda Diversion (VC1)
- Vangorda Creek & Shrimp Creek (VC2)
- Grum Pit (VC3)
- Shrimp Creek/Dixon Creek (VC4)
- Vangorda Creek (VC5)

Notes:

1. Aerial photography acquired by Peregrine Aerial Surveyors Inc. and Eagle Mapping in August 2012.
2. Orthophotography prepared by Critigen Canada Corp.

N

0 320 640 960 1,280

Metres

Created by: CRITIGEN

FIGURE 2-6

Grum Dump Area: Local Surface Water Catchments

Faro Mine Remediation Project

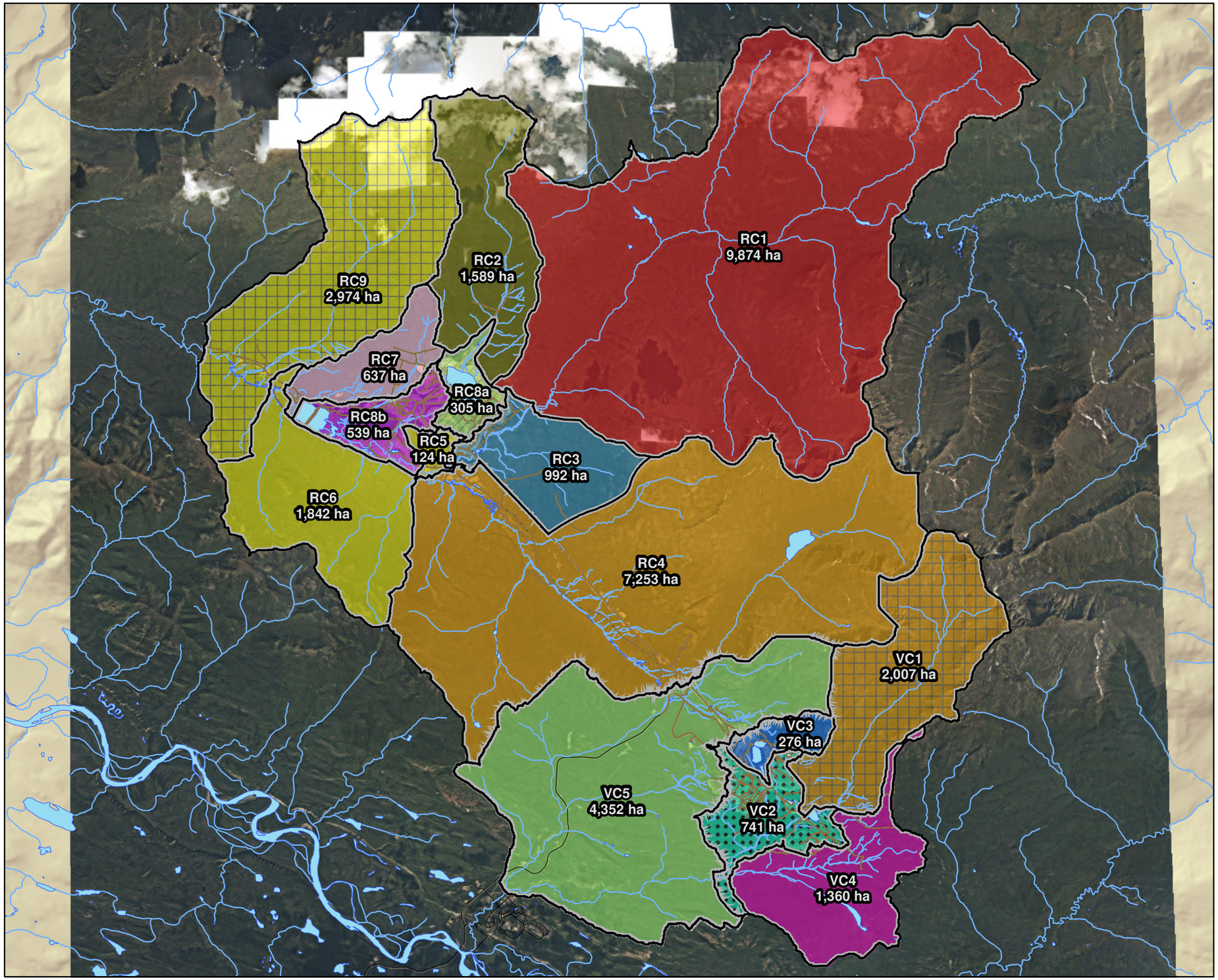

VICINITY MAP

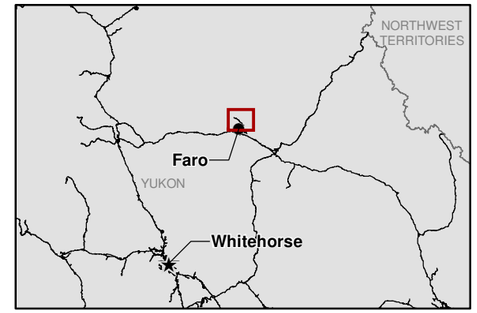

LEGEND

- Roads Unpaved
- Faro Site Watercourse
- Faro Site Waterbody
- Catchment Boundary

Catchment Areas Tributary to Rose Creek

- North Fork Rose Creek (Upper) (RC1)
- Faro Creek & Faro Creek Diversion (RC2)
- North Fork Rose Creek (Lower) (RC3)
- South Fork Rose Creek (RC4)
- Rose Creek Diversion (RC5 + RC6)
- Upper Guardhouse Creek/North Wall Interceptor (RC7)
- Faro Pit (RC8a)
- Tailings Area (RC8b)
- Rose Creek (RC9)

Catchment Areas Tributary to Vangorda Creek

- Vangorda Creek & Vangorda Diversion (VC1)
- Vangorda Creek & Shrimp Creek (VC2)
- Grum Pit (VC3)
- Shrimp Creek/Dixon Creek (VC4)
- Vangorda Creek (VC5)

Notes:
1. Aerial photography acquired by Peregrine Aerial Surveyors Inc. and Eagle Mapping in August 2012.
2. Orthophotography prepared by Critigen Canada Corp.

N

0 1,050 2,100 3,150 4,200
Metres

Created by:
CRITIGEN

FIGURE 2-7
Regional Surface Water Subcatchments
Faro Mine Remediation Project

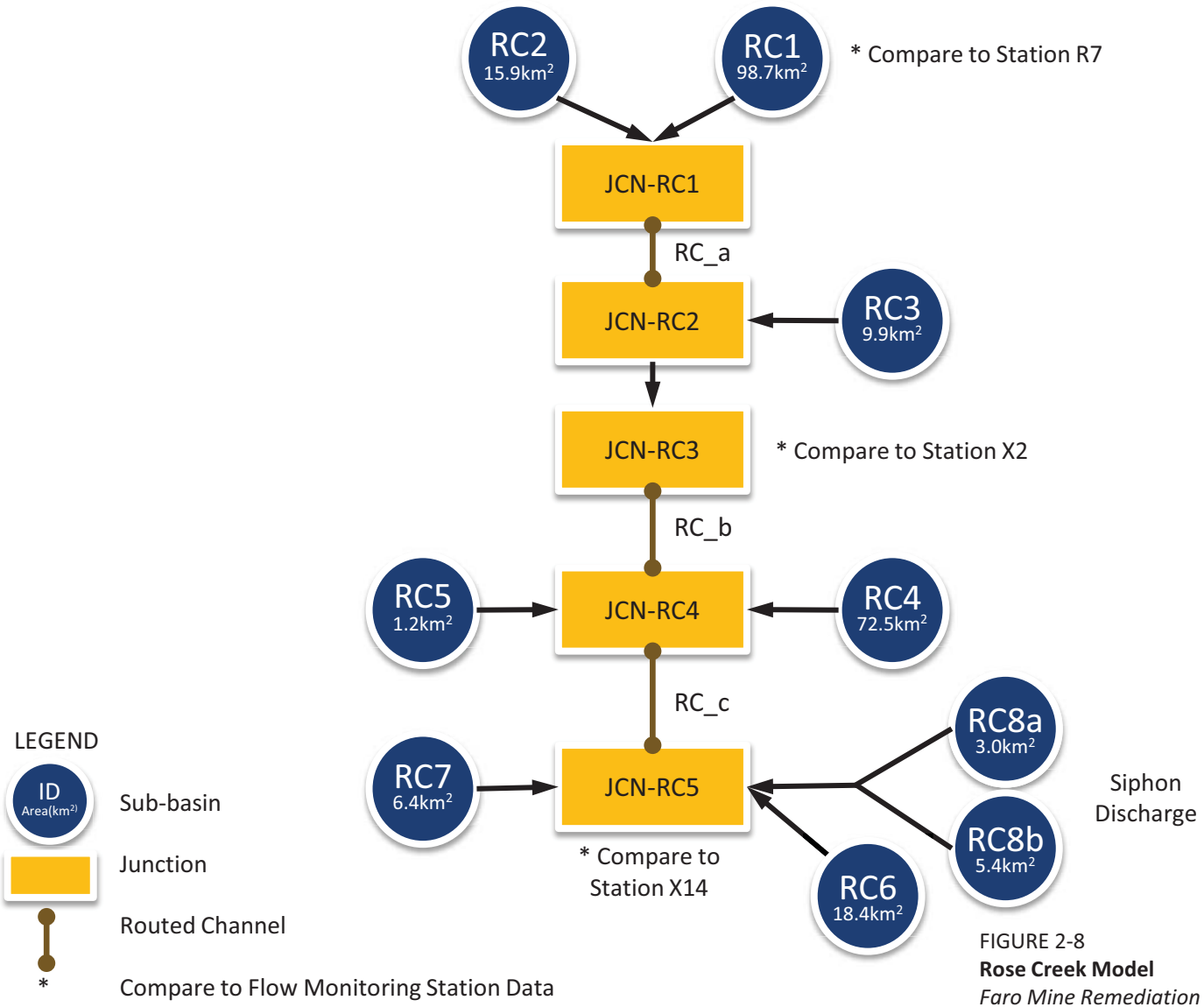

FIGURE 2-8
Rose Creek Model
Faro Mine Remediation Project

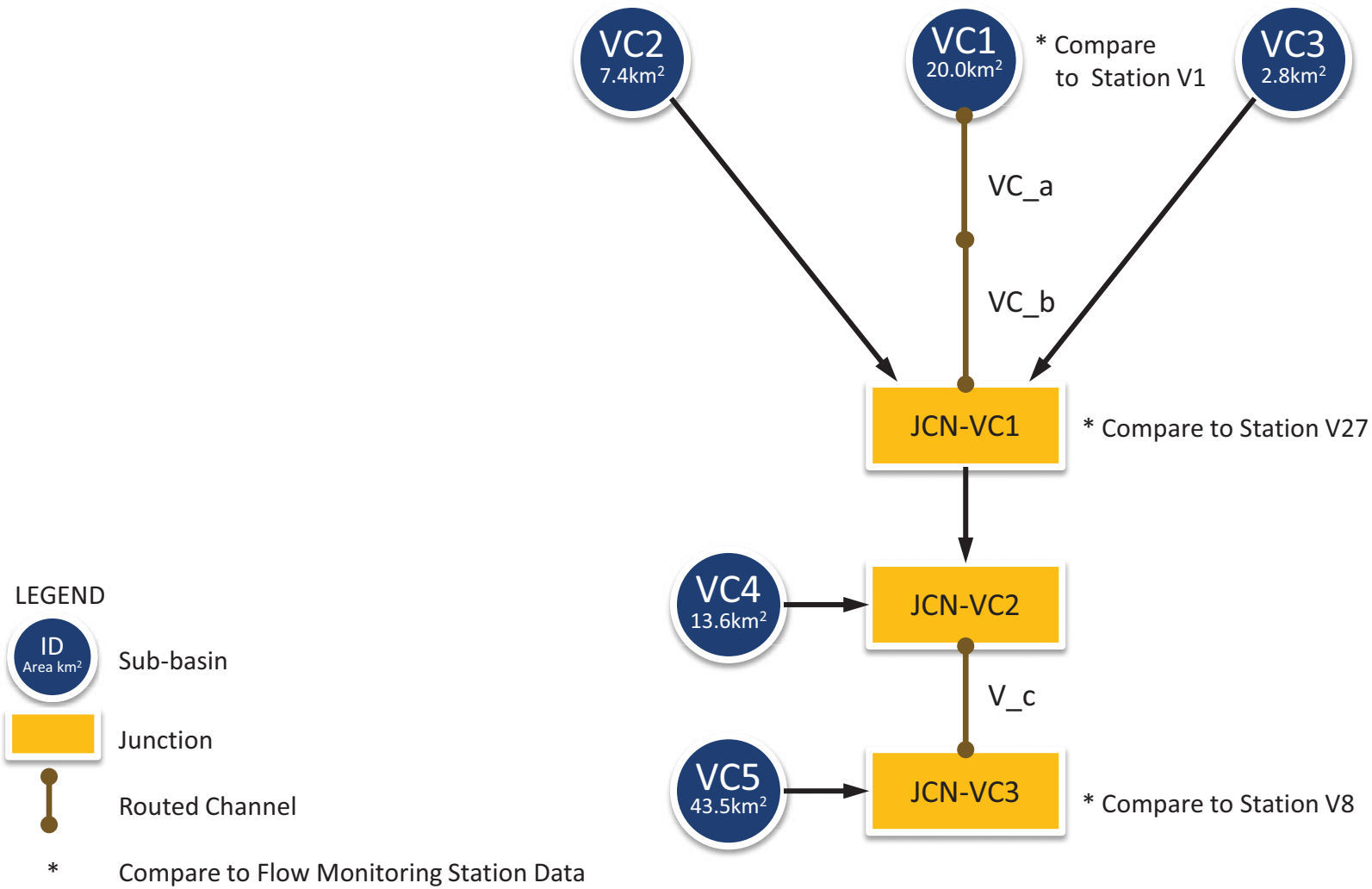

FIGURE 2-9
Vangorda Creek Model
Faro Mine Remediation Project

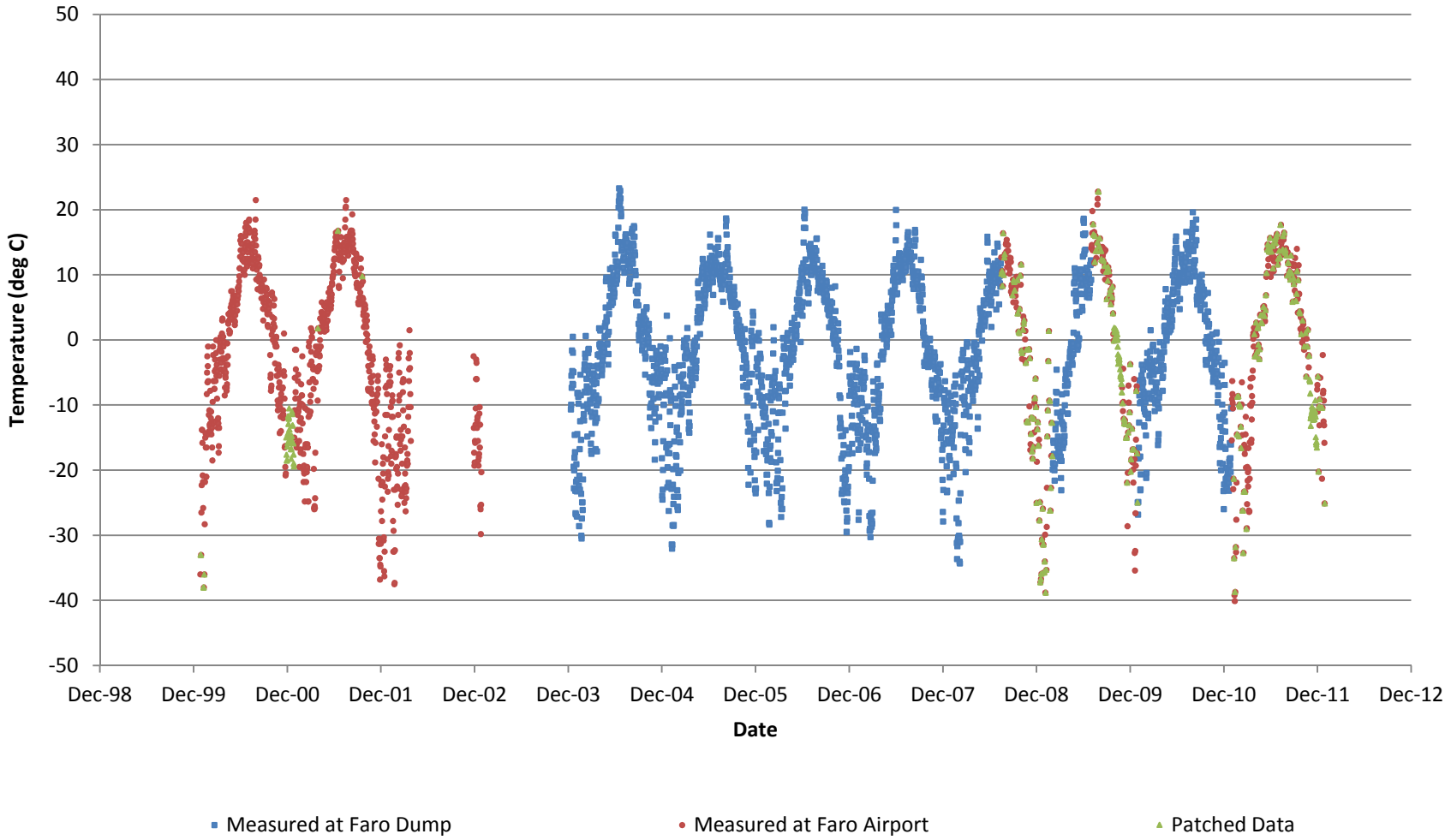

FIGURE 2-10
Faro Dump: Temperature Record by Data Source
Faro Mine Remediation Project

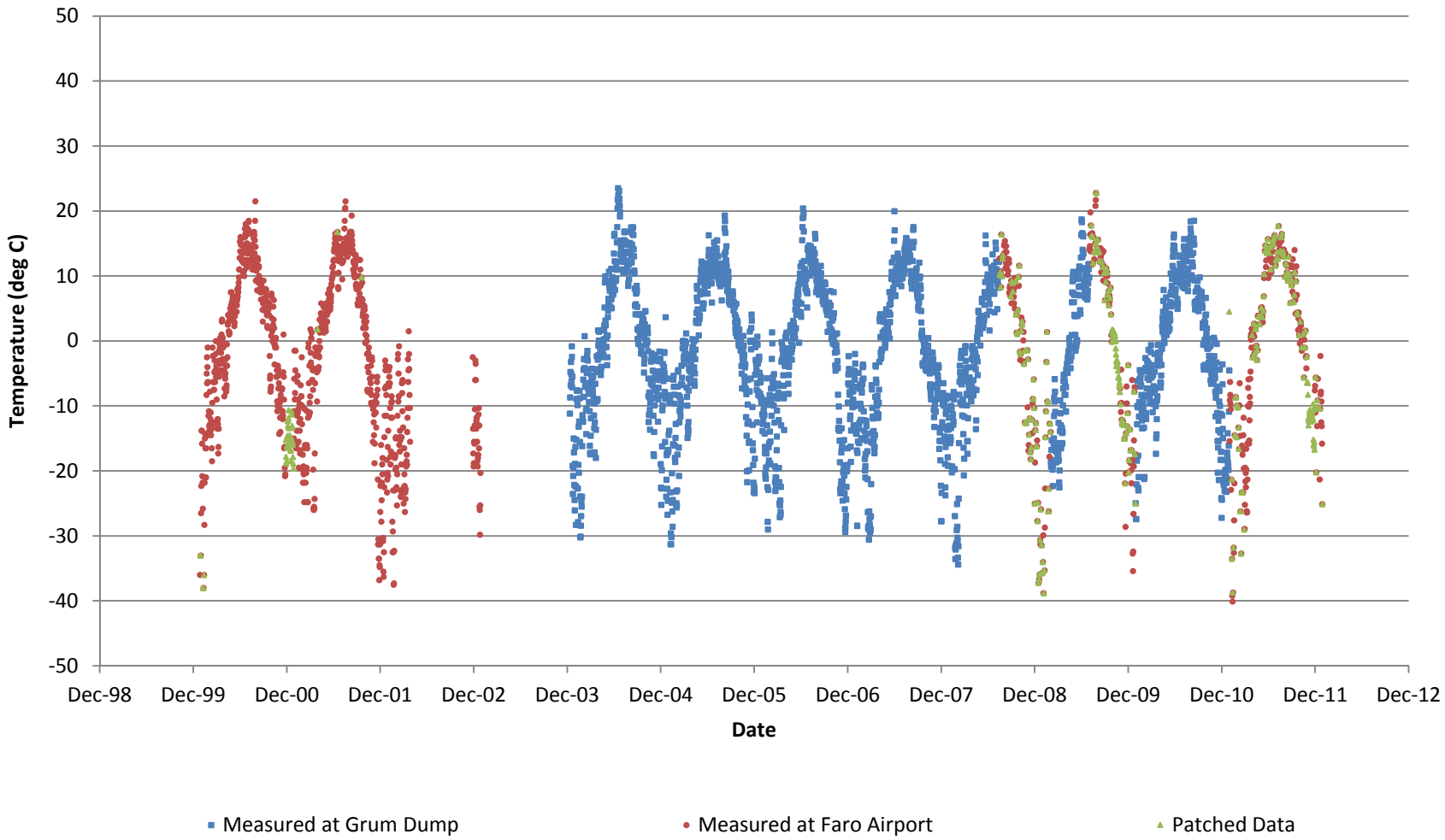

FIGURE 2-11
Grum Dump: Temperature Record by Data Source
Faro Mine Remediation Project

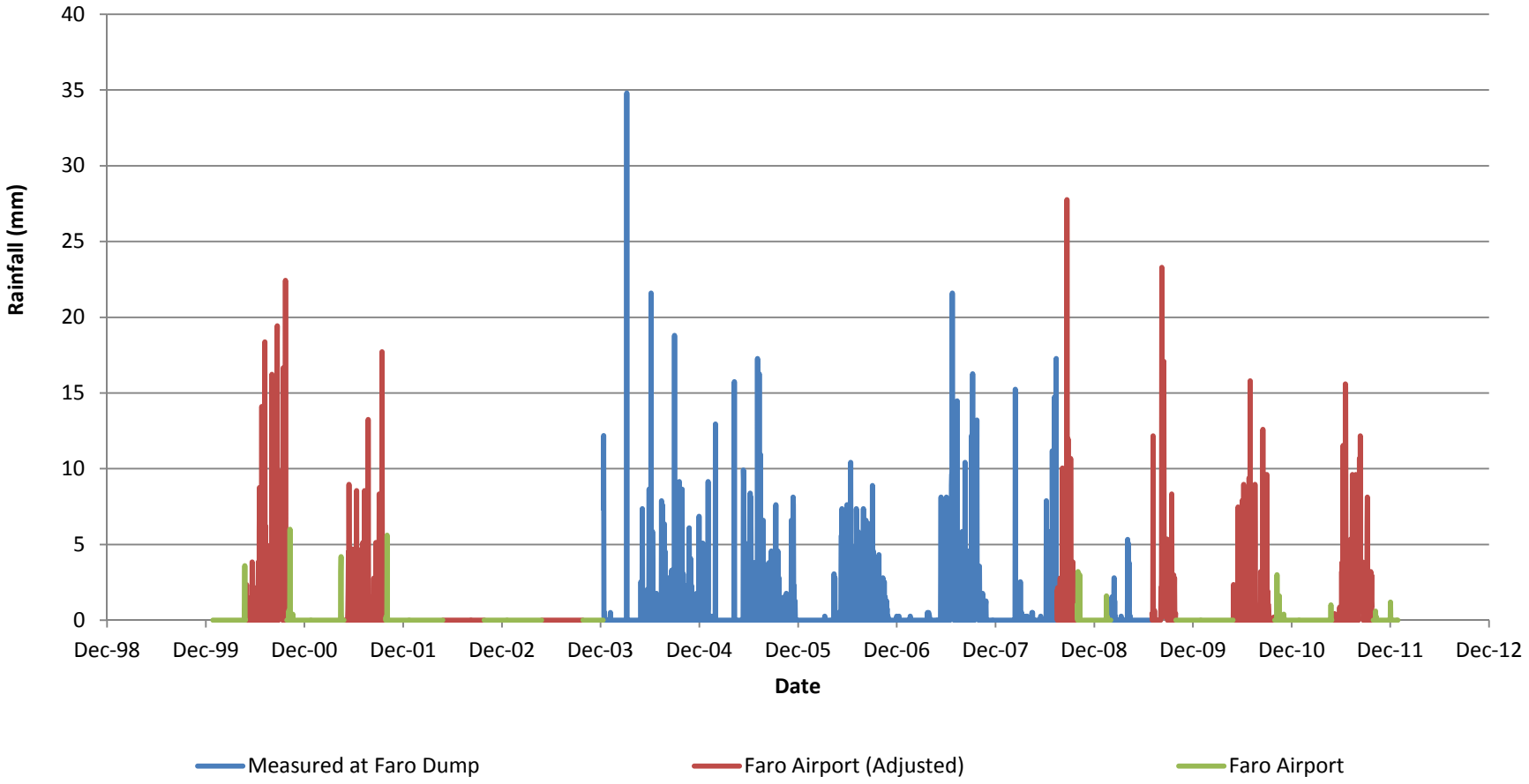

FIGURE 2-12
Faro Dump: Rainfall Record by Data Source
Faro Mine Remediation Project

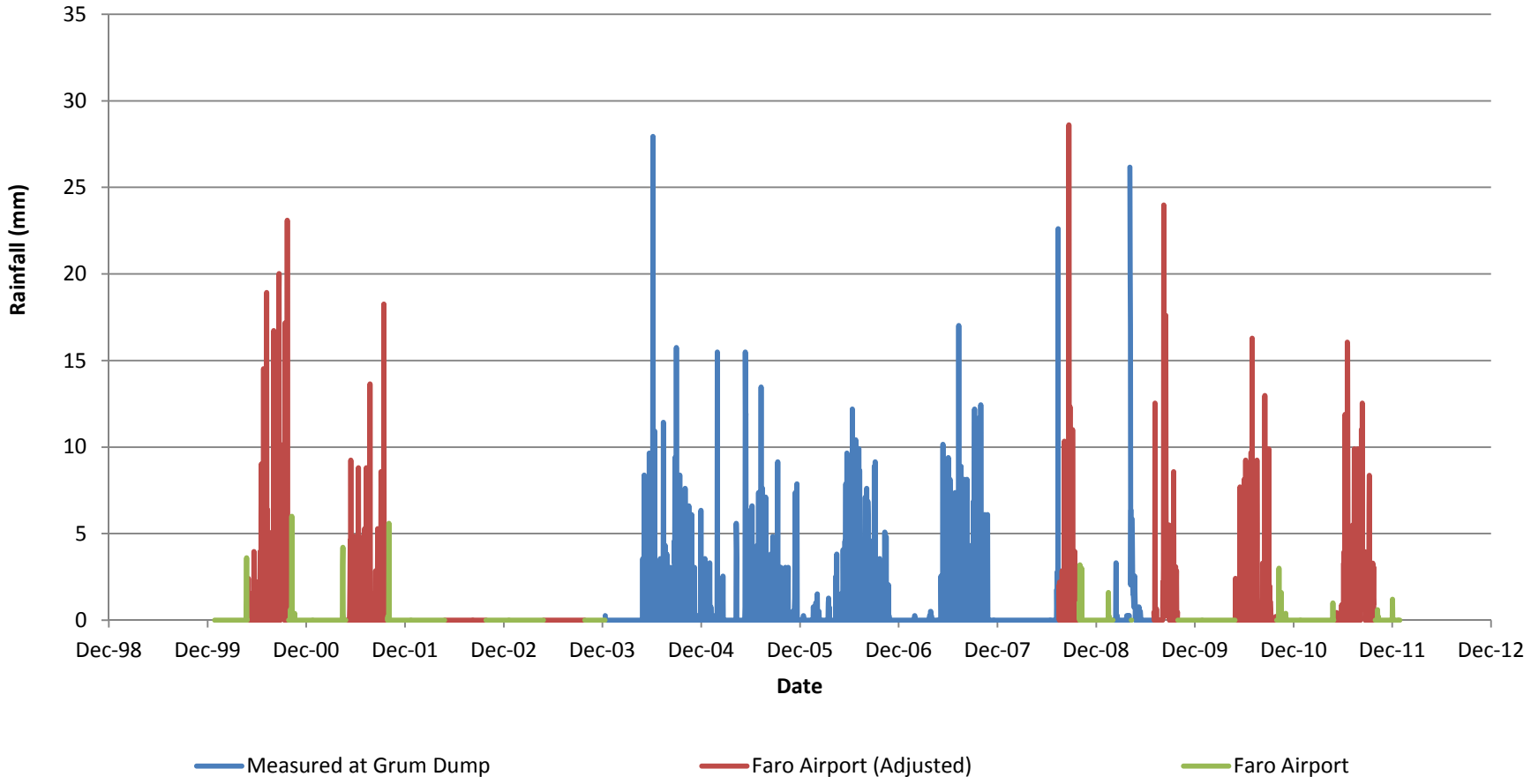

FIGURE 2-13
Grum Dump: Rainfall Record by Data Source
Faro Mine Remediation Project

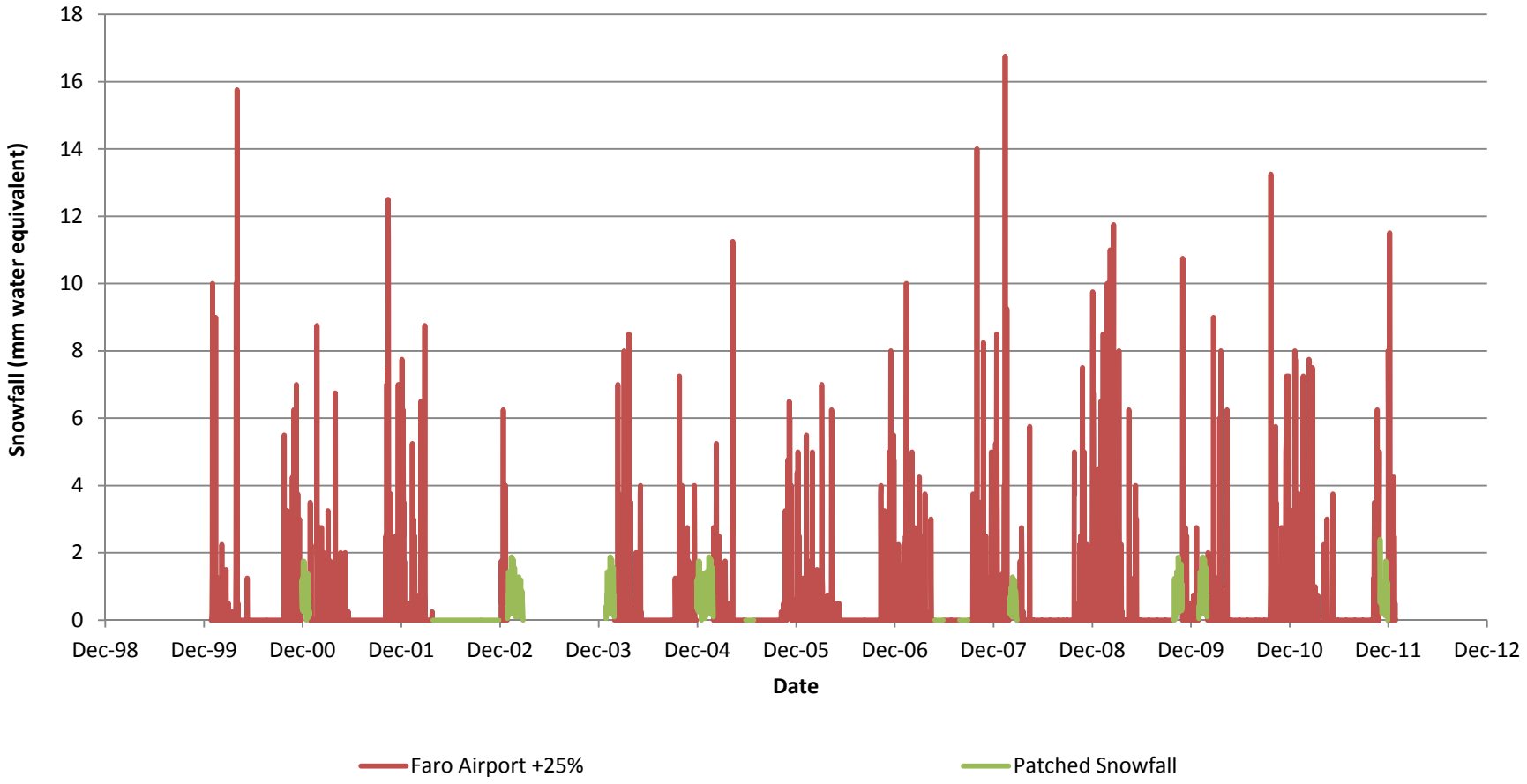

FIGURE 2-14
Faro Mine Complex Snowfall Estimate
Faro Mine Remediation Project

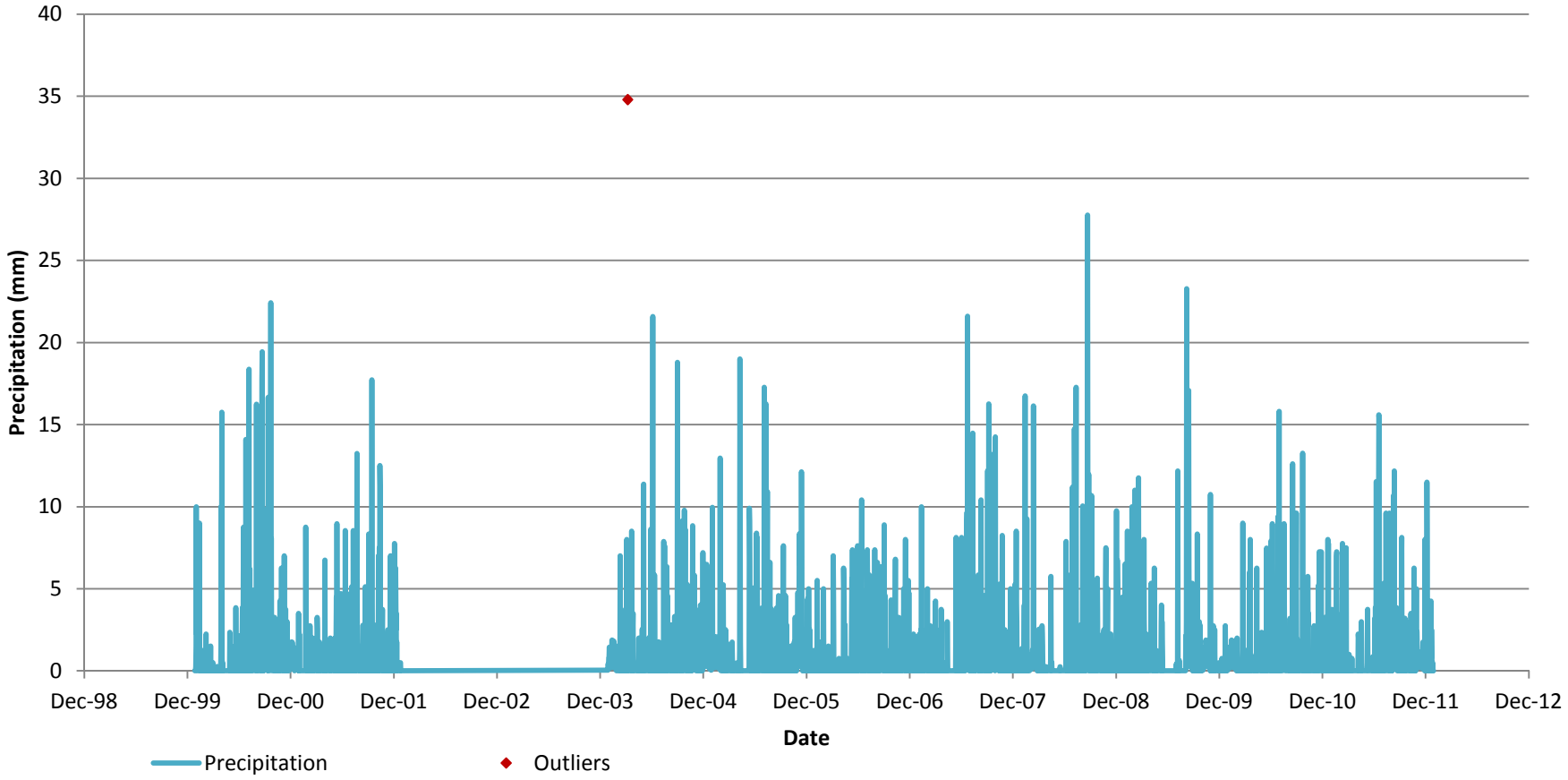

FIGURE 2-15
Faro Dump Area Daily Precipitation Estimate
Faro Mine Remediation Project

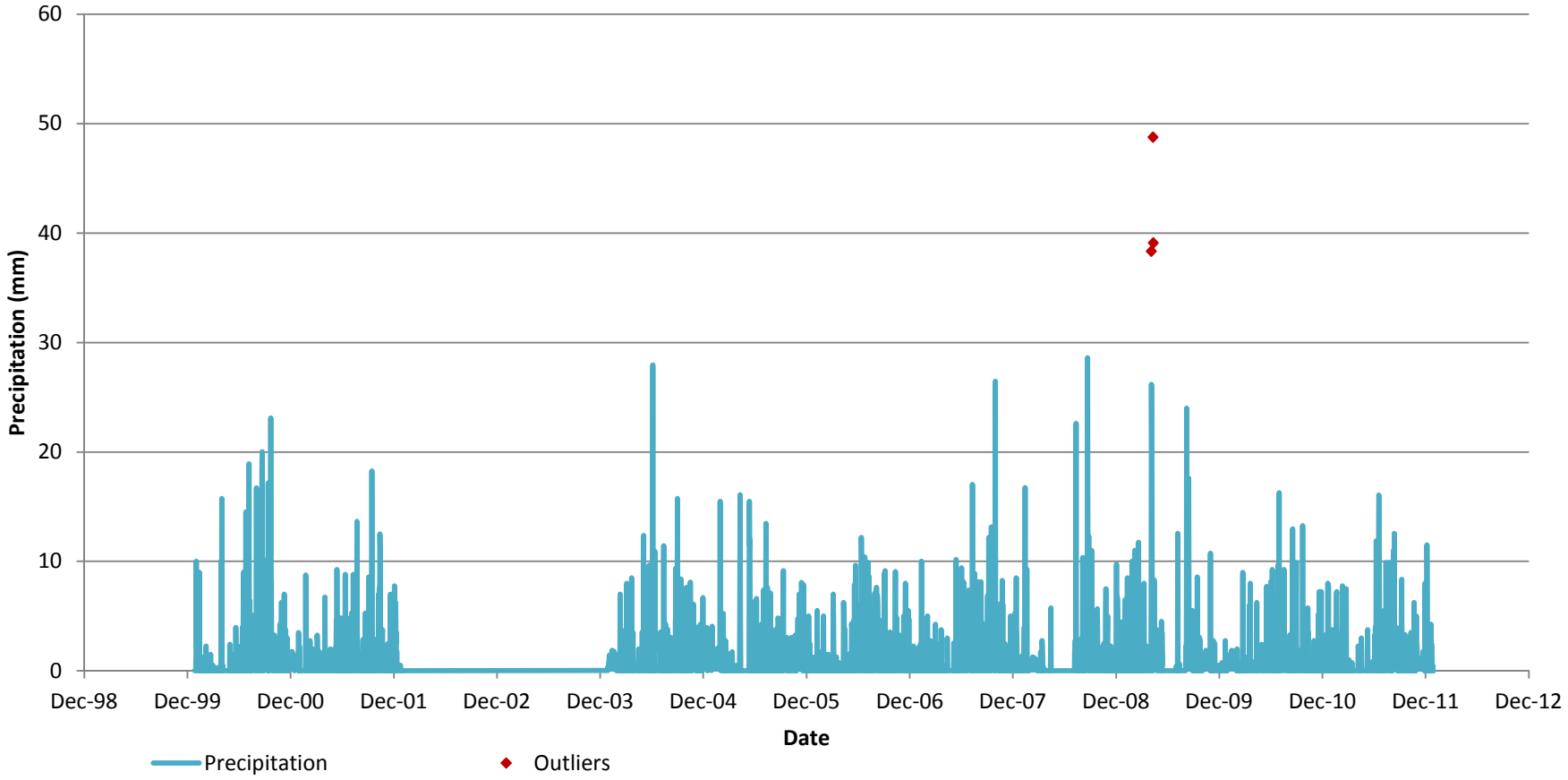

FIGURE 2-16
Grum Dump Area Daily Precipitation Estimate
Faro Mine Remediation Project

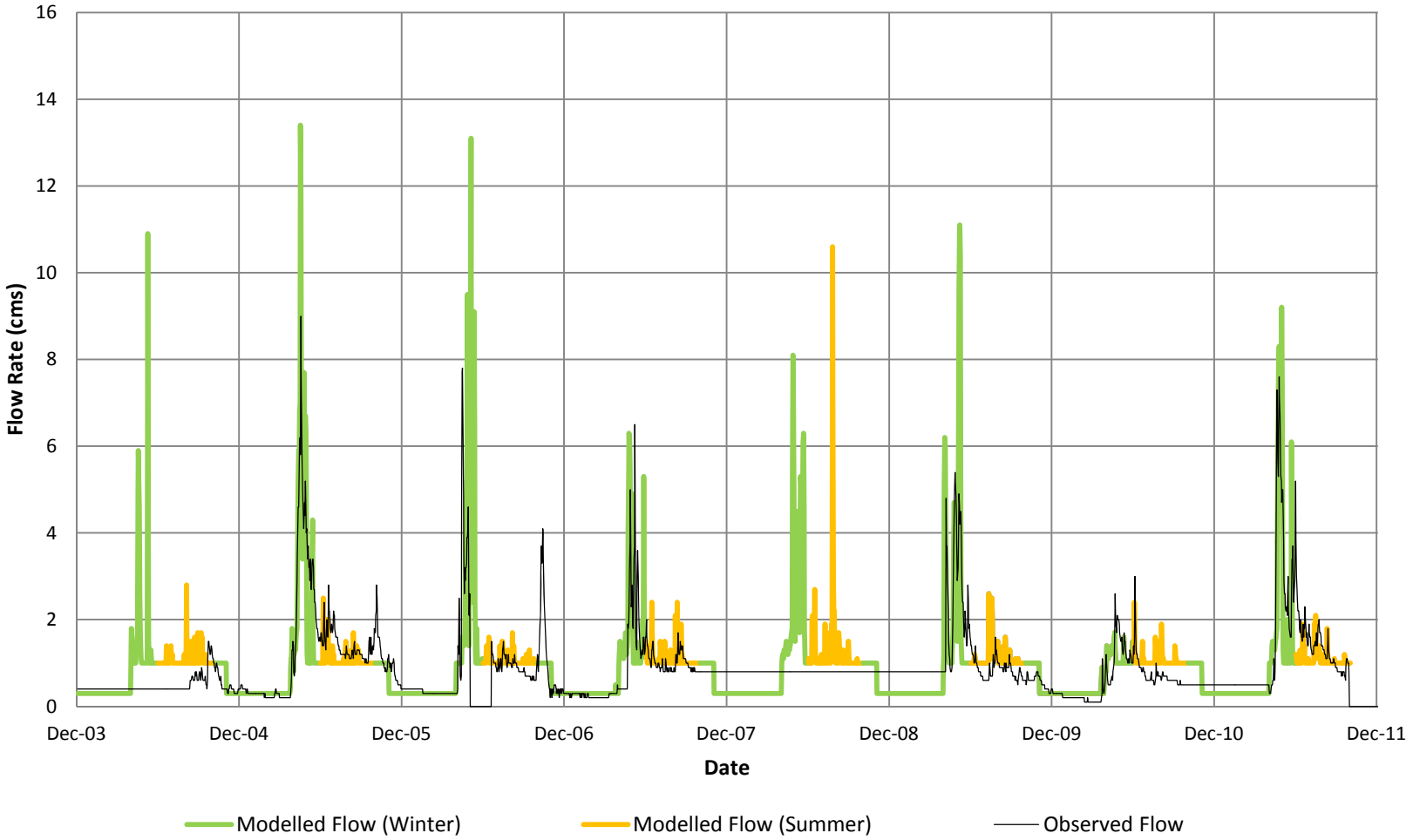

FIGURE 2-17
Modelled vs. Observed Flow at Station R7, 2004-2011
Faro Mine Remediation Project

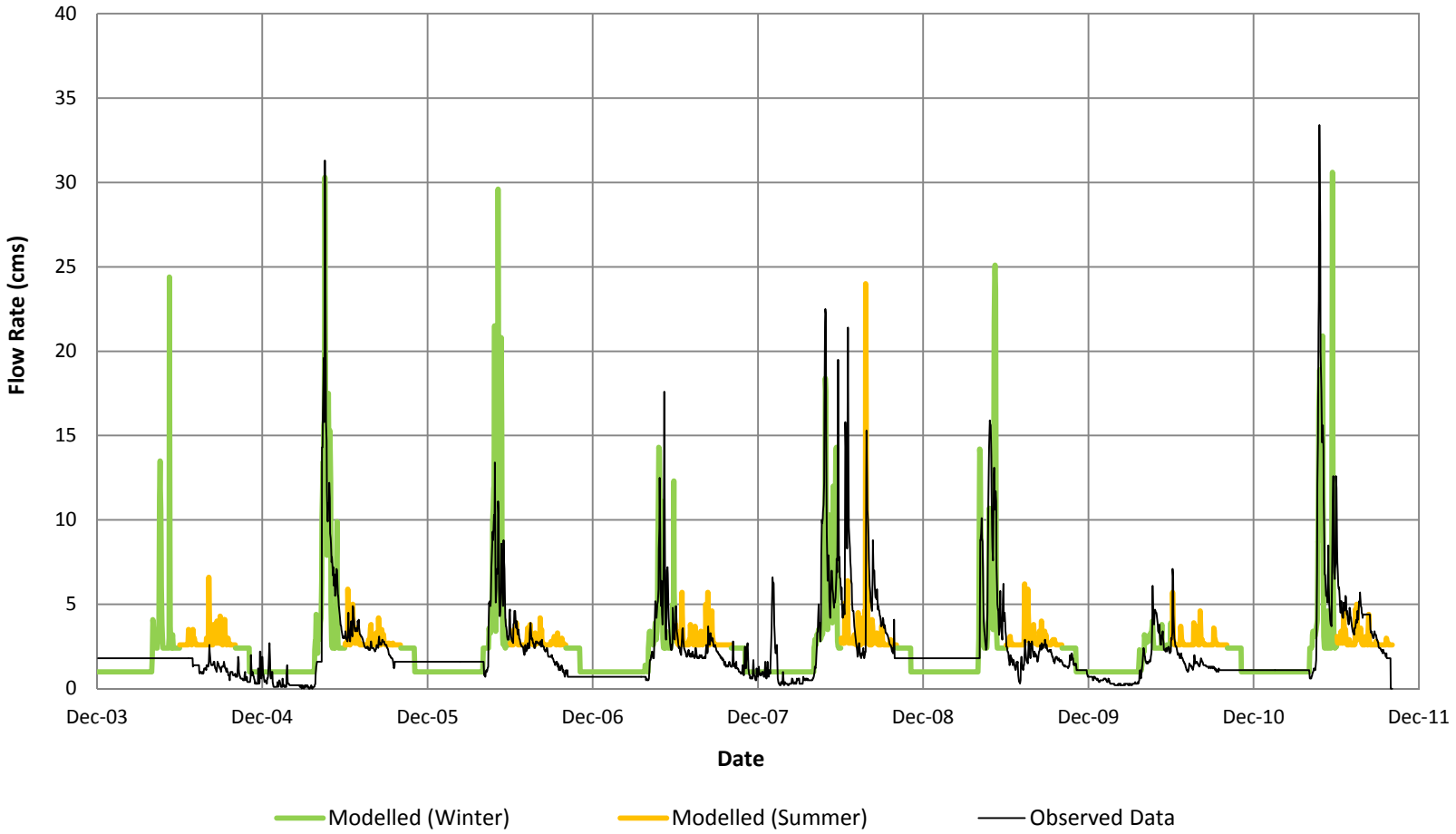

FIGURE 2-18
Modelled vs. Observed Flow at Station X14, 2004-2011
Faro Mine Remediation Project

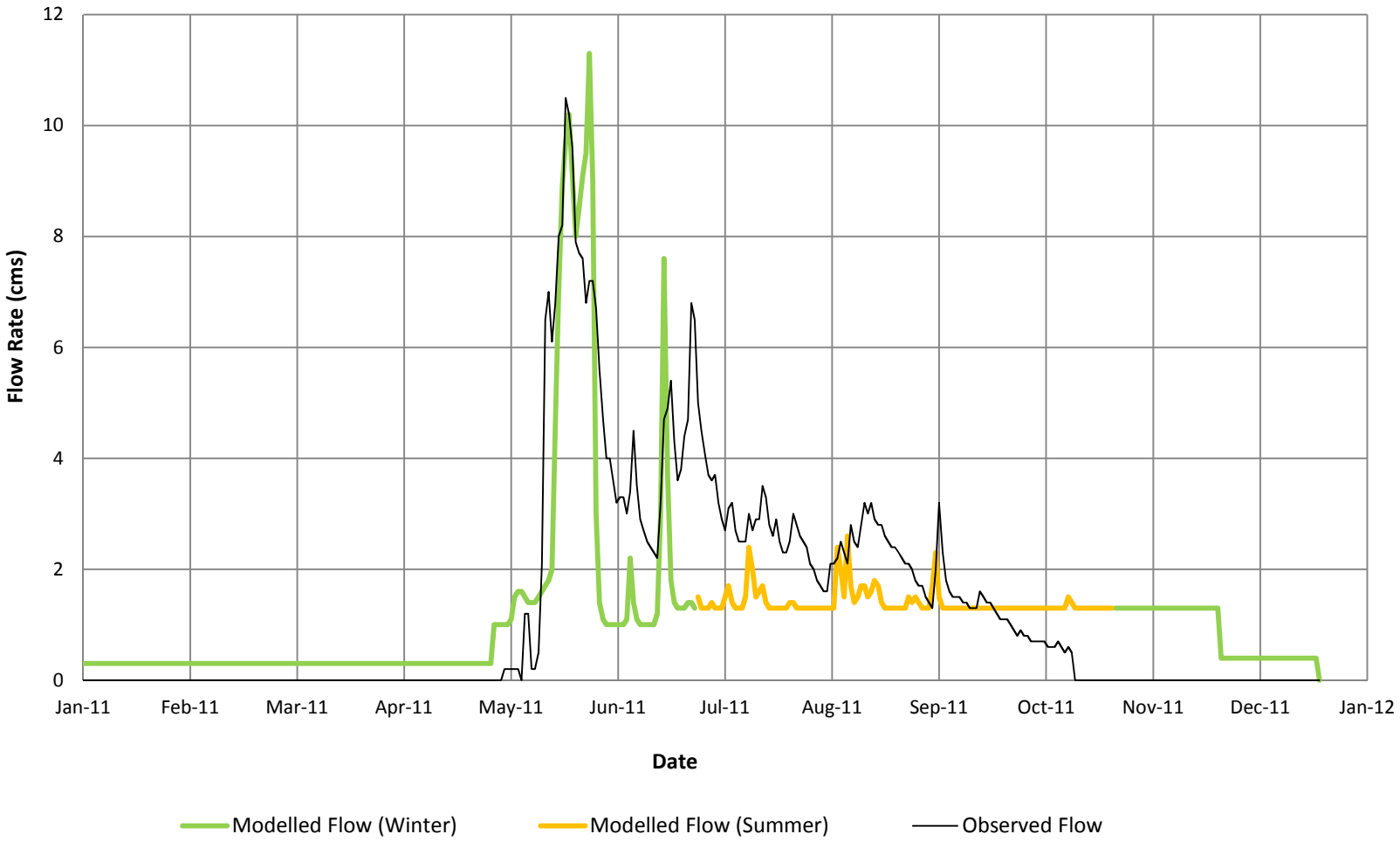

FIGURE 2-19
Modelled vs. Observed Flow at Station X2, 2011
Faro Mine Remediation Project

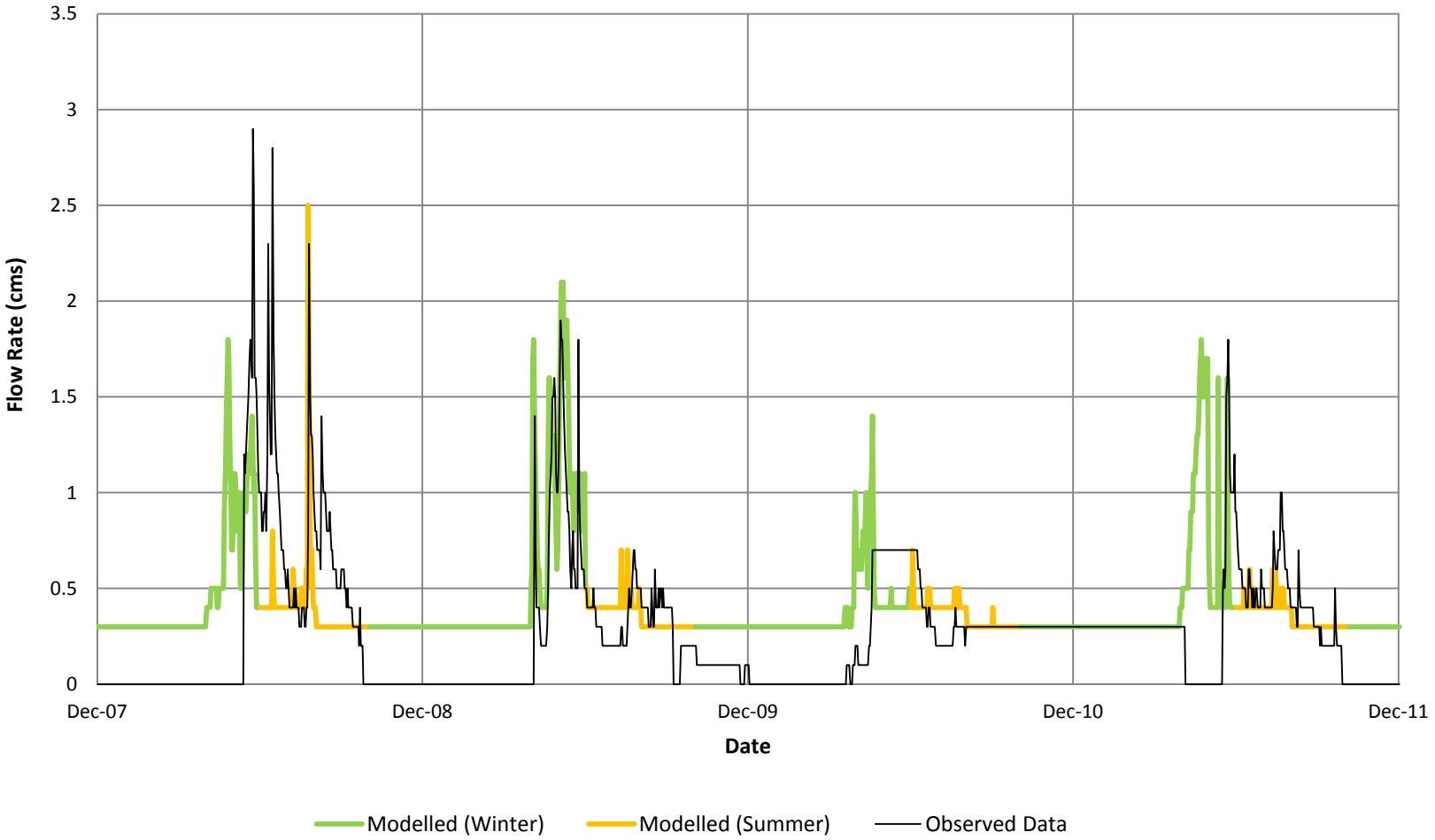

FIGURE 2-20
Modelled vs. Observed Flow at Station V1, 2008-2011
Faro Mine Remediation Project

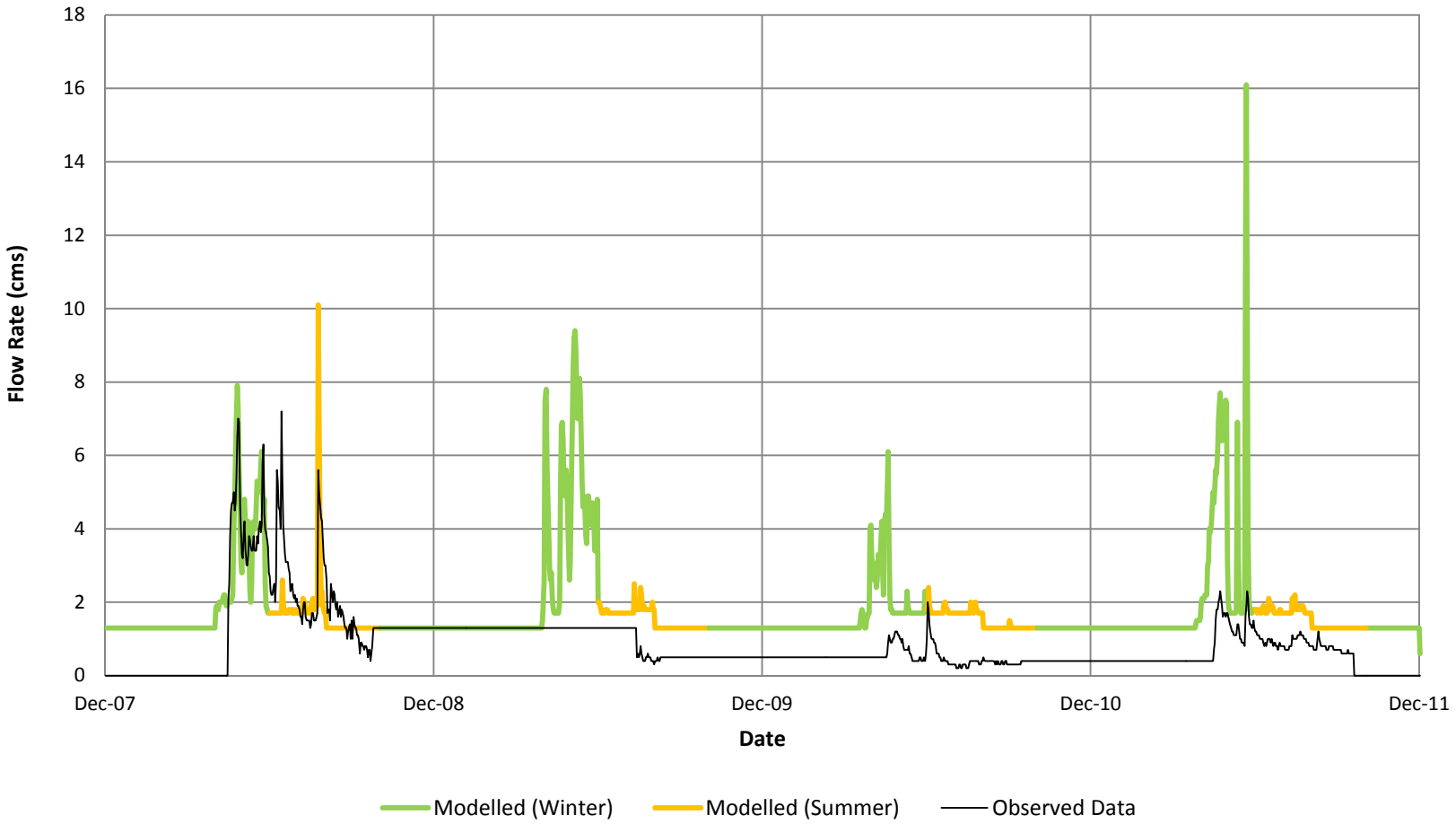

FIGURE 2-21
Modelled vs. Observed Flow at Station V8, 2008-2011
Faro Mine Remediation Project

SECTION 3

Groundwater Flow Modelling

This section describes the development, calibration, and application of GW flow models that are being used to support the FMRP.

3.1 Groundwater Flow Modelling Objectives

GW flow modelling is required to gain insight into subsurface flow processes and how these processes can be influenced to benefit the FMRP. The GW models use meteorological and hydrological data, along with drainage basin and aquifer characteristics, to compute GW flows and GW elevations (heads) throughout the modelled domain under assumed hydrogeological and operational conditions. Because it is anticipated that the GW flow models will evolve as knowledge of the FMC evolves and as FMRP needs change, the GW modelling objectives are divided into near-term and potential longer-term objectives.

3.1.1 Near-term Groundwater Flow Modelling Objectives

The near-term GW flow modelling objectives described herein are associated with the current modelling effort, which focuses on an approximately 262-square-kilometre (km^2) area of the Rose Creek drainage basin, as shown on Figure 3-1. A similar GW flow model will be developed to focus on a portion of the Vangorda Creek drainage basin during later stages of the FMRP; this will help inform decisions related to management of the Vangorda/Grum Area. The GW flow models described herein were designed as tools to help the project team anticipate and respond to hydrological system behaviour that may result from implementing proposed actions. Specifically, the near-term GW flow modelling objectives are as follows:

- Help inform the subsurface interception system (SIS) conceptual designs at the Zone 2 Outwash and CVD subareas and support potential modifications to the existing S-Wells system.
- Help test and inform the CSM components that are related to GW flow.
- Gain insight into the locations and nature of GW-SW interaction.
- Help inform the development of the subsurface reactive transport model of the Rose Creek Alluvial Aquifer (RCAA) beneath the RCTA (described further in Section 4.5).
- Reduce conceptual errors associated with how the GoldSim model handles GW flow and forecasts SIS effectiveness.
- Help inform the adaptive management plan (AMP) as it relates to anticipated GW flow conditions.

3.1.2 Potential Longer-term Groundwater Flow Modelling Objectives

To the extent the GW flow models are periodically updated and used, GW flow modelling could include the following longer-term objectives:

- Enhance the utility of the GW flow models by incorporating newly collected field data to further evaluate GW flow conditions of interest in support of the FMRP.
- Evaluate potential alternative designs and configurations of each SIS.
- Evaluate the performance of each SIS to assess the opportunity to enhance remedial effectiveness.
- Provide a basis for additional enhancements to the GoldSim model to improve its predictive capabilities by reducing uncertainties associated with GW flow conditions at locations of interest.
- Provide improved datasets for input into the GoldSim model, which will be used to support the preparation of the project proposal/*Yukon Environmental and Socio-economic Assessment Act* submittal.
- Help inform subsequent phases of the Faro WTP design, AMP, and other components of the FMRP, as needed.

3.2 Groundwater Modelling Approach

The overall approach to GW flow model development includes constructing, calibrating, and applying three-dimensional (3D), physically based, spatially distributed, steady-state numerical models. These models were developed in anticipation of needing to address a wide range of GW questions during the FMRP's implementation. As such, even though the more common GW questions asked of the FWMT tend to relate to existing and potential SIS locations, the domains of the GW flow models were built to facilitate the evaluation of GW conditions beyond just the local scale. With this in mind, the approach to establishing GW flow modelling domains included translating more regional geological and hydrological components of the CSM, in addition to the more local-scale CSM components, into the mathematical design of the numerical GW flow models. Establishing GW flow models that simulate larger portions of the GW flow system of the Rose Creek drainage basin is advantageous for the following reasons because the GW flow models:

- Avoid imposing closer lateral boundaries that would require the estimation of specified GW fluxes or heads.
- Provide a framework for examining a wider range of GW questions.
- Provide the opportunity to improve the overall utility of the models for the FMRP.

Ultimately, two separate models were developed under this effort. While both models share the same overall domain extent, the RCAA Subarea model provides enhanced resolution near the RCTA, whereas the NFRC Subarea model provides enhanced resolution in the NFRC drainage area. Both GW flow models were set up to compute cell-by-cell, steady-state GW inflows, outflows, and elevations (heads).

3.3 Groundwater Data Sources

A large amount of GW data has been collected at the FMC since the 1990s and has been summarized in several technical documents. The specific GW data required as model inputs for the Rose Creek GW models are summarized herein.

3.3.1 Topography

Present-day topography for the FMC was assembled from LiDAR data collected during October 2011 and provided by TerraRemote, whereas the topographic information for the outlying areas was obtained from 20-m digital elevation model (DEM) data obtained from YG, as shown on Figure 3-2. The LiDAR and DEM data were used to help establish the top elevation of the GW flow models. The pre-mining topography was derived from the 20-m DEM data and was used to develop lower layers in the GW flow models.

3.3.2 Bathymetry of Faro Pit and Bench Plan of Zone 2 Pit

The bathymetry of the Faro Pit and the benching plan of the Zone 2 Pit were used to develop boundary conditions, layering, and assignment of hydrogeologic properties in the GW flow models at appropriate pit locations and depths. The dataset for the Faro Pit was based on data collected by CH2M HILL during the 2012 field season for the Faro Pit (Laberge, 2012a, 2012b). The data set for the Zone 2 Pit was based on information obtained from RGC (1996).

3.3.3 Rose Creek Hydrographic Network

A hydrographic dataset was compiled to define the river boundaries for the GW models. Hydrographic mapping was developed using the LiDAR data and the 1:3600-scale stereo photography, acquired by Peregrine Aerial Surveyors Inc. and Eagle Mapping during August 2012 and prepared by Critigen Canada Corp., to gather 3D elevations of major flow lines and major body water edges (Critigen, 2013). Other hydrometric data were compiled using data from the 20-m DEM. Both datasets focused on the streams and pit lakes that are most relevant to the FMRP.

3.3.4 Geological and Hydrogeological Properties

Several geological and hydrogeological investigations have been conducted at the various sites within the RCAA and NFRC subareas. Surficial geological information (Bond, 1999), shown on Figure 3-3, was used to help delineate aquifer property zonation in the models. Geological information on the composition and layout of the various

bedrock types for the entire region near the Rose Creek drainage basin was obtained from Curragh Resources Inc. (1987) and Access Mining Consultants (1996). This information was used to assign particular types of bedrock zones to the GW flow models.

Hydrogeological information used in the GW modelling effort includes boring logs, geological cross sections, and aquifer testing results. Selected soil boring logs and geological cross sections were used to gain insight into the types (e.g., alluvium, till/overburden, tailings, waste rock, weathered bedrock, and indurated bedrock) and thicknesses of subsurface materials present at locations of interest. These assisted the FWMT to refine layer elevations and assign zones of hydraulic conductivity in the GW flow models. A focus was placed on identifying the bedrock topography and overburden isopachs, shown on Figures 3-4 and 3-5, respectively, that were established from well boring logs. Aquifer testing results provided the quantitative hydraulic information of the subsurface materials, which was the basis for the initial hydraulic conductivity values used in the GW flow models.

Pertinent hydrogeological information was obtained from the following reports:

- S-wells (SRK, 2006b, 2009a, 2010a)
- Zone 2 (SRK, 2007, 2009b, and 2011; BGC Engineering, Inc. [BCG], 2006)
- Emergency Tailings Area (ETA) (SRK, 2006a, 2006b, 2008; RGC, 2010)
- CVD/RCAA (Golder, 1973, 1975, 1979, 1980a, 1980b, 1980c, 1991; SRK, 1991; RGC 1996, 2006b)
- WRD wells installed in 2012 (CH2M HILL, 2013a)

3.3.5 Areal Groundwater Recharge

Groundwater recharge from precipitation (GW_{ppn}) is a primary input of water into the GW flow models. Initial values of GW_{ppn} were estimated using the average annual precipitation at the FMC (AECOM, 2009) using the methods described in Turner (1985).

3.3.6 Treatment System Water Flows

Pumping well and drain seepage flows were used to help define boundary conditions in the GW models and assess model calibration. Information about each SIS was obtained from the following reports:

- Zone 2 Pit (SRK, 2007, 2011; DES, 2011, 2012a)
- S-wells (SRK, 2009a, 2010b, 2011; BGC, 2006; RGC, 2012; DES, 2011, 2012a)
- ETA (RGC, 2010; DES, 2011, 2012a)

3.3.7 Surface Water Flows

SW flow information can be examined to assess changes in discharge along stream reaches, providing a flow calibration target along the modelled river reaches. Stream-flow data for the NFRC upstream from the Rock Drain (YG, 2012) were examined; however, no clear trends of stream gain or loss were identified that would allow comparison to the modelled stream reaches. Downstream from the Rock Drain, data presented in Laberge (2005a) suggest that the NFRC is a slightly losing reach. However, this observation is inconsistent with historical data, which suggest that GW contamination near the S-Wells system is impacting NFRC water quality. Additional information is necessary about both of these areas to better understand the relationship between the NFRC and the underlying aquifer. DES performed additional NFRC stream loading surveys in 2010 (DES, 2010a, 2010b). However, these data were not available to CH2M HILL in time for inclusion in this report.

3.3.8 Groundwater Levels

GW level data were obtained from the emLine database (DES, 2012b) and the Environmental Quality Information System (EQuIS) database currently being developed by CH2M HILL. These data were used to develop GW elevation targets for the calibration phase of the GW flow modeling effort. Further details on the use of these data are provided in Section 3.5.

3.4 Groundwater Model Construction

The numerical model design is the result of translating the CSM into a form suitable for numerical modelling. The Rose Creek GW flow models were developed following these steps:

1. Select numerical GW flow model code.
2. Establish a model domain and developing model grids.
3. Spatially distribute land surface elevation and subsurface hydraulic parameter values.
4. Establish boundary conditions for GW flow.
5. Select a time discretization approach appropriate for evaluating the field problem and fulfilling the near-term modeling objectives, as discussed in Section 3.1.1.

Sections 3.4.1 through 3.4.5 describe the methodology for executing these five design steps.

3.4.1 Groundwater Model Code Selection

The MODHMS Version 1 code (HydroGeoLogic, Inc. [HGL], 2011) was selected for the GW flow models in conjunction with Groundwater Vistas Version 6 (Environmental Simulations, Inc. [ESI], 2012), which was used as the pre- and post-processing graphical user interface. MODHMS is a physically based, spatially distributed numerical modeling code that includes several packages for simulating 3D groundwater flow and solute transport. MODHMS is an enhanced version of three numerical modeling codes: MODFLOW (McDonald and Harbaugh, 1988; Harbaugh et al., 2000; Hill et al., 2000; Harbaugh, 2005); MT3DMS (Zheng, 1990; Zheng and Wang, 1999; Zheng, 2010); and RT3D (Clement, 1997). The MODHMS code was selected for the following reasons:

- The near-term and potential longer-term modelling objectives require a code that can simulate drying and rewetting of subsurface zones to allow for evaluations of unsteady flow resulting from periodic and spatial wet and dry conditions. Further, the code must be able to simulate SW-GW interactions.
- MODHMS is the product of more than 15 years of development and is built on the United States Geological Survey (USGS) MODFLOW model. MODFLOW has been used extensively in GW evaluations worldwide for more than 20 years.
- MODHMS has been benchmarked and verified, meaning that the numerical solutions generated by the code have been compared with one or more analytical solutions, subjected to scientific review, and used on previous modelling projects. Verification of the code confirms that MODHMS can accurately solve the governing equations that constitute the mathematical model.
- CH2M HILL has experience applying MODHMS to assess complicated hydrogeological problems.
- MODHMS has the flexibility to incorporate additional features of the physical system should the FMRP require it in the future. For example, it can be set up to treat the hydrological system rigorously and mechanistically by mathematically representing surface and subsurface domains as one holistic system. When set up in this manner, it would not be necessary to presume stream stages or locations of losing or gaining portions of streams, or to manually link approximations of the SW and GW systems separately. Key processes that control the interaction of SW and GW can be inherently simulated as part of the numerical solution.

The MODHMS user's manual (HGL, 2011) contains additional information on the code.

3.4.2 Groundwater Model Domain

Space is continuous in the real world, but a numerical model must use discrete space to represent the hydrological system. The simplest way to discretize space is to subdivide the study area into many subregions (i.e., grid blocks) of the same size. If smaller grid blocks are necessary to avoid numerical instabilities, spacing these grid blocks uniformly across the entire modelling domain can lead to very long simulation run times. It is typically advantageous to use relatively small grid blocks only in key areas of the modelling domain where more resolution in the numerical solution is desired. Using larger grid blocks in areas of the modelling domain located away from the main areas of interest is a typical grid-building strategy, especially when the model domain represents a large geographic area. This strategy seeks to maximize the resolution of the numerical solution in

areas of interest within the modelling domain, while minimizing model run times. This grid-building strategy was implemented for this modelling effort and is described in the following subsections.

3.4.2.1 Areal Characteristics of Groundwater Flow Model Grids

The FWMT developed two GW flow model grids that each mathematically represents a 262-km² area encompassing a portion of the Rose Creek drainage basin. The locations of the lateral model domain boundaries shown on Figures 3-1, 3-6, and 3-7 were selected to coincide with natural hydrological features, such as watershed boundaries and streams, to help establish a regional hydrological framework around the subareas of interest. Figures 3-6 and 3-7 depict areal views of the grids, which are areally discretized into grid-block (i.e., cell) spacings ranging from 10 to 100 m. The finer cell spacings are located in two general subareas, as follows:

- **NFRC, Zone 2 Pit and Outwash, and S-Wells Subarea (NFRC Subarea).** This subarea is of interest because of elevated concentrations of constituents of interest between the Faro Pit and NFRC, north of the RCTA (Figure 3-6).
- **RCTA and CVD Subarea (RCAA Subarea).** This subarea is of interest because of the tailings situated upgradient from the CVD, which is considered the last line of defence for capturing contaminated GW before it migrates to downgradient receiving waters (Figure 3-7).

Cell spacings were refined in these particular subareas to make the models suitable for addressing the near-term modelling objectives. Cell spacings were refined in two separate model grids, as opposed to both subareas within one model grid, to avoid excessively long runtimes that would have resulted from having such refinements in one model grid.

3.4.2.2 Vertical Characteristics of Groundwater Flow Model Grids

The FWMT developed six vertically stacked model layers to provide a 3D representation of the subsurface system in the Rose Creek drainage basin, as shown on Figures 3-8 through 3-10. Table 3-1 summarizes the generalized definition of model layers in different portions of the domain. As Table 3-1 indicates, the model layers do not represent the same geological material throughout the domain; therefore, the model layers do not represent strict geological layers in all locations. Rather, the subsurface is vertically subdivided into six numerical layers that provide adequate vertical resolution for solving the governing GW flow equations.

Elevation datasets for the present-day and pre-mining land surfaces (Figure 3-2) and the top of the inferred weathered bedrock (Figure 3-4) were used to define the initial vertical characteristics of the model grids. The top of Model Layer 4 was modified in the vicinity of the former Zone 2 Pit using bench plan information (RGC, 1996) to represent the lower elevation of the excavated bedrock surface within the Zone 2 pit. Additional layers were then added between and below these layers by subtracting selected constant thicknesses from the overlying layer interfaces. Table 3-2 lists the minimum, maximum, and average thicknesses of the model layers over the whole domain and also just within the areas with refined cell spacings of 100 m^2.

TABLE 3-1
Generalized Groundwater Flow Model Layering
Faro Mine Remediation Project

Model Layer	Upland Areas	Midland Areas[a]	Lowland Areas[b]
1	Weathered Bedrock	Waste Rock/Overburden	Waste Rock/ Overburden/Tailings
2	Weathered Bedrock	Waste Rock/ Overburden/Weathered Bedrock	Overburden
3	Weathered/Indurated Bedrock	Waste Rock/ Overburden/Weathered Bedrock	Overburden
4	Indurated Bedrock	Weathered/Indurated Bedrock	Weathered Bedrock
5	Indurated Bedrock	Indurated Bedrock	Indurated Bedrock
6	Indurated Bedrock	Indurated Bedrock	Indurated Bedrock

[a] More indicative of the NFRC Subarea model.
[b] More indicative of the RCAA Subarea model.

TABLE 3-2
Minimum, Maximum, and Average Model Layer Thicknesses
Faro Mine Remediation Project

	NFRC Subarea		RCAA Subarea	
Model Layer	**Whole Model Domain (m)**	**Region of Refined Cells (m)**	**Whole Model Domain (m)**	**Region of Refined Cells (m)**
1	3 to 94 (8.0)	3 to 94 (16.4)	3 to 90 (4.4)	3 to 30 (7.5)
2	5 to 23 (5.4)	5 to 23 (5.5)	5 to 29 (6.9)	5 to 29 (13.3)
3	5 to 23 (5.4)	5 to 23 (5.5)	4 to 28 (6.8)	4 to 28 (12.5)
4	15 to 20 (15.5)	15 to 20 (16.6)	15 to 20 (15.0)	15 to 20 (15.0)
5	10 to 10 (10.0)	10 to 10 (10.0)	10 to 15 (10.0)	10 to 15 (10.0)
6	25 to 100 (99.5)	25 to 100 (98.4)	100 to 100 (100.0)	100 to 100 (100.0)

Notes:
Values represent the minimum to maximum layer thicknesses with the arithmetic mean listed in parentheses. Arithmetic means that appear equal to the minimum values indicate that localized adjustments to the layer thicknesses were made to either match monitoring well screens or pit excavations.
The region of refined cells corresponds to the 10×10 m cells depicted on Figures 3-6 and 3-7.

3.4.3 Groundwater Model Parameters

After the structure of a model grid is established, cell-by-cell parameter values must be distributed throughout the GW flow model domain. The steady-state GW flow models described herein require cell-by-cell horizontal and vertical hydraulic conductivity (K_h and K_v respectively) input values. These cell-by-cell K_h and K_v values are grouped into zones (K zones) that represent distinct hydrogeological materials and provide a method for assigning the K_h and K_v values throughout the models. The method used to assign model cells to a particular K zone involved first assigning generalized material properties to the various layers of the model based on general surficial geology (Figure 3-3) and a generalized bedrock type based on Access Mining Consultants (1996). After refining the 100-m grid cells down to 10 m, the K zones inside the refined areas were modified to more accurately represent K zones on the finer scale and "smooth out" the coarser-scale zone boundaries from the larger-scale model. These K zones were examined layer by layer and in cross section to confirm that the zone boundaries coincided with the proper materials and elevations. The K zones were further refined by examining site-specific features, cross sections, and refinements made during the calibration process, as discussed in Section 3.5.

Data resulting from slug, packer, and aquifer tests and professional judgment formed the basis for the initial K_h and K_v values in the GW flow models, before calibration. The initial K_h values used in the models varied by site and subarea. In the RCAA Subarea model, the prevalence of deep alluvium and mine tailings warranted different values than in the NFRC Subarea model where waste rock, thin alluvium, and weathered bedrock are the dominant material types. In the NFRC Subarea model, the initial K_h values in the region of refined cells ranged from approximately 1 to 130 metres per day (m/day) in the alluvial zones (SRK, 2006a, 2007, 2009a), 0.5 to 15 m/day in the overburden zones (waste rock and till) (SRK, 2006a, 2009a), and from $1x10^{-4}$ to 5 m/day in the less permeable zones representing weathered and indurated bedrock (SRK, 2006a, 2009a; RGC, 2012).

In the RCAA Subarea model, the initial K_h values in the region of refined cells ranged from approximately 0.1 to 50 m/day in the alluvial zones (RGC, 2006a), 0.01 to 3.0 m/day in the overburden zones (till and tailings), and from $1x10^{-4}$ to 1 m/day in the less-permeable zones representing weathered and indurated bedrock (SRK, 2009a). In both subarea models, the K_v values were initially assigned according to an assumed K_h:K_v (i.e., vertical anisotropy) ratio of 10:1 for each model layer. Thus, K_v was initially parameterized on a cell-by-cell basis by dividing each K_h value by a value of 10. Section 3.5 describes how these values were modified during the calibration process.

3.4.4 Groundwater Model Boundary Conditions

Boundary conditions for GW flow models are mathematical statements (i.e., rules) that specify head or GW flux at particular locations within the model domain. The following four types of boundary conditions were used to develop the GW flow models:

- **Specified Head:** Head is specified.
- **Specified Flux:** Volumetric GW flux is specified.
- **Head-dependent Flux:** GW fluxes are internally computed according to the difference between the boundary head and the head being computed for that cell and multiplied by a conductance term (if applicable, depending on the type of head-dependent flux boundary)
- **No-flow:** GW can flow parallel to the boundary but not across it

Figures 3-11 and 3-12 and Table 3-3 summarize the boundary conditions used with the GW flow models.

TABLE 3-3
Summary of Boundary Conditions
Faro Mine Remediation Project

Hydrologic Process	Specified-head Boundary	Specified-flux Boundary	Head-dependent Flux Boundary
GW Recharge from Precipitation		X	X
CVD Toe Drain			X
GW-SW Interaction	X		X
GW Pumping		X	X
GW Discharge to Land Surface			X
Subsurface Outflow Beneath Rose Creek			X

Notes:
No-flow boundaries coincide with the active lateral boundaries of the domain in all model layers and with the bottom of Model Layer 6, with the exception of the head-dependent flux boundary assigned at the exit cells beneath Rose Creek.
Figures 3-11 and 3-12 present a graphical depiction of these boundary conditions.

3.4.4.1 Specified Head

Heads were specified in the Faro Pit, the pond above the Rock Drain on the NFRC, the Intermediate Pond, and the Polishing Pond. A specified head of 1,141 m above the Canadian Geodetic Vertical Datum of 1928 (CGVD28) was assigned in Model Layer 1 cells that represent the Faro Pit Lake. A specified head of 1,098 m CGVD28 was assigned in Model Layer 1 cells that represent the pond above the Rock Drain. These specified heads are based on the results of a hydrometric survey (Critigen, 2013).

Specified heads of 1,028 m and 1,046 m were assigned to the Polishing Pond and Intermediate Pond, respectively. These values represent approximate average stages computed from pond elevation data collected from 2004 through early 2012.

3.4.4.2 Specified Fluxes

Specified flux boundaries add or remove a specified volumetric flow to or from a model cell. Specified fluxes were used to define GW_{ppn} and water pumped from wells.

An areal GW recharge term is applied to Model Layer 1 that represents GW_{ppn}. An initial GW_{ppn} rate of 23 millimetres per year (mm/yr) was initially assigned areally across the entire model domain based on the methods described in Turner (1985). This magnitude of GW_{ppn} represents approximately 6 percent of the 2003 through 2008 annual average precipitation rate of 366 mm/yr (AECOM, 2009). The GW recharge term was adjusted during the calibration process, as described in Section 3.5. In the upland areas where weathered bedrock is exposed, the amount of GW_{ppn} is less certain because no infiltration data are available for these areas. For this

reason, the recharge seepage face boundary was used in the higher elevations in the model. The recharge seepage face boundary is an extension of the typical MODFLOW recharge package with the added capability of removing GW if the water table rises above land surface. In other words, the models were set up to simulate rejected GW recharge in the higher elevations to avoid having ponded GW levels at those locations and avoid overestimating GW_{ppn}.

Water is currently pumped from three wells in the model domain: well CH12-Z2-PW001 in the buried Zone 2 Pit and wells SRK08-SPW2 and SRK08-SPW3 in the S-Wells SIS, and each is represented by a specified flux boundary condition. A fourth specified flux boundary was added, representing the forced upwelling and sump configuration currently operating at the ETA. Even though the water leaving the ETA is not from an extraction well per se, the quantity of water leaving the aquifer is known because of the sump discharge records, and is therefore simulated as a well (specified flux). Pumping rates were taken from the previous studies referenced in Section 3.3.6.

The specified fluxes from pumping were simulated using the fracture well (FWL) package of MODHMS (HGL, 2011), which has added capabilities over the standard MODFLOW Well package. The FWL package withdraws the user-specified flux if the modelled aquifer system can support the specified extraction rates. However, if the modelled aquifer cannot support the pumping (when modelled GW levels approach a specified pumping water level), the FWL package reduces the pumping based on the surrounding head and K_h and K_v in the aquifer. This functionality makes the FWL boundary include elements of both a specified flux and a head-dependent flux boundary condition.

Because the GW flow models described herein are steady-state models reflecting average hydrologic conditions, the pumping associated with the Faro Pit Lake and Intermediate Pond is not actively simulated. The SW-GW interaction associated with the Faro Pit and Intermediate Pond is governed by the difference between the assigned average stages in these SW bodies (which do not change in the simulations) and the modelled heads in the underlying aquifer (Model Layer 1) and the hydraulic conductivity of the bottom sediments of these SW bodies. Thus, the modelled subsurface outflow from these SW bodies also reflects average conditions.

3.4.4.3 Head-dependent Flux

Streams and general head boundaries (GHB) are the two types of traditional head-dependant flux boundary conditions used in the model. Streams and selected surface water features of interest were assigned as river boundaries and represent the predominant type of head-dependent flux boundary used in the GW flow models. This boundary type was assigned with the assistance of a LiDAR-based, 3D hydrographic dataset that provides a 3D representation of streams and surface water bodies within the mine-impacted area of the Rose Creek drainage basin.

The river package requires input of stream stage and conductance (computed from streambed length, width, thickness, and hydraulic conductivity) that specifies the resistance to water exchange between the stream and modelled GW system. The 3D hydrometric dataset was converted into a polyline ESRI Shapefile, which was later translated to the GW flow model grids. The stream polyline ESRI Shapefile contains attribute fields of the conductance term components, as well as the river stage at the upstream and downstream ends of each polyline. Other attributes include an assumed river bottom approximately 1 m below the river stage and initial assumed K_v of 0.086 m/day (1×10^{-4} cm/sec), consistent with silty sand (Freeze and Cherry, 1979). Groundwater Vistas was used to linearly interpolate the stream polyline endpoint information to Model Layer 1 of each model grid. This step translated most of the stream information to the model grids; however, some of the boundaries required manual adjustments to maintain consistency between the two subarea model grids. Other modifications were subsequently made to this boundary in the refined areas of each subarea model during the calibration process discussed in Section 3.5.

A GHB was assigned at the lateral exit boundary in Model Layers 1 through 6 at the downstream end of the RCAA. The GHB was designed to allow GW flow out of the model domain based on a continuation of the average stream and GW gradient downstream from the CVD to the edge of the model domain (approximately 0.005 m/m). GHB boundaries include a conductance term (computed as the product of cell area and hydraulic conductivity divided by the GHB distance) used in conjunction with hydraulic gradients to control the flow of GW into or out of the

boundary. The stage of Rose Creek is estimated at about 1,003 m near the downgradient edge of the model, and the head of the GHB was set to 998 m at a distance of 1,000 m (representing a gradient of 0.005 metres per metre [m/m]). The hydraulic conductivity of the GHB boundary varied by layer in accordance with estimated values within each layer (i.e., 30 m/day in alluvium and 0.01 m/day in weathered bedrock).

3.4.4.4 No Flow

The lateral model boundaries depicted on Figures 3-11 and 3-12 that are not simulated as specified-head, specified-flux, or head-dependent flux boundaries are simulated as no-flow boundaries. The bottom of the deepest model layer (i.e., Model Layer 6) is also assigned as a no-flow boundary.

Inherent with the assignment of no-flow boundaries at these locations is the assumption that these boundaries coincide with locations of GW divides. The no-flow assumption for the lower model layers might not be valid at all locations along the lateral boundaries. However, these lateral model boundaries were purposely located far enough from the subareas of interest to avoid adverse boundary effects that could result from conceptualization errors along the margin of the GW flow modelling domain.

3.4.5 Groundwater Model Time Discretization

Time is continuous in the physical system, but a numerical model must describe the field problem at discrete time intervals. The GW flow models were set up to simulate steady-state flow conditions. As such, the hydraulics associated with the modelled GW flow system do not change over time. As discussed in Section 3.5.2, the averaging period for the steady-state GW flow models, 1998 through 2012, was selected on the basis of available FMC GW elevation data.

3.5 Groundwater Model Calibration

Model calibration is a process of tuning a numerical model to simulate observed subsurface flow conditions in the field (as described with measured data) to within a reasonable degree of accuracy. This section discusses the calibration approach, targets, process, and results.

3.5.1 Groundwater Model Calibration Approach

As previously discussed, finer cell spacings are located in two separate subareas of the GW flow modelling domain: the NFRC and RCAA subareas, shown on Figures 3-6 and 3-7. Because these individual models are focused in different subareas with different types of field data against which to calibrate, the model calibration approach was tailored to each subarea model.

The FWMT implemented a calibration approach that included a combination of manual and autocalibration techniques to achieve sufficient, effective calibration. This approach consisted of three general phases. The first phase included initial model setup, defining locations with field-derived parameter values, and establishing approximate parameter fields, which resulted in a reasonably close match to both quantitative and qualitative targets, as discussed in Section 3.5.2. The second phase implemented autocalibration techniques using numerical optimization software to obtain the best fit to the calibration targets. The third phase involved interpreting the autocalibration results with respect to the quantitative and qualitative calibration targets and further constraining parameter values to either maintain consistency with or refine the CSM.

Because the modelling effort included the development of two different GW flow models with cell refinements in different portions of the domain, the two models were calibrated simultaneously with the goal of maintaining as much consistency between the models as practical. The primary calibration parameters included the K_h and K_v, the GW_{ppn} rate, and stream and lake/pond bed permeabilities.

3.5.2 Groundwater Model Calibration Targets

Calibration targets are defined as the selected field-measured values that quantify site conditions of interest with consideration to data quality and reliability. Qualitative and quantitative calibration targets were selected to evaluate the progress of calibration during the GW flow model development.

Measured heads, averaged over the period of record for each of the selected site monitoring wells (from 1998 to 2012), served as quantitative calibration targets. These data were examined during the target selection process to assess whether temporal biases or anomalous data existed. Head targets at the S-Wells area were only averaged from 2009 and, later, to account for the operation of the S-Wells SIS that began pumping early in 2009. Figure 3-13 depicts the locations of the calibration target wells selected for this effort for each subarea GW flow model. The qualitative calibration targets include average vertical head differences at locations of vertical well pairs, time-series drawdowns in the RCAA Subarea measured during aquifer testing at the CVD in 2012, general GW flow patterns, and observed discharges of groundwater to drains. Calibration summary statistics were computed to provide a measure of each model's ability to replicate the quantitative calibration-target head values. Head calibration was evaluated using the following summary statistics:

- Residual error, computed as the modelled head value minus the target head value.
- Mean error (ME), computed as the sum of all residual errors divided by the number of observations.
- Coefficient of determination (R^2), computed as the square of the correlation coefficient.
- Root mean squared error (RMSE), computed as the square root of the mean of all residual squared errors.
- RMSE divided by the range of target head values (RMSE/range).

During the quantitative calibration, the FWMT implemented the following goals:

- Minimize spatial bias of residual errors in key areas of the domain.
- Minimize residual error, ME, RMSE, and RMSE/range values.
- Maintain R^2 values as close to unity as possible.

3.5.3 Groundwater Model Calibration Process

The following sections provide an overview of the calibration process implemented for each of the GW flow models.

3.5.3.1 NFRC Subarea Model

The first stage of model calibration used the initial model configuration and parameter values of the NFRC Subarea model to assess initial quantitative and qualitative calibration before making any changes. This step provided a benchmark against which improvements to model calibration could be compared. Then, the configuration of K zone and recharge zone boundaries were further adjusted, as appropriate, in the refined grid area to improve model performance relative to calibration targets. Minor adjustments were made to the K zone values, recharge zone values, and river boundary configurations to improve this initial calibration.

The next stage involved adding new K zones, as necessary, to give the model more flexibility in routing GW and better matching calibration targets. Fourteen additional K zones specific to the NFRC Subarea were added to the model to achieve this flexibility:

- Six zones representing the lowland /alluvial valley of NFRC (one each in the three uppermost model layers upstream and downstream from the Rock Drain)
- Two zones representing glacial till east and west of NFRC
- One zone representing buried alluvium/colluvium in Model Layers 2 and 3 upgradient from the S-Wells
- One zone representing the east portion of the WRDs
- One zone representing buried waste rock in the Zone 2 Pit
- One zone representing the shallow rock-filled collector trench at the S-Wells
- One zone representing the Rock Drain in a portion of the Haul Road
- One zone representing weathered bedrock beneath NFRC in Model Layer 4

The new K zone values were then manually adjusted to better fit calibration targets. The additional number of parameter zones made tracking progress more time-consuming. It was at this stage of calibration that PEST

autocalibration software was employed (Doherty, 2004, 2010). PEST software objectively and routinely reduces the difference between measured field values and the corresponding quantitative calibration targets through an iterative approach. Qualitative targets were not included in PEST autocalibration. When using a property zone approach, PEST can modify the parameter values (K and recharge) but not the configuration of these property zones. As such, PEST can only operate within the structure and flexibility of the model it is given.

PEST effectively reduced the residual errors of the modelled heads; however, PEST software lacks professional judgement and the resulting parameter values typically require a thorough review of the results. Thus, the final stage of the NFRC Subarea model calibration involved further modifying the PEST-derived parameters so that optimized parameter values were within reasonable limits, K_h:K_v ratios were sensible, and the GW balance information was reasonable.

3.5.3.2 RCAA Subarea Model

The first stages of the RCAA Subarea model calibration were similar to those of the NFRC Subarea model. However, the RCAA modelling effort replicated aquifer testing conducted in the CVD Area in 2012, as well as autocalibration. The 2012 aquifer testing effort spanned from September 28, 2012 to October 7, 2012 and is summarized in the *CVD Interception System Investigation Data Technical Memorandum* (CH2M HILL, 2013b). A separate transient RCAA model was developed to calibrate the model to the aquifer test drawdown data. The details of model setup and calibration drawdown curves are provided in Appendix B.

Calibrating to steady-state heads and the aquifer tests was an iterative process: results from one model were incorporated into the other until satisfactory calibration to both steady-state heads and aquifer test drawdown was achieved. Calibration to the aquifer test data resulted in relatively small-scale hydraulic conductivity zone changes near the CVD, whereas calibration to steady-state heads involved evaluation of the entire RCAA Subarea.

The RCAA Subarea model was also qualitatively calibrated to vertical hydraulic gradients observed during the 2012 potentiomanometer field study (CH2M HILL, in preparation). The intent was to match the direction of flow between SW and GW (or the gradient direction) but not the magnitude of the gradient because the model grid spacing is not appropriate for such a comparison. In the fall of 2012, vertical hydraulic gradients were measured at 16 locations in Rose Creek downgradient from the CVD, the X13 drainage channel and the lower portion of the North Diversion Channel. The direction of GW flow was consistently measured to be upward (gaining SW bodies) with the exception of the southwest-flowing reach of Rose Creek just downstream from X14 and the end of the armored section of the North Diversion Channel (as it flows into native valley bottom sediments and starts to run parallel to the X13 ditch). At these locations the direction of the vertical hydraulic gradient was downward. The calibrated model matches the direction of the vertical hydraulic gradient at all observed locations.

3.5.3.3 Subarea Model Reconciliation

Following calibration of the NFRC and RCAA Subarea models, parameters were reconciled so that the parameter zone configurations and values were in agreement between both models to the extent practical. Discrepancies in the final heads and GW balances between the two models were inevitable, given the variations in cell resolutions, particularly where boundary conditions are assigned within the areas of grid refinement. GW balances for these models are presented in Section 3.5.4.3.

3.5.4 Groundwater Model Calibration Results

3.5.4.1 Parameter Values

Figure 3-14 presents the calibrated distributions of K_h for each model layer and subarea model. Calibrated K_h values range from 1×10^{-4} to 95 m/day (1.2×10^{-7} to 0.1 cm/sec) with one higher value specified for the S-Wells collector trench (500 m/day or 0.6 cm/sec). The high K_h assumed for the S-Wells collector trench reflects typical hydraulic conductivity values for designed fill materials that tend to be coarse-grained and well-sorted. K_h values assigned for the WRDs—including the main rock dumps, the Haul Road and Rock Drain, and Zone 2 backfill materials—ranged from 1 m/day to 85 m/day ($1.2x10^{-3}$ to 0.1 cm/sec).

Table 3-4 compares K_h estimates derived from aquifer tests conducted at various locations throughout the FMC. The relatively low values of the modelled K_h for weathered bedrock are likely representative for a large portion of

the modelled areas; however, there may be localized areas of higher permeability, depending on the degree of weathering. For example, in the S-Wells area, the K_h value estimated at SRK08-SPW1 is higher than that arrived at by calibration, suggesting that the weathered bedrock could be more permeable at this location than is assumed in the model. However, caution must be exercised when comparing estimated and modelled values because the simplifying assumptions associated with analytical and numerical methods are not consistent. Numerical models have fewer restrictive simplifying assumptions than the analytical equations used to estimate aquifer properties from field data. Future modelling efforts associated with the S-Wells area would benefit from additional data collection regarding the distribution of higher-permeability weathered bedrock beneath the FMC.

TABLE 3-4
Estimated and Modelled Hydraulic Conductivity
Faro Mine Remediation Project

Location	Site	Material Type	Estimated K_h (m/day)	Modelled K_h (m/day)	Screen Interval (mbgs)
BH4	Zone 2[a]	Alluvium/Till	40 to 100	85	0 to 2.5
BH6	Zone 2[a]	Alluvium	100 to 130	30	4.3 to 5.9
P05-04	Zone 2[a]	Alluvium	50 to 60	30	2.2 to 6.4
PW3	Zone 2[a]	Alluvium	45 to 60	30	5.5 to 7.4
SRK08-SPW1	S-Wells[b]	Weathered Bedrock	$8.6x10^{-1}$	$7.5x10^{-2}$	13 to 28
SRK08-SPW2	S-Wells[b]	Weathered Bedrock	4.3	4	10 to 13
South-Central Rose Creek Valley near CVD	CVD Area[c]	Alluvium	60.5	5 to 50	-
Northern Rose Creek Valley near CVD	CVD Area[c]	Alluvium	43.2	5 to 50	-
Tailings	Tailings Ponds[c]	Tailings	$1.7x10^{-3}$	0.05 to 2	-
Intermediate Dam	Intermediate Dam[c]	Dam	$2.6x10^{-2}$	$1x10^{-4}$	-
CVD	CVD [c]	Dam	$8.6x10^{-3}$	$1x10^{-4}$	-
Pond Sediments	PP & IP[c]	Pond Sediments	$7.8x10^{-5}$	$2x10^{-5}$	-
Basal Till	CVD Area[c]	Basal Till	$2.6x10^{-2}$	0.01 to 0.1	-
Slope Till	CVD Area[c]	Slope Till	$2.6x10^{-1}$	1 to 3	-
Bedrock	CVD Area[c]	Bedrock	$8.6x10^{-2}$	$2x10^{-3}$	-
CH12-014-MW003 and CH12-014-MW007	Faro Waste Rock[d]	Weathered Bedrock	$1x10^{-2}$	$1x10^{-2}$	26.1 to 35.3 46.3 to 61.6
CH12-014-MW003 and CH12-014-MW007	Faro Waste Rock[d]	Competent Bedrock	$1x10^{-3}$	$2.5x10^{-3}$	26.1 to 35.3 46.3 to 61.6
SRK05-ETA-BR2	ETA[e]	Bedrock	$3.7x10^{-3}$	$1x10^{-3}$	12 - 23.6 (packer test interval)
ETA sediments	ETA[e]	Alluvium	17.3	50	several wells

Notes:
mbgs = metre below ground surface
[a] SRK (2007)
[b] SRK (2006a)
[c] RGC (2006b)
[d] CH2M HILL (2013a)
[e] SRK (2006b)

The calibrated K_v values equate to K_h:K_v ratios of 1:1 to 500:1. Typically K_h:K_v ratios are between 1:1 and 1,000:1 in natural aquifer systems. As such, these values are reasonable considering the depositional environment that shaped the hydrostratigraphic zones beneath the site.

Figure 3-15 shows the calibrated distribution of GW_{ppn}. These GW recharge fluxes are internally computed using the specified GW_{ppn} rate, K_v of the shallow model layers, and simulated water table elevation, as described in Section 3.4.4.2. The calibrated GW_{ppn} rate ranges from 3.7 mm/yr in the upland areas to approximately 50 mm/yr on the WRDs, with the majority of the modelled area equal to approximately 14 mm/yr (about 4 percent of the annual precipitation).

River cell conductances were also modified during calibration by adjusting the associated hydraulic conductivity term (starting value 0.086 m/day). The hydraulic conductivity associated with these conductance terms were increased to 0.2 to 3 m/day in several reaches, where necessary to increase GW-SW interaction.

3.5.4.2 Groundwater Elevations

Tables 3-5 and 3-6 provide summary statistics that characterize the match between modelled and target heads for both GW flow models. Figure 3-16 compares modelled and target head data. Data presented on Figure 3-16 indicate strong agreement between modelled and target heads. Because the points fall both above and below, and close to, the 1:1 correlation line, no global bias in modelled heads is evident from Figure 3-16. Table 3-5 summarizes the statistics that quantify the goodness-of-fit between the modelled and target heads.

TABLE 3-5
Summary Statistics for Modelled Heads
Faro Mine Remediation Project

Summary Statistic	NFRC Whole Domain	RCAA Whole Domain	NFRC Subarea Model	RCAA Subarea Model
ME (m)	0.13	0.02	-1.26	0.28
R^2	1.00	1.00	0.99	1.00
RMSE (m)	2.26	2.49	2.67	2.02
Range of Target Head Values (m)	168.86	168.86	104.32	141.37
RMSE/Range (percent)	1.3	1.5	2.6	1.4
Number of Targets	205	205	53	152

Figure 3-17 presents maps of head residual errors. These maps assisted the FMWT to identify whether spatial bias was present in the head residual errors; such bias would be revealed by clusters of wells in which similar residual errors occur. These figures indicate there is little spatial bias in the modelled heads.

Figure 3-18 shows modelled potentiometric surfaces. The complexity of the potentiometric surface contours decreases with depth, indicating that the modelled GW flow system transitions from a shallow, topographically controlled system to a deeper, regionally controlled system. Much of the complexity of the GW flow system depicted in the shallower layers is because large portions of these layers are unsaturated; therefore, there is no modelled lateral flow in these areas. The deeper GW flow system layers are more saturated throughout the model domain, resulting in more continuous and regular GW flow patterns. Overall, the patterns of GW flow shown on Figure 3-18 fit this geographic setting, which includes shallow GW levels interacting with surface drainages and a decreasing SW-GW interaction with depth.

Figure 3-19 shows the modelled depth to GW, which ranges from 0 to no more than 15 m near the CVD area. At the S-Wells and Zone 2 outwash areas, the modelled depth to GW is approximately 5 m or less. In some areas, such as WRDs and the Rock Drain, the depth to GW values exceed 60 m and correspond to locations where mining activities have significantly altered the landscape.

TABLE 3-6
Comparison of Modelled and Target Heads
Faro Mine Remediation Project

Well	Model Layer	Target Head (m CGVD28)	Modelled Head (m CGVD28)	Residual Error (m)	Subarea Model
BH12A	1	1157.92	1156.23	-1.69	NFRC
BH13A	1	1179.87	1181.90	2.03	NFRC
BH14A	1	1152.94	1146.12	-6.82	NFRC
BH14B	1	1152.59	1146.07	-6.52	NFRC
BH4	1	1094.66	1094.41	-0.25	NFRC
DP-4	1	1080.73	1079.09	-1.64	NFRC
P09-SIS4	1	1083.52	1080.17	-3.35	NFRC
S1B	1	1080.70	1079.28	-1.42	NFRC
SRK05-SP1A	1	1084.73	1083.41	-1.32	NFRC
SRK05-SP1B	1	1084.63	1083.38	-1.25	NFRC
SRK05-SP4B	1	1083.51	1080.12	-3.39	NFRC
BH13B	2	1180.25	1182.04	1.79	NFRC
BH2	2	1094.66	1094.49	-0.17	NFRC
BH5	2	1092.62	1093.82	1.20	NFRC
BH6	2	1094.04	1094.25	0.21	NFRC
BH7B	2	1095.17	1094.64	-0.53	NFRC
CH12-014-MW007	2	1108.98	1102.94	-6.04	NFRC
P05-04	2	1094.62	1094.37	-0.25	NFRC
P09-SIS1	2	1082.42	1079.59	-2.83	NFRC
P09-SIS2	2	1083.11	1079.92	-3.19	NFRC
P09-SIS3	2	1083.36	1080.10	-3.26	NFRC
P09-SIS5	2	1084.00	1080.47	-3.53	NFRC
P09-SIS6	2	1083.98	1080.69	-3.29	NFRC
P96-7	2	1120.03	1115.05	-4.98	NFRC
RGC-PW3	2	1094.67	1094.34	-0.33	NFRC
S3	2	1082.93	1079.99	-2.94	NFRC
SRK05-SP6	2	1086.12	1088.81	2.69	NFRC
SRK08-P12B	2	1095.67	1095.28	-0.39	NFRC
SRK08-P13B	2	1093.90	1092.88	-1.02	NFRC
SRK08-SP7B	2	1079.15	1079.13	-0.02	NFRC
SRK08-SP8B	2	1075.93	1074.74	-1.19	NFRC
BH12B	3	1155.22	1153.40	-1.82	NFRC
BH7A	3	1095.13	1094.75	-0.38	NFRC
S1A	3	1080.21	1079.23	-0.98	NFRC
S2A	3	1080.15	1079.06	-1.09	NFRC
S2B	3	1080.30	1079.04	-1.26	NFRC
SRK05-SP2	3	1084.63	1084.75	0.12	NFRC
SRK05-SP3B	3	1084.43	1081.69	-2.74	NFRC
SRK05-SP5	3	1079.89	1078.93	-0.96	NFRC
SRK08-P12A	3	1095.69	1095.36	-0.33	NFRC
SRK08-P13A	3	1093.63	1092.85	-0.78	NFRC
SRK08-SBR3	3	1084.81	1086.63	1.82	NFRC

TABLE 3-6
Comparison of Modelled and Target Heads
Faro Mine Remediation Project

Well	Model Layer	Target Head (m CGVD28)	Modelled Head (m CGVD28)	Residual Error (m)	Subarea Model
SRK08-SP8A	3	1077.00	1074.89	-2.11	NFRC
BH8	4	1105.16	1097.39	-7.77	NFRC
P96-6	4	1090.31	1090.42	0.11	NFRC
SRK05-SP3A	4	1083.53	1081.87	-1.66	NFRC
SRK05-SP4A	4	1082.89	1081.04	-1.85	NFRC
SRK08-SBR2	4	1080.42	1080.85	0.43	NFRC
SRK08-SBR4	4	1079.59	1080.86	1.27	NFRC
SRK08-SP7A	4	1079.03	1079.46	0.43	NFRC
BH10A	5	1094.27	1095.49	1.22	NFRC
SRK08-SBR1	5	1080.39	1081.22	0.83	NFRC
BH10B	6	1094.25	1098.54	4.29	NFRC
CH12-204-MW005A	1	1011.39	1011.65	0.26	RCAA
NA05-2S	1	1046.62	1048.14	1.52	RCAA
P01-05A	1	1047.54	1048.32	0.78	RCAA
P01-05B	1	1047.12	1048.34	1.22	RCAA
P01-07A	1	1049.47	1050.96	1.49	RCAA
P01-07B	1	1049.49	1050.95	1.46	RCAA
P01-08A	1	1052.11	1052.47	0.36	RCAA
P03-03-09	1	1055.46	1055.05	-0.41	RCAA
P03-04-05	1	1048.48	1050.14	1.66	RCAA
P03-04-06	1	1048.55	1050.14	1.59	RCAA
P03-04-07	1	1048.51	1050.14	1.63	RCAA
P03-04-08	1	1048.69	1050.14	1.45	RCAA
P03-04-09	1	1048.47	1050.14	1.67	RCAA
P03-05-08	1	1051.90	1052.72	0.82	RCAA
P03-06-05	1	1050.35	1052.06	1.71	RCAA
P03-06-06	1	1050.52	1052.06	1.54	RCAA
P03-07-07	1	1051.61	1052.61	1.00	RCAA
P03-07-08	1	1052.21	1052.61	0.40	RCAA
P05-02	1	1014.88	1015.52	0.64	RCAA
SRK08-P09	1	1142.84	1125.22	-17.62	RCAA
SRK08-P11B	1	1135.65	1137.18	1.53	RCAA
X16A	1	1011.75	1011.87	0.12	RCAA
X16B	1	1011.75	1011.87	0.12	RCAA
X17A	1	1012.29	1013.35	1.06	RCAA
X17B	1	1011.75	1013.36	1.61	RCAA
X18A	1	1014.71	1014.71	0.00	RCAA
X18B	1	1015.19	1014.71	-0.48	RCAA
X21-96A	1	1047.80	1049.11	1.31	RCAA
X21-96B	1	1047.67	1049.11	1.44	RCAA
X25-96A	1	1028.86	1028.60	-0.26	RCAA
CH12-014-MW003	2	1152.76	1151.54	-1.22	RCAA

TABLE 3-6
Comparison of Modelled and Target Heads
Faro Mine Remediation Project

Well	Model Layer	Target Head (m CGVD28)	Modelled Head (m CGVD28)	Residual Error (m)	Subarea Model
CH12-204-MW005B	2	1011.39	1011.67	0.28	RCAA
ETA-05-04	2	1102.69	1098.84	-3.85	RCAA
MW1	2	1015.19	1016.44	1.25	RCAA
MW2	2	1015.19	1017.01	1.82	RCAA
NA05-11	2	1055.26	1055.82	0.56	RCAA
NA05-2D	2	1046.77	1048.15	1.38	RCAA
NA05-9D	2	1054.01	1054.56	0.55	RCAA
P01-03	2	1028.79	1028.52	-0.27	RCAA
P01-06	2	1047.81	1049.06	1.25	RCAA
P01-07C	2	1049.55	1050.93	1.38	RCAA
P01-07D	2	1049.35	1050.75	1.40	RCAA
P01-08B	2	1051.58	1052.49	0.91	RCAA
P01-08C	2	1051.07	1052.48	1.41	RCAA
P01-09A	2	1055.07	1055.82	0.75	RCAA
P01-09B	2	1054.71	1055.81	1.10	RCAA
P01-10A	2	1055.51	1055.60	0.09	RCAA
P01-10B	2	1054.68	1055.60	0.92	RCAA
P03-01-05	2	1055.22	1056.41	1.19	RCAA
P03-01-06	2	1055.17	1056.34	1.17	RCAA
P03-01-07	2	1055.11	1056.34	1.23	RCAA
P03-01-08	2	1055.41	1056.34	0.93	RCAA
P03-01-09	2	1055.36	1056.34	0.98	RCAA
P03-02-05	2	1054.48	1055.45	0.97	RCAA
P03-02-06	2	1054.48	1055.45	0.97	RCAA
P03-02-07	2	1054.86	1055.45	0.59	RCAA
P03-02-08	2	1054.95	1055.45	0.50	RCAA
P03-02-09	2	1054.99	1055.45	0.46	RCAA
P03-03-05	2	1054.18	1055.04	0.86	RCAA
P03-03-06	2	1054.27	1055.04	0.77	RCAA
P03-03-07	2	1054.17	1055.04	0.87	RCAA
P03-03-08	2	1054.45	1055.04	0.59	RCAA
P03-04-04	2	1048.54	1050.14	1.60	RCAA
P03-05-03	2	1051.74	1052.72	0.98	RCAA
P03-05-04	2	1051.68	1052.72	1.04	RCAA
P03-05-05	2	1051.57	1052.72	1.15	RCAA
P03-05-06	2	1051.80	1052.72	0.92	RCAA
P03-05-07	2	1051.69	1052.72	1.03	RCAA
P03-06-01	2	1050.33	1052.06	1.73	RCAA
P03-06-02	2	1050.36	1052.06	1.70	RCAA
P03-06-03	2	1050.44	1052.06	1.62	RCAA
P03-06-04	2	1050.39	1052.06	1.67	RCAA
P03-07-04	2	1051.77	1052.60	0.83	RCAA

TABLE 3-6
Comparison of Modelled and Target Heads
Faro Mine Remediation Project

Well	Model Layer	Target Head (m CGVD28)	Modelled Head (m CGVD28)	Residual Error (m)	Subarea Model
P03-07-05	2	1051.67	1052.60	0.93	RCAA
P03-07-06	2	1052.22	1052.60	0.38	RCAA
P03-08-02	2	1040.32	1038.71	-1.61	RCAA
P03-08-03	2	1040.64	1038.71	-1.93	RCAA
P03-08-04	2	1040.61	1038.71	-1.90	RCAA
P03-08-05	2	1040.80	1038.71	-2.09	RCAA
P03-08-06	2	1041.15	1038.71	-2.44	RCAA
P03-08-07	2	1042.88	1038.71	-4.17	RCAA
P03-08-08	2	1043.27	1038.71	-4.56	RCAA
P03-09-07	2	1014.91	1015.98	1.07	RCAA
P03-09-08	2	1015.01	1015.98	0.97	RCAA
P03-09-09	2	1014.79	1015.98	1.19	RCAA
P05-01-04	2	1015.96	1016.61	0.65	RCAA
P05-01-05	2	1015.61	1016.61	1.00	RCAA
P05-01-06	2	1015.56	1016.61	1.05	RCAA
P05-03	2	1015.22	1017.22	2.00	RCAA
P96-8A	2	1106.51	1104.73	-1.78	RCAA
RGC-PW1	2	1015.11	1016.53	1.42	RCAA
SRK04-3B	2	1097.94	1094.13	-3.81	RCAA
SRK05-ETA-BR1	2	1097.79	1095.83	-1.96	RCAA
SRK08-P10A	2	1101.41	1101.30	-0.11	RCAA
SRK08-P10B	2	1104.54	1101.16	-3.38	RCAA
SRK08-P11A	2	1135.68	1137.07	1.39	RCAA
X24-96A	2	1029.29	1028.61	-0.68	RCAA
X24-96B	2	1030.24	1028.61	-1.63	RCAA
CH12-204-MW001A	3	1016.40	1016.47	0.07	RCAA
P01-01A	3	1012.20	1012.63	0.43	RCAA
P01-02A	3	1017.36	1019.01	1.65	RCAA
P01-02B	3	1019.77	1019.01	-0.76	RCAA
P01-04A	3	1029.71	1028.11	-1.60	RCAA
P01-07E	3	1049.52	1050.75	1.23	RCAA
P01-09C	3	1054.68	1055.80	1.12	RCAA
P01-09D	3	1054.24	1055.80	1.56	RCAA
P01-11	3	1017.16	1017.85	0.69	RCAA
P03-01-03	3	1055.14	1056.41	1.27	RCAA
P03-01-04	3	1055.28	1056.41	1.13	RCAA
P03-02-03	3	1054.51	1055.45	0.94	RCAA
P03-02-04	3	1054.51	1055.45	0.94	RCAA
P03-03-02	3	1054.28	1055.04	0.76	RCAA
P03-03-03	3	1054.19	1055.04	0.85	RCAA
P03-03-04	3	1054.30	1055.04	0.74	RCAA
P03-04-02	3	1048.93	1050.15	1.22	RCAA

TABLE 3-6
Comparison of Modelled and Target Heads
Faro Mine Remediation Project

Well	Model Layer	Target Head (m CGVD28)	Modelled Head (m CGVD28)	Residual Error (m)	Subarea Model
P03-04-03	3	1048.91	1050.15	1.24	RCAA
P03-05-02	3	1051.84	1052.72	0.88	RCAA
P03-07-02	3	1051.75	1052.60	0.85	RCAA
P03-07-03	3	1051.73	1052.60	0.87	RCAA
P03-08-01	3	1040.35	1038.71	-1.64	RCAA
P03-09-02	3	1015.54	1016.14	0.60	RCAA
P03-09-03	3	1015.54	1016.14	0.60	RCAA
P03-09-04	3	1015.34	1016.14	0.80	RCAA
P03-09-05	3	1015.16	1016.14	0.98	RCAA
P03-09-06	3	1015.27	1016.14	0.87	RCAA
P05-01-01	3	1015.90	1016.74	0.84	RCAA
P05-01-02	3	1015.72	1016.74	1.02	RCAA
P05-01-03	3	1015.55	1016.74	1.19	RCAA
P09-ETA2	3	1062.50	1060.81	-1.69	RCAA
P96-8B	3	1106.58	1104.71	-1.87	RCAA
SRK04-3A	3	1098.14	1094.12	-4.02	RCAA
X21-96C	3	1047.47	1049.11	1.64	RCAA
CH12-204-MW001B	4	1017.22	1016.57	-0.65	RCAA
CH12-204-MW002B	4	1017.28	1016.76	-0.52	RCAA
P01-01B	4	1012.08	1012.65	0.57	RCAA
P01-04B	4	1029.59	1028.11	-1.48	RCAA
P03-01-02	4	1055.09	1056.41	1.32	RCAA
P03-02-01	4	1054.53	1055.45	0.92	RCAA
P03-02-02	4	1054.52	1055.45	0.93	RCAA
P03-03-01	4	1054.28	1055.05	0.77	RCAA
P03-04-01	4	1048.82	1050.15	1.33	RCAA
P03-05-01	4	1051.78	1052.72	0.94	RCAA
P03-07-01	4	1051.85	1052.60	0.75	RCAA
P03-09-01	4	1015.88	1016.13	0.25	RCAA
P09-C1	4	1016.81	1017.00	0.19	RCAA
P09-C3	4	1018.14	1017.54	-0.60	RCAA
P09-ETA1	4	1063.89	1060.88	-3.01	RCAA
SRK05-ETA-BR2	4	1098.61	1094.74	-3.87	RCAA
X24-96D	4	1029.11	1028.59	-0.52	RCAA
CH12-204-MW003B	5	1015.77	1016.96	1.19	RCAA
P03-01-01	5	1055.18	1056.41	1.23	RCAA
P09-C2	6	1016.15	1017.62	1.47	RCAA

Notes:
Target head values were computed by averaging available field-measured heads.
Residual error was computed as modelled head value minus target head value.

3.5.4.3 Steady-state Groundwater Balance

Table 3-7 lists the components of the combined modelled GW balance for Model Layers 1 through 6. The GW balance is reported for the individual subarea GW flow models as well as the entire active domains to illustrate the magnitudes of the GW balance components at different spatial scales. Figure 3-20 shows the locations of the subareas used for computing the GW balance terms. Data in Table 3-7 indicate that approximately 20 and 211 litres per second (L/sec) of GW flows through the NFRC and RCAA subareas, respectively.

TABLE 3-7
Modelled Groundwater Balance
Faro Mine Remediation Project

	GW Inflow Rate (L/sec)					GW Outflow Rate (L/sec)			
GW Inflow Component	**NFRC Whole Domain**	**RCAA Whole Domain**	**NFRC Subarea**	**RCAA Subarea**	**GW Outflow Component**	**NFRC Whole Domain**	**RCAA Whole Domain**	**NFRC Subarea**	**RCAA Subarea**
GW Recharge from Precipitation	85	92	4	2	GW Pumping	5	4	2	0
GW Recharge from Streams	427	463	8	134	GW Discharge to Streams	440	479	5	147
GW Recharge from Ponds and Pit Lakes	4	1	3	0	GW Discharge to Ponds and Pit Lakes	4	2	2	0
Subsurface Inflow	0	0	5	75	Subsurface Outflow	21	21	11	15
					GW Discharge to Drains	46	50	0	49
Total GW Inflows	516	556	20	211	Total GW Outflows	516	556	20	211

Note:
Values are rounded to the nearest L/sec.

3.6 Groundwater Model Application

The calibrated GW flow models described previously were used to conduct predictive simulations to support the evaluation of potential remedial strategies that could be implemented to reduce the volume of contaminated GW leaving the FMC. More specifically, these simulations provided forecasts that provide insight into the potential effectiveness of each modelled SIS at capturing mine-impacted GW that discharges to Rose Creek and its tributaries. These predictive simulations were conducted to provide additional information to inform prioritization decisions on when certain elements of work should be pursued. Further, these predictive simulations serve as a first step to develop reliable engineering designs that should be further pursued to intercept contaminated GW at the FMC.

The following section discusses how the calibrated GW flow models were modified to simulate the operation of existing and hypothetical GW extraction systems and the results obtained from these predictive simulations.

3.6.1 Setup for Predictive Groundwater Simulations

The predictive simulations described herein maintain consistency with model parameters achieved via calibration and initial boundary conditions, except for new boundary conditions implemented to simulate a hypothetical SIS.

3.6.1.1 Particle Tracking

A GW particle-tracking approach was implemented with the predictive modelling to forecast the potential effectiveness of select GW extraction systems. MODPATH Version 3 (Pollock, 1994) was used to track the GW particles both forward (i.e., downgradient) and in reverse (i.e., upgradient) from various locations within the models to delineate the hydraulic capture zones. In both NFRC Subarea model simulations described below, MODPATH was used to track particles forward to delineate modelled regions of hydraulic capture of these systems based on the particle's ending location (destination). Reverse particle tracking was used in the RCAA

Subarea model where particles originated from the depth intervals corresponding to the extraction depth intervals to delineate the hydraulic capture zones. Both forward and reverse particle tracking was conducted to provide examples of each approach in this report. Because no GW extraction systems in the RCAA Subarea currently exist, particle tracking was not performed to assess existing conditions.

3.6.1.2 NFRC Subarea Model

The NFRC Subarea model encompasses two areas in which SISs were simulated: one as an existing system and one as a future, hypothetical system. In the S-Wells area, an existing SIS is operational and was simulated as part of the calibrated model. At the Zone 2 Pit and Outwash area, an existing pumping well is screened in the deep aquifer beneath the pit and was included in the calibrated model. CH2M HILL submitted a conceptual SIS system design for the Zone 2 Outwash area, and the operation of this system was simulated in a predictive model run (CH2M HILL, 2012). Based on the calibration simulations performed with the NFRC Subarea model, the existing S-Wells SIS and Zone 2 Pit extraction well was simulated as described below. The conceptual Zone 2 Outwash SIS was then added to the S-Wells and Zone 2 Pit extraction well systems in a post-calibration predictive simulation.

S-Wells Area

The S-Wells area currently includes an SIS that has been in place since the winter of 2008-2009 (RGC, 2012). The S-Wells SIS consists of a shallow and a deep GW component. The shallow component includes a shallow rock-filled interceptor trench coupled with a central sump and pumping well SRK08-SPW3. The deep component consists of two pumping wells screened in the deep aquifer (SRK08-SPW1 and SRK08-SPW2). Pumping from well SRK08-SPW1 ceased in early 2010, and only SRK08-SPW2 is now operational to capture the deeper GW (RGC, 2012). In the NFRC Subarea model, the interceptor trench was simulated with a four-cell zone of high K_h (500 m/day) to represent the permeable material present in the trench. SRK08-SPW3 was included as a pumping well in one of the high K cells and screened in Model Layers 1 and 2. The pumping rate was set at a constant 86.4 cubic metres per day (m^3/day) (1 L/sec). SRK08-SPW2 was included as a pumping well with a constant rate of 103.7 m^3/day (1.2 L/sec) and screened in Model Layer 3 only.

Zone 2 Pit and Outwash

The Zone 2 Pit extraction well was included in the calibrated model as an extraction well screened in Model Layer 4 with a constant pumping rate of 170 m^3/day (approximately 2 L/sec). No SIS is currently installed in the Zone 2 Outwash area. The Zone 2 Outwash SIS conceptual design consists of a permeable trench with four paired alluvial/bedrock aquifer extraction wells equally spaced along its length (CH2M HILL, 2012). The assumed trench depth is approximately 13 mbgs (approximate combined thickness of Model Layers 1 through 3), and the trench is assumed to be backfilled with coarse granular material. The trench was simulated with a MODFLOW drain package approximately 350 m long by 15 m wide and 15 m deep with a K_h value of 500 m/day (these approximate dimensions were only used to compute the model conductance term). The drain elevation was set 1 m above the bottom of Model Layer 3.

The GW flow out of the simulated trench is computed internally by MODHMS and represents the combined flux to the shallow wells in the trench. A deep well is paired with each shallow trench extraction well to directly extract GW from the weathered bedrock. These deep wells were simulated using four wells in Model Layer 4 beneath the simulated trench. GW extraction rates for these deeper wells were set above the likely maximum yield from the model to allow the FWL package of MODHMS to compute the maximum steady-state yield for these wells.

3.6.1.3 RCAA Subarea Model

The calibrated RCAA Subarea model was modified by adding nine hypothetical extraction wells in the alluvial and weathered bedrock aquifers. These wells are screened at various depths to capture mine-impacted GW flowing in the RCAA beneath the RCTA and downstream impoundments. The calibration of the GW model to the drawdown observed during 2012 aquifer testing was a critical step in confirming that the model could replicate the response of the aquifer near the CVD to pumping. Because the operation of the future CVD SIS will exert stresses on the RCAA that are similar to those exerted during aquifer testing, calibration to the 2012 aquifer test is an ideal approach to gaining confidence that the model can accurately simulate the performance of an SIS constructed in the CVD area.

3.6.2 Groundwater Model Application Results

This section presents the results of the modeling simulations performed in both the NFRC and RCAA subareas.

3.6.2.1 NFRC Subarea Model

Figure 3-21 depicts the results of the particle tracking associated with the existing Zone 2 Pit extraction well and the S-Wells SIS. The red areas indicate capture of the Zone 2 Pit extraction well (CH12-Z2-PW001), whereas the purple and yellow areas indicate capture areas of SRK08-SPW2 and SRK08-SPW3, respectively. The light and dark blue areas indicate areas with GW that eventually discharges to the NFRC and Faro Pit, respectively. Light brown areas indicate areas with GW that flows to downgradient locations not otherwise indicated. These results indicate a potentially large extent of capture from the Zone 2 Pit extraction well and the S-Wells SIS. Figure 3-21 also indicates potentially large GW source areas of GW to Faro Pit and the NFRC.

Figure 3-22 depicts the results of the particle tracking associated with the existing Zone 2 Pit extraction well and S-Wells SIS along with a hypothetical trench and deep bedrock SIS in the Zone 2 Outwash. The green areas on Figure 3-22 indicate the capture area of the Zone 2 Outwash SIS. The extents of the modelled hydraulic capture areas are similar to those shown on Figure 3-21, with the exception that additional GW is captured by the Zone 2 Outwash SIS. In many places, the GW that is simulated to discharge to NFRC under current conditions would be captured by the Zone 2 Outwash SIS, according to the model. These results suggest that the SIS configurations modelled may be effective at intercepting contaminated GW. However, these results should be considered preliminary at best. Additional fieldwork and analysis is required in the NFRC Subarea to help reduce the predictive uncertainty associated with the NFRC Subarea model. Additional configurations will continue to be explored with the model in the remaining weeks of FY12.

3.6.2.2 RCAA Subarea Model

Figure 3-23 illustrates the modelled GW flow patterns under current, steady-state conditions in the RCAA near the CVD. The lateral GW flow direction arrows were developed by creating a gridded potentiometric surface for each model layer and computing GW flow directions on 100-m centres. The GW flow direction arrows are only illustrated in saturated regions of each model layer because the unsaturated zones do not have lateral GW flow in the model. The GW flow directions in Model Layer 1 are complex, primarily because of the interaction of GW with the specified-head boundary conditions imposed on the Polishing Pond and Intermediate Pond, as well as the recharge boundaries reflecting infiltration of mine-affected water migrating into the RCTA from the ETA. GW flow directions in Model Layer 2 and deeper show the expected pattern of GW moving into the RCAA from the uplands to the north and south and GW within the RCAA moving west toward X14.

For the predictive simulation that includes an SIS operating downstream of the CVD, the total flow rate required to fully capture the RCAA was estimated to be approximately 107 L/sec (1,700 United States gallons per minute) from nine hypothetical extraction wells. The colored particle traces shown on Figure 3-24 reflect which extraction well each particle is captured by, thereby collectively providing a representation of the portion of the aquifer captured by each extraction well in the SIS. GW particle traces indicate that particles move between and through portions of model layers while en route to the hypothetical CVD SIS. Overall, it is clear that the simulated operation of the CVD SIS results in a full capture of modelled GW moving through the RCAA; no particles continue to migrate downstream toward Rose Creek. Additional SIS configurations including the potential use of slurry wall systems to reduce the inflow of clean GW into the SIS will continue to be explored with the model in the remaining weeks of FY12.

3.6.3 Groundwater Model Use and Limitations

No model is a perfect simulator of reality. Nevertheless, the GW flow models described herein are powerful tools that can provide useful insight into flow and transport processes within the physical system. However, the fundamental assumptions inherent in these models and the adequacy of their input data should be considered when using model output to help make important site management decisions. The model output should be scrutinized and used in conjunction with observational site data and professional judgment.

The GW flow models described herein were used primarily to address questions related to subsurface flow. The GW flow models provide steady-state solutions to the governing GW flow equations and forecast GW flow conditions that could result from long-term implementation of subsurface components of the FMRP. Transient (time-varying) solutions to the governing GW flow equations may also be required to address questions related to seasonal or long-term trends in GW flow conditions.

Output from the GW flow models may be geographic, graphic (e.g., discharge hydrograph), or tabular time-series data (e.g., spreadsheet format) and are available at each model cell in the 3D GW flow model domain. Portions of the GW flow model input and outputs may be linked with or used the following modelling tools:

- SW balance information in the GoldSim model
- Rates of GW discharge to SW bodies to facilitate development of SW flow models
- Subsurface hydraulic and physical transport parameter information for subsurface geochemical modelling

In turn, the GoldSim model, the SW flow, and the geochemical models may provide inputs into the GW flow models in regard to SW availability and stage.

As with any mathematical model, the GW flow models developed to support the FMRP design, construction, and implementation are only able to approximate processes of physical systems. Models are inherently inexact because the mathematical description of the physical system is imperfect and the understanding of interrelated physical processes is incomplete. However, CH2M HILL incorporated enough detail of the physical system into the GW flow models to fulfill the near-term modelling objectives described in Section 3.1.1.

REGIONAL MAP

LEGEND

- Roads Unpaved
- Faro Site Watercourse
- Faro Site Waterbody
- Groundwater Flow Modelling Boundary

Notes:
1. Aerial photography acquired by Peregrine Aerial Surveyors Inc. and Eagle Mapping in August 2012.
2. Orthophotography prepared by Critigen Canada Corp.

N

0 850 1,700 2,550 3,400

Metres

Created by: CRITIGEN

FIGURE 3-1
Active Groundwater Flow Modelling Domain within the Rose Creek Drainage Basin
Faro Mine Remediation Project

Pre-mining Topography

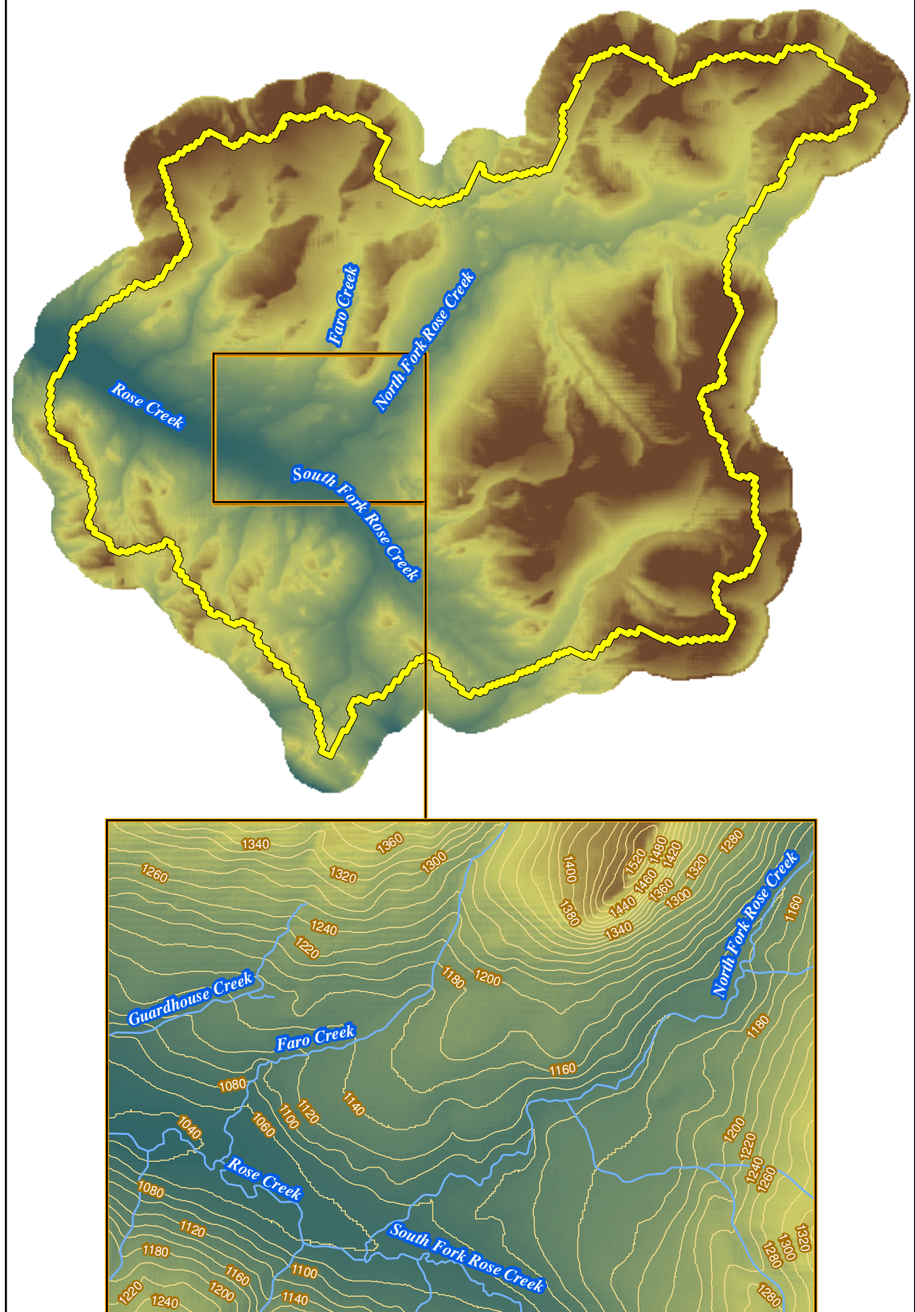

Present-day Topography

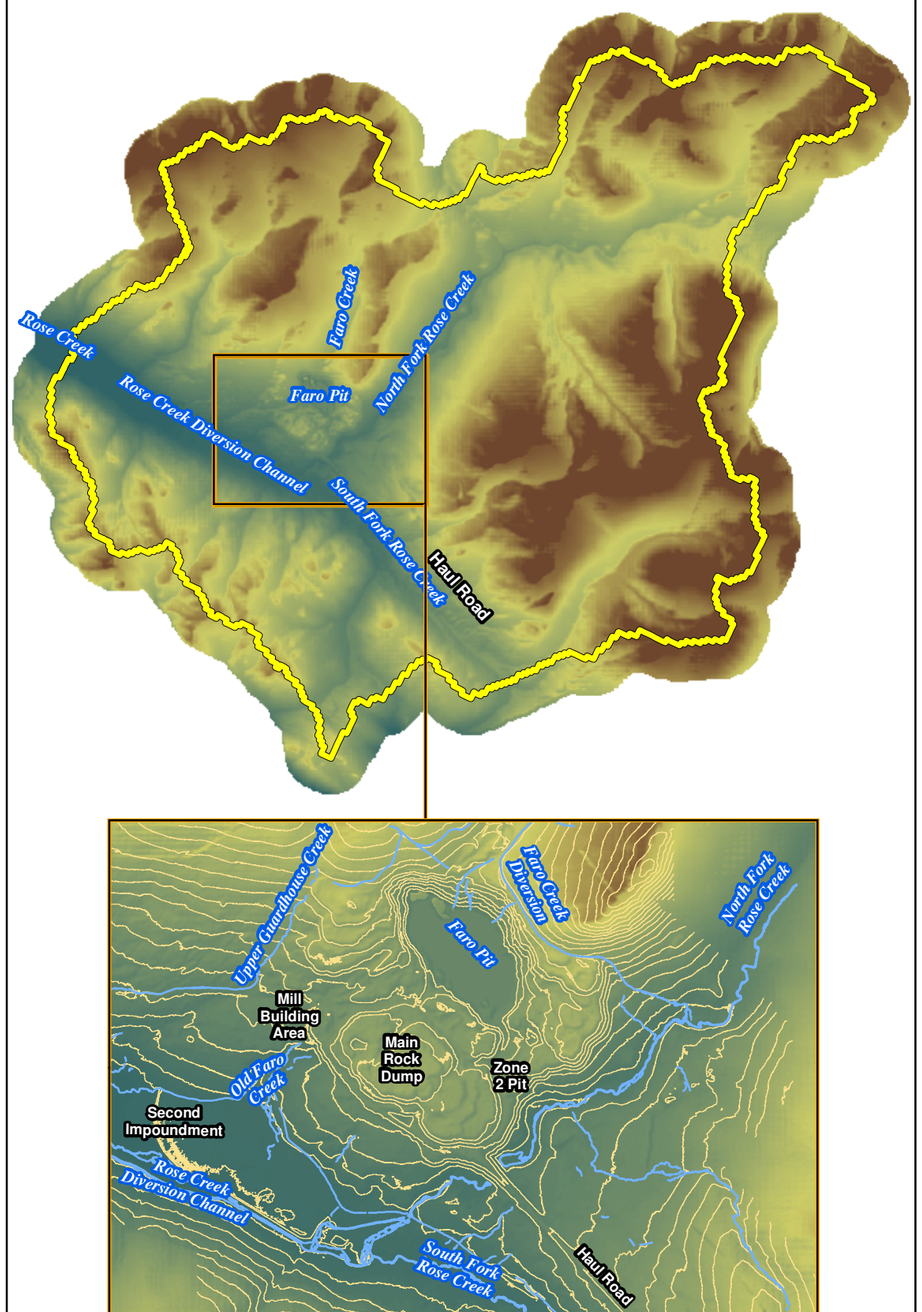

REGIONAL MAP

LEGEND

- Land Surface Elevation Contour (m CGVD28)
- Stream
- Groundwater Flow Modelling Boundary

Elevation (m CGVD28)

2,041

994

Note:
Contours are displayed at an interval of 20 metres.

N

0 1,675 3,350 5,025 6,700
Metres
Main Map Scale

0 500 1,000 1,500 2,000
Metres
Inset Scale

Created by:
CRITIGEN

FIGURE 3-2
Land Surface Topography
Faro Mine Remediation Project

CH2MHILL

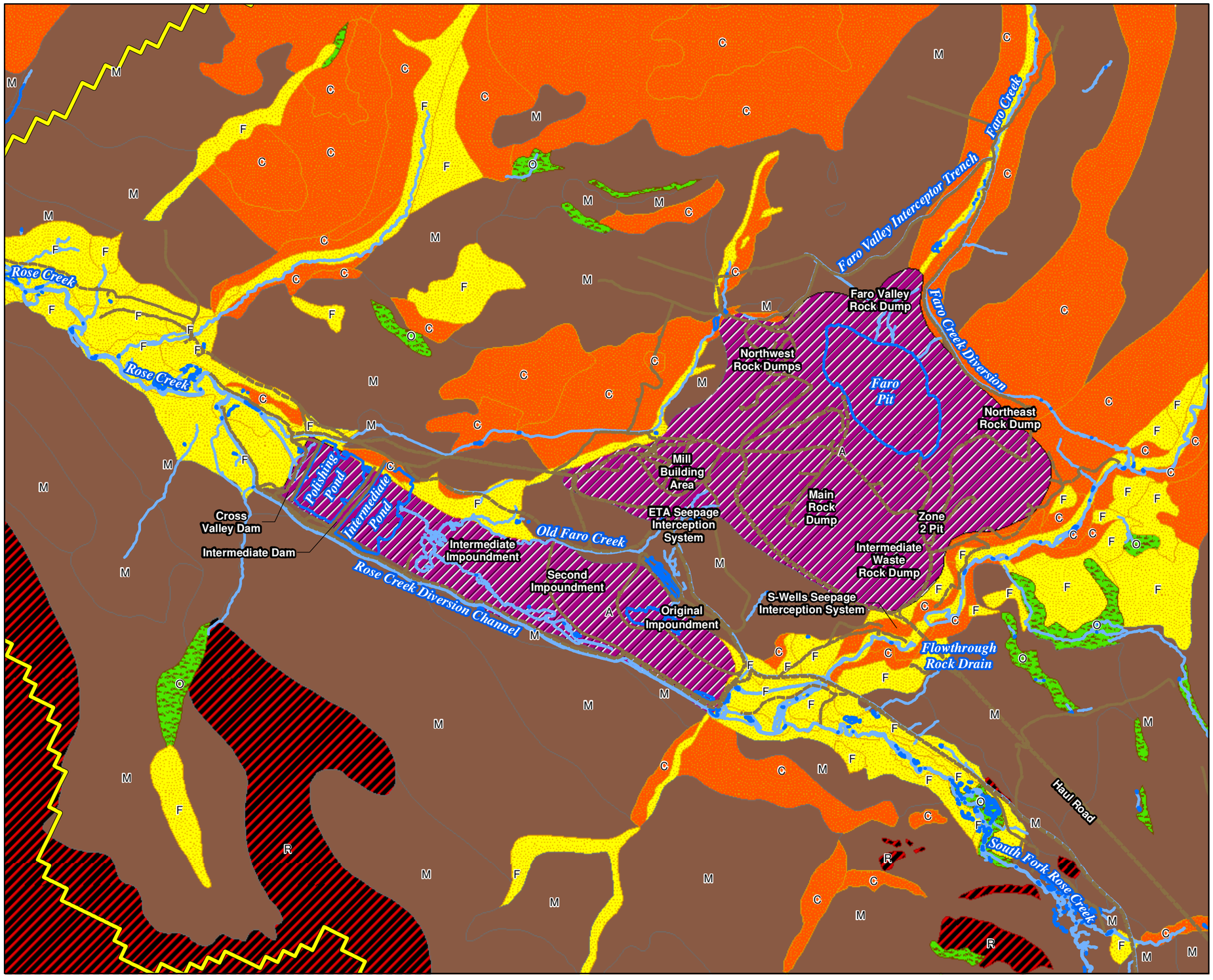

VICINITY MAP

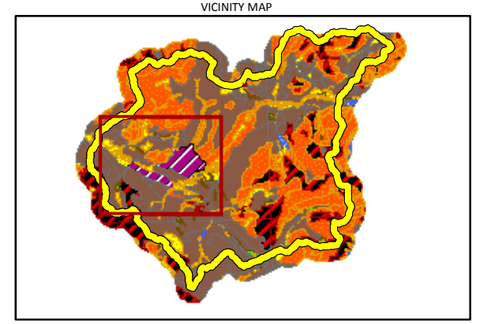

LEGEND

- Roads Unpaved
- Stream
- Lake, Pool, or Pond
- Groundwater Flow Modelling Boundary

Surficial Material

- Anthropogenic (A)
- Colluvium (C)
- Fluvial (F)
- Lacustrine (L)
- Morainal/Till (M)
- Organics (O)
- Bedrock (R)

Note:
Surficial Geology Source
http://ygsftp.gov.yk.ca/standardized_geodatabases_ArcGIS_9

N

0 300 600 900 1,200
Metres

Created by:
CRITIGEN

FIGURE 3-3
Surficial Geology
Faro Mine Remediation Project

CH2MHILL

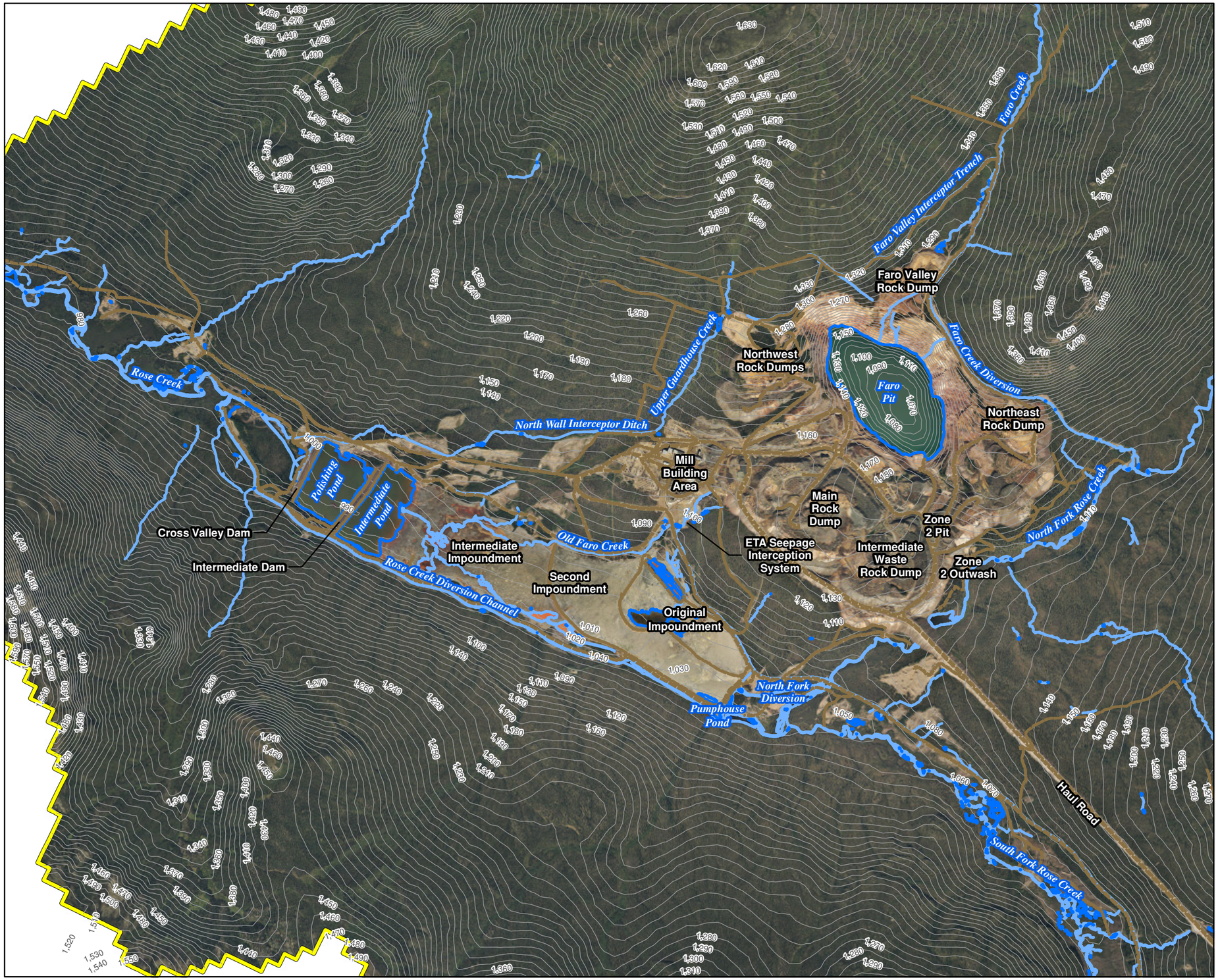

VICINITY MAP

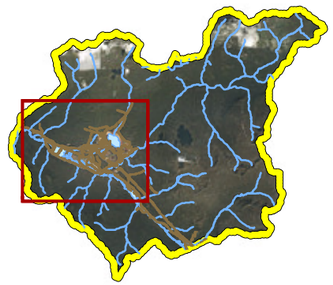

LEGEND

- Bedrock Elevation Contour (m CGVD28)
- Roads Unpaved
- Stream
- Lake, Pond, or Pool
- Groundwater Flow Modelling Boundary

Notes:
1. Contours are displayed at an interval of 5 m.
2. Contours represent the inferred top elevation of weathered bedrock.
3. Aerial photography acquired by Peregrine Aerial Surveyors Inc. and Eagle Mapping in August 2012.
4. Orthophotography prepared by Critigen Canada Corp.

N

0 300 600 900 1,200

Metres

Created by: CRITIGEN

FIGURE 3-4
Modelled Bedrock Topography
Faro Mine Remediation Project

VICINITY MAP

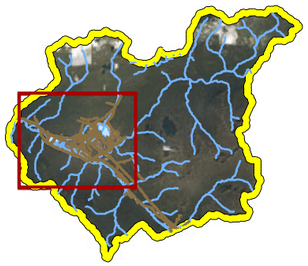

LEGEND

- Contour of Overburden Thickness (m)
- Roads Unpaved
- Stream
- Lake, Pond, or Pool
- Groundwater Flow Modelling Boundary

Notes:

1. Contours are displayed at an interval of 5 m.
2. Contours represent the difference between the top elevation of Model Layer 1 and the bedrock topography illustrated on Figure 3-4.
3. Aerial photography acquired by Peregrine Aerial Surveyors Inc. and Eagle Mapping in August 2012.
4. Orthophotography prepared by Critigen Canada Corp.

N

0 300 600 900 1,200

Metres

Created by: CRITIGEN

FIGURE 3-5

Modelled Overburden Isopach

Faro Mine Remediation Project

CH2MHILL

R:\FAROMINE_20000342\MAPFILES\WATERMODELANALYSISRPT\FIG03_05.MXD ECLARK 2/15/2013 2:42:27 PM

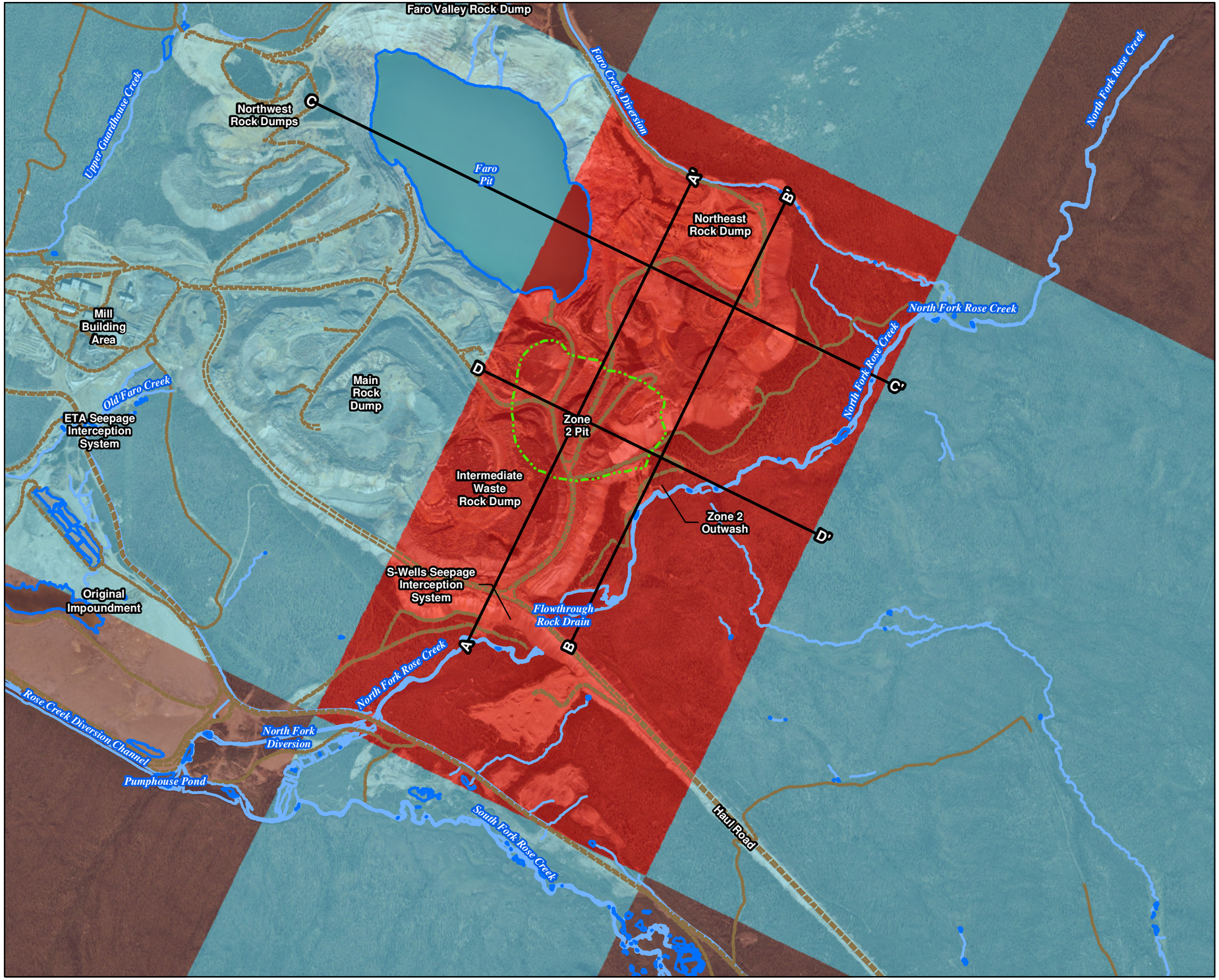

VICINITY MAP

LEGEND

- Roads Unpaved
- Stream
- Lake, Pond, or Pool
- Approximate Zone 2 Pit Outline
- Groundwater Flow Modelling Boundary
- Cross Section Line

Model Grid Spacing Zone

- Region of 10×10 m Cells
- Region of Transition Cells
- Region of 100×100 m Cells

Notes:

1. Profile views of the model grid along A-A' and B-B' are provided on Figure 3-8, whereas those along C-C' and D-D' are provided on Figure 3-9.
2. Aerial photography acquired by Peregrine Aerial Surveyors Inc. and Eagle Mapping in August 2012.
3. Orthophotography prepared by Critigen Canada Corp.

N

0 160 320 480 640

Metres

Created by: CRITIGEN

FIGURE 3-6

Active Groundwater Flow Model Grid Spacing in the NFRC Subarea: Areal View

Faro Mine Remediation Project

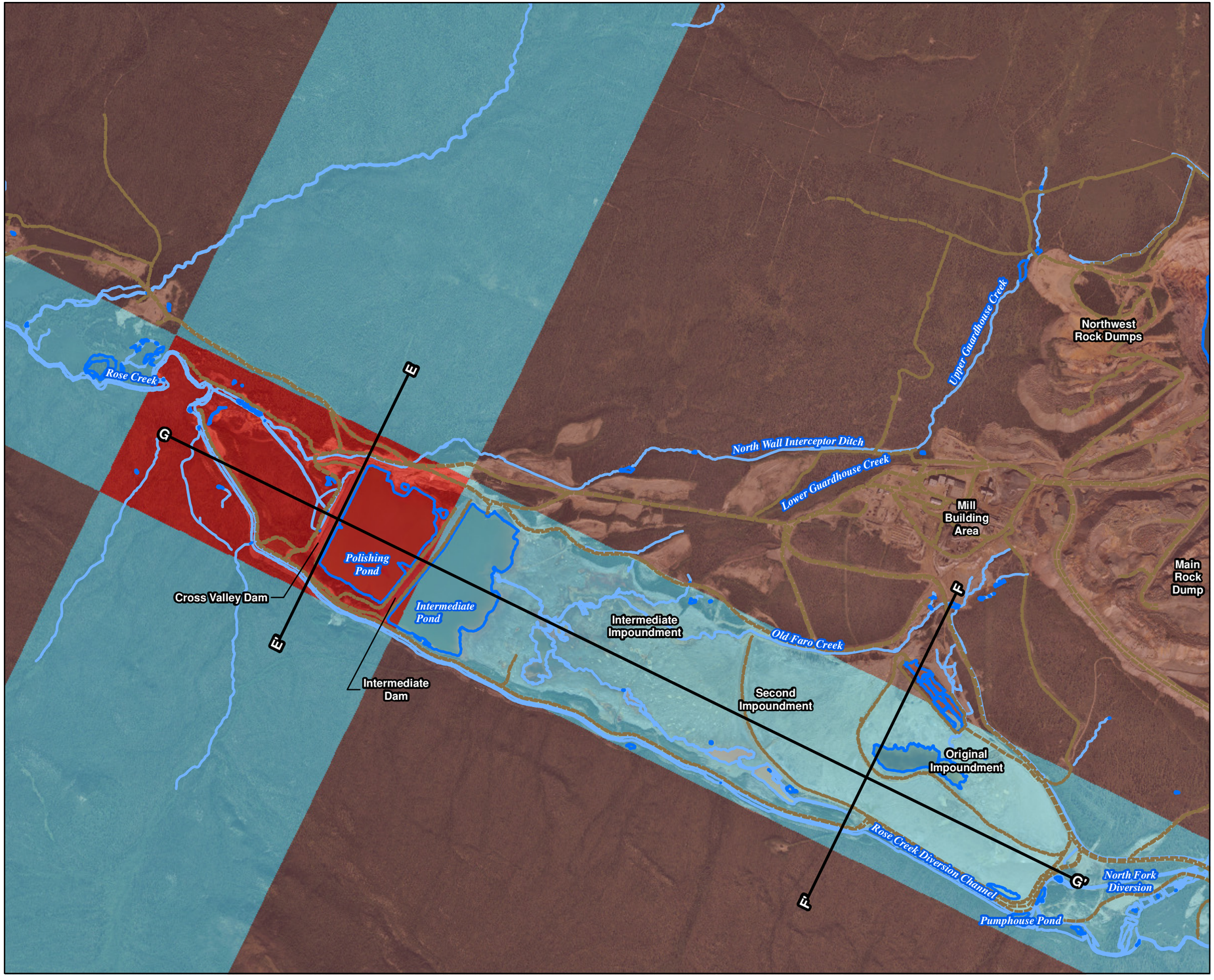

VICINITY MAP

LEGEND

- Roads Unpaved
- Stream
- Lake, Pond, or Pool
- Groundwater Flow Modelling Boundary
- Cross Section Line

Model Grid Spacing Zone

- Region of 10×10 m Cells
- Region of Transition Cells
- Region of 100×100 m Cells

Notes:

1. Profile views of the model grid along E-E', F-F', and G-G' are provided on Figure 3-10.
2. Aerial photography acquired by Peregrine Aerial Surveyors Inc. and Eagle Mapping in August 2012.
3. Orthophotography prepared by Critigen Canada Corp.

N

0 180 360 540 720

Metres

Created by: CRITIGEN

FIGURE 3-7

Active Groundwater Flow Model Grid Spacing in the RCAA Subarea: Areal View

Faro Mine Remediation Project

R:\FAROMINE_20000342\MAPFILES\WATERMODELANALYSISRPT\FIG03_07.MXD ECLARK 2/25/2013 3:33:28 PM

CH2MHILL

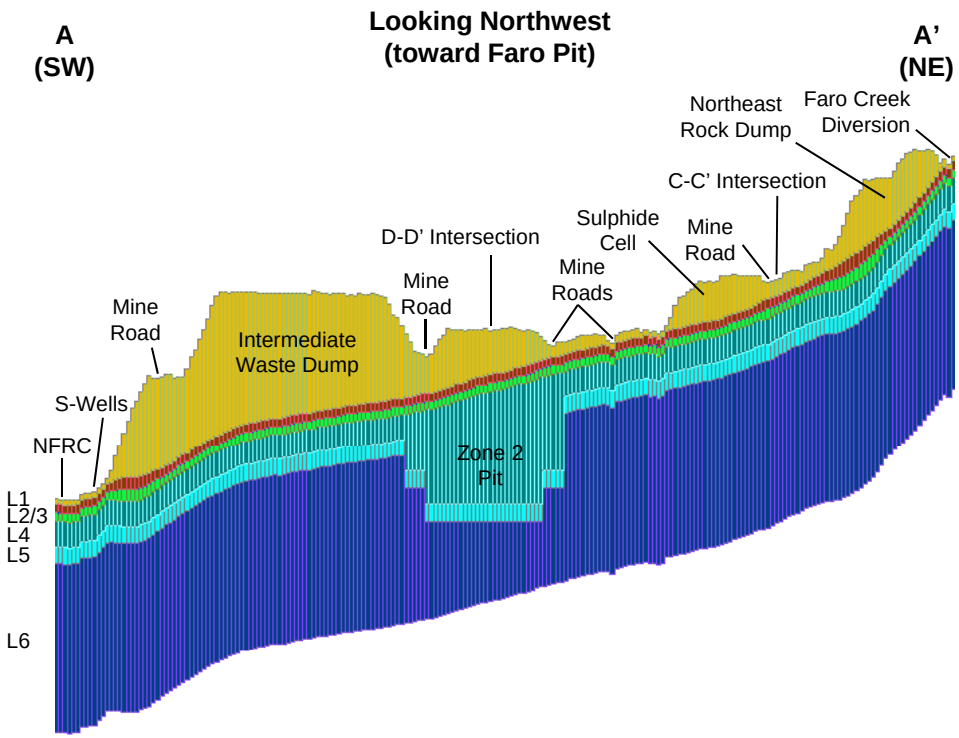

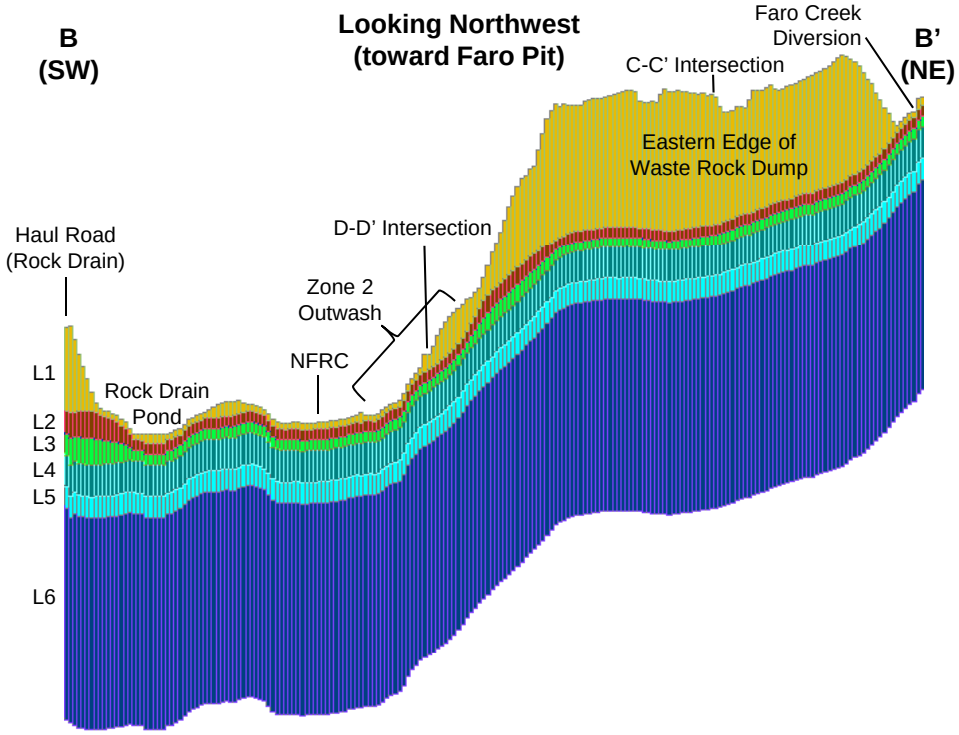

Notes
1. Images are not to scale and are vertically exaggerated by a factor of 4.
2. Figure 3-6 depicts the locations of A-A' and B-B'.

FIGURE 3-8
Profile Views of the NFRC Subarea Model Grid along A-A' and B-B'
Faro Mine Remediation Project

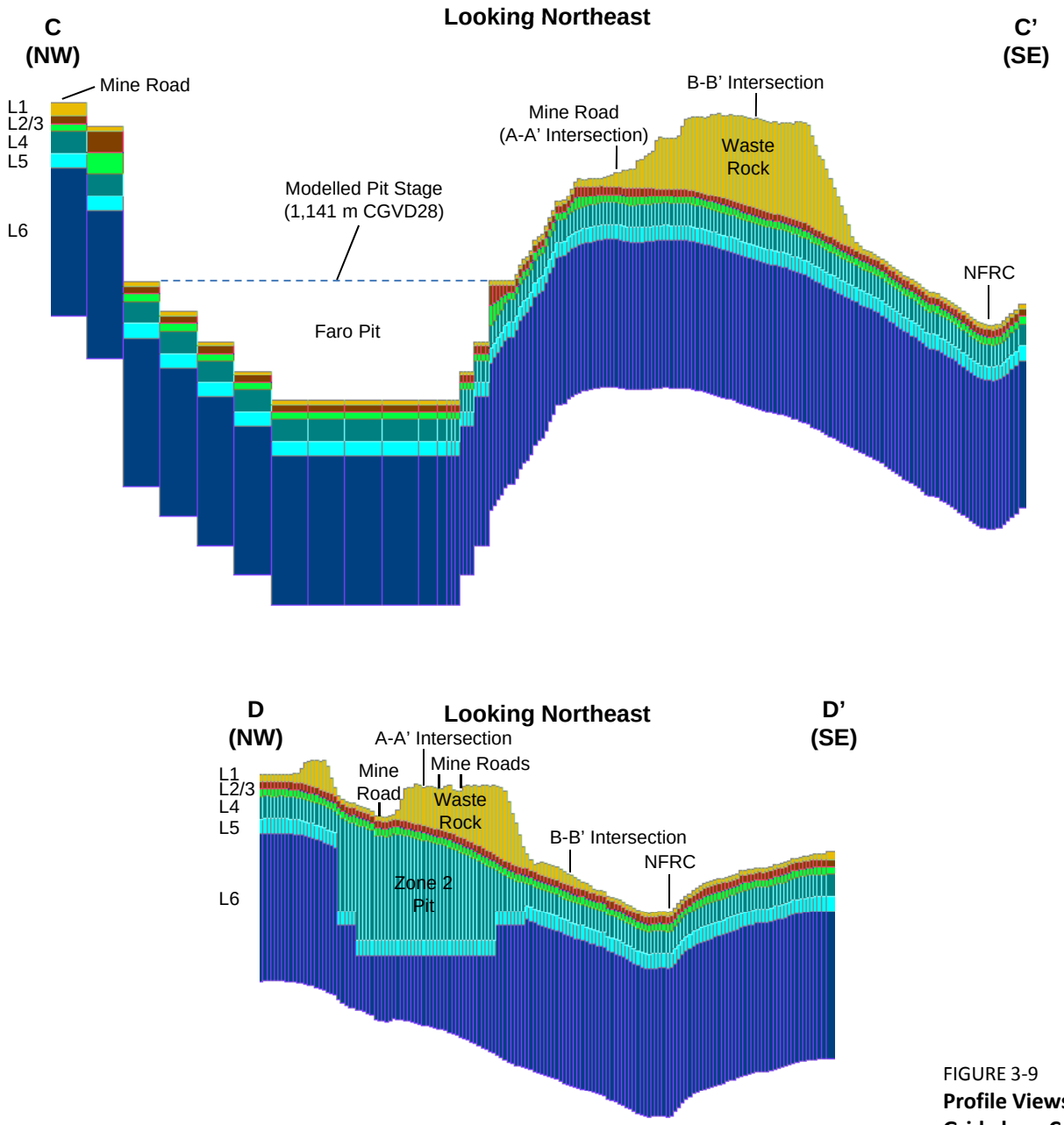

Notes
1. Images are not to scale and are vertically exaggerated by a factor of 4.
2. Figure 3-6 depicts the locations of C-C' and D-D'.

FIGURE 3-9
Profile Views of the NFRC Subarea Model Grid along C-C' and D-D'
Faro Mine Remediation Project

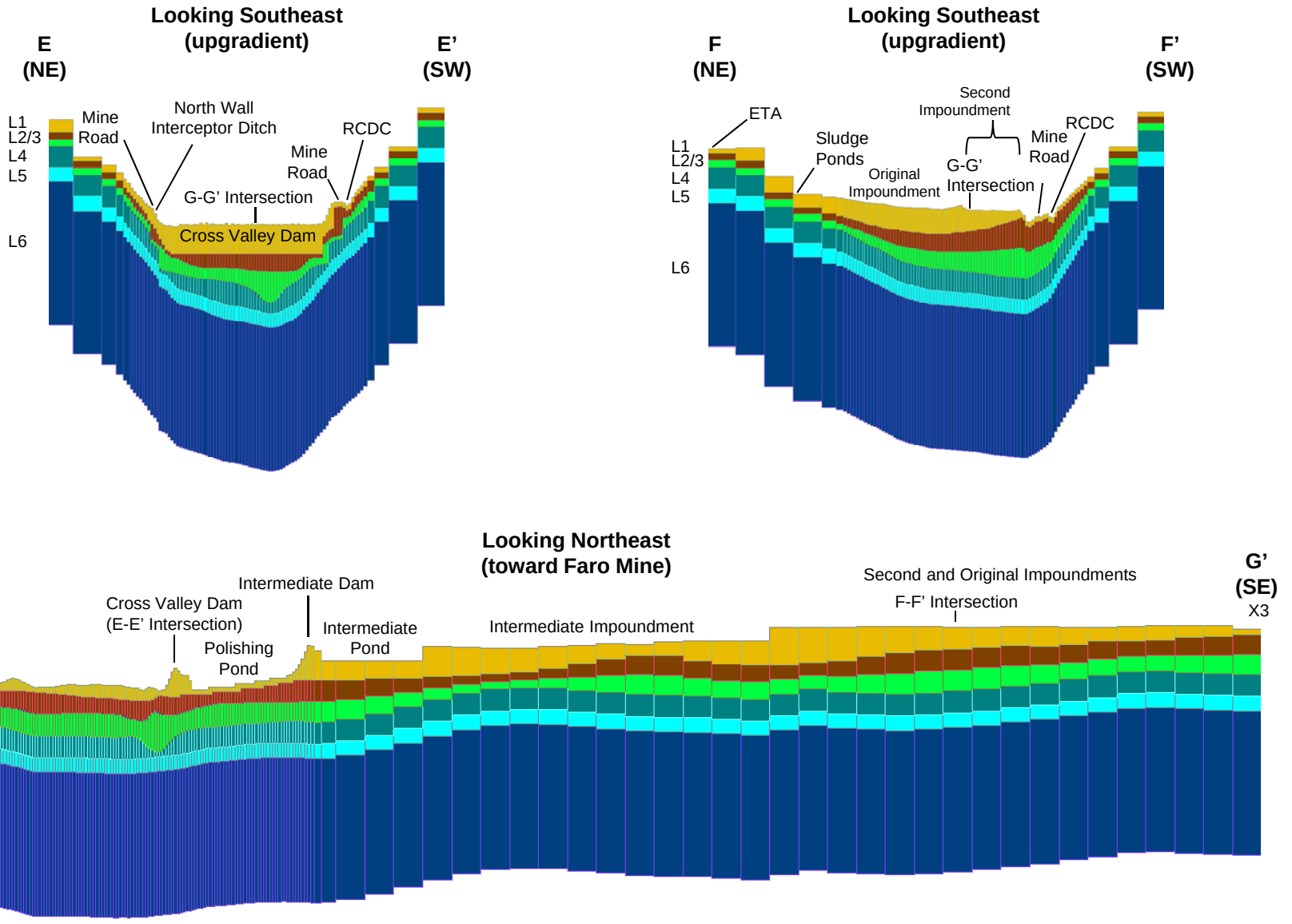

Notes
1. Images are not to scale and are vertically exaggerated by a factor of 5.
2. Figure 3-7 depicts the locations of E-E', F-F', and G-G'.

FIGURE 3-10
Profile Views of the RCAA Subarea Model Grid along E-E', F-F', and G-G'
Faro Mine Remediation Project

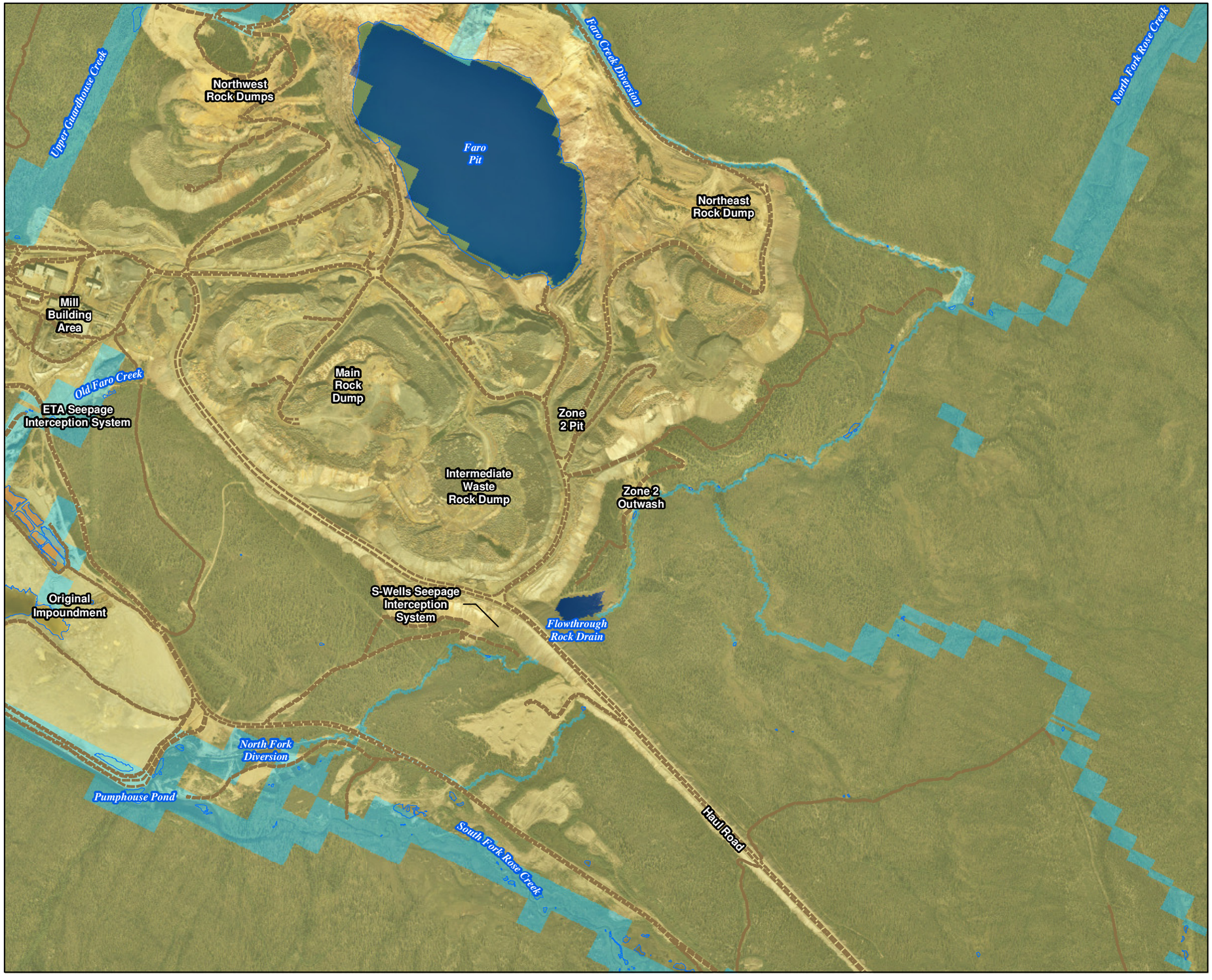

VICINITY MAP

LEGEND

- Roads Unpaved
- Lake, Pond, or Pool

Boundary Condition

- Specified Flux (Groundwater Recharge from Precipitation)
- Specified Head (Faro Pit Lake and Ponds)
- Head-dependent Flux (Streams)
- Groundwater Flow Modelling Boundary (No-flow Boundary)

Notes:

1. A no-flow boundary is also located at the bottom of Model Layer 6.
2. Aerial photography acquired by Peregrine Aerial Surveyors Inc. and Eagle Mapping in August 2012.
3. Orthophotography prepared by Critigen Canada Corp.

N

0 150 300 450 600

Metres

Created by: CRITIGEN

FIGURE 3-11

Groundwater Flow Model Boundary Conditions: NFRC Subarea Model

Faro Mine Remediation Project

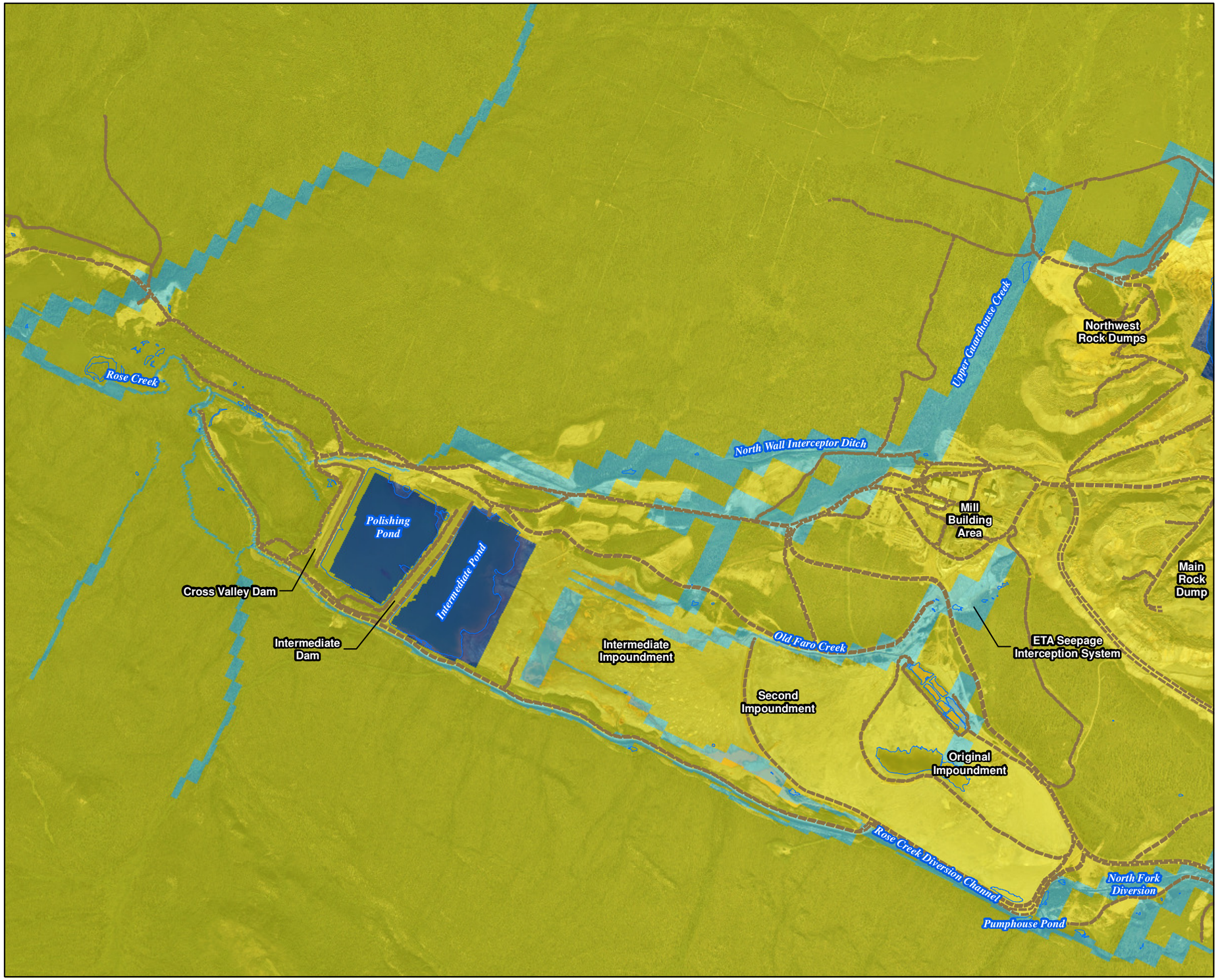

VICINITY MAP

LEGEND

- Roads Unpaved
- Lake, Pond, or Pool

Boundary Condition

- Specified Flux (Groundwater Recharge from Precipitation)
- Specified Head (Faro Pit Lake and Ponds)
- Head-dependent Flux (Streams)
- Groundwater Flow Modelling Boundary (No-flow Boundary)

Notes:

1. A no-flow boundary is also located at the bottom of Model Layer 6.
2. Aerial photography acquired by Peregrine Aerial Surveyors Inc. and Eagle Mapping in August 2012.
3. Orthophotography prepared by Critigen Canada Corp.

N

0 180 360 540 720

Metres

Created by: CRITIGEN

FIGURE 3-12

Groundwater Flow Model Boundary Conditions: RCAA Subarea Model

Faro Mine Remediation Project

R:\FAROMINE_20000342\MAPFILES\WATERMODELANALYSISRPT\FIG03_12.MXD ECLARK 2/25/2013 1:39:21 PM

CH2MHILL

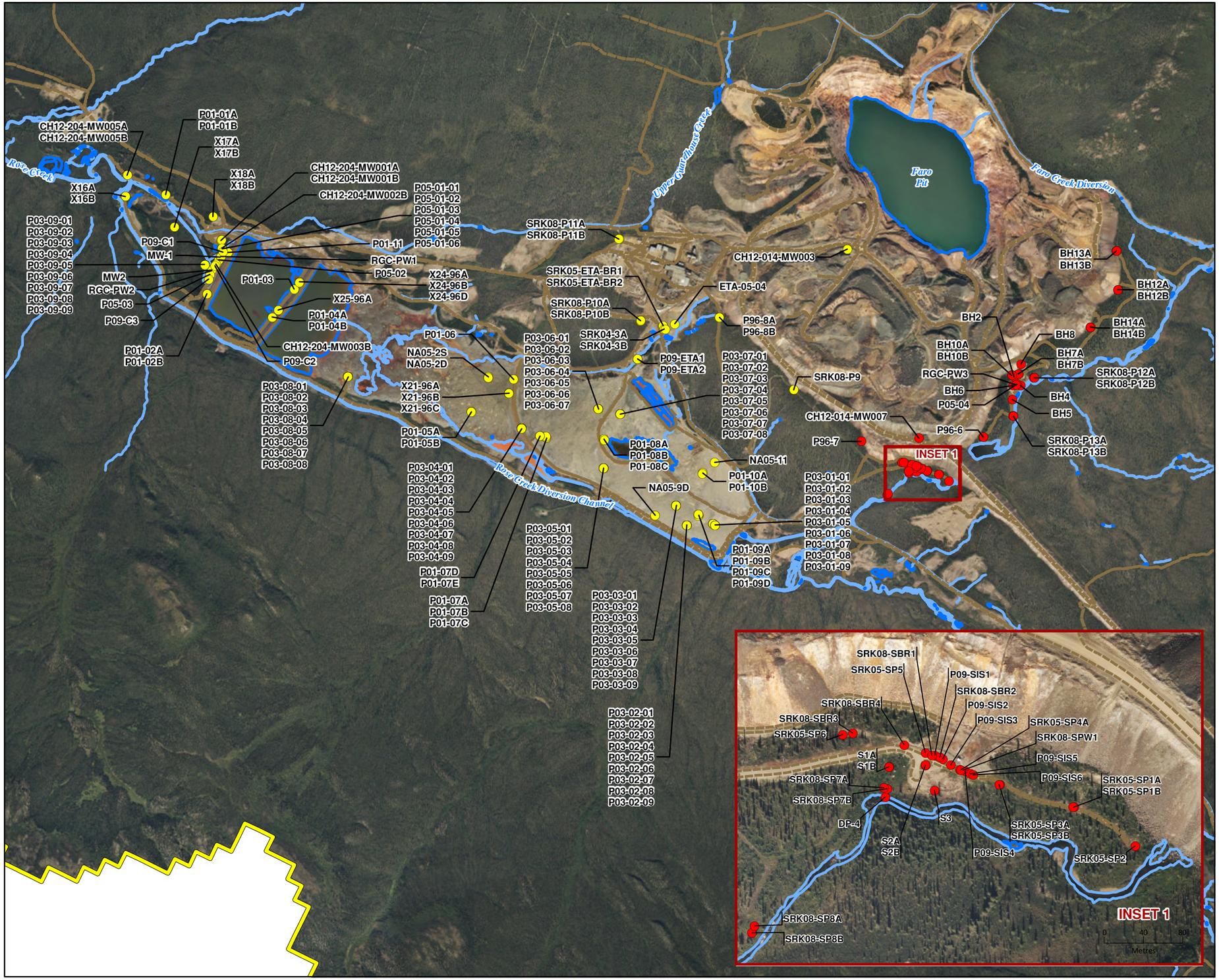

VICINITY MAP

LEGEND

- RCAA Subarea Model Target Head Location
- NFRC Subarea Model Target Head Location
- Roads Unpaved
- Stream
- Lake, Pond, or Pool
- Groundwater Flow Modelling Boundary

Notes:

1. Aerial photography acquired by Peregrine Aerial Surveyors Inc. and Eagle Mapping in August 2012.
2. Orthophotography prepared by Critigen Canada Corp.

N

0 300 600 900 1,200

Metres

Created by: CRITIGEN

FIGURE 3-13

Groundwater Model Calibration Target Locations

Faro Mine Remediation Project

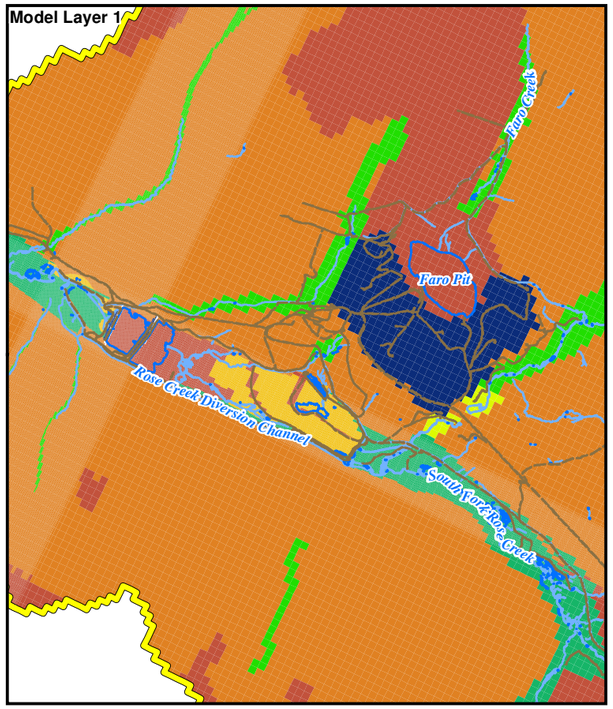

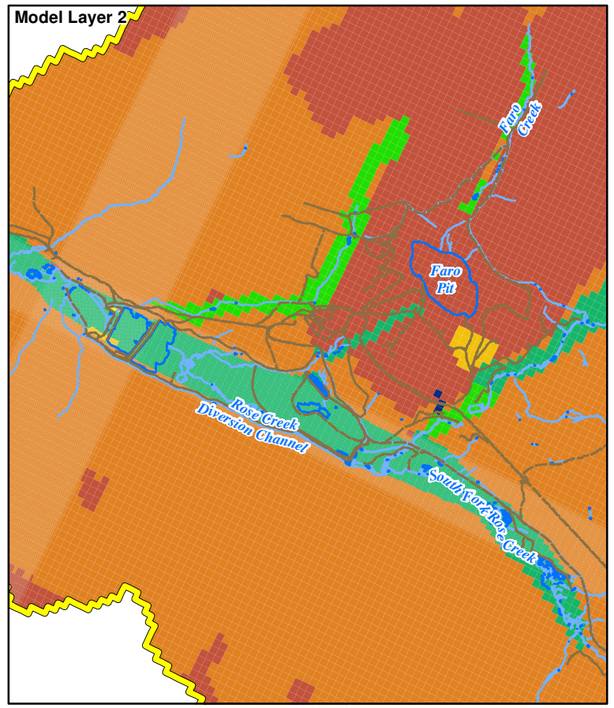

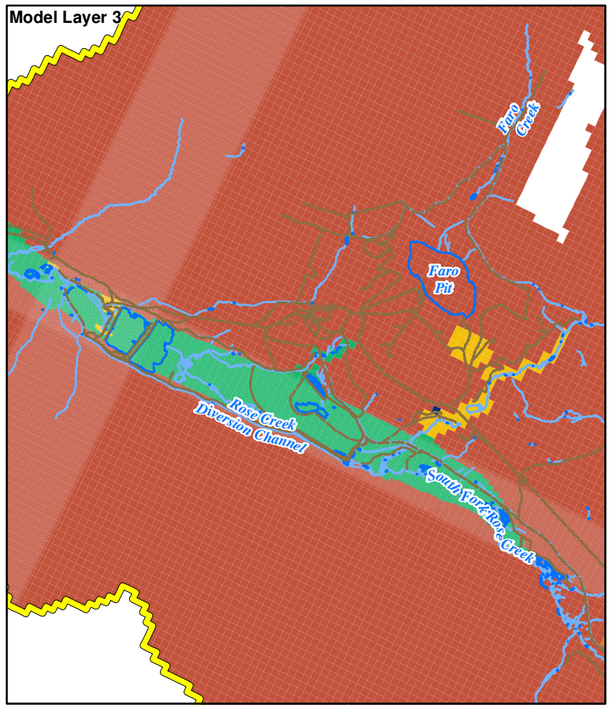

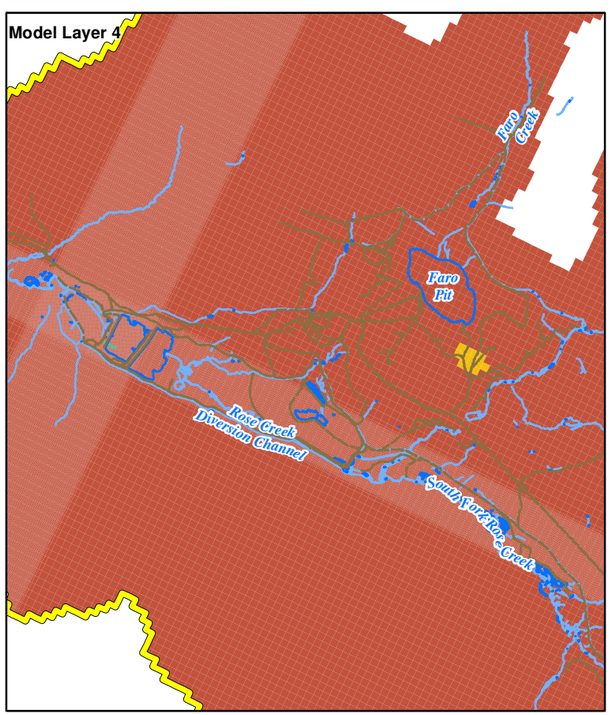

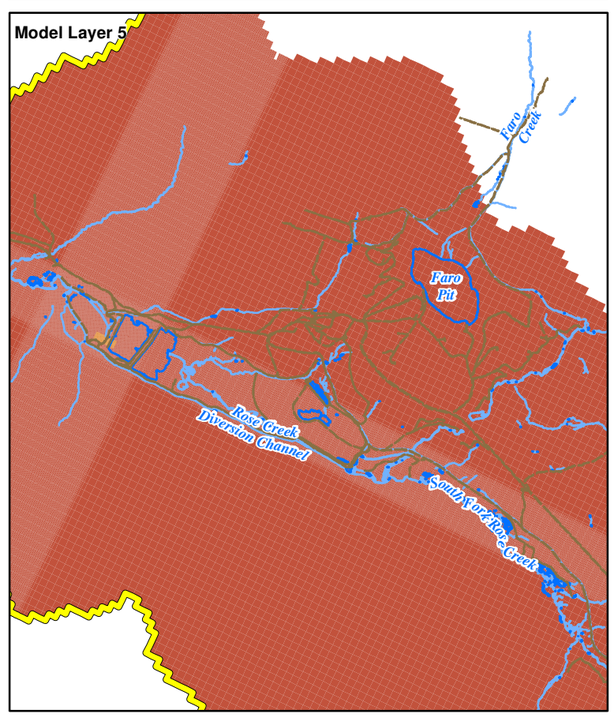

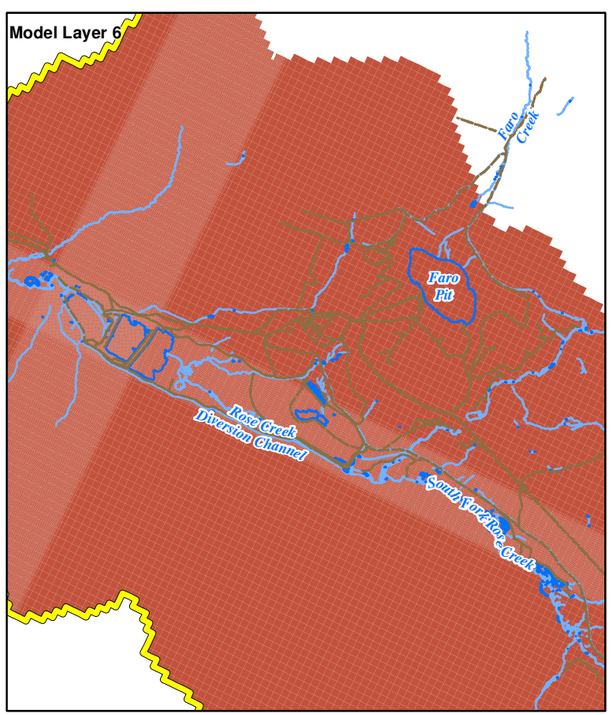

VICINITY MAP

LEGEND

- Roads Unpaved
- Stream
- Lake, Pond, or Pool
- Groundwater Flow Modelling Boundary

Horizontal Hydraulic Conductivity (m/day)

- <= 0.1
- 0.1 to 1
- 1 to 5
- 5 to 10
- 10 to 25
- 25 to 50
- 50 to 75
- 75 to 195

Notes:
1. Horizontal hydraulic conductivity taken from the RCAA Subarea Model.
2. Aerial photography acquired by Peregrine Aerial Surveyors Inc. and Eagle Mapping in August 2012.
3. Orthophotography prepared by Critigen Canada Corp.

N

0 1,000 2,000 3,000 4,000
Metres

Created by: CRITIGEN

FIGURE 3-14
Modelled Horizontal Hydraulic Conductivity
Faro Mine Remediation Project

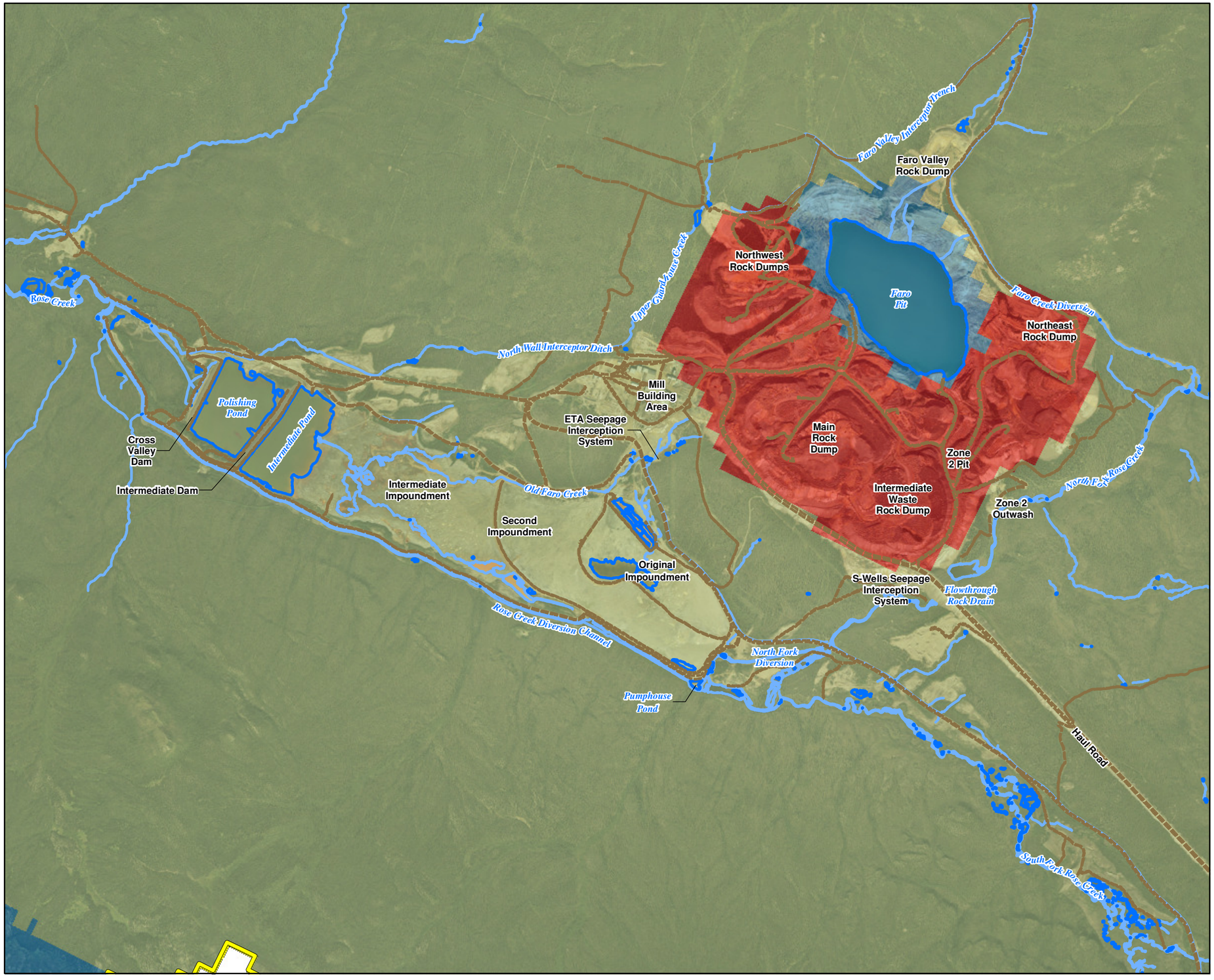

VICINITY MAP

LEGEND

- Roads Unpaved
- Stream
- Lake, Pond, or Pool
- Groundwater Flow Modelling Boundary

Groundwater Recharge from Precipitation (mm/yr)

- 3.7
- 14.6
- 51.1

Notes:
1. Groundwater recharge taken from the RCAA Subarea Model.
2. Aerial photography acquired by Peregrine Aerial Surveyors Inc. and Eagle Mapping in August 2012.
3. Orthophotography prepared by Critigen Canada Corp.

N

0 250 500 750 1,000
Metres

Created by: CRITIGEN

FIGURE 3-15
Modelled Groundwater Recharge
Faro Mine Remediation Project

CH2MHILL

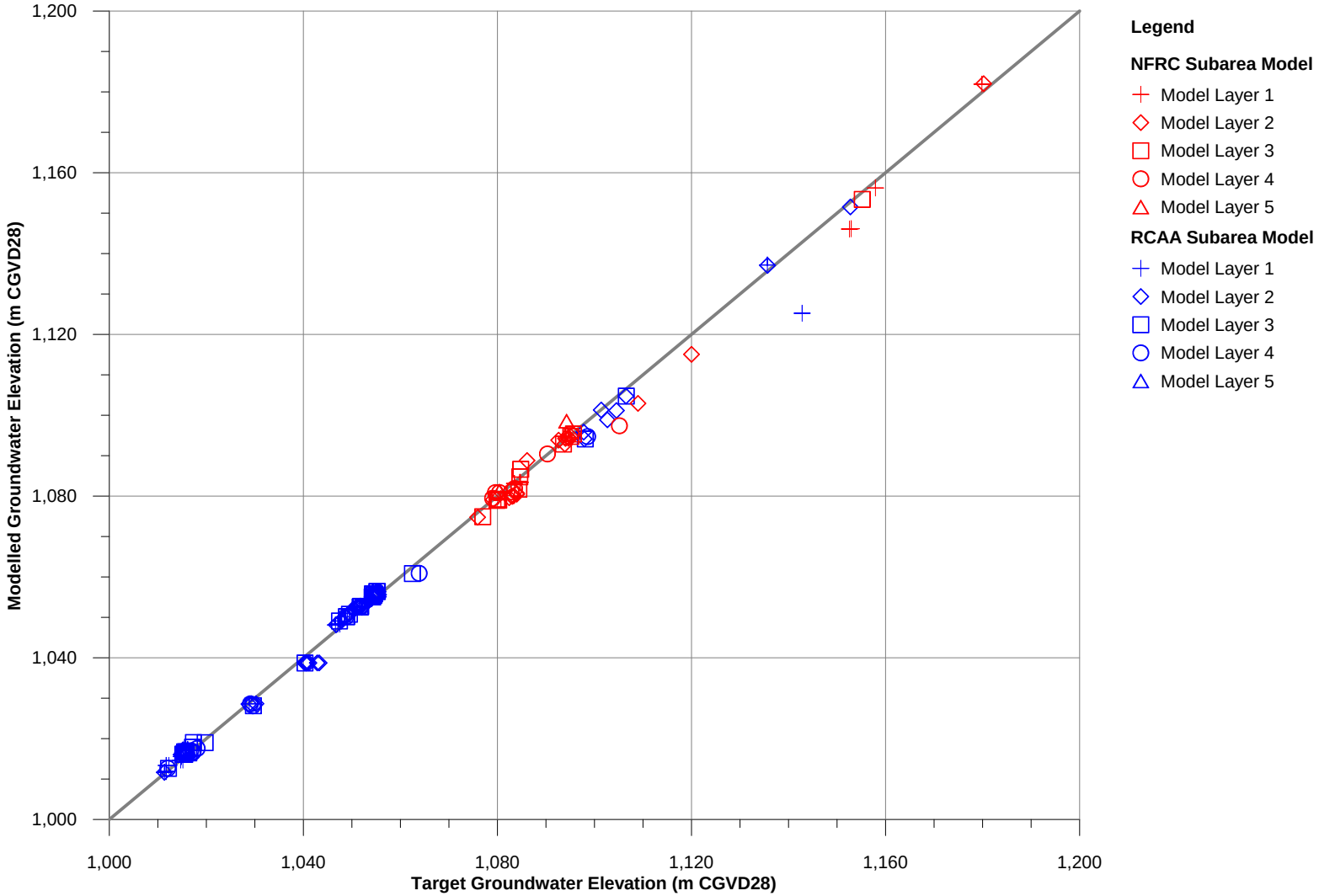

FIGURE 3-16
Modelled versus Target Groundwater Elevations
Faro Mine Remediation Project

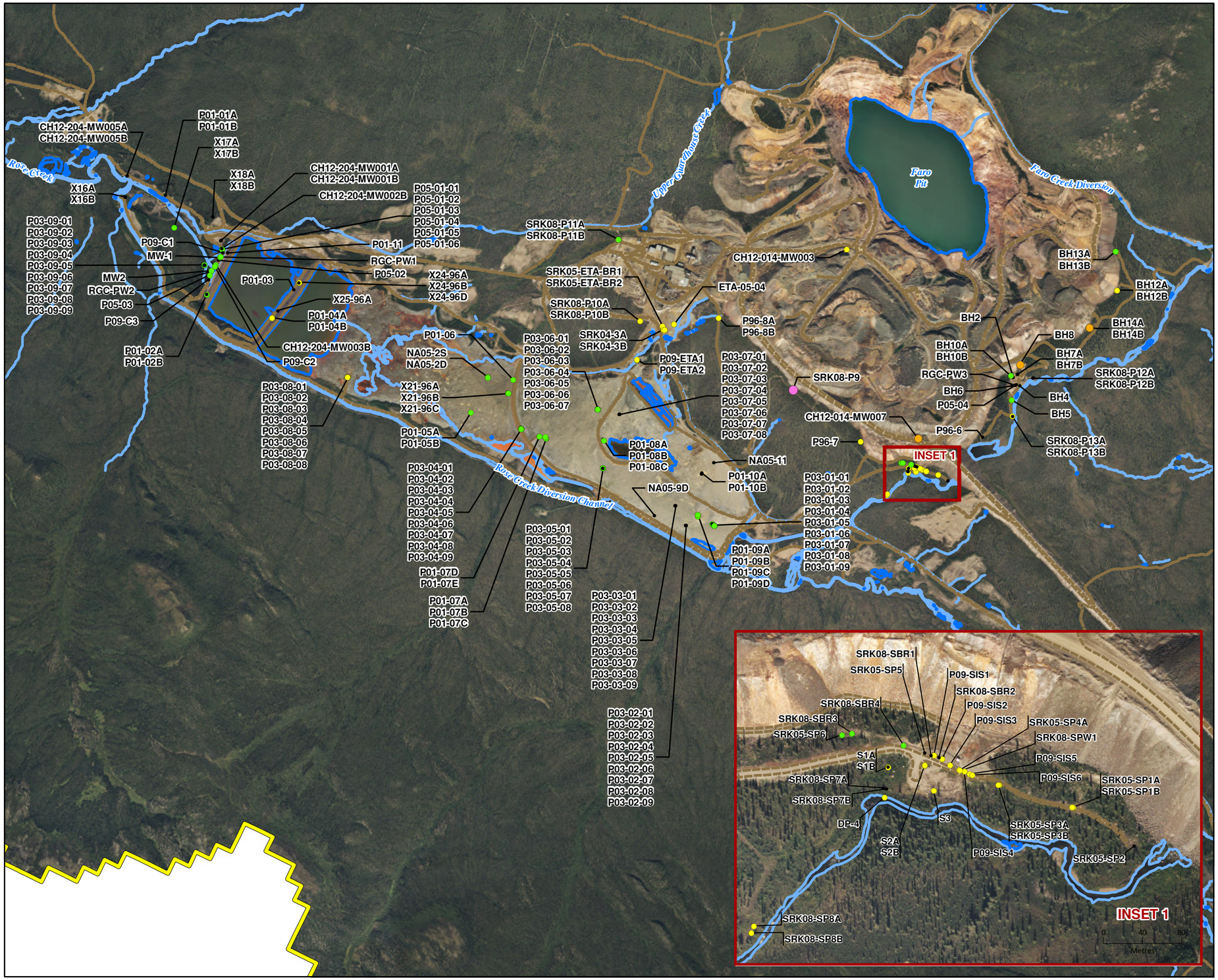

VICINITY MAP

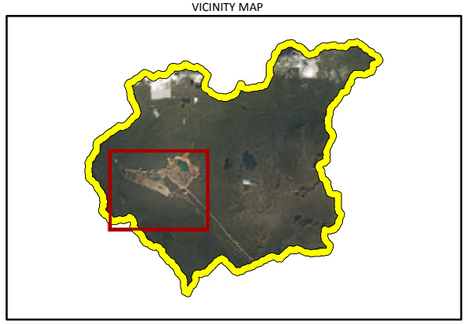

LEGEND

Residual Error (m)

- 10 to 17.7
- 5 to 10
- 1 to 5
- -1 to 1
- -5 to -1
- -10 to -5
- -17.7 to -10

Roads Unpaved

Stream

Lake, Pond, or Pool

Groundwater Flow Modelling Boundary

Notes:

1. Residual error equals the modelled head valve minus the target head valve.
2. Aerial photography acquired by Peregrine Aerial Surveyors Inc. and Eagle Mapping in August 2012.
3. Orthophotography prepared by Critigen Canada Corp.

N

0 300 600 900 1,200

Metres

Created by: CRITIGEN

FIGURE 3-17

Spatial Distribution of Residual Errors in Modelled Groundwater Elevations

Faro Mine Remediation Project

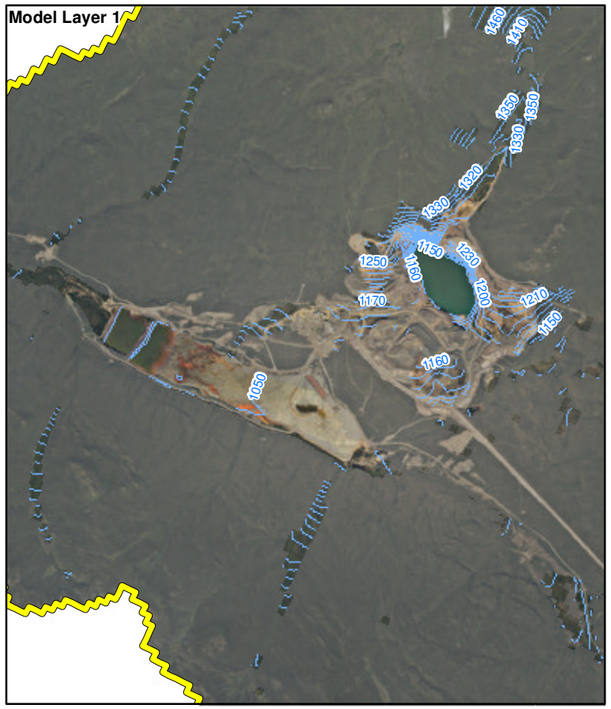

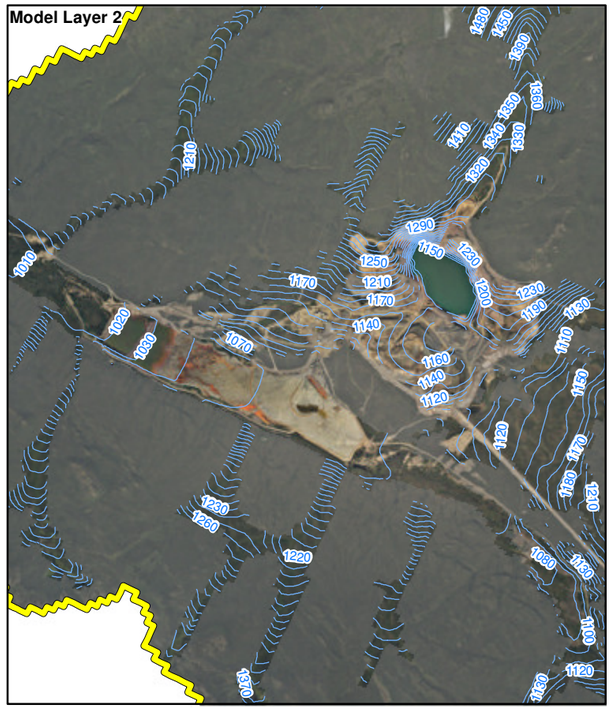

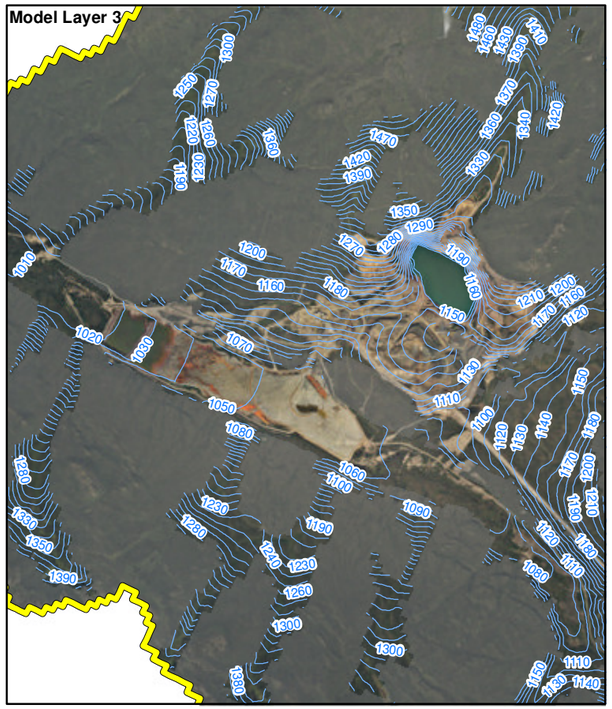

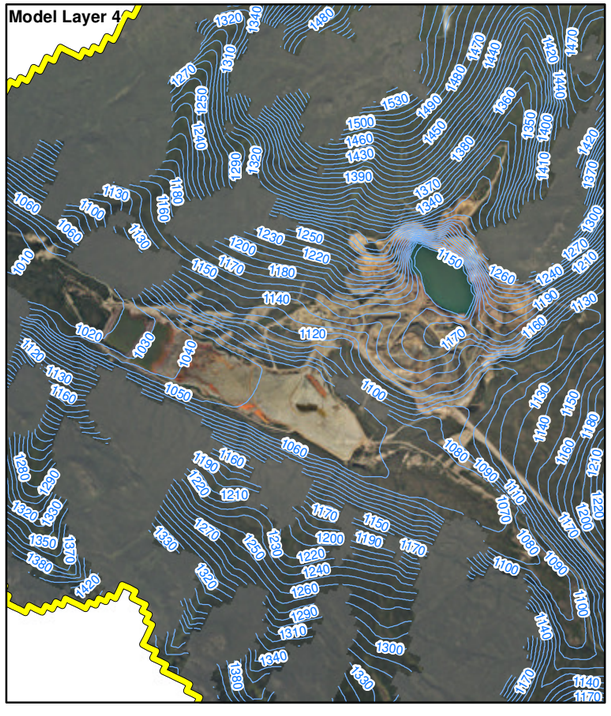

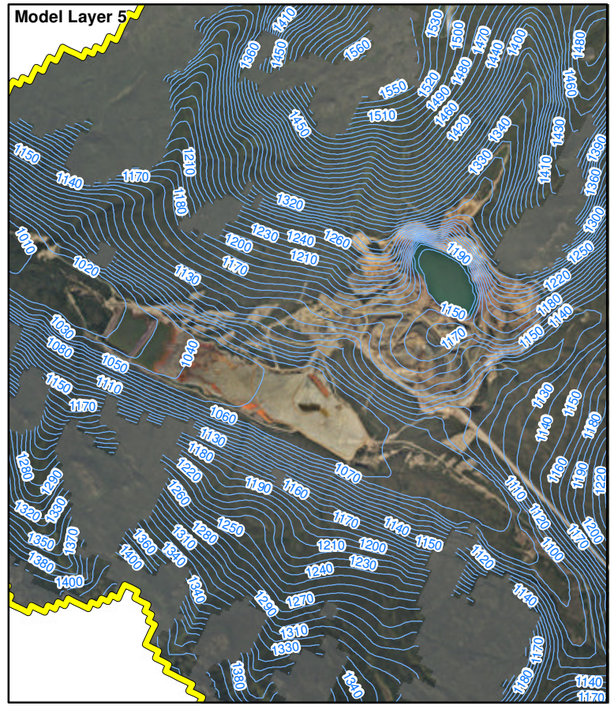

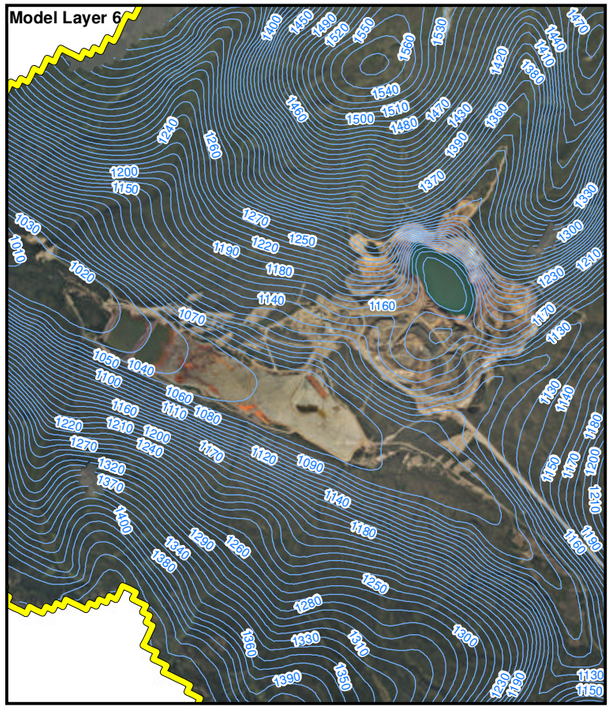

VICINITY MAP

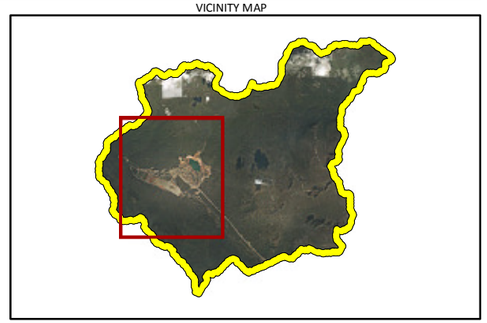

LEGEND

- Potentiometric Surface Contour (m CGVD28)
- Dry Cell
- Groundwater Flow Modelling Boundary

Notes:
1. Contours are displayed at an interval of 10 metres.
2. Aerial photography acquired by Peregrine Aerial Surveyors Inc. and Eagle Mapping in August 2012.
3. Orthophotography prepared by Critigen Canada Corp.

N

0 1,000 2,000 3,000 4,000

Metres

Created by: CRITIGEN

FIGURE 3-18
Modelled Potentiometric Surfaces
Faro Mine Remediation Project

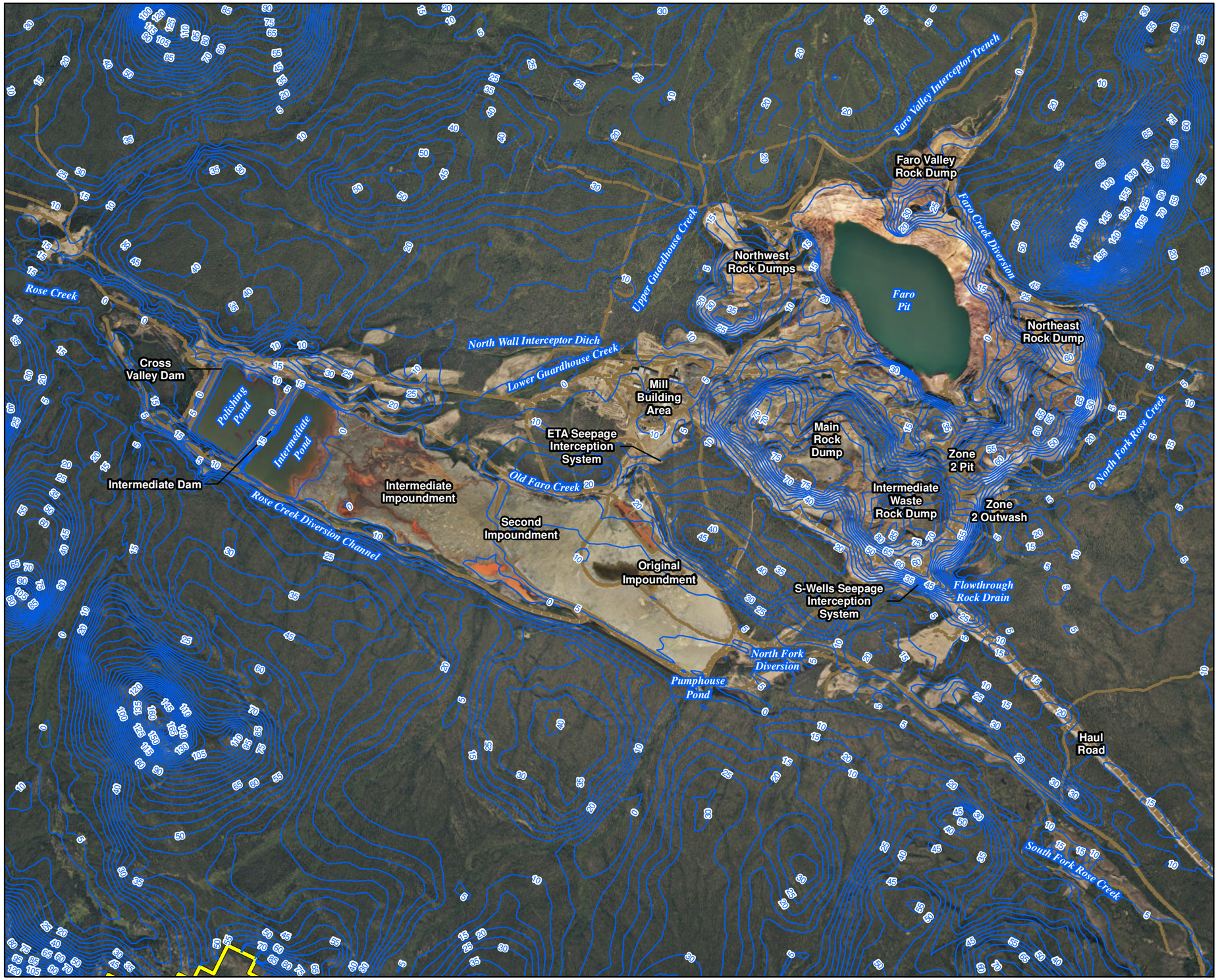

VICINITY MAP

LEGEND

- Roads Unpaved
- Contour of Depth to Groundwater (m bgs)
- Groundwater Flow Modelling Boundary

Notes:
1. Contours are displayed at an interval of 5 m.
2. Aerial photography acquired by Peregrine Aerial Surveyors Inc. and Eagle Mapping in August 2012.
3. Orthophotography prepared by Critigen Canada Corp.

N

0 250 500 750 1,000
Metres

Created by:
CRITIGEN

FIGURE 3-19
Modelled Depth to Groundwater
Faro Mine Remediation Project

CH2MHILL

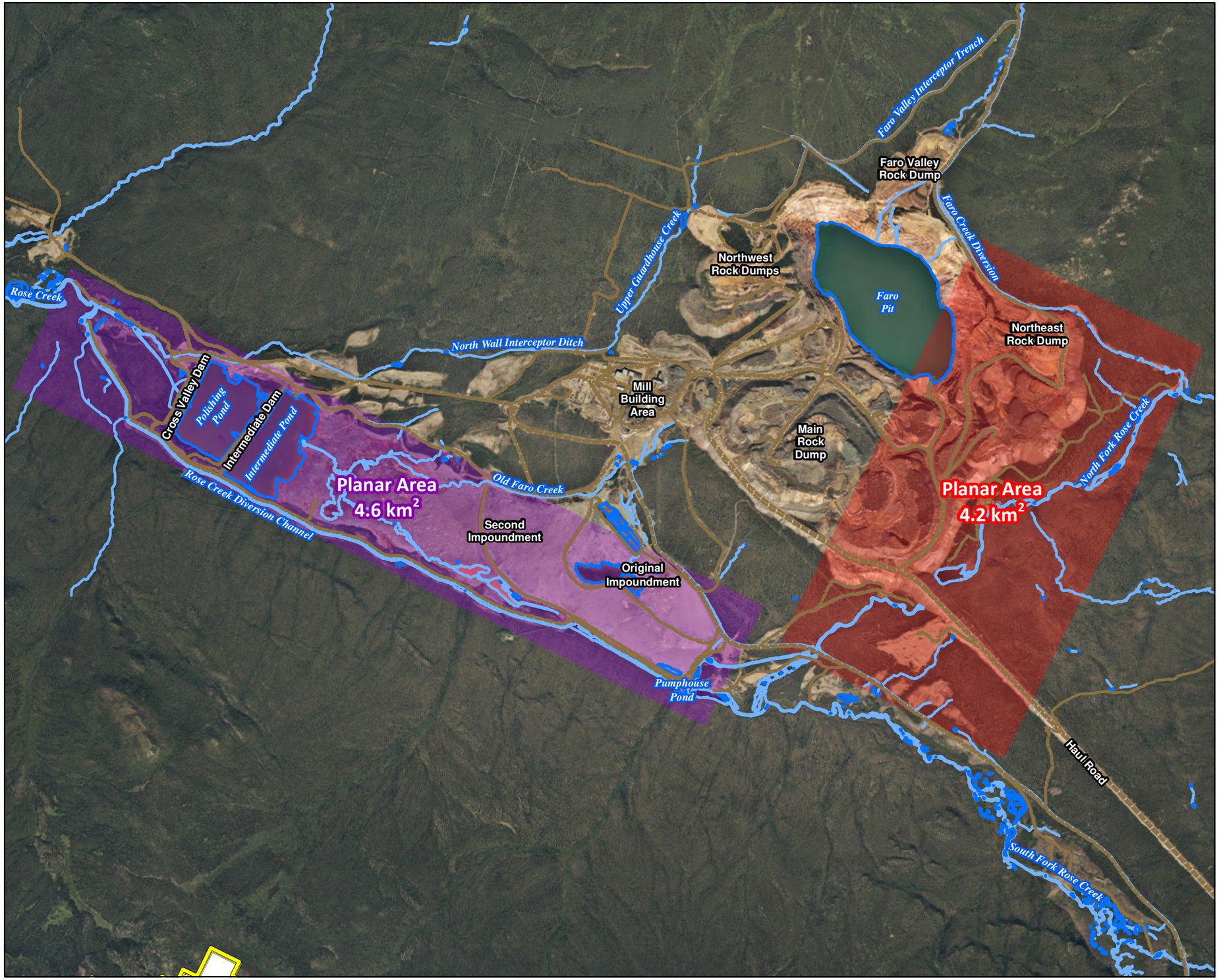

VICINITY MAP

LEGEND

- Roads Unpaved
- Stream
- Lake, Pond, or Pool
- Groundwater Balance Subarea: RCAA Subarea Model
- Groundwater Balance Subarea: NFRC Subarea Model
- Groundwater Flow Modelling Boundary

Notes:
1. Aerial photography acquired by Peregrine Aerial Surveyors Inc. and Eagle Mapping in August 2012.
2. Orthophotography prepared by Critigen Canada Corp.

N

0 250 500 750 1,000
Metres

Created by: CRITIGEN

FIGURE 3-20
Subareas Used to Compute Groundwater Balances in the NFRC and RCAA Subarea Models
Faro Mine Remediation Project

CH2MHILL

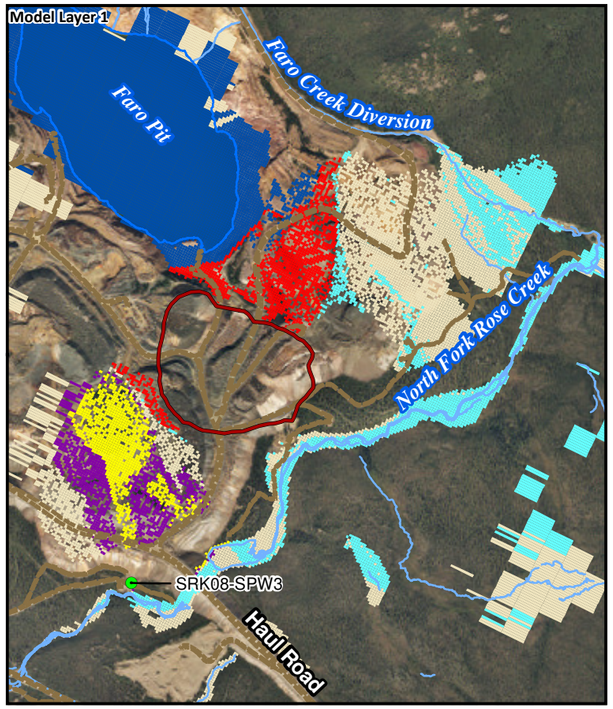

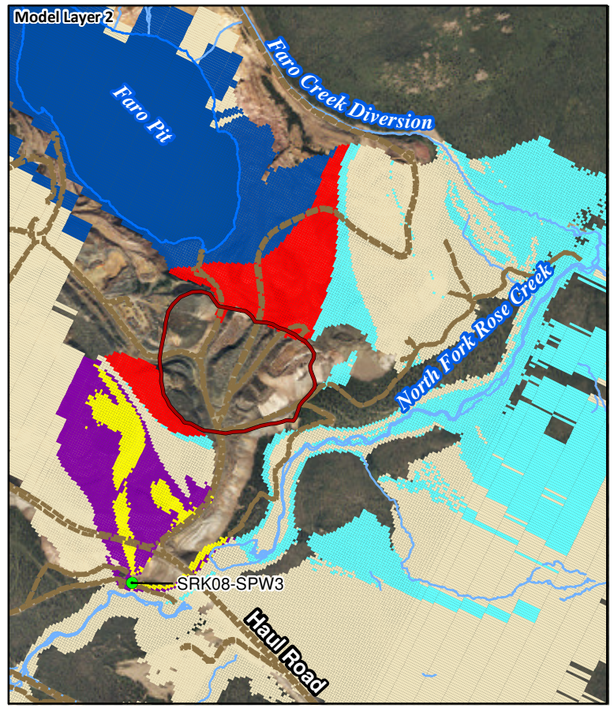

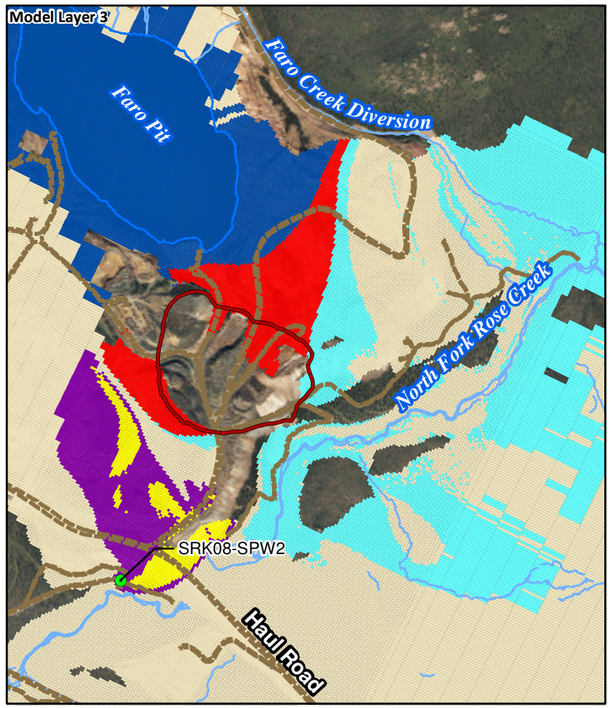

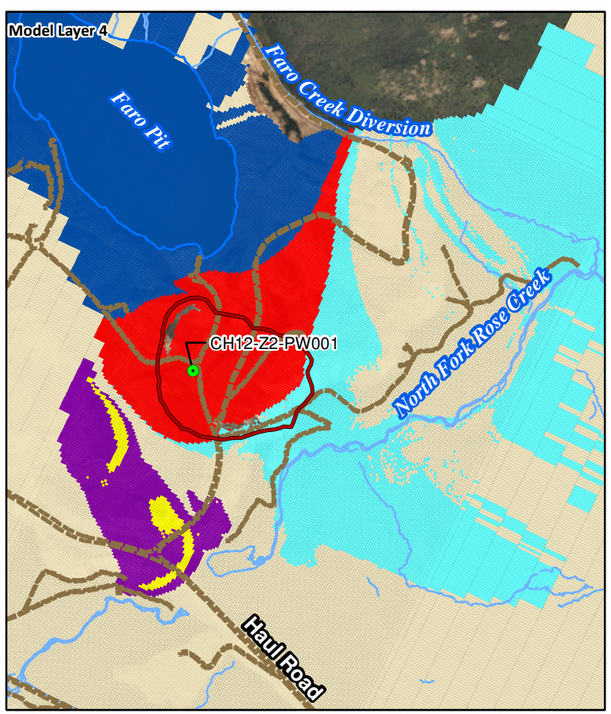

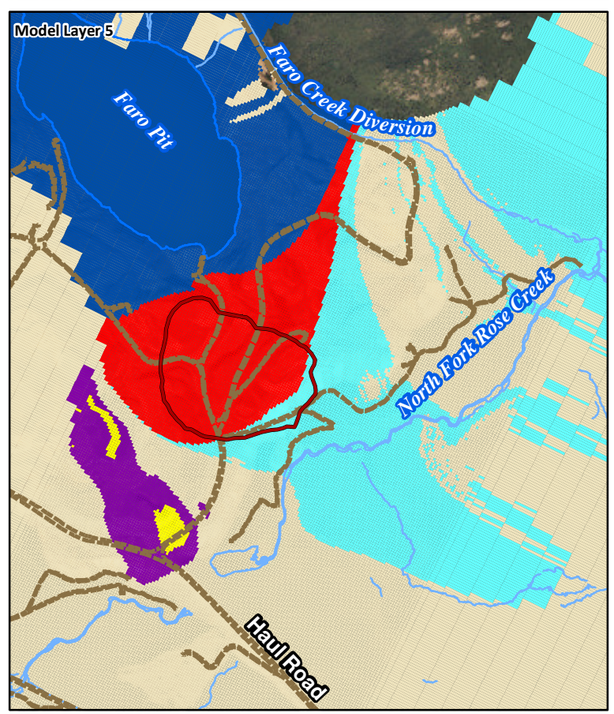

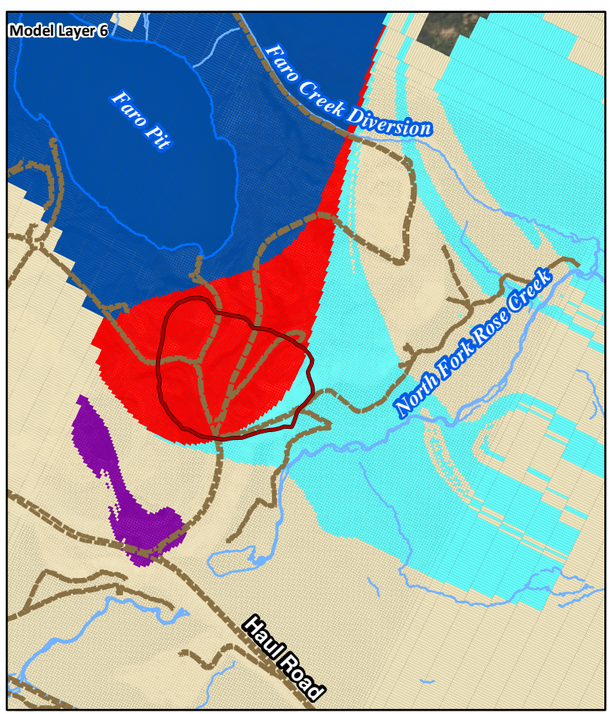

VICINITY MAP

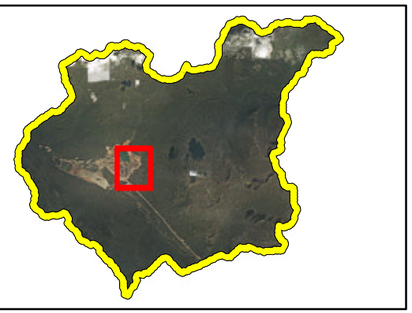

LEGEND

- Modelled Extraction Well
- Roads Unpaved
- Streams
- Lake, Pond, or Pool
- Zone 2 Pit Outline

Destination of Modelled Particle

- CH12-Z2-PW001
- SRK08-SPW3
- SRK08-SPW2
- NFRC
- Faro Pit
- Downgradient Location Not Otherwise Indicated

Notes

1. Particle starting cells are symbolized by a color representing the destination at which the particle ended.
2. Particles were started at the vertical midpoints of each cell and tracked forward (downgradient) until reaching the feature indicated in the legend.
3. Areas with no assigned destination color indicate the model layer is dry at that particular model cell.
4. CH12-Z2-PW001 is screened in Model Layer 4, SRK08-SPW2 is screened in Model Layer 3, and SRK08-SPW3 is screened in Model Layers 1 and 2.
5. Aerial Photography acquired by Peregrine Aerial Surveyors Inc. and Eagle Mapping in August 2012.
6. Orthophotography prepared by Critigen Canada Corp.

N

0 240 480 720 960

Metres

Created by: CRITIGEN

FIGURE 3-21

Modelled Hydraulic Capture of the Existing S-Wells SIS and the Zone 2 Pit Extraction Well

Faro Mine Remediation Project

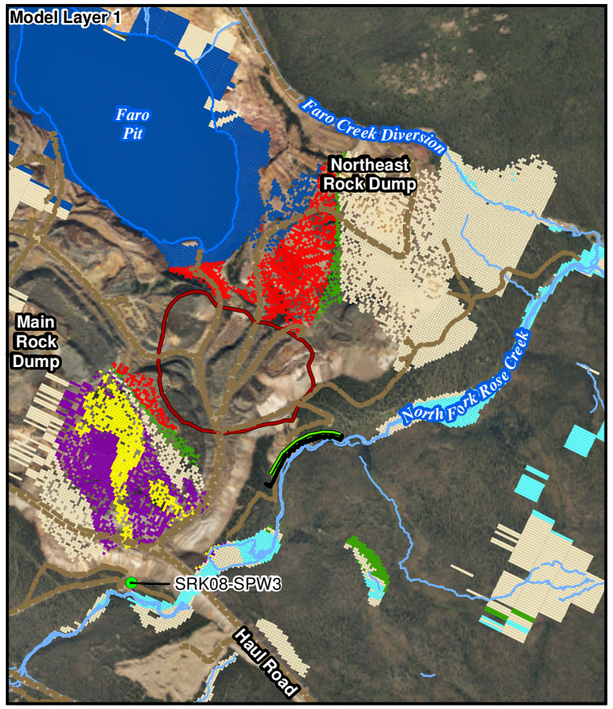

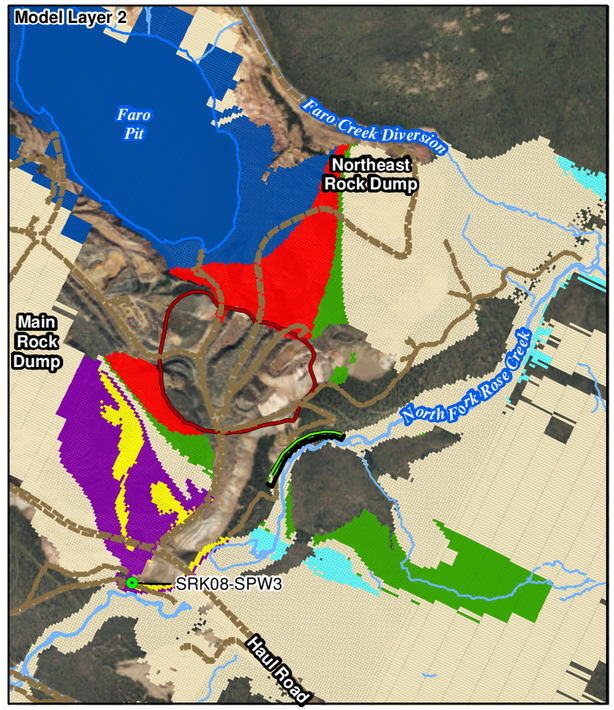

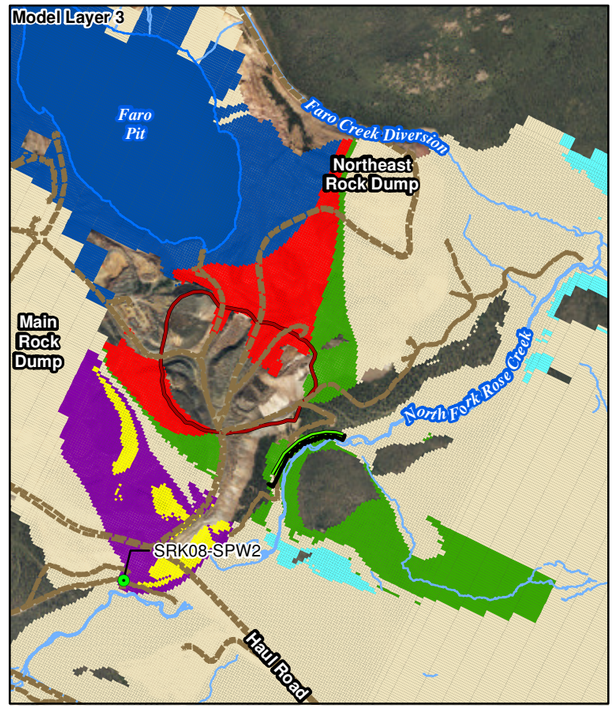

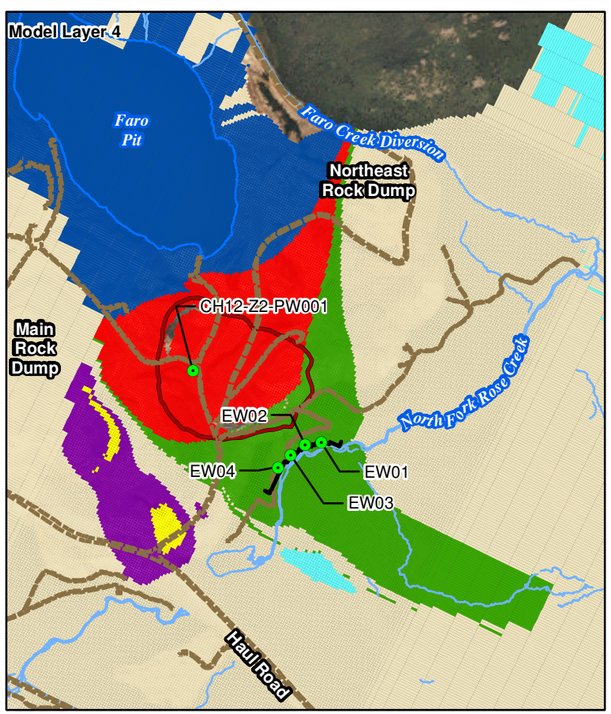

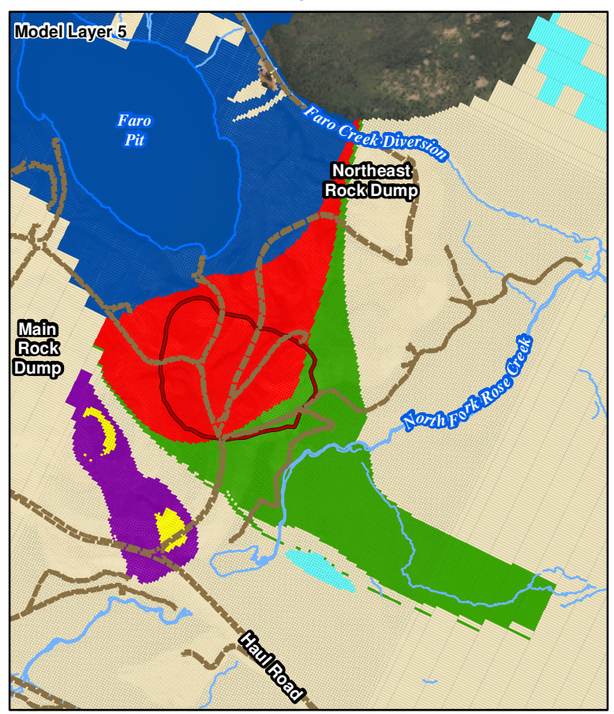

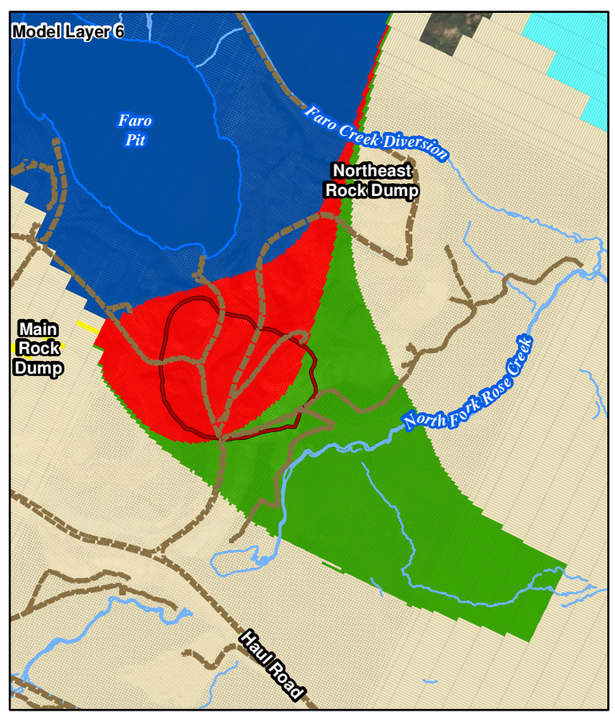

VICINITY MAP

LEGEND

- Modelled Extraction Well
- Hypothetical Slurry Wall
- Modelled Zone 2 Outwash Trench
- Roads Unpaved
- Stream
- Lake, Pond, or Pool
- Zone 2 Pit Outline

Destination of Modelled Particle

- CH12-Z2-PW001
- SRK08-SPW3
- SRK08-SPW2
- NFRC
- Faro Pit
- Hypothetical Zone 2 Outwash SIS
- Downgradient Location Not Otherwise Indicated

Notes

1. Particle starting cells are symbolized by a color representing the destination at which the particle ended.
2. Particles were started at the vertical midpoints of each cell and tracked forward (downgradient) until reaching the feature indicated in the legend.
3. Areas with no assigned destination color indicate the model layer is dry at that particular model cell.
4. CH12-Z2-PW001 is screened in Model Layer 4; SRK08-SPW2 is screened in Model Layer 3; SRK08-SPW3 is screenedin Model Layers 1 and 2; hypothetical Zone 2 OutwashTrench is located in Model Layers 1, 2, and 3; and EW01through EW04 (hypothetical Zone 2 Outwash bedrockextraction wells) are screened in Model Layer 4.
5. Aerial Photography acquired by Peregrine Aerial Surveyors Inc. and Eagle Mapping in August 2012.
6. Orthophotography prepared by Critigen Canada Corp.

N

0 240 480 720 960

Metres

Created by: CRITIGEN

FIGURE 3-22

Modelled Hydraulic Capture of the Zone 2 Pit and Outwash Under Assumed Operation of a Hypothetical SIS

Faro Mine Remediation Project

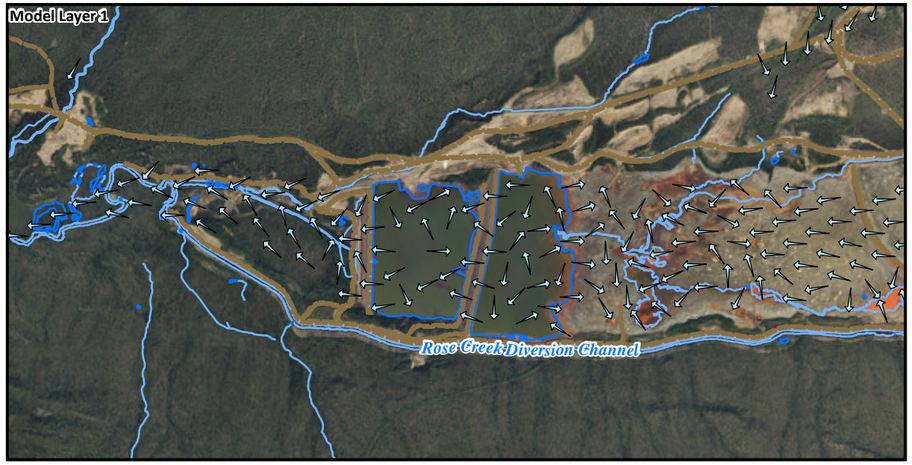

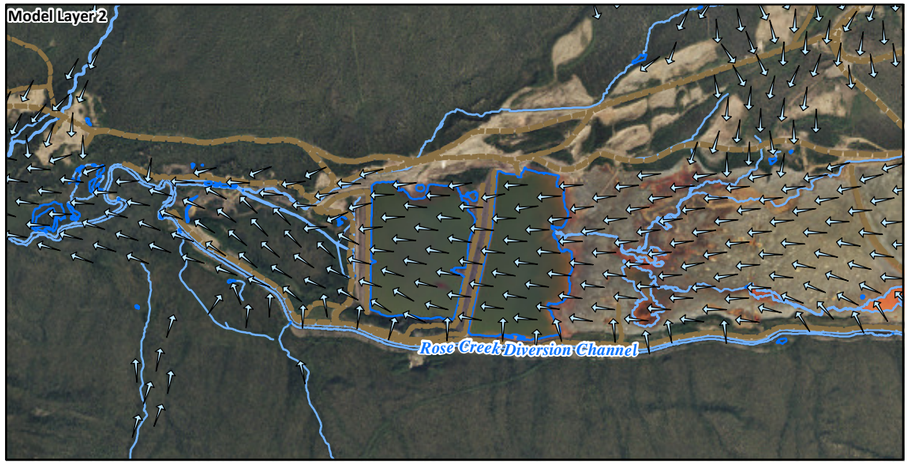

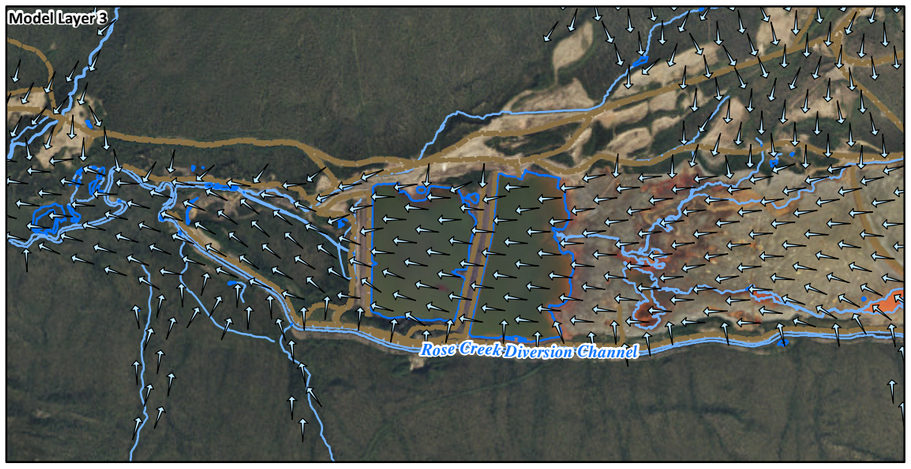

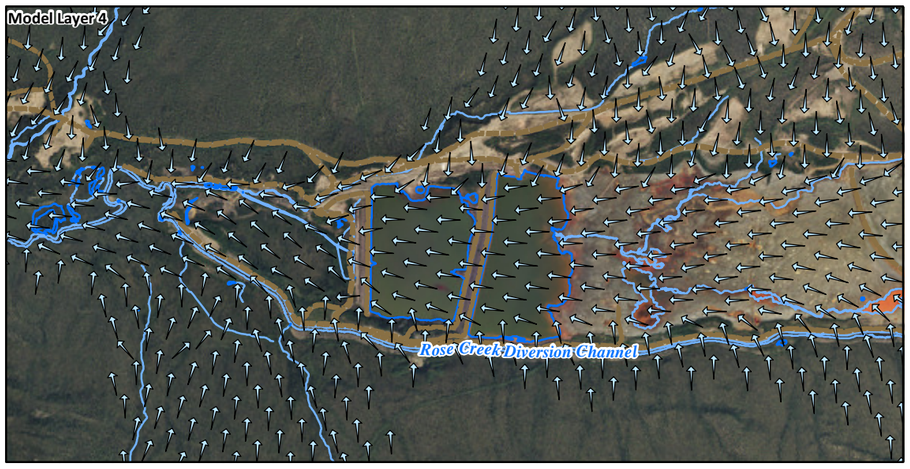

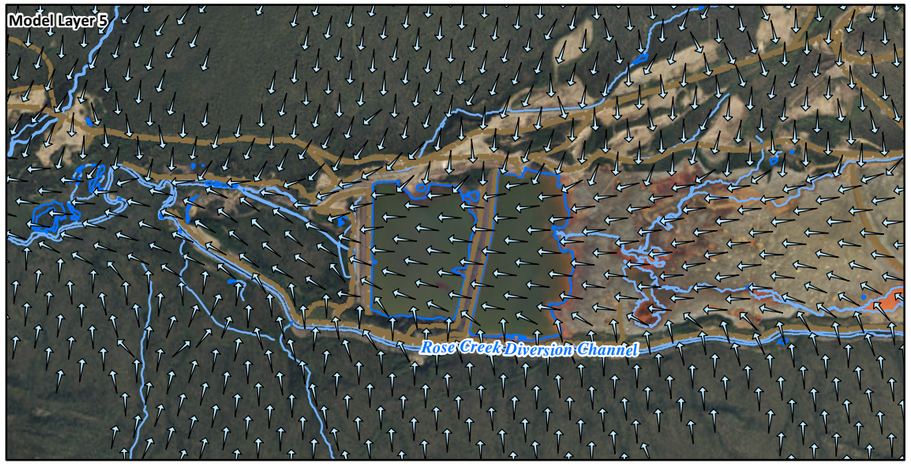

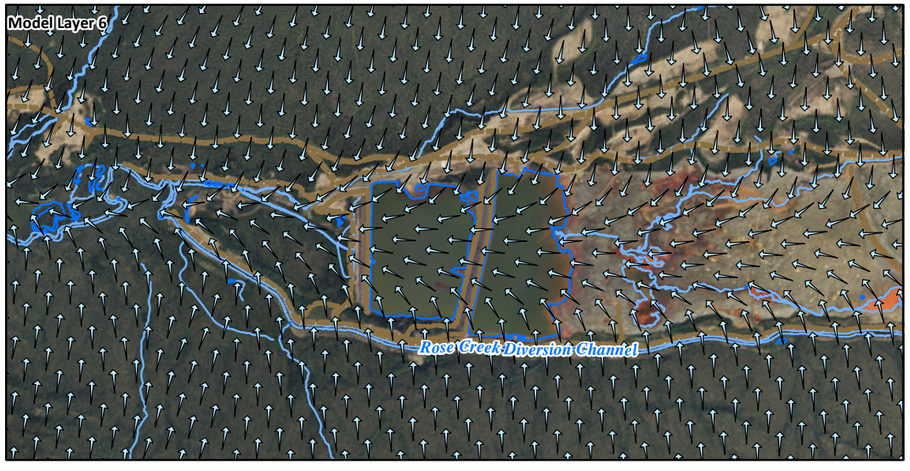

VICINITY MAP

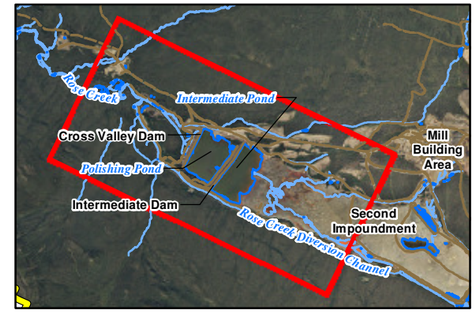

LEGEND

- Lateral Groundwater Flow Direction
- Roads Unpaved
- Stream
- Lake, Pond, or Pool
- Groundwater Flow Modelling Boundary

Notes
1. Lateral groundwater flow direction arrows are displayed on 100-m centers in the saturated portions of each model layer.
2. Aerial photography acquired by Peregrine Aerial Surveyors Inc. and Eagle Mapping in August 2012.
3. Orthophotography prepared by Critigen Canada Corp.

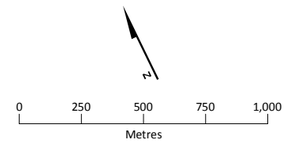

Created by:
CRITIGEN

FIGURE 3-23
Modelled Groundwater Flow Pathways in the RCAA Subarea Model Under Existing Conditions
Faro Mine Remediation Project

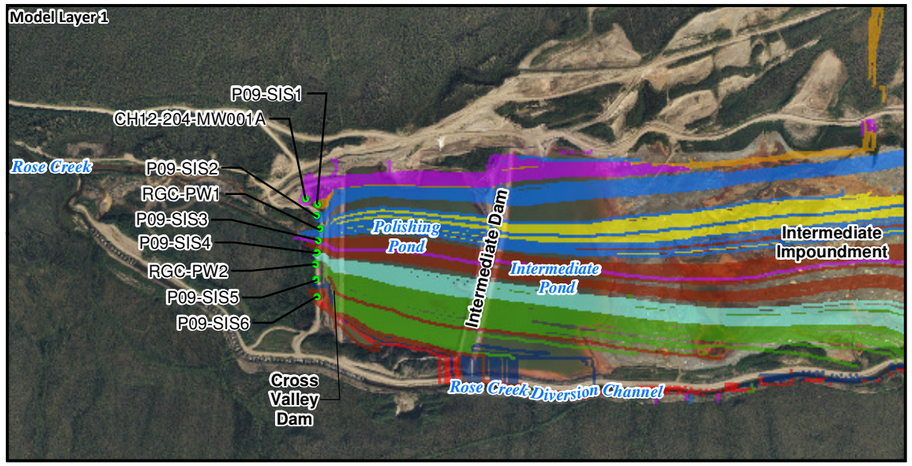

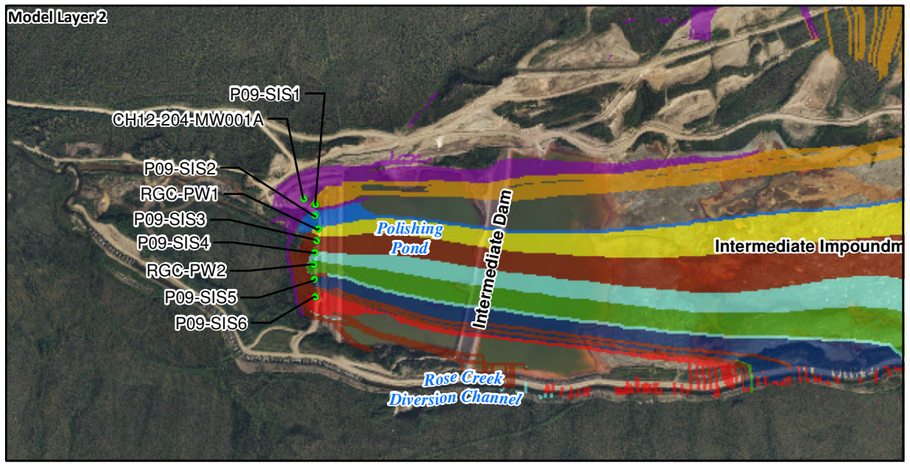

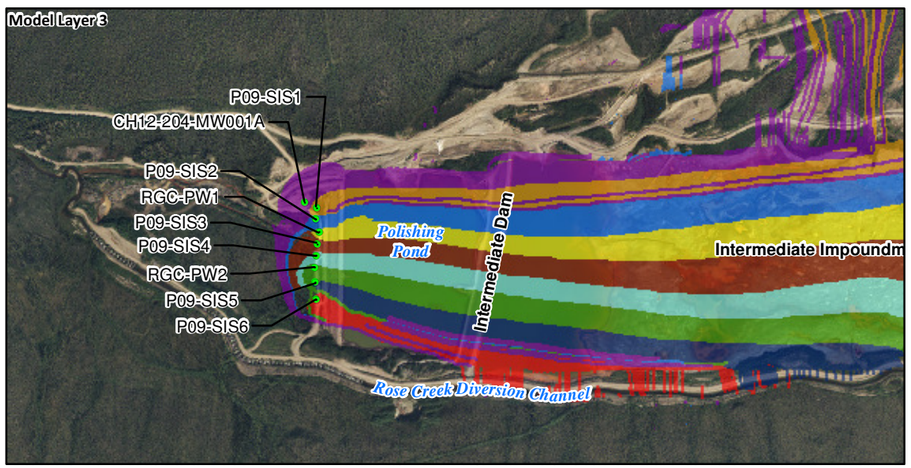

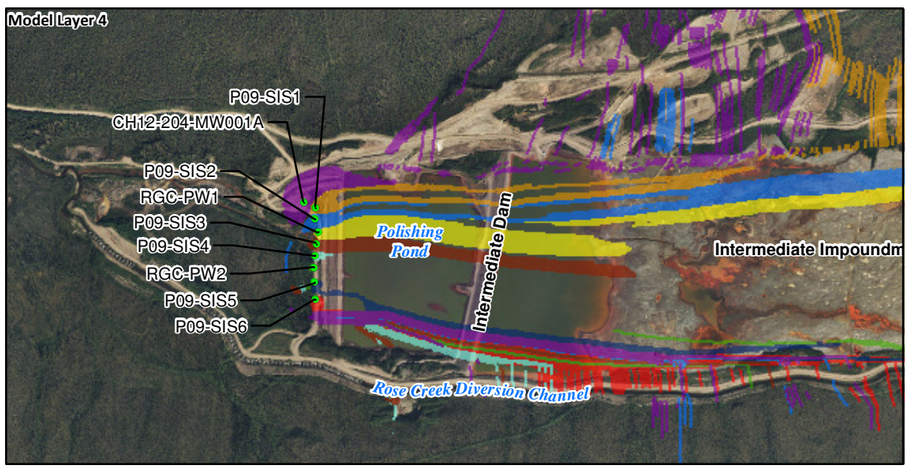

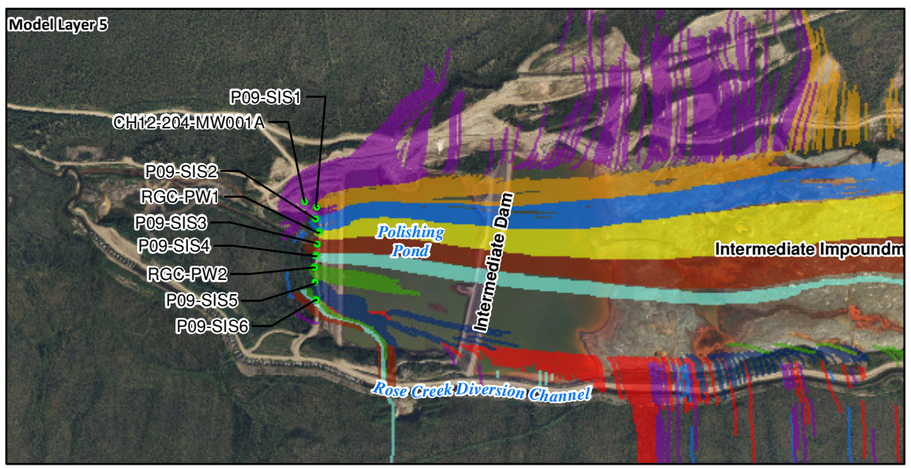

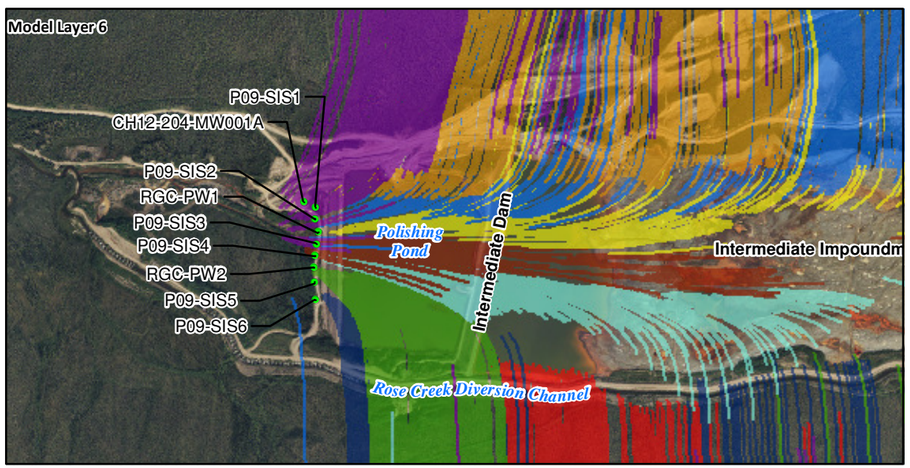

VICINITY MAP

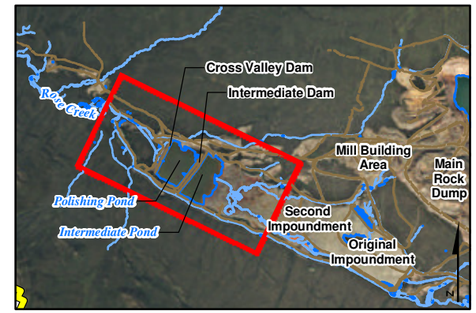

LEGEND

- Modelled Extraction Well
- MW-1A Particle Trace
- SIS1 Particle Trace
- SIS2 Particle Trace
- PW-1R Particle Trace
- SIS3 Particle Trace
- SIS4 Particle Trace
- PW2 Particle Trace
- SIS5 Particle Trace
- SIS6 Particle Trace

Notes
1. Particles were started at the upper, middle, and lower portions of each extraction well in Model Layers 2, 3, and 4 and tracked in reverse (upgradient) to delineate each capture zone.
2. Particle traces are only displayed for a given layer where the particles travel through that layer.
3. Aerial photography acquired by Peregrine Aerial Surveyors Inc. and Eagle Mapping in August 2012.
4. Orthophotography prepared by Critigen Canada Corp.

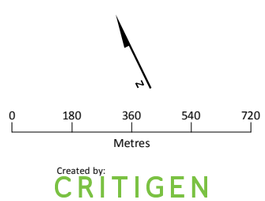

Created by: CRITIGEN

FIGURE 3-24
Modelled Hydraulic Capture Downgradient from the Cross Valley Dam Under Assumed Operation of a Hypothetical SIS
Faro Mine Remediation Project

SECTION 4

Geochemical Modelling

This section describes the development, calibration, and application of geochemical models that are being used to support the FMRP.

4.1 Geochemical Modelling Objectives

The overall geochemical modelling objective for the site is to build reliable predictive tools for future geochemical conditions. These geochemical tools integrate flow and chemistry of SW and GW with geochemical properties of solid materials (i.e., WRDs, tailings, and subsurface porous media). They will be used to inform remediation alternatives, identify important locations and constituents for continued testing and monitoring, and help assess potential ecological risk at designated receptor areas

The FY12 objectives associated with the geochemical modelling task were to evaluate the geochemical loading components of the existing GoldSim model and make improvements where appropriate. Notably, there was no reactive mixing associated with the Faro Pit or individual WRDs at the catchment level within the GoldSim model. The existing SRK tailings model was only developed for zinc and sulphate and did not account for reactive mixing and transport within the RCAA underlying the RCTA. Some key constituents of GW, including zinc, lead, and iron, are not consistent with current observed data at key locations, such as the Faro Pit Lake and the CVD. Accordingly, elements of the GoldSim model have been examined using geochemical reactive transport and reactive mixing models. These models account for known geochemical processes that occur between source and receiving areas and are designed to improve the predictive capabilities of the GoldSim model.

4.2 Geochemical Modelling Approach

In an effort to present the geochemical modelling approach used, a brief background and history of development for the GoldSim model is merited. SRK developed three main spreadsheet-based geochemical models for the FMC, as follows (SRK, 2004b, 2005, 2006c, 2009; GEEC, 2010):

- WRD model
- Faro Pit Lake model
- Tailings model

The WRD and tailings models were incorporated into the GoldSim model, whereas the Pit Lake model was left unfinished. To date, none of the SRK spreadsheet models has been made available to CH2M HILL for examination, manipulation, or for further enhancement, and it is not anticipated that these models will be available in the future. However, some components of these models are available within the existing GoldSim model. Moreover, within the GoldSim model, there are calculations established for each modelled WRD that do provide some limited insight into how SRK established the WRD geochemical spreadsheet-based models. Discussions referencing the GoldSim model in the remainder of this section refer to the original model (GEEC, 2010), referred to as model version 1.0 in a separate GoldSim update document (CH2M HILL, 2013b), unless otherwise described as the “updated” GoldSim model. Although numerous updates and additions have been implemented (CH2M HILL, 2013b), nearly all of the chemical parameters and formulas have thus far remained unchanged in the GoldSim model.

The individual WRD calculations provide the root geochemical loading for the majority of the GoldSim model. The Faro portion of the GoldSim model has 33 individual WRDs divided among eight defined catchments. GoldSim accounts for the site conceptual geochemical model as follows:

- Precipitation falling on each WRD leaches components of the waste rock into underlying GW. The chemistry of the infiltrating water was assigned on the basis of the observed mineralogy and geochemical properties of the associated WRD.

- The water chemistry assigned to each WRD was chosen among 11 water types defined in the GoldSim model. These water types were formulated from observed seep data from the site and were grouped into type categories by chemical properties. Either one type or a combination of two or three of these water types was assigned to each WRD.
- The assumed proportion of infiltrating precipitation and the mapped area of each WRD were used to calculate the total flow contributed by each WRD. Combined with the assigned water chemistry, the GoldSim model calculates mass loading of each chemical component to underlying groundwater.
- Hydraulic inputs and chemical loading from multiple WRDs contribute to the discharge from each catchment, referred to as "nodes" within the GoldSim model. Some individual WRDs contribute hydraulic inputs and chemical loading to more than one catchment or node. Flow and loading is split between the Faro Pit Lake and the surrounding seven catchments, with flow fractions based on pre-mining topography.
- Each WRD is assigned a neutralization potential, acid-generating potential, and neutralization potential depletion rate. When 70 percent of the neutralization potential is depleted, the water chemistry begins a linear transition of each component from present to "future" water chemistry, which is assigned with a different individual or set of water chemistry types. The future water chemistry is more acidic and metal-rich than the present, unless the WRD in question has a greater neutralization potential than acid-generating potential.

The water types assigned in the GoldSim model represent average concentrations of many seep samples from a variety of locations. As a result, there is uncertainty associated not only in the averaging process but also in the variability of source materials, even within the same chemical type. In addition, the GoldSim model simulates the mixing of WRD inputs at the catchment level using a simple mass balance approach. It does not account for reactive mixing that may result in the removal of a fraction of the dissolved constituents from solution, contributions to solution from the aquifer matrix, or resulting adjustments in pH and acidity. Consequently, the geochemical loading at the catchment level is unrealistic in some cases. Significant differences between modelled and observed concentrations have been noted at several model nodes.

Similarly, the Faro Pit Lake component of the GoldSim model, which receives portions of the catchment discharges described previously, uses simple mass balance equations for mixing in Faro Pit Lake and does not account for geochemical reactions that occur when Faro Pit Lake inputs are combined. For example, current iron concentrations predicted by the GoldSim model for Faro Pit Lake are 360 times the observed values. Iron is an important water quality parameter that plays a role in determining pH and acidity and, when precipitated, acts as an effective scavenger of trace metals. These reactions, if not considered, can result in very large errors in predicting downstream and future concentrations of key parameters such as pH, sulphate, zinc, and lead concentrations.

On the basis of these observed inconsistencies, along with the recommendation of the independent peer review panel to account for reactive transport in the model, an external reactive mixing model, PHREEQC, developed by Parkhurst and Appelo (1999), was applied to both the catchment-level mixing and the Faro Pit Lake mixing as a tool to improve the agreement of GoldSim model and observed sampling results. These models are discussed in Section 4.4.

A portion of the flow from the WRD catchments contributes to the RCAA, which lies beneath the Rose Creek Tailings Impoundment. Westward upgradient flow in the RCAA is assigned a background groundwater chemistry in the GoldSim model, and infiltration through the tailings is assigned loading estimates developed by SRK (2005). Prediction of current zinc concentrations at the CVD is greatly overestimated by the GoldSim model, indicating the need for improvements in this portion of the model as well.

The RCTA model, described in Section 4.5, was the most challenging of the SRK models to improve, given the size and complexity of the system, but it was also the model requiring the greatest modification as it was only partially completed. Sulphate had been modelled as an annual loading term via infiltration through tailings to the RCAA. Zinc had also been modelled but is likely overestimated (SRK, 2005). The remaining groundwater chemical

constituents were expressed as a ratio to sulphate. The GoldSim model is missing several non-tailings input components that contribute load and flow estimates for the RCAA and does not incorporate the wealth of data collected in this area. As with the Faro Pit Lake and WRD areas, the GoldSim model does not account for reactions occurring during mixing of these inputs or interaction with the aquifer solids, which could greatly overestimate the future concentrations and rate of transport of trace metals in the RCAA. Therefore, a separate reactive transport model has been developed to incorporate and account for the detailed subsurface information that has been collected in the RCTA. This model, developed using the PHAST code (Parkhurst et al., 2010), is not designed to replace the GoldSim model but rather to provide a more rigorous, independent check on the parameters and assumptions used for this area and, ultimately, to identify improvements to the GoldSim model's predictive capabilities.

4.3 Geochemistry Data Sources

The hydraulic and chemical input parameter data used in the reactive mixing models constructed for the Faro Pit Lake and WRDs were exported directly from the GoldSim model (as revised and updated by CH2M HILL, in preparation) and represent the consolidation of the data used in the SRK (2009c) spreadsheet water-quality model, as described in GEEC (2010).

Lateral hydraulic input data and generalized aquifer property data that were incorporated into the PHAST simulations of the RCTA were imported from early versions of the RCAA Subarea model, which is described in Section 3. Infiltration rates were assigned as a function of grain size at the top of the PHAST model domain, which was adopted from a previous study carried out by SRK (2005). Chemical input parameter data for the PHAST simulations were compiled from historical GW, tailings porewater, and SW data available in the EQuIS database from the RCTA and ETA for 2002 until 2012.

4.4 Reactive Mixing – Faro Pit Lake and Waste Rock Dump Modelling

This section describes the development of geochemical reactive mixing models of the Faro Pit Lake and Faro WRDs. The purpose for developing these models is to support the continued calibration and refinement of the existing GoldSim model. Previous water quality modelling efforts for Faro Pit Lake and the Faro WRDs were summarized from the SRK (2009c) spreadsheet water quality models and used to construct the previous version of the GoldSim Model, as described in GEEC (2010). Although the GoldSim model is a useful tool for assessing simple mass balance and mass transport problems, the current version overestimates some water quality constituent concentrations, such as iron and zinc, in several key locations. This is in part because the model does not account for geochemical processes and reactions that occur during mixing and movement through the aquifer, such as reduction/oxidation (redox), mineral precipitation, and adsorption, that result in the removal of a fraction of the dissolved constituents from solution along with adjustments in pH and acidity. Some constituent concentrations are also underestimated by the GoldSim model, potentially due to uncertainty associated with averaging highly variable component water chemistries. The following subsections describe the construction and calibration of new reactive mixing models developed to provide additional insight into how the GoldSim model might be improved from a geochemical perspective.

The application of the Pit Lake and WRD models described below represents a first phase in the GoldSim improvement process. Given the effort that has gone into developing the spreadsheet models comprising GoldSim, the hope is to use these geochemical models to replace GoldSim calculations only at selected points in the model calculation process (i.e., locations of key mixing). Though true geochemical mixing and reactions occur continuously, it was not the intent to model all of these processes explicitly, but rather to provide the most efficient means possible to support and improve the GoldSim model. As such, the Faro Pit Lake model's initial objective was to account for reactions occurring in Faro Pit Lake to see if the difference between the GoldSim model predictions and observed conditions may be accounted for in the simplest manner possible. The same is true for the WRD model – the approach is to account for mixing reactions only where the mixtures are calculated by the GoldSim model (i.e., beneath mixed-waste WRDs and at the catchment discharge node). It was the hope of this study that these model insertions would improve the fit to observed data and explain key processes to be

applied to future predictive modelling. The plan was for more complexity to be added only if deemed necessary on the basis of the current model results.

4.4.1 Faro Pit Lake and Waste Rock Dump Model Construction

The models for the Faro Pit Lake and Waste Rock Dumps were constructed using the same software and approach and similar calibration techniques; therefore, the models are described together in this and subsequent sections. Because these models are equilibrium chemistry mixing models, they do not have many of the properties associated with groundwater flow models or flow/transport models so descriptions of parameters and boundary conditions will differ from those presented in Sections 3 and 4.5.

4.4.1.1 Faro Pit Lake and Waste Rock Dump Code Selection

Geochemical simulations were run using the USGS PHREEQC code (Parkhurst and Appelo, 1999), a publically available modelling software program that allows for complex geochemical reactions in low-temperature aqueous applications, combined with the Lawrence Livermore National Laboratories thermodynamic database. Although PHREEQC has the capabilities to simulate kinetic reactions, the reactive mixing models developed for this study assume instantaneous equilibrium in the mixtures and reactions simulated. The Faro Pit Lake model simulates reactive mixing, within the shallow lake depths, of inflowing groundwater from surrounding sources. In the WRD model, a single catchment has been chosen (X23) to identify the pertinent geochemical reactions that occur during subsurface mixing and transport of infiltrating WRD waters in the aquifer. Because transport distances between WRD source areas and the Faro Pit Lake and catchment area receiving waters are relatively small, a groundwater transport component was not considered necessary for these models. Transport was applied to the larger-scale tailings area, described in Section 4.5.

4.4.1.2 Faro Pit Lake and Waste Rock Dump Model Domain

Figure 4-1 presents a map showing the Faro Pit Lake and WRD model domain boundaries. The Faro Pit Lake domain includes the lake itself and surrounding WRDs that drain into the lake. Figure 4-2 shows the lateral extent of the Faro Pit Lake model domain, which was designed to include all of the hydraulic and chemical inputs to the Faro Pit. The domain of the Faro Pit Lake reactive mixing model is the upper zone of the Faro Pit Lake itself and the surrounding area. The area draining to the pit is roughly bounded by the Faro Valley North (FVN) WRD to the north, the Ramp Zone Dump (RZD) WRD to the south, the Northeast WRD (NEL, NEU) to the east, and the Northwest Rock Dumps to the west.

Figure 4-3 shows the extent of the WRD model domain, which is defined by the outer edges of the X23 catchment, as defined in the GoldSim model. Only this catchment has thus far been modelled because it is serving as a test case for the use of PHREEQC as a supplement to the GoldSim model. If this method is found to be successful, the remaining catchments will be modelled in a similar manner. In the WRD simulations, the delineations of the individual catchments are important to the mixing of the WRDs. It was assumed that the individual WRDs contributing to a given catchment were as identified in GEEC (2010). The X23 catchment was selected for the first catchment-level WRD mixing model because it captures flow and constituent loading of groundwater from many of the individual WRDs. The drainage outflow from this catchment is at seepage location FCS-4, as shown on Figure 4-3. This constitutes the X23 catchment discharge node in the GoldSim model and the calculated water quality parameters at this node are used as input to other evaluations, such as the RCTA and the Faro WTP design.

4.4.1.3 Faro Pit Lake and Waste Rock Dump Model Parameters

Faro Pit Lake Model Parameters

The reactive mixing model for the Faro Pit Lake was designed to mix all of the input water compositions in the same relative proportions as in the GoldSim model and compare results with those from the GoldSim model. The PHREEQC model incorporated the following parameters:

- Simulated GoldSim Model inputs (flow and water quality) to the Faro Pit Lake over the course of 2012
- Initial Faro Pit Lake storage volume of 17,877,410 m^3 (half of estimated total volume in the updated GoldSim model (CH2M HILL, in preparation), representing upper 25 m, the assumed mixing reaction zone)

- Initial Faro Pit Lake composition is represented by the sample collected from X22B on January 23, 2006 (this analysis is considered an initial condition for the purposes of modelling the effects of the inflows)

Constituent loading data for the Faro Pit Lake were compiled from the GoldSim model for the input waters and converted to average concentrations using the cumulative flow volumes over 2012, as shown in Table 4-2. The composition of water that reports to the Faro Pit was highly variable depending on the water source, with ranges in pH from 2.8 to 7.9 and alkalinity values from less than 1 to 199 milligrams per litre (mg/L). Concentrations of sulphate in the input waters ranged from 15 to 22,853 mg/L. Metal loading from the contributing waters was highly variable depending on the source water, with the low-grade ore stock pile "C" (LGSP C) seepage water contributing the greatest aluminum, iron, and zinc concentrations, as shown in Table 4-1. The tabulated volumetric fluxes of all the hydraulic inputs were used to calculate the relative mixing fraction of the hydraulic and chemical loading input parameters, as shown in Table 4-2. The initial conditions assigned to the upper Faro Pit Lake at the start of the model simulation represented the largest component, accounting for about 70 percent of the final Faro Pit Lake composition. Background water, represented by the leakage from the FCD and runoff that was not associated with a specific WRD, was the second largest inflow component, accounting for about 14 percent of the final mixture. Once the inflow waters were mixed in the relative proportions identified in Table 4-2, the mixture was reacted with additional constituent loading included to represent the interaction of the submerged pit walls with the pit lake. The submerged pit wall loading estimation was calculated from the pit wall loading term in the GoldSim model that was not associated with a hydraulic flow component and was converted to a concentration using an estimated volume of Faro Pit Lake water in contact with the pit walls.

Many of the calculated water chemistries in the GoldSim model, representing runoff and seepage from the WRDs, were not chemically balanced (cation-anion imbalances of greater than 5 percent), and some did not represent realistic environmental water samples (e.g., pH below 3 with nonzero alkalinity). Therefore, modifications to the PHREEQC input water chemistries were made to account for the chemical inaccuracies in the GoldSim model input parameters. Where no water temperature value was indicated in the GoldSim model, water temperature was assumed to be the same as that of the current Faro Pit Lake, represented by the temperature data collected from X22B on May 5, 2012. Where pH values were unavailable, estimations of pH were adopted from the seepage monitoring results presented in SRK (2009b). Modifications to the PHREEQC input water chemistries, such as the manual balancing of calcium, magnesium, and sulphate concentrations, were made to adjust individual chemical constituents to the input water composition to facilitate cation-anion balancing and simulating realistic environmental waters. In the GoldSim model, the chemical composition of water reporting to the Faro Pit through leakage from the FCD and runoff that was not associated with a specific WRD was estimated to be relatively "clean" water (i.e., near neutral pH and lower metals concentrations in comparison to the nearby WRD seepage) and representative of background water quality conditions. However, results from field investigations of seepage water quality on the north wall of the Faro Pit (spring and fall 2012 seep surveys) indicate that this assumption of background water quality conditions was underestimating the constituent loads coming from the FCD leakage and runoff not associated with a specific WRD. Therefore, water chemistry results from three seep locations along the north wall of the Faro Pit (A30, SRK-FD40, and CH-FP-30, shown on Figure 4-4) that contribute the largest volume of water to the Faro Pit Lake from the north wall were selected as representative of background water quality conditions. Water quality data from these three seep locations comprise the updated background water composition provided in Table 4-1.

Waste Rock Dump Mixing Model Parameters

Similar to the model for the Faro Pit Lake, construction of the WRD catchment-level reactive mixing model used the calculated constituent loading and volumetric fluxes for each WRD as defined in the GoldSim model. Without access to the original SRK WRD spreadsheet models and supporting parameter calculations, the understanding of the input water chemistry derivations was limited. Therefore, the approach to the WRD modelling for this study was to evaluate the water quality conditions of the individual WRDs at the catchment level. In the GoldSim model, there are 33 individual WRDs divided among eight defined catchments, as shown on Figure 4-3. Hydraulic inputs and chemical loading from multiple WRDs contribute to the discharge for each catchment (e.g., X23). Some individual WRDs contribute hydraulic inputs and chemical loading to more than one catchment. For example,

seepage from the low-grade ore stockpile "A" (LGSP A) WRD reports to both the X23 catchment and the Main Pit (MP) catchment (GEEC, 2010).

The X23 catchment was modelled as the test case and is described in this section. Because the X23 catchment captures runoff and seepage from many of the individual WRDs and because calibration of water quality conditions at the X23 catchment discharge node (FCS-4) is essential to many of the other modelling efforts (Faro Pit Lake, RCTA, WTP), the X23 catchment was selected to be the first catchment-level reactive mixing model constructed. Average seepage chemistries for X23 catchment were compiled using the GoldSim model and were designed to be representative of current (neutral) conditions. These seepage chemistries were assigned to each hydraulic input and mixed in relative proportion to the flows that report to the X23 discharge node, shown on Figure 4-3. Table 4-3 provides the seepage chemistries and corresponding WRDs that were used as input parameters to the X23 catchment model. Since the water types used by the GoldSim model to make up the water chemistry were made from average values of a wide variety of seepage samples, some components were adjusted to achieve electrical neutrality and geochemical consistency, as was done in the Faro Pit Lake model. Where seepage type mixtures were required to simulate seepage water quality from individual WRDs (e.g., Upper Northwest WRD, NWU), the mixtures were allowed to precipitate several relevant mineral phases if the solution became oversaturated: calcite, magnesite, gibbsite, rhodochrosite, siderite, smithsonite, cerussite, anglesite, gypsum, and ferric iron hydroxide ($Fe[OH]_3$), as discussed in Table 4-3. In addition, calcite, magnesite, and iron hydroxide were assumed to be present in the matrix and therefore could dissolve to a limited degree. Ferric iron hydroxide and calcite were also modeled as trace metal adsorbents, with adsorption parameters for the former included in the thermodynamic database with PHREEQC and the latter taken from published studies of zinc and cadmium adsorption (Zachara et al., 1991, 1993). These mineral phases were selected based on observations made during field investigations.

4.4.1.4 Faro Pit Lake and Waste Rock Dump Model Boundary Conditions

A conceptual schematic drawing of the Faro Pit Lake model boundary conditions is illustrated on Figure 4-5 and includes descriptions of the key factors influencing the chemical composition of the Faro Pit Lake. Inputs to the Faro Pit Lake mixing model were derived from the GoldSim model and include the following sources: precipitation; WRD and pit wall runoff; WRD seepage; runoff not assigned to a particular WRD; FCD leakage; chemical loading from the submerged pit walls; and additional inflows from the S-wells, Zone 2, and Intermediate Dam Pond collection systems. Hydraulic outflow from the Faro Pit occurs through pumping pit lake water to the WTP. Active pumping of the Faro Pit Lake typically occurs during 5 months of the year, from mid-late April through mid-late September. Although discharge from the Faro Pit Lake to the WTP is a known outflow component, incorporation of outflow into the geochemical mixing model was beyond the initial scope of work. Therefore, the mixing model only simulates the hydraulic and chemical inputs to the lake and assumes the Faro Pit Lake acts as a hydraulic sink and there are no water losses from the Faro Pit Lake to the underlying aquifer or through pumping. Calculated mean annual precipitation values were applied to the surfaces of the WRDs and pit walls, and precipitation reports to the Faro Pit Lake as either surface runoff or seepage, and representative chemistries were assigned to each of the influent waters, as discussed in Table 4-1. Precipitation that falls directly on the Faro Pit Lake was not assigned a chemical composition in the GoldSim model, and the volume of precipitation was directly incorporated into the calculated Faro Pit Lake storage term. In this way, GoldSim assumes precipitation to be pure water with no dissolved solids—not an unreasonable assumption in this environment of high total dissolved solids (TDS) waters. Leakage from the FCD infiltrates through the WRDs and reports to the Faro Pit Lake as seepage. These waters are each assigned the same chemistry as designated in the GoldSim model. Although there are undoubtedly reactions that occur between WRD infiltration and arrival of these waters at the Faro Pit Lake, these were not taken into account in the Faro Pit Lake model in the interest of simplicity and efficiency, as described at the beginning of this section.

TABLE 4-1
Chemical Compositions for the Input Waters – Faro Pit Lake, Current Conditions Reactive Transport Model
Faro Mine Remediation Project

Solution		1	2	3	4	5	6	7	8	9	10	11	12	13	14	15	16	17	18	19	20	21	22	23	24	25	26
Constituent	Abbreviation	S-WELLS	Zone 2	DVT (INTERMEDIATE POND)	NEL_RUNOFF	NEU_RUNOFF	FVS_RUNOFF	FVN_RUNOFF	LGSP A_RUNOFF	LGSP C_RUNOFF	SWPWD_RUNOFF	RD_RUNOFF	RZD_RUNOFF	NEL_SEEPAGE	NEU_SEEPAGE	FVS_SEEPAGE	FVN_SEEPAGE	LGSPA_SEEPAGE	LGSPC_SEEPAGE	SWPWD_SEEPAGE	RD_SEEPAGE	RZD_SEEPAGE	FC_DIVERSION_LOSS (BACKGROUND)	STARTING_PL_CHEMISTRY_ X22B23JAN2006	A30-22SEP2012 SAMPLE	FD40-22SEP2012 SAMPLE	CH-FP-30-22SEP2012 SAMPLE
Temperature (degrees C)	Temp	6.46	6.46	6.46	6.46	6.46	6.46	6.46	6.46	6.46	6.46	6.46	6.46	6.46	6.46	6.46	6.46	6.46	6.46	6.46	6.46	6.46	6.46	1.20	5.84	5.46	5.97
pH (s.u.)	pH	6.2	7.6	4.7	7.9	7.9	3.7	3.7	2.8	2.8	3.7	7.7	7.9	7.9	7.9	3.7	3.7	2.8	2.8	3.7	7.7	7.9	3.0	7.6	3.6	2.8	7.0
pe	pe	8	8	8	8	8	8	8	8	8	8	8	8	8	8	8	8	8	8	8	8	8	8	8	8	8	8
Redox	redox	pe	pe	pe	pe	pe	pe	pe	pe	pe	pe	pe	pe	pe	pe	pe	pe	pe	pe	pe	pe	pe	pe	pe	pe	pe	pe
Units	units	mg/L	mg/L	mg/L	mg/L	mg/L	mg/L	mg/L	mg/L	mg/L	mg/L	mg/L	mg/l	mg/l	mg/l	mg/l	mg/l	mg/l	mg/l	mg/l	mg/l	mg/l	mg/l	mg/l	mg/l	mg/l	mg/l
Density	density	1	1	1	1	1	1	1	1	1	1	1	1	1	1	1	1	1	1	1	1	1	1	1	1	1	1
Sodium	Na	16.8	21	7.78	0.59	0.59	0.89	0.89	3.66	3.66	0.89	1.85	9.01	5.92	5.92	8.92	8.92	37	40	8.92	18.5	90	3.43	22	3.64	3.64	2.59
Potassium	K	6.95	6.74	2.61	0.37	0.37	0.65	0.65	0.52	0.52	0.65	0.70	1.48	3.66	3.66	6.46	6.46	5.19	5.74	6.46	6.98	14.8	1.23	9.20	1.58	1.18	0.69
Calcium	Ca	202	180	133	12.1	12.1	17.2	17.2	32	32	17.2	21	17.8	121	121	172	172	318	352	172	214	178	51	146	64	53	21
Magnesium	Mg	229	187	45	9.27	9.27	25	25	59	59	25	22	23	93	93	252	252	594	658	252	224	229	56.1	65	62	75	4.03
Chloride	Cl	1.99	1.48	2.88	0.15	0.15	0.33	0.33	8.74	8.74	0.33	0.14	0.085	1.52	1.52	3.34	3.34	87	97	3.34	1.40	0.85	4.10		5.00	5.00	0.50
Iron	Fe	65	12.1	76	0.00080	0.00080	22	22	262	262	22	0.14	0.038	0.0080	0.0080	223	223	2618	2897	223	1.40	0.38	4.96	0.0000010	1.17	10.5	0.030
Manganese	Mn	8.53	3.27	13.3	0.0085	0.0085	2.07	2.07	31	31	2.07	0.39	0.018	0.085	0.085	21	21	310	344	21	3.93	0.18	3.15	2.78	2.99	4.75	0.00068
Sulfate	SO4	1705	1190	734	45	45	253	253	2065	2065	253	140	156	448	448	2533	2533	20646	22853	2533	1399	1559	490	688	530	675	15.5
Alkalinity (total, as CaCO3)	Alkalinity	121	158	38	19.9	19.9	0.95	0.95	0.41	0.41	0.95	15.8	11.3	199	199	9.54	9.54	4.06	4.50	9.54	158	113	15		1.00	1.00	57
Arsenic	As	0.20	0.036	0.28	0.000023	0.000023	0.068	0.068	0.11	0.11	0.068	0.00028	0.000025	0.00024	0.00023	0.68	0.68	1.07	1.19	0.68	0.0028	0.00025	0.00042	0.0000010	0.0054	0.0051	0.00013
Zinc	Zn	92	26	57	0.29	0.29	27	27	731	731	27	2.03	0.38	2.95	2.95	275	275	7309	8090	275	20	3.82	44	13.2	48	61	0.0092
Cadmium	Cd	0.40	0.083	0.077	0.00020	0.00021	0.14	0.14	1.19	1.19	0.14	0.0023	0.0010	0.0021	0.0020	1.36	1.36	11.9	13.2	1.36	0.023	0.010	0.068	0.0000010	0.074	0.093	0.000034
Cobalt	Co	0.19	0.055	0.094	0.000081	0.000081	0.056	0.056	0.57	0.57	0.056	0.0046	0.00090	0.00081	0.00081	0.56	0.56	5.72	6.33	0.56	0.046	0.0090	0.13	0.041	0.11	0.20	0.00010
Copper	Cu	1.00	0.20	0.98	0.00019	0.00019	0.34	0.34	15.4	15.4	0.34	0.0056	0.0018	0.0019	0.0019	3.39	3.39	154	170	3.39	0.056	0.018	0.82	0.0010	0.81	1.20	0.00027
Nickel	Ni	0.37	0.15	0.086	0.0044	0.0044	0.093	0.093	0.51	0.51	0.093	0.016	0.0069	0.044	0.044	0.93	0.93	5.10	5.65	0.93	0.16	0.069	0.13	0.10	0.14	0.17	0.00050
Aluminum	Al	8.04	1.57	1.71	0.00030	0.00030	2.74	2.74	22	22	2.74	0.032	0.00076	0.0030	0.0030	27	27	223	247	27	0.32	0.0076	7.04	0.0000010	7.88	9.57	0.018
Lead	Pb	0.18	0.037	0.016	0.000020	0.000020	0.060	0.060	0.067	0.067	0.060	0.0010	0.00067	0.00020	0.00020	0.60	0.60	0.67	0.74	0.60	0.010	0.0067	0.19	0.0000010	0.33	0.17	0.00013

Notes:
Where pH values were unavailable, pH was estimated from Gomm (2010).
Where temperature data was unavailable, temperature was estimated using the value from the May 5, 2012 sample collected from Faro Pit Lake at station X22B.

This page intentionally left blank.

TABLE 4-2
Relative Mixing Fractions of the Input Waters – Faro Pit Lake, Current Conditions Reactive Transport Model
Faro Mine Remediation Project

Input Solution	Input Solution Title	Location Description	Volume (m^3), Cumulative for 2012	Mixing Fraction [a]
1	S-wells	S-wells collection	92,972	0.4%
2	Zone 2	Zone 2 collection	70,217	0.3%
3	DVT (Intermediate Pond)	Intermediate Pond collection	1,283,940	5.1%
4	NEL_runoff	Lower Northeast Dump - runoff	26,663	0.1%
5	NEU_runoff	Upper Northeast Dump - runoff	81,344	0.3%
6	FVS_runoff	Faro Valley South - runoff	34,310	0.14%
7	FVN_runoff	Faro Valley North - runoff	144,230	0.57%
8	LGSPA_runoff	Low Grade Stockpile A - runoff	11,954	0.05%
9	LGSPC_runoff	Low Grade Stockpile C - runoff	11,954	0.05%
10	SWPWD_runoff	Southwest Pit Wall Dump - runoff	55,881	0.22%
11	RD_runoff	Ranch Dump - runoff	5,182	0.02%
12	RZD_runoff	Ramp Zone Dump - runoff	14,182	0.06%
13	NEL_seepage	Lower Northeast Dump - seepage	49,605	0.2%
14	NEU_seepage	Upper Northeast Dump - seepage	151,339	0.6 %
15	FVS_seepage	Faro Valley South - seepage	63,831	0.25%
16	FVN_seepage	Faro Valley North - seepage	268,330	1.1%
17	LGSPA_seepage	Low Grade Stockpile A - seepage	22,241	0.09%
18	LGSPC_seepage	Low Grade Stockpile C - seepage	22,241	0.09%
19	SWPWD_seepage	Southwest Pit Wall Dump - seepage	103,964	0.41%
20	RD_seepage	Ranch Dump - seepage	9,642	0.04%
21	RZD_seepage	Ramp Zone Dump - seepage	26,385	0.1%
22	A30, FD40, CH-FP-30 [b] (mixture)	Faro Creek Diversion - background	1,372,828	5.4%
23	Existing Pit Lake (upper 25 meters)	Faro Pit lake	17,877,410	70.8%
24-26	A30, FD40, CH-FP-30 [b] (mixture)	North Faro Pit wall seeps - runoff	3,466,400	13.7%
	Totals		**25,267,045**	**100%**

Notes:
[a] Mixing fraction of N. wall faro pit: A30, 37% (350 L/min); SRK-FD40, 43% (400 L/min); and CH-FP-30, 20% (190 L/min).
[b] Assignment of Faro Creek Diversion leakage and runoff not associated with a particular WRD.

The upper portion of the Faro Pit Lake mixes with runoff and seepage water, and limited mixing is assumed to occur with the deeper portions of the Faro Pit Lake. Equilibrium reactions of the upper portion of the Faro Pit Lake with atmospheric oxygen and carbon dioxide affect the redox properties and the dominant chemical species present. Additional chemical loading to the Faro Pit Lake occurs through water-rock interactions occurring near the submerged pit walls. Limited mixing of the upper Faro Pit Lake with the deeper, more alkaline parts of the Faro Pit Lake introduces acid-buffering capacity to neutralize acidic influent waters.

Figure 4-6 provides a conceptual schematic drawing of the WRD model boundary conditions and includes descriptions of the key factors influencing the chemical composition of the individual WRDs. Input hydraulic fluxes and constituent loading to the WRD mixing model was derived from the GoldSim model and generally includes the application of mean annual precipitation to the surface of individual WRDs that report to a given catchment as either runoff or seepage. GoldSim model water chemistries were assigned to each of the WRDs that contribute flow and constituent loading to the catchment, as shown in Table 4-3. The X23 catchment model was run assuming groundwater mixing and reactions beneath WRDs of mixed water types, followed by atmospheric equilibration during mixing of all streams at the discharge point of the catchment (FCS-4).

4.4.2 Faro Pit Lake and Waste Rock Dump Geochemical Model Calibration

The next three subsections describe the approach to calibration, identify the observed data that serve as the calibration targets, and recount the process by which calibration was executed. Section 4.4.2.4 presents the results of the calibration, with implications on the current GoldSim model and future tasks. The limitations of the PHREEQC modeling approach are discussed in Section 4.4.2.5.

4.4.2.1 Faro Pit Lake and Waste Rock Dump Model Calibration Approach

The overall approach to model calibration was to use geochemical reaction models to adjust the current assumed GoldSim model water chemistry in an attempt to better match observed water quality conditions in key areas of the FMC. The first step in this calibration approach was to develop the PHREEQC models described previously. Using PHREEQC, simulations were performed to evaluate the appropriateness of the input parameters and assumptions within the GoldSim model used to simulate current (observed) water quality conditions. The initial versions of the PHREEC Faro Pit Lake and WRD reactive mixing models used as many of the input parameters from the GoldSim model as possible to compare the modelled 2012 results against the GoldSim model output and observed calibration targets.

4.4.2.2 Faro Pit Lake and Waste Rock Dump Model Calibration Targets

Figure 4-7 shows the calibration targets selected for the reactive mixing model simulations. Modelled current water quality conditions in the Faro Pit Lake and at FCS-4 were compared to water quality results obtained from the May 5, 2012 pit lake sample collected at X22B and an average of April 2011_March 2012 surface water sample collected at FCS-4. The average of 2012 chemistry for station X23 was also examined for reasons explained in Section 4.4.2.4.

4.4.2.3 Faro Pit Lake and Waste Rock Dump Model Calibration Process

The construction of the PHREEQC Faro Pit Lake model required modifications to some of the original GoldSim model input parameters that were either out of cation-anion balance or beyond the capability of the GoldSim model for water quality estimations. Representative water chemistries were assigned to each of the hydraulic input waters to the Faro Pit Lake, and the electrical balance of each hydraulic input water was calculated in PHREEQC. Where the calculated imbalance between cations and anions was greater than 5 percent, manual adjustments to the dominant cations and dominant anion were made to shift the water chemistry toward electroneutrality. While PHREEQC can modify and balance waters within the program, ion balancing was done manually to keep key constituent relationships in place. In most cases, adjustments were made to the concentrations of calcium or magnesium (dominant cations) and sulphate (dominant anion) to achieve electroneutrality without significantly altering the chemical signature of the water. The process of balancing the input waters has highlighted uncertainty for the water quality estimates that are propagated through the GoldSim model and have the potential to limit the its predictive capabilities.

Although the GoldSim model assumed a fully-mixed reservoir, field investigations suggest that the Faro Pit Lake is not uniformly mixed, and a thermocline and chemocline exist at depth (Laberge, 2012a; SRK, 2004a). The reactive mixing model accounted for this shift in conceptual understanding by assuming that most geochemical reactions between the Faro Pit Lake and the influent waters occur in an upper portion of the lake. Partial saturation of the upper Faro Pit Lake with atmospheric oxygen and carbon dioxide was achieved by fixing the saturation index (SI) of oxygen dissolved O_2 gas to -1.6, and the SI of carbon dioxide dissolved CO_2 gas to -2.5 in the model. The SI values selected were estimated from the speciation and mineral saturation calculations carried out in PHREEQC on the calibration target sample from X22B.

TABLE 4-3
Chemical Compositions for the Input Waters - X23 Catchment, Current Conditions WRD Reactive Mixing Model
Faro Mine Remediation Project

Seepage Type		F1	F2 WASTE	F2 ORE	F3 WASTE	F3 ORE	OTHER 1	OTHER 2	OTHER 3	OTHER 4	OTHER 5	OTHER 6	Mix 1: 70% F1, 20% F2 waste, 10% F3 waste	Mix 2: 95% F1, 5% F2 waste	Mix 3: 90% F1, 10% F2 waste	Mix 4: 50% F1, 50% F2 waste	Mix 5: 40% F1, 60% F2 waste	Mix 6: 90% F2 waste, 10% F3 waste	Mix 7: 40% F1, 40% F2 waste, 20% F3 waste	Mix 8: 50% F1, 30% F2 waste, 20% F3 waste
Waste Rock Dumps		----	FTE, SPB	----	MMW, MME, FTW, SWPWD, MESC, IDSC, NELS	CHSP, LGSP A, LGSP C	OXSP	NEL, NEU	RZD	NWL	MGSP	----	NWU, NWM	UPL	LPL	RD, OHRW, NEO, Z2E	OHRE, Z2W	MDW	MSW	ID
Constituent	**Abbreviation**																			
pH (s.u.)	pH	7.82	7.22	6.92	4.26	3.28	2.45	7.84	7.88	7.57	2.53	4.31	6.70	6.95	6.94	6.88	6.87	6.62	6.55	6.56
pe	pe	4	4	4	4	4	4	4	4	4	4	4	2.59	3.71	3.57	3.21	3.17	2.82	2.82	2.79
Units	units	mg/L	mg/L	mg/L	mg/L	mg/L	mg/L	mg/L	mg/L	mg/L	mg/L	mg/L	mg/L	mg/L	mg/L	mg/L	mg/L	mg/L	mg/L	mg/L
Density (kg/L)	density	1	1	1	1	1	1	1	1	1	1	1	1	1	1	1	1	1	1	1
Sodium	Na	26	10.7	43	8.92	37	10.0	5.92	90	20	2.70	3.08	21	26	25	19	17	11	17	18
Potassium	K	6.44	7.51	12.1	6.46	5.19	0.00	3.66	14.8	9.83	0.00	1.31	6.67	6.51	6.56	6.99	7.10	7.43	6.89	6.78
Calcium	Ca	144	284	520	172	318	378	121	178	569	289	65	462	330	353	539	585	787	612	566
Magnesium	Mg	125	338	497	286	633	1849	87	244	631	631	88	22	15.2	16.3	25	28	38	29	27
Chloride	Cl	1.42	1.39	10.3	3.34	87	342	1.52	0.85	2.05	2.00	0.91	1.61	1.42	1.42	1.41	1.40	1.59	1.79	1.80
Iron	Fe	0.12	2.68	37	223	2618	6748	0.01	0.38	0.40	3896	44	7.87	0.085	0.13	0.48	0.57	8.48	15.7	15.6
Manganese	Mn	0.15842	7.7082	37.541	20.717	310.38	936	0.085267	0.17525	20.879	356.63	4.0856	3.74	0.54	0.92	3.94	4.70	9.04	7.31	6.56
Sulfate	SO4	732	2002	3576	2400	20484	34507	468	1502	3720	35827	698	1155	797	860	1370	1498	2048	1578	1451
Alkalinity	Alkalinity	182	134	203	9.5	4.06	1.00	199	113	375	1.38	8.75	245	159	157	142	139	218	312	317
Arsenic	As	0.0003	0.0053	0.0030	0.678	1.074	0.136	0.00024	0.00025	0.0005	291	0.0036	0.069320082	0.000524064	0.00077784	0.002807702	0.003315224	0.072872883	0.138373442	0.137863972
Zinc	Zn	3.04	38	226	275	7309	6930	2.95	3.82	66	15759	69	37	4.77	6.50	20	24	61	71	68
Aluminum	Al	0.04	0.60	0.19	27	223	502	0.0030	0.0076	0.16	309	12.8	0.00018	0.00026	0.00026	0.00024	0.00024	0.00017	0.00016	0.00016

Note:
All concentrations are in mg/L unless otherwise specified; seepage types are defined in Gomm (2010); mixtures allowed for the precipitation of calcite, gibbsite, ferric iron hydroxide, and/or dolomite where saturation indexes were greater than zero; mixing fractions of individual WRDs are as designated in Gomm (2010).

CHSP	Crusher Stockpile
FTE	Fuel Tank Dump E
FTW	Fuel Tank Dump W
ID	Intermediate Dump
IDSC	Intermediate Dump Sulphide Cell
LGSP A	Low Grade Stockpile A
LGSP C	Low Grade Stockpile C
LPL	Lower Parking Lot Dump
MDW	Main Dump West
MESC	Main East Sulphide Cell
MGSP	Medium Grade Stockpile
MME	Mt. Mungly East
MMW	Mt. Mungly West
NEL	Lower Northeast Dump
NELS	Lower Northeast sulphide cell
NEO	Outer Northeast Dump
NEU	Upper Northeast Dump
NWL	Lower Northwest Dump
NWM	Middle Northwest Dump
NWU	Upper Northwest Dump
OHRE	Outer Haul Road East
OHRW	Outer Haul Road West
OXSP	Oxide Fines Stockpile
RD	Ranch Dump
RZD	Ramp Zone Dump
SPB	Stock Piles Base
SWPWD	Southwest Pit Wall Dump
UPL	Upper Parking Lot Dump
Z2E	Zone 2 East
Z2W	Zone 2 West

This page intentionally left blank.

TABLE 4-4
Relative Mixing Fractions of Seepage from Individual Waste Rock Dumps – X23, Current Conditions Reactive Transport Model
Faro Mine Remediation Project

Waste Rock Element	Abbreviation	Relative Percent Contributing to Each Catchment (m^3)							
		X23	MP	X2	RCV	Z2[a]	NFRC	GHU	GHL
Faro Valley North	FVN	----	37.4%	----	----	----	----	----	----
Faro Valley South	FVS	----	8.9%	----	----	----	----	----	----
Medium Grade Ore Stockpile	MGSP	14.7%	----	----	----	----	----	----	----
Crusher Stockpile	CHSP	1.6%	----	----	----	----	----	----	----
Oxide Fines Stockpile	OXSP	2.1%	----	----	----	----	----	----	----
Low Grade Stockpile A	LGSPA	1.8%	3.1%	----	----	----	----	----	----
Upper Northwest Dump	NWU	4.3%	----	----	----	----	----	76.3%	7.0%
Middle Northwest Dump	NWM	7.5%	----	----	----	----	----	23.7%	17.3%
Lower Northwest Dump	NWL	3.8%	----	----	----	----	----	----	30.3%
Mt. Mungly West	MMW	2.4%	----	----	----	----	----	----	----
Mt. Mungly East	MME	2.8%	----	----	----	----	----	----	----
Fuel Tank Dump W.	FTW	0.7%	----	----	----	----	----	----	----
Fuel Tank Dump E.	FTE	7.5%	----	----	----	----	----	----	----
Upper Parking Lot Dump	UPL	----	----	----	----	----	----	----	29.0%
Lower Parking Lot Dump	LPL	----	----	----	----	----	----	----	16.4%
Stock Piles Base	SPB	6.2%	----	----	----	----	----	----	----
Low Grade Stockpile C	LGSPC	2.0%	3.1%	----	----	----	----	----	----
South West Pit Wall Dump	SWPWD	1.6%	14.5%	----	----	----	----	----	----
Main Sulphide Cell	MESC	5.7%	----	----	----	----	----	----	----
Intermediate Sulphide Cell	IDSC	----	----	15.6%	----	----	----	----	----
Ranch Dump	RD	3.0%	1.3%	----	----	----	----	----	----
Ramp Zone Dump	RZD	----	3.7%	0.6%	----	9.0%	----	----	----
Main Dump West	MDW	13.7%	----	----	----	----	----	----	----
Main Dump East	MDE	16.2%	----	11.4%	28.5%	----	----	----	----
Intermediate Dump	ID	----	-----	50.3%	-----	5.3%	-----	-----	-----
Outer Haul Road West	OHRW	2.3%	----	8.6%	71.5%	----	----	----	----
Outer Haul Road East	OHRE	----	----	13.5%	----	----	----	----	----
North East Sulphide Cell	NELS	----	----	----	----	4.3%	0.5%	----	-----
Outer Northeast Dump	NEO	----	0.0%	----	----	----	----	----	----
Zone 2 West	Z2W	----	----	----	----	1.3%	----	----	----
Zone 2 East	Z2E	----	----	----	----	52.9%	12.6%	----	----
Lower Northeast Dump	NEL	----	6.9%	----	----	17.9%	42.7%	----	----
Upper Northeast Dump	NEU	----	21.1%	----	----	9.2%	44.2%	----	----
TOTALS	**ALL DUMPS**	**100%**	**100%**	**100%**	**100%**	**100%**	**100%**	**100%**	**100%**

Notes:
[a] Z2 catchment contributions back-calculated from Gomm (2010).

GHL Lower Guardhouse Creek catchment
GHU Upper Guardhouse Creek catchment
MP Main Pit (Faro) catchment
NFRC North Fork Rose Creek catchment
RCV Rose Creek Valley catchment
X2 Catchment draining near stream monitoring location X2
X23 Catchment draining near seep monitoring location X23
Z2 Catchment draining near Zone 2 drainage area

The PHREEQC model also assumes limited mixing of the upper Faro Pit Lake with the deeper parts of the lake, which serve as a source of alkalinity (supported by aqueous chemistry at depth) and a sink for precipitated minerals. While the PHREEQC program calculates SIs for the mineral phases in the Lawrence Livermore National Laboratories database, it is up to the user to determine which minerals are expected to precipitate based on field observations. The minerals that were allowed to precipitate in the Faro Pit Lake reactive mixing model were gibbsite ($Al[OH]_3$), $Fe(OH)_3$, and calcite ($CaCO_3$). While precipitated gibbsite and $Fe(OH)_3$ were not allowed to redissolve, $CaCO_3$ redissolution was permitted in the model to simulate the limited mixing of the upper portion of the lake and the more alkaline deeper part of the lake. Attenuation of metals onto mineral surfaces was accounted for in the model through the precipitation of $Fe(OH)_3$ and surface reactions involving $Fe(OH)_3$ according to the surface-complexation reactions derived from Dzombak and Morel (1990) and incorporated into the PHREEQC program.

The WRD reactive mixing model is currently in the process of calibration to observed water quality at the FCS-4 and X23 sample stations. Early in the calibration process, it became obvious that chemical signature observed at FCS-4 would not be matched closely due most likely to model inputs and the variability of the chemistry at this location. Station X23 was added for comparison during calibration to examine which site had the greatest potential for successfully matching the simulated water chemistries based on GoldSim model mixing proportions. Because the GoldSim WRD model feeds into the Faro Pit Lake model in some cases, many of the modifications described in the previous paragraphs were also applied to the chemical composition of runoff and seepage from the WRDs at the X23 catchment level. Due to the more extensive interactions with the aquifer matrix involved in these reactions, a larger mineral suite was included in this model. Precipitation and dissolution of $Fe(OH)_3$, $CaCO_3$, and magnesite were allowed, and precipitation of gibbsite, siderite, rhodocrosite, smithsonite, cerussite, anglesite, and gypsum were allowed if the solution became oversaturated in any of these minerals. These minerals were selected based on field observations and preliminary PHREEQC analysis of observed seeps and groundwater. The adsorption of metals onto mineral surfaces was accounted for in the model in the same manner described for the Faro Pit Lake model. A starting concentration of $Fe(OH)_3$ in the aquifer matrix was assigned based on core data and field observations. Additional $Fe(OH)_3$ that precipitated during simulated mixing provided additional adsorptive capacity. In addition, calcite was assigned as an exchange surface for calcium, cadmium, and zinc, based on published literature (Zachara et al., 1991, 1993).

4.4.2.4 Faro Pit Lake and Waste Rock Dump Model Calibration Results

Results from the Faro Pit Lake PHREEQC simulations were sent to post-processing spreadsheets to convert the model output to constituent concentrations in mg/L. The PHREEQC model results were compared to the GoldSim model results for the 2012 modelled time period, and relative percent differences between modelled and observed water quality conditions were calculated, as shown in Table 4-5. In general, the GoldSim model underestimates the concentration of sulphate and the amount of alkalinity in the Faro Pit Lake for current conditions. The GoldSim model also overestimates the concentrations of iron, zinc, and aluminum. Because the GoldSim model does not account for precipitation of minerals and adsorption reactions, the concentrations of metals are high compared to actual measured concentrations. In contrast, output from the PHREEQC reactive mixing model is more consistent with the currently observed water quality of the Faro Pit Lake. Concentrations of alkalinity were closer to the calibration target once an alkalinity source at depth was introduced to the model. pH and concentrations of sulphate and iron calculated in PHREEQC were within 5 percent of the calibration target concentration. Concentrations of potassium calculated by PHREEQC were a relatively close match—within 10 percent of the calibration target. Results from the Faro Pit Lake PHREEQC model overestimate the concentrations of calcium but to a lesser extent than the overestimations calculated in the GoldSim model. Results from the PHREEQC model underestimated the concentrations of magnesium and chloride. The overestimations and underestimations of constituent concentrations calculated by the PHREEQC model are likely attributable to the particular mineral phases selected to participate in the Faro Pit Lake reactions and the uncertainty and limitations associated with the input parameters used.

TABLE 4-5
Observed Versus Modelled Water Quality Results – Faro Pit Lake, Current Conditions
Faro Mine Remediation Project

	Current Conditions				
Constituent	**Observed**	**Modelled (GoldSIM)**	**Relative Percent Difference**	**Modelled (PHREEQC)**	**Relative Percent Difference**
pH (s.u.)	7.27	6.85	6%	7.24	0.5%
Alkalinity (total, as CaCO3)	98	11	160%	89	9.7%
Sodium	19	17	12%	19	1%
Potassium	8.01	7.05	13%	7.44	7%
Calcium	152	122	22%	170	11%
Magnesium	85	62	31%	70	18%
Chloride	1.80	1.53	16%	1.25	36%
Iron	0.075	27	199%	0.07	3%
Manganese	3.41	5.59	48%	4.50	27%
Sulphate	715	348	69%	754	5%
Arsenic	0.00040	0.036	196%	0.084	35%
Zinc	25	40	45%	41	47%
Cadmium	0.022	0.052	82%	0.069	104%
Cobalt	0.059	0.074	23%	0.084	35%
Copper	0.024	0.99	191%	0.16	147%
Nickel	0.15	0.11	32%	0.13	13%
Aluminum	0.036	2.20	194%	0.000047	199%
Lead	0.0023	0.0080	111%	0.0070	102%

Notes:
All units are mg/L unless otherwise noted.
Observed data are from X22B May 5, 2012 sample.

Similar to the post-processing of the Faro Pit Lake results, results from the WRD PHREEQC simulations for the X23 catchment were converted to constituent concentrations in mg/L. The PHREEQC model results were compared to the GoldSim model results over the same 2012 modelled time period, and relative percent differences between modelled and observed water quality conditions were calculated, as shown in Table 4-6. For the X23 catchment, neither the GoldSim model nor the PHREEQC catchment-level reactive mixing model was able to closely simulate the current observed water quality conditions at FCS-4. This discharge location has very low alkalinity (average of 9 mg/L but commonly not detected) and high iron (over 500 mg/L), yet a less acidic pH than would be expected under these conditions (6.3). Though this is not chemically impossible, it likely represents a transitional state because groundwater is actively emerging at the surface and flowing in this area while mixing with other surface water (e.g., FCS-3). The mixing proportions dictated by the GoldSim model prevent matching of all three key parameters (pH, iron, and alkalinity) at FCS-4. The GoldSim mixing model is close on pH and not too far off on iron, but greatly overestimates alkalinity. The PHREEQC parameters were adjusted to varying results, with two of these three being matched, but never all three. It was found during calibration that the water chemistry at location X23, though not the final discharge point of the catchment, was more easily matched by the PHREEQC model. An increase to the solubility of the $Fe(OH)_3$ phase in the PHREEQC database was necessary to account for the observed iron concentration, but solubility of ferric hydroxide minerals as a group is highly variable and so this adjustment was considered reasonable. The fit of X23 but not of FCS-4 suggests that this more fresh emergence from the subsurface (X23) is more suited to the proportions suggested by the GoldSim model. Table 4-6 compares PHREEQC results that best matched X23 and compares them to both GoldSim and FCS-4 data. The results suggest that the groundwater chemistry flowing through the X23 catchment is undergoing complex changes that are not captured by GoldSim and are not helped significantly by equilibrium modeling with these settings. Key

constituents such as zinc and arsenic are greatly overestimated at the current input proportions. The next steps require alteration of input proportions and most likely input chemistry as well. Without known chemical properties and processes accounted for, future prediction of water chemistry will be highly uncertain.

The results of the Faro Pit Lake model indicate that inputs to the shallow aquatic environment of the lake can be made to reasonably match observed conditions (with some refinement still needed), thus providing a useful improvement to the GoldSim model as an integrated unit. Seasonal changes in lake chemistry may play an important role that is not yet accounted for in the model, so additional measurements are recommended to assess this condition, as is discussed in Section 5.

The test case of the X23 catchment WRD model showed that adding a reactive mixing module was useful in explaining downgradient groundwater chemistry (X23 seep station). However, after rigorous testing, it was discovered that the module alone does not significantly improve the fit to observed data at the discharge point of the catchment (FCS-4). This indicates that more refinement is necessary for the model to be a trustworthy predictor of future conditions. More detailed recommendations are provided in Section 5.

TABLE 4-6
Observed Versus Modelled Water Quality Results – X23 Catchment, Current Conditions
Faro Mine Remediation Project

Constituent	FCS-4 (average Apr11-Mar12)	X23 (average 2012)	PHREEQC	GoldSim
Sodium	59	58	13.8	15
Potassium	12.6	17.8	5.85	6.64
Calcium	428	461	417	246
Magnesium	738	1191	1318	331
Iron	525	249	226	442
Manganese	74	123	100	56
Chloride	14.2	14.0	14.3	14.8
Alkalinity	9.46	23	38	113
Sulphate	5554	7943	7934	4535
pH, s.u.	6.36	5.85	5.63	6.23
Aluminum	1.29	0.10	0.018	37
Arsenic	0.0049	0.0070	40	6.56
Cadmium	0.035	0.32	0.18	0.23
Cobalt	0.75	1.78	2.23	1.83
Copper	0.068	0.59	1.45	0.023
Nickel	0.72	2.04	2.20	2.09
Lead	0.072	0.0050	0.45	0.00000010
Zinc	315	881	955	995

Note: All concentrations are in mg/L unless otherwise noted.

4.4.3 Faro Pit Lake and Waste Rock Dump Model Use and Limitation

The PHREEQC reactive mixing models that were developed for the Faro Pit Lake and WRDs at the catchment-level were intended to provide a more rigorous, independent evaluation of the water quality assumptions and input parameters that are currently implemented in the GoldSim model. In addition, the PHREEQC models were designed as tools to identify potential modifications that would improve the conceptual understanding of the geochemical processes influencing the Faro Pit Lake and WRD water quality conditions. The results of the Faro Pit Lake PHREEQC model accounted for the reactive mixing and equilibrium reactions, which provided better agreement between modelled and observed water quality results than previously achieved with the simple mass balance used in the GoldSim model. However, substantial uncertainty was uncovered for the input parameters

and assumptions associated with the original SRK WRD model, and the limitations of the GoldSim model to simulate complex geochemical processes occurring in nature.

The WRD PHREEQC reactive-mixing model attempted to more closely approximate observed water quality results by incorporating reactive mixing, mineral precipitation, and sorption reactions. However, the results from the PHREEQC simulations to date have not been consistent enough with observed conditions at the X23 catchment node. It is necessary to further investigate the assumptions and input parameters that went into the SRK WRD model to reduce the amount of uncertainty that is carried through to the water quality estimations and predictions.

Although PHREEQC is a useful tool to simulate the geochemical reactions taking place in the Faro Pit Lake and WRDs, it is a simplification of a complex natural system and is limited by the assumptions and input parameters used by the model. Results from the PHREEQC reactive-mixing model should be used as a tool to simulate complex geochemical reactions to highlight functions within the GoldSim model that can be improved to provide more accurate forecasting of water quality conditions. One approach to achieving this objective would be to incorporate PHREEQC directly into the GoldSim model. While there are methods to generate a feedback loop of results between GoldSim and PHREEQC, the implementation of that type of process has not yet been tested for application to the GoldSim model.

4.5 Reactive Subsurface Transport Modelling

The RCTA is one of the most studied areas of the FMC, with numerous monitoring wells in tailings, the RCAA, and bedrock, along with surface seeps and channels, all with extensive time-series histories of water quality. Numerous reports interpret these data, including water quality of seepage through tailings (SRK, 2005), loads and water balance estimates (RGC, 2006b), zinc attenuation estimates (SRK, 2006c), and acid rock drainage source identification (RGC, 2011). The original spreadsheet model and current GoldSim model incorporate only a subset of the known contributions to the RCAA and essentially none of the data collected in this area. This makes it difficult, if not impossible, to assess the GoldSim model's ability to predict future water quality. Major shortcomings of the current GoldSim model include the lack of inputs from several locations, including infiltration of surface water that flows onto the tailings (thus altering the infiltrating water's chemistry), GW underflow from Guardhouse Creek drainage, and underflow from WRD areas to the east of ETA. As with the Faro Pit Lake and WRD areas, the GoldSim model does not account for reactions occurring while these inputs are mixing or interacting with the aquifer solids, which could greatly overestimate the future concentrations and rate of transport of trace metals in the RCAA.

To assess the reliability of the GoldSim model in forecasting future water quality conditions, a separate model has been constructed to incorporate and account for the detailed information that has been collected in this area. The model is not designed to replace the GoldSim model but to provide a more rigorous, independent check of the parameters and assumptions used for this area and, ultimately, to point out improvements that would assist in more appropriate and efficient design. This may include more accurate inputs to the GoldSim model to improve its predictive capabilities of water quality.

4.5.1 Reactive Subsurface Transport Model Construction

4.5.1.1 Reactive Subsurface Transport Model Code Selection

The USGS geochemical transport code PHAST (Parkhurst et al., 2010) was chosen to model the reactive transport of selected constituents in the RCAA beneath the RCTA and downgradient impoundments. PHAST combines GW flow and solute transport with PHREEQC (Parkhurst and Appelo, 1999), which accounts for solute speciation, mineral solubility, and adsorption reactions. Using hydraulic parameters and boundary conditions from the RCAA Subarea model (described in Section 3) and representative GW chemistry from monitoring well data around the area, the PHAST model was designed to account for the various input flows and loads from all sides of the RCTA. With this tool, known water chemistry may be assigned to calibrated flows into and out of the RCAA.

Conventional transport codes, either stand-alone or expressions that may be applied to the GoldSim model, rely on dispersion and effective porosity to estimate conservative velocity and dilution during transport. PHAST uses these relationships, as well. The other transport codes account for adsorption process by assuming a soil-water partition

coefficient, commonly referred to as "K_d", for a constituent of interest. The K_d value is usually reported in the literature as a range of values spanning several orders of magnitude (Allison and Allison, 2005) because adsorption is very much specific to site materials and chemical characteristics of the GW. The K_d parameter implicitly assumes an infinite capacity of the porous medium to adsorb the constituent; there is no maximum adsorption capacity, making its use limited to more dilute conditions. The models incorporate the K_d parameter into a retardation factor, which slows the calculated velocity of the constituent during subsurface transport. In many cases, adsorption reactions are essentially irreversible and if the adsorption capacity is not met, the solute is not simply retarded but is removed from the system entirely. In these cases, the retardation assumption can be very different from reality. The PHAST model bypasses these assumptions by explicitly modelling the adsorption process using site-specific chemistry and mineralogy, which provides a much more realistic model of this process. By assigning a concentration of an adsorbing mineral phase to the model, there is a ceiling on how much the media may be able to adsorb per constituent. In addition, solubility criteria contained in PHAST are important to put limits on sulphate and metals concentrations, and some precipitated solids add to the aquifer adsorption capacity to retard the transport of trace metals, such as zinc and cadmium. Conventional transport models do not consider chemical precipitation criteria.

Because there is considerable information on the GW chemistry, tailings chemistry, and mineralogy present in the RCAA, site-specific geochemical parameters were assigned to provide a more accurate model of FMC processes. Model uncertainty will be more clearly identified and quantified using these tools because the parameters controlling concentrations (e.g., adsorption capacity, controlling mineral phases, and reactions during mixing) are accounted for and may be adjusted within reasonable values. Without these parameters, only input concentrations may be adjusted, which could lead to inaccurate forecasting.

4.5.1.2 Reactive Subsurface Transport Model Domain

Figure 4-8 shows the extent of the RCAA reactive transport model domain. It was designed to roughly extend between the SW monitoring stations X2 (east) and X14 (west) and bound on the south by the RCD channel and the north by the edge of the tailings impoundment. The X2 and X14 locations were chosen as upgradient and downgradient boundaries to potentially tie in with the GoldSim model catchment outlets so that water chemistry changes between one and the other may be altered or substituted based on the results of the PHAST modelling.

In the interest of keeping the model as simple as possible, it was made rectangular with a total length of 5,200 m and width of 750 m. The lateral grid spacing is 50 m by 50 m, and the model is composed of a single layer, 25 m thick, which is the inferred average saturated thickness of the RCAA. Though there are variations in physical and chemical properties throughout the thickness of the RCAA, a single layer was used in the interest of simplicity. The model may be expanded to multiple layers in the future, as necessitated by the FMRP. The bedrock was not included in this model for simplicity, as well as the fact that constituent movement and loading are much smaller in bedrock than in the RCAA. It is recognized so that there are vertical differences in GW flow and composition to various degrees throughout the RCAA. To keep the model effective but simple, the hydraulics were combined from the three alluvial layers of the RCAA Subarea model (described in Section 3) and water chemistry was selected at key locations to represent the average of the variable vertical profile. The uniform PHAST model grid is shown on Figure 4-9.

4.5.1.3 Reactive Subsurface Transport Model Parameters

Hydraulic parameters for the PHAST model are hydraulic conductivity, specific storage, and effective porosity. A uniform K_h value of 30 m/day (both in the longitudinal and transverse directions) was assigned based on average values used in the RCAA Subarea model. It was assumed that K_h was 10 times K_v. Specific storage was set to 0.001 m^{-1}, reflecting semiconfined conditions. For numerical efficiency, the model was set to confined conditions so the saturated thickness and transmissivity remained constant during the simulations. Effective porosity was set to 0.1 based on professional judgment.

The physical transport parameter dispersivity was set to 20 m in the longitudinal direction (i.e., parallel with the primary GW flow direction) based on the 5,200-m scale of the system (Xu and Eckstein, 1995; Al-Suwaiyan, 1996). The common assumption was applied, where longitudinal dispersivity is 10 times the transverse dispersivity which, in turn is 10 times the vertical dispersivity. With a one-layer model, effects of K_v and vertical dispersivity were negligible.

Chemical parameters for PHAST involve two basic categories: (1) specifying solution chemistry for the various initial conditions and fluxes into and out of the model and (2) specifying porous media chemical properties that limit GW concentrations via precipitation and adsorption. The solution chemistry distribution is discussed in Section 4.5.1.4. A mineral suite that was judged to be controlling GW chemistry was developed on the basis of previous studies, current field observations, and pre-PHAST PHREEQC analysis of GW data performed in this study. PHREEQC was used to examine the mineral phases that were at or near saturation in the various waters around the RCTA. The selected minerals are listed in Table 4-7. All of these were designated as either "present in the aquifer matrix" or "could potentially form during GW mixing."

TABLE 4-7
Mineral Phases Assigned to PHAST Model for Solubility Constraints
Faro Mine Remediation Project

Mineral	Formula	SI [a]	Matrix Concentration [b]	Notes
Ferric Hydroxide	$Fe(OH)_3$	0.0	0.25	
Calcite	$CaCO_3$	0.0	2.0	
Dolomite	$CaMg(CO_3)_2$	0.0	2.0	to dissolve only
Rhodochrosite	$MnCO_3$	0.0	0.0	
Siderite	$FeCO_3$	0.0	0.0	
Hydrated Zinc Carbonate	$ZnCO_3\_H_2O$	0.0	0.0	
Cerussite	$PbCO_3$	0.0	0.0	
Gypsum	$CaSO_4\_2H_2O$	0.3	0.0	
Anglesite	$PbSO_4$	0.0	0.0	
Aluminum Hydroxide	$Al(OH)_3$	0.0	0.0	
Amorphous Silica	SiO_2	0.0	10.0	

Notes:
[a] Saturation Index, the degree of saturation or oversaturation of a mineral phase, assigned as a limit in the model.
[b] Assigned as moles surrounding each litre of groundwater.

The PHREEQC module of PHAST calculates the SI for every mineral phase in its database. The SI is defined as the log (IAP/Ksp), where IAP is the product of ion activities that make up the mineral, and Ksp is the solubility-product constant of that mineral. If the two products are the same, their ratio is one and therefore the log of that ratio (the SI) is zero. This indicates the mineral is in equilibrium with the water, or the water is said to be saturated with that mineral. If the SI is less than zero, the water is undersaturated so that precipitation of the mineral is not favoured, but the mineral could dissolve if present in the matrix. If the SI is above zero, the water is said to be oversaturated and precipitation may occur. The user selects mineral phases that PHAST will precipitate if their SI becomes larger than the user-defined level. For the list of minerals in Table 4-7, the SI threshold was zero, with two exceptions. Dolomite does not usually precipitate directly out of solution but can dissolve if the solution becomes undersaturated. This mineral was therefore set only to dissolve but not to precipitate. The other exception was gypsum, which was assigned an SI threshold of 0.3, slightly oversaturated. This was done because PHREEQC analysis of measured water chemistries commonly found the SI for gypsum to be in the 0.0 to 0.3 range so setting the threshold at 0.3 provides a site-specific setting for this important mineral. Note that most minerals were assigned a zero concentration in the matrix in Table 4-7. This was done because they are not present in areas of diluted GW, and assigning a concentration would result in these minerals dissolving into those waters and producing erroneous results.

Some mineral phases also act as adsorbents of ions, particularly trace metals. The most common of these are the iron oxides/hydroxides, whose surfaces attract trace metal ions such as zinc (Zn^{2+}), cadmium (Cd^{2+}), or lead (Pb^{2+}). The more freshly precipitated forms of iron are the most effective adsorbents due to their much higher surface area. A common chemical formula used for these solids is $Fe(OH)_3$. The abundance of this mineral was estimated based on historical measured iron content of background core samples, which ranged from 2.3 to 12.2 percent (SRK, 2006c). It was assumed that $Fe(OH)_3$ constitutes roughly 10 percent of the total iron in a given alluvial soil

deposit (Parkhurst et al., 1996). A range of 0.23 to 1.22 percent $Fe(OH)_3$ in an aquifer matrix corresponds to 0.25 to 1.35 moles of $Fe(OH)_3$ surrounding each liter of GW, assuming a total porosity of 0.3 and solids density of 2.65 kilograms per litre. A value of 0.25 moles per litre (mol/L) was assigned for the matrix concentration of $Fe(OH)_3$ during calibration. The adsorptive properties of this solid were assigned the default values in the database, which were taken from Dzombak and Morel (1990). Note that this mineral was allowed to precipitate if it became oversaturated, as shown in Table 4-7, so additional adsorbent was created when this occurred during simulations. In addition to $Fe(OH)_3$, $CaCO_3$ is also known to act as an adsorbent, with published exchange equilibria for zinc and cadmium (Zachara et al., 1991, 1993). These relationships were added to the PHAST model in the form of ion exchange reactions for use in this study. It was conservatively assumed that the actively exchanging concentration of $CaCO_3$ was 0.05 mol/L.

There are a number of other potential adsorbents for trace metals, including organic matter that was described in detail in a previous study (SRK, 2006c), along with aluminum hydroxide and clay minerals. The adsorption parameters included in the model are tied to specific mineral phases, but the calibrated quantities may be viewed as inclusive of all adsorbents present in the matrix.

4.5.1.4 Reactive Subsurface Transport Model Initial Conditions

The hydraulic portion of the PHAST model was run under steady-state assumptions so boundary fluxes and heads were constant throughout reactive transport simulations. The model required initial GW heads for all nodes for calculation purposes, and for this, a single value of 1,070.5 m CGVD28 was assigned—the approximate head at the upgradient end. The remaining boundary conditions are described in the next section.

Chemical initial conditions were selected from historical data from monitoring wells at key locations in the model domain. As Section 4.5.2 describes, the calibration period was from 2002 until 2012 so the initial GW chemistry was set as a blend of available data from 2002. Because some areas in the domain were not monitored until 2004, some data from that year were used, assuming the chemistry at those wells was not changing significantly between 2002 and 2004. An extensive survey of GW chemistry data was conducted to view changes in GW chemistry over time and space, as well as to examine the quality of the available data. Figure 4-10 shows the wells whose data were used to form the initial conditions. Water quality at each well represents the approximate chemistry of the GW near that well. To blend the chemistry between the well locations, a feature of PHAST allows a linear interpolation of water chemistry in one coordinate direction. The green arrows on Figure 4-10 depict the blending directions of initial water chemistry between upgradient and downgradient end members. The blending was done for two separate zones of the tailings area: north and south. These zones have shown different water chemistry in observed data, especially in the area of the Intermediate Dam and Polishing Ponds. GW in the immediate vicinity of the RCD channel was assigned the chemistry of X3 upgradient from the Fuse Plug (where a transition between gaining and losing RCD channel conditions begins) and from X10 below the Fuse Plug. Historical data show X10 to be slightly higher in TDS and sulphate than X3; otherwise, the two are of similar chemistry.

4.5.1.5 Reactive Subsurface Transport Model Boundary Conditions

The PHAST model domain lies within the much larger GW flow model grid described in Section 3. GW fluxes at the northern, eastern, and southern boundaries of the PHAST model were directly imported from the RCAA Subarea model to maintain consistency and connection between the modelling efforts. The calculated fluxes were combined for the alluvial layers of the RCAA Subarea model (Model Layers 1 through 3) and excluded the bedrock layers. The relative magnitude of flux entering these boundaries is displayed in colour code along the grid boundaries on Figure 4-11. The western boundary of the PHAST model was assigned a constant head of 1,013 m CGVD28, consistent with the RCAA Subarea model and measured heads in this area.

Infiltration of precipitation and SW into the top of the PHAST model domain was derived from the estimates made in a previous study of tailings infiltration (SRK, 2005c) in which the tailings were divided into 11 zones of coarse and fine tailings. The average infiltration values from that study of 34 mm/yr (coarse) and 16 mm/yr (fine) were applied to respective fine and coarse zones, shown on Figure 4-12. Though this distribution of infiltration was not used in the RCAA Subarea model, the average infiltration over the entire tailings area is very similar between the two models.

Representative water chemistry was assigned to every point of influx into the PHAST model domain. Like the initial chemical conditions, influx was assigned using historical water chemistry data. In most cases, data indicated no significant change in water chemistry for the inputs during the calibration period of 2002 through 2012. For these, an average of historical data was made for a constant input, as shown on Figure 4-11. The two input fluxes that were set to change chemical composition with time were GW inflow from the ETA and infiltration through tailings. For the ETA, historical data at X23 have shown marked increase in sulphate and metals concentrations over recent years. Though station FCS-4 more accurately represents flow that is directly entering the RCTA, a much more complete chemical record exists for X23; therefore, this station was used for the calibration period.

For infiltration through the RCTA, shown on Figure 4-12, the projected sulphate loading from the SRK (2005c) study, which is also incorporated in the GoldSim model, was used as a basis for the chemical changes over time. A sulphate loading value for each of the 11 simulated years (2002 through 2012) was estimated by regressing the SRK (2005c) model data using a quadratic fit, shown on Figure 4-13. Each tonne per year (tonne/yr) value was converted to a sulphate concentration, using the infiltration rate and area of each the 11 infiltration subareas shown on Figure 4-12. PHAST requires a chemically balanced analysis (i.e., total positive ion equivalents equal total negative ion equivalents) for water chemistry inputs or else either unrealistic results will be produced or the model may not converge. The GoldSim model used a mass ratio of sulphate to the other chemical constituents based on a selected tailings porewater sample. However, the resulting water chemistry is far from balanced, and an alternate tailings porewater sample, P01-09A from September 24, 2003, was used to calculate sulphate equivalent ratios of other ions. This porewater sample was selected as a representative of high-TDS tailings porewater that also showed a well-balanced, complete chemical analysis. Table 4-8 provides the calculated ratios.

Although loading estimates were also made for zinc in previous work (and included in the GoldSim model), these were not used in the PHAST model. Instead, the equivalent ratio of sulphate to zinc in the representative tailings porewater sample (P01-09A) was used to calculate zinc concentrations. This is assumed to be a more accurate loading of zinc because there are several mineral phases that likely exert controls on zinc concentrations that were not considered in the previous work. In fact, the report on this work calls this fact out and suggests that the loading estimates may be overly conservative (SRK, 2005c). The calculated zinc concentrations from the original loading estimates are approximately double those used in the PHAST model. The PHAST model concentrations were checked, and zinc appeared to be near saturation with controlling mineral phases. If the previous values were used, zinc minerals would be oversaturated; therefore, the concentrations are not realistic.

The detailed distribution of sulphate loading from SRK (2005c) was not available; only the total tonnes/yr values over time for the entire RCTA were available in the report and in the GoldSim model. The calculated average sulphate loading values were applied to each of the 11 infiltration zones, and the area and assigned infiltration rate for each zone were used to calculate a weighted average concentration of sulphate that infiltrates through each zone in each simulated year. Using the equivalent ratios in Table 4-8, complete water chemistry for each zone and each simulation year were calculated and assigned to the PHAST model. As a result, each of the 11 infiltration zones was assigned an infiltration water chemistry for each of the 11 simulated calibration years (2002 through 2012) for a total of 121 infiltration water chemistries in each model run. The strength of each zone's set of water chemistries was altered during calibration, as the following paragraph describes.

A portion of ETA discharge is known to flow onto the surface of the tailings and eventually infiltrate to the aquifer (Christoph Wels, RGC; personal communication, 2013). To separate this infiltration from the average annual tailings infiltration, the ETA infiltration was assigned immediately west of the tailings, as shown on Figure 4-12. Though in reality the infiltration likely intermingles with tailings further east, this simple method helped to more easily track this component and change during calibration. Because the tailings provide a much stronger source of constituents than X23 water alone, this small portion of ETA discharge was assigned the chemistry of the nearest of the 11 tailings infiltration zones, area IIIN-f, shown on Figure 4-12.

TABLE 4-8
Calculated Porewater Sulphate Ratios for Water Chemistry Constituents
Faro Mine Remediation Project

Station ID	P01-09A	Value Used in Calculations	Notes	SO_4 Equivalent Ratio
Date	09/24/03			
pH	5.9			
Temp	3.2			
SO_4	77,600	75,864	Adjusted to meet ion equivalent balance	1
Fe	35,900	36,909	Adjusted to meet ion equivalent balance	8.37E-01
Zn	5,520	5,520		1.07E-01
Mg	633	633		3.30E-02
Ca	495	495		1.56E-02
Mn	243	243		5.60E-03
Na	100U	50	Half of reporting limits and actual measured value on September 26, 2002	1.38E-03
K	100U	50	Half of reporting limits and actual measured value on September 26, 2002	8.09E-04
Pb	1.6	1.6		9.78E-06
Ba	1U	0.5	Value represents max detected at P01-9A	4.61E-06
Cu	1U	0.5	Value represents max detected at P01-9A	9.96E-06
Ni	1	1		2.16E-05
As	0.5U	0.3	Value represents max detected at P01-9A	1.90E-09
Co	0.3U	0.2	Value represents max detected at P01-9A	4.30E-06
Cd	0.05U	0.03	Value represents max detected at P01-9A	3.38E-07

Notes:
Concentrations in mg/L.
100U = Nondetect with value indicating the reporting limit.

4.5.1.6 Reactive Subsurface Transport Model Time Discretization

The PHAST model conducts the most intensive calculations to move from initial conditions to applied fluxes and infiltration during early simulation times. The time steps during this period were therefore made small (1 day) for the first 13 days, then 10 days, until one-fifth of a year (73 days) had passed. At that point, the model was run with a constant time step of 18.25 days (one-twentieth of a year). This produced acceptable model numerical stability with reasonable run times for the 11-year calibration period. Post-calibration runs of the model over a 54-year time period used a maximum time step of 73 days.

4.5.2 Reactive Subsurface Transport Geochemical Model Calibration

The CSM of the RCTA reveals that recent increases in GW concentrations of sulphate and trace metals have been caused by two principal inputs to the GW system: ETA drainage, and infiltration through tailings. Concentrations of these constituents have been increasing for the past 10 years in ETA sources, and modelling of the tailings (SRK, 2005c) and of the ETA sources (SRK, 2009c) predicted an increase from both sources for the next 100 to 200 years. Observed GW monitoring well data in the RCTA has shown a marked increase in sulphate over the past 10 years, along with an increase in trace metals in some wells. The PHAST model was calibrated over the 2002 through 2012 period, which has the most complete chemical record during which these increases have been observed.

4.5.2.1 Reactive Subsurface Transport Model Calibration Approach

The calibration was initially aimed at matching trends in sulphate over the calibration period in the target locations. Sulphate behaves much more conservatively than trace metals, and matching these data emphasized adjustment of the hydraulic and dispersive model parameters of the model. Concentrations from tailings

infiltration were based on the modelled values from a previous study (SRK, 2005c) so these concentrations were also subject to adjustments during sulphate calibration.

Once an acceptable visual match to sulphate concentrations was achieved, attention was turned towards matching zinc concentrations. Zinc was designated as a representative of the less conservative trace metals, whose concentrations are more strongly influenced by adsorption and precipitation reactions during mixing and transport. Commonly associated with cadmium in source materials, zinc is more plentiful and therefore more clearly tracked in GW than cadmium, as well as the more strongly attenuated lead. Of the trace metals of concern at the FMC, zinc is expected to be the first identified to break through in GW monitoring wells and is therefore best used for calibration. During this calibration phase, the amount and binding strength of adsorbent material (namely $Fe[OH]_3$ and $CaCO_3$) present in the aquifer matrix were adjusted to match observed zinc data to a reasonable degree.

As noted, in the interest of simplicity, the model was restricted to one layer representing the RCAA. In reality, there is a complex distribution of constituents with depth, with different trends in the various monitoring well clusters. The approach of the model calibration was to produce a reasonable fit of highly variable data, with an emphasis on matching general longer-term concentration trends, and not every short-term concentration fluctuation, at a given location.

4.5.2.2 Reactive Subsurface Transport Model Calibration Targets

The monitoring well locations shown as green circles on Figure 4-9 were selected to be the calibration targets for the study. Though not all wells had complete chemical records for the entire calibration period, they are considered representative of the general areas in which they are located. The emphasis of the calibration was placed on the downgradient locations at the CVD (P01-02A and P01-11) and the Intermediate Dam Pond (P01-03 and X25-96A) because the main objective of this study relates to forecasting water quality changes of GW leaving the site towards potential downgradient receptor areas. The RCAA beneath the RCTA, as well as the tailings themselves, are far too complex to account for all observed data trends; therefore, an approximate match to the key constituents was the goal for wells in the tailings area upgradient of the Intermediate Dam and Polishing Ponds.

4.5.2.3 Reactive Subsurface Transport Model Calibration Process

Model output was sent to post-processing software and spreadsheets, where simulated data were compared graphically to observed data from each of the target wells during the calibration period. Model parameters were adjusted on the basis of this comparison, and these adjustments were documented for each model run. For the sulphate matching process, the parameters that were adjusted from the starting values included model boundary fluxes, initial water chemistry distribution, and infiltration water chemistry. The model accounts for sulphate precipitation (via gypsum solubility) and adsorption reactions, but these were not altered during the sulphate stage of the calibration.

The tailings infiltration water chemistry adjustments were made with the goal of preserving: (1) the ratio of sulphate to the other chemical constituents (described in Section 4.5.1.5) and (2) the relative changes in sulphate through time, as modelled by SRK (2005c). To accomplish this, a multiplication factor was applied to each of the 11 infiltration zones shown on Figure 4-12. All zones had a starting factor of 1.0. If a factor was adjusted for a zone, it would be applied to all constituents in all modeled annual concentrations for that zone, preserving points (1) and (2) above.

As described, a 900-m^2 area was assigned for a portion of the ETA flow to infiltrate vertically through the downgradient end of the tailings area. A starting value of 20 percent of the average ETA flow was adjusted during calibration. The water chemistry from the nearest tailings infiltration zone, area IIIN-f (shown on Figure 4-12), was used for this area and was only altered if it was deemed necessary to alter that zone's multiplication factor, as described in the previous paragraph.

Once sulphate matches were deemed adequate, the zinc output was examined, and calibration was continued to match observed data. This stage of calibration required less effort, as many of the same parameters that factored in the sulphate simulations played major roles in matching zinc data. The main adjustments made during this calibration phase were in adsorption parameters that work to attenuate zinc migration while having little effect

on sulphate concentrations. Some adjustments were made to other parameters to strike the best compromise between the sulphate and zinc fits to data.

4.5.2.4 Reactive Subsurface Transport Model Calibration Results

The results of the calibration are provided in Figures 4-14a and 4-14b, displaying model matches to the target well locations for sulphate and zinc, respectively. The calibrated model parameters are provided in Table 4-9. These matches to observed data were considered adequate given the complexity of the FMC, variability in the data and inherent uncertainties of model parameters, and modelling objectives discussed in Section 4.1. Work will continue to improve this calibration and test sensitivity to predicted future conditions. The greatest emphasis in the calibration was in matching CVD well data, as these are the furthest downgradient and represent GW that will move offsite if not captured and, if captured by design wells, will determine future levels of treatment required.

TABLE 4-9
Calibrated PHAST Model Parameters
Faro Mine Remediation Project

Parameter	Value	Units	Notes
Hydraulic Conductivity, horizontal	30	m/day	
Hydraulic Conductivity, lateral	30	m/day	
Hydraulic Conductivity, vertical	3	m/day	
Effective Porosity	0.1		
Specific Storage	0.001	1/m	
Dispersivity, longitudinal	20	m	
Dispersivity, lateral	2	m	
Dispersivity, vertical	0.2	m	
South Boundary Groundwater Flux	variable	m/day	Imported directly from groundwater flow model
North Boundary Groundwater Flux	variable	m/day	Imported directly from groundwater flow model
East Boundary Groundwater Flux	variable	m/day	Imported directly from groundwater flow model
West Boundary Constant Head	1013	m above mean sea level	
ETA Infiltration Through Tailings	0.35	L/sec	10% of average measured flow at FCS-4
Infiltration Concentration Factors (unitless multipliers to adjust concentration)			
IIIN-c	1		
IIIN-f	1		
IIIS-c	1		
IIIS-f	0.4		
IIN-c	1		
IIN-f	1		
IIS-f	1		
IN-c	1		
IN-f	1		
IS-c	0.4		
IS-f	1		
Concentration of $Fe(OH)_3$ in matrix	0.25	mol/L	Correlates with approximately 2.3% total iron (see Section 4.5.1.3
Concentration of calcite in matrix	0.05	mol/L	

The match to well P01-11 is slightly underestimated in sulphate concentration because of a compromise to avoid overestimation of zinc at this well. Specialized zones of differing adsorbent concentrations could be created to improve the fit, but this was not done in the absence of data to justify such distinctions. Other targets that showed less than ideal matches, such as P03-06-4, are most likely the result of using initial condition water chemistry that is not fully representative in some areas. A decision was made during model construction to use actual water analyses for target well initial conditions, rather than vertical averaging. This was done because the chemical profiles are highly variable, often with very high concentrations near the tailings/alluvium interface, and averaging the profile would skew the concentrations towards these very high values. Instead, actual analyses from near the middle of the profile were used, and not all of these necessarily represent the bulk of the GW flowing though these areas. More detailed selection of representative chemistry, or possibly additional model layering, may occur to address this in the future if such activity is considered warranted to meet project objectives. For P03-06-4, the simulated sulphate concentration was greater than observed (shown on Figure 4-14a), and other wells in this cluster showed sulphate values similar to simulated values. Zinc concentrations, by contrast, were matched fairly well at this location (shown on Figure 4-14b), demonstrating the heterogeneous nature of the water chemistry.

Figure 4-15 summarizes sulphate concentrations across the entire model domain at selected times during calibration. The influence of ETA inflow is clearly visible on the north side, but infiltration through tailings also plays a critical role. During initial stages of calibration, it was assumed (based on previous work) that the majority of the increasing sulphate concentrations observed near the Intermediate Dam Pond and CVD wells had drainage from the WRD area (and ETA in particular) as their source (RGC, 2011). Infiltration through tailings was thought to be less important and, as such, was originally modelled as an average flux over the entire ETA. It became clear that the observed flows from ETA (averaging about 3.5 litres per second at FCS-4) and estimated underflow from areas further west were not sufficient to account for the observed concentrations. At that point, the RCTA was divided into the 11 recharge zones (SRK, 2005c) so that more flexibility in distribution of recharge could be applied. Only after this alteration to the model was made could the data be fit at the northern CVD and Intermediate Dam Pond wells, which indicates that the tailings are playing a significant role as the source of these concentrations. The final calibration included adjusting the multiplication factor for infiltration areas IS-c and IIIS-f to 40 percent of their original concentrations, as shown in Table 4-9. The rest of the areas were left at initial values. A finer-scale alteration of all 11 zones will likely provide a better fit to the data but that was not performed at this stage. An autocalibration technique may be applied in the future if a finer-scale alteration is deemed useful.

What is presented here represents an initial calibration. As more data become available and refinement is requested, parameters and possibly model structure will continue to be adjusted. The model is viewed as a working, improving tool in which the most up-to-date knowledge of hydraulic and geochemical data are applied.

4.5.3 Reactive Subsurface Transport Geochemical Model Application

The calibrated model was used to simulate future conditions in the downgradient areas of the domain, namely, the Intermediate Dam Pond and CVD areas. This was also an opportunity to compare model output with that of the GoldSim model, which has output data for both Intermediate Dam Pond and CVD. It is assumed in this scenario that no corrective measures, such as covers or diversions, are implemented.

4.5.3.1 Setup for Predictive Reactive Subsurface Transport Simulations

Simulation of future conditions used the same hydraulic and static chemical boundary conditions and parameters of the calibration. The two dynamic chemical boundary conditions, ETA inflow and infiltration through tailings, were extended through time using the existing GoldSim model settings as a basis. Projected sulphate concentrations from X23 drainage catchment in the GoldSim model, which incorporates all flows contributing to catchment outflow, were downloaded for a 50-year period (2006 through 2056). Because the constituents in the GoldSim model are not chemically balanced, the equivalent ratios of sulphate to all other constituents were compiled from the averages of X23 data used in the calibration. In a similar manner to the method used for tailings infiltration for the calibration, complete water chemistry was assigned for each modelled year of ETA inflow along the 800-m reach of the north model boundary.

The tailings infiltration was modelled in the same manner used in calibration. The GoldSim model values of average sulphate tonnes/yr, obtained from SRK (2005c), were downloaded from the model. These values were spaced in 2-year intervals, and the years in between were calculated by interpolation between each pair of data points. The annual tonnes/yr were then converted to sulphate concentrations and, in turn, to complete water chemistries using the same equivalent ratios reported in Table 4-8.

The model was run from 2002 through 2056. Sulphate and zinc concentrations were again used as the principal indicators of future conditions. Figure 4-16 shows the projected increases in sulphate between 2012 and 2056. The same mineral solubility and adsorption constraints were maintained for this PHAST model run as those set in calibration so that as more highly concentrated seepage enters the aquifer, mineral phases such as gypsum and $Fe(OH)_3$ were precipitated out of solution by the model to maintain specified equilibrium.

4.5.3.2 Reactive Subsurface Transport Model Application Results

The results of the applied model are focused on the CVD and Intermediate Dam Pond areas and are shown on Figures 4-17a and 4-17b, respectively. The two wells representing each area were used as calibration targets, and their observed data are also provided on the figures for perspective. Also included in these figures is the GoldSim model output for the two areas. Because the GoldSim model is not a spatially distributed numerical model, the output should be viewed as a general average of conditions. As demonstrated during calibration and observed in previous studies (e.g., RGC, 2011), the northern wells in the CVD and Intermediate Dam Pond area show a stronger mining influence than the southern wells, resulting in higher projected sulphate and zinc concentrations. The sulphate simulations results shown on Figure 4-17a illustrate this difference, with the GoldSim model results falling in between recent data, as expected. The PHAST model captures the spatial difference and the leading edge of higher concentrations but also predicts a stronger rise in sulphate than the GoldSim model does.

For zinc concentrations at the CVD, Figure 4-17a shows the GoldSim model predictions far above those of observed and PHAST-simulated results. This is likely due to: (1) strong overestimates of tailings infiltration loading, as discussed previously and noted in the original study and (2) the lack of accounting for precipitation and adsorption reactions that reduce zinc and other metal concentrations during mixing and transport. The PHAST simulations were calibrated to the observed data and predict a much gentler rise in zinc concentrations over the next 40 to 50 years.

The PHAST mode simulation at the Intermediate Dam Pond well P01-03 clearly overestimates zinc concentrations. This is likely because of localized variations in zinc source and the potential overestimation of infiltration concentrations in the designated ETA infiltration area (Figure 4-12), which were assumed to be identical to tailings porewater. However, it is interesting to note that even with this overestimation the model correctly predicts the low downgradient zinc concentrations at CVD well P01-11. This demonstrates the strong metals attenuation potential of the aquifer at the leading edge of the sulphate plume migration. The model in its present state predicts zinc levels will rise but remain below 0.2 mg/L at CVD over the next 40 years. The most critical variables to this prediction are the amount of adsorption capacity present in the aquifer and the future loading levels of zinc into the aquifer.

Figure 4-18 shows predicted sulphate concentrations over the entire grid area for selected years. The increased sulphate predicted for the ETA is shown to continue to influence the area and, to a lesser degree, the tailings infiltration increases load downgradient.

4.5.3.3 Reactive Subsurface Transport Model Use and Limitations

The PHAST transport model was designed to examine present GoldSim model assumptions and to suggest revisions and additions to the GoldSim model to better serve the objectives of the FMRP. The results of the PHAST modelling account for the spatially different distribution of affected GW between north and south and predict a stronger rise in sulphate in the near future, as compared to forecasts from the GoldSim model. This is likely caused by PHAST accounting for input fluxes from all sides of the tailings area rather than only upgradient and ETA underflows. By accounting for precipitation and adsorption reactions, PHAST more accurately simulates a strong attenuation of zinc in the CVD and Intermediate Dam Pond area, whereas the GoldSim model does not include these reactions and, as a result, greatly overpredicts zinc concentrations.

The PHAST model results should be used to augment the GoldSim model to correct for these key parameters and inputs. The method of implementation is still being developed but may involve running the GoldSim model first to provide input parameters to PHAST (principally ETA inflow) then running PHAST to provide a refined output for use in assessing downgradient concentrations.

Like all models, the PHAST model is a simplified approximation of a natural complex system and is therefore subject to inaccurate representations. The overlying tailings body is a highly complex, heterogeneous mixture of materials that produce porewater ranging in concentrations over several orders of magnitude. The RCAA is also heterogeneous, with varying vertical chemical variations. The fact that PHAST was constructed as a single-layer model forces a gross averaging of these variations; as such, the predicted GW concentrations will be rough approximations at best. The model does, however, fulfill its purpose of accounting for key chemical controls on concentrations during mixing and transport. Though the effects of these reactions will vary with the composition of the aquifer matrix, it is important to account for them in a manner that considers known thermodynamic relationships. The PHAST model does not account for flow in tailings (saturated or unsaturated); only inputs to the RCAA from tailings porewater. The PHAST model also does not account for flow or transport associated with the underlying bedrock.

Other than infiltration of ETA surface flow, the PHAST model does not account for the infiltration of SW that flows onto the surface of the tailings. This infiltration was incorporated into the RCAA Subarea model, discussed in Section 3, but was left out of the PHAST model at this stage. It will be added as the models are further developed.

The most sensitive chemical parameters of the model are the concentrations of the source water inputs and the adsorptive capacity of the aquifer matrix. These represent model uncertainties that would benefit most from additional data collection. Continued monitoring of the deepest tailings pore water at as many locations as possible is recommended, along with choosing new borings in unmonitored areas, such as the northwestern area of the tailings. The adsorptive capacity estimates will be supported by a series of cores collected from aquifer solids beneath and downgradient from the RCTA. The cores may be analyzed for reactive iron oxide/hydroxides via a series of selective extractions. A number of these tests have been initiated, and additional locations should be selected. Finally, GW monitoring wells should be installed in the northwest area of the model domain, upgradient of the Intermediate Dam Pond, in tandem with the suggested tailings porewater monitoring in this area. Additional wells north of this area would be useful to better characterize influx to the RCAA from hydraulic and chemical standpoints.

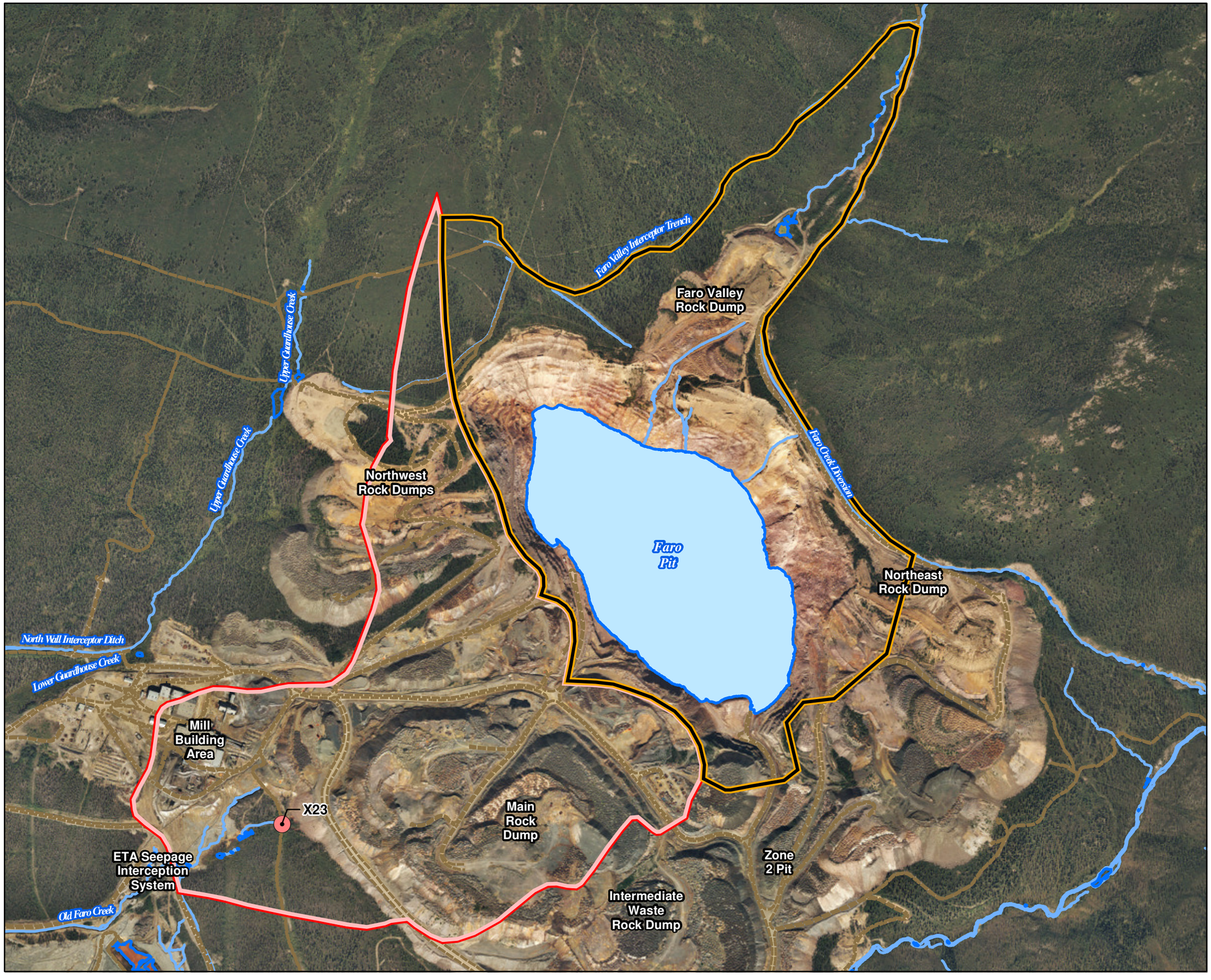

VICINITY MAP

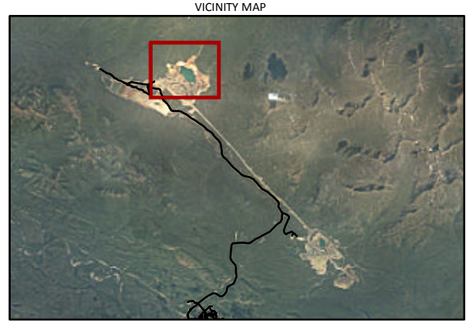

LEGEND

- Collection node for the X23 Catchment
- Roads Unpaved
- Stream
- Lake, Pond, or Pool
- Faro Site Waterbody (Faro Pit)
- Waste Rock Dump Geochemical Model Boundary (X23)
- Faro Pit Lake Geochemical Model Boundary

Notes:

1. Aerial photography acquired by Peregrine Aerial Surveyors Inc. and Eagle Mapping in August 2012.
2. Orthophotography prepared by Critigen Canada Corp.

N

0 160 320 480 640

Metres

Created by: CRITIGEN

FIGURE 4-1

Study Area for Geochemical Mixing Models

Faro Mine Remediation Project

CH2MHILL

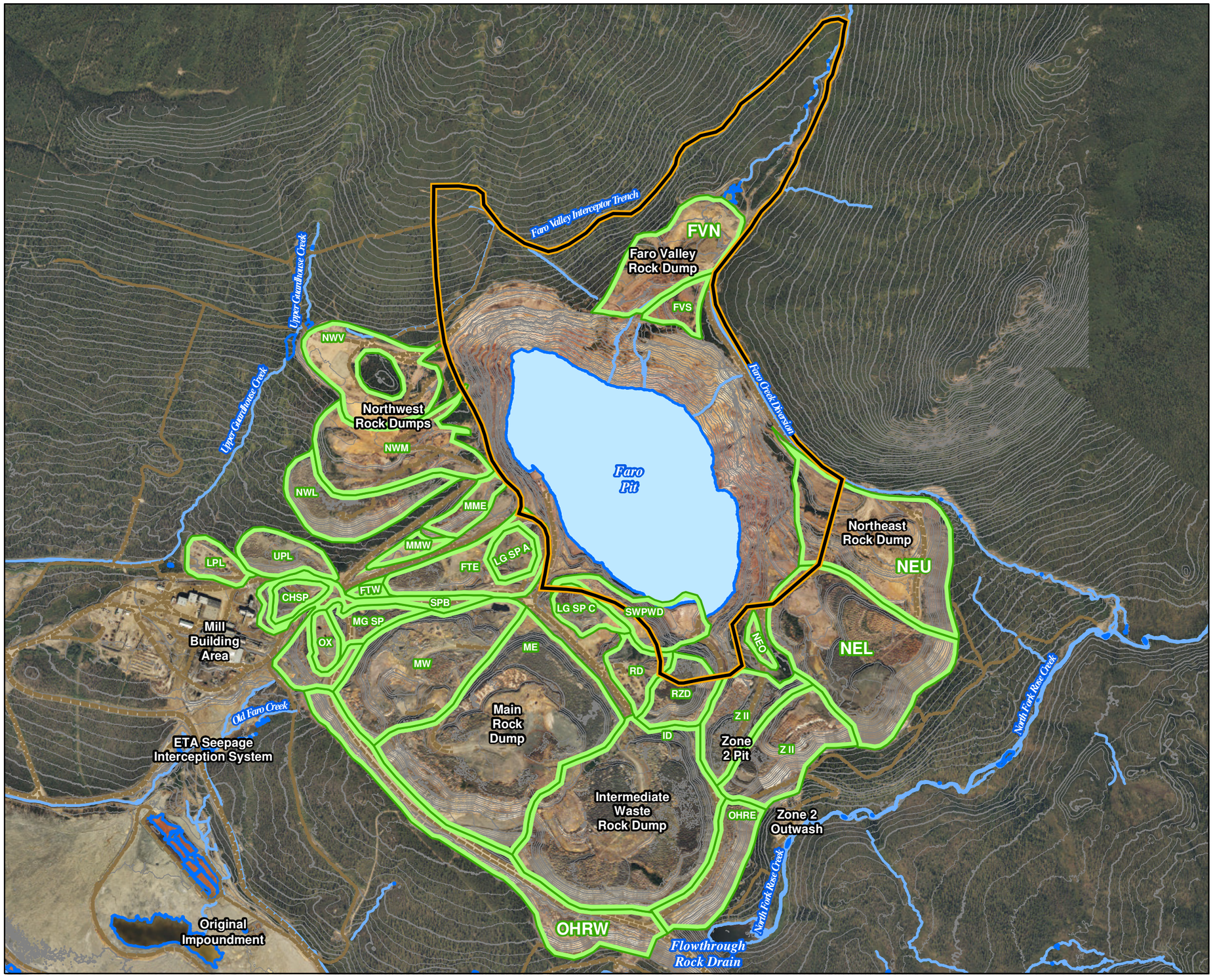

VICINITY MAP

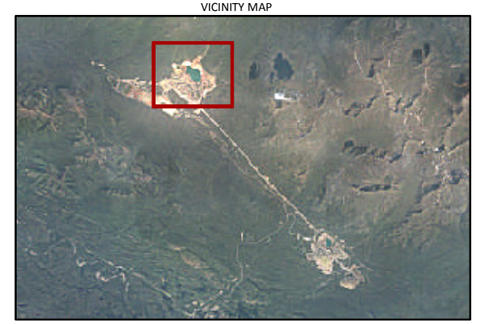

LEGEND

- Elevation Contours
- Roads Unpaved
- Stream
- Lake, Pool, or Pond
- Faro Site Waterbody (Faro Pit)
- Waste Rock Dump Area (WRD)
- Faro Pit Lake Geochemical Model Boundary

Notes:

1. Aerial photography acquired by Peregrine Aerial Surveyors Inc. and Eagle Mapping in August 2012.
2. Orthophotography prepared by Critigen Canada Corp.

N

0 190 380 570 760

Metres

Created by: CRITIGEN

FIGURE 4-2

Faro Pit Reactive Mixing Model Domain

Faro Mine Remediation Project

CH2MHILL

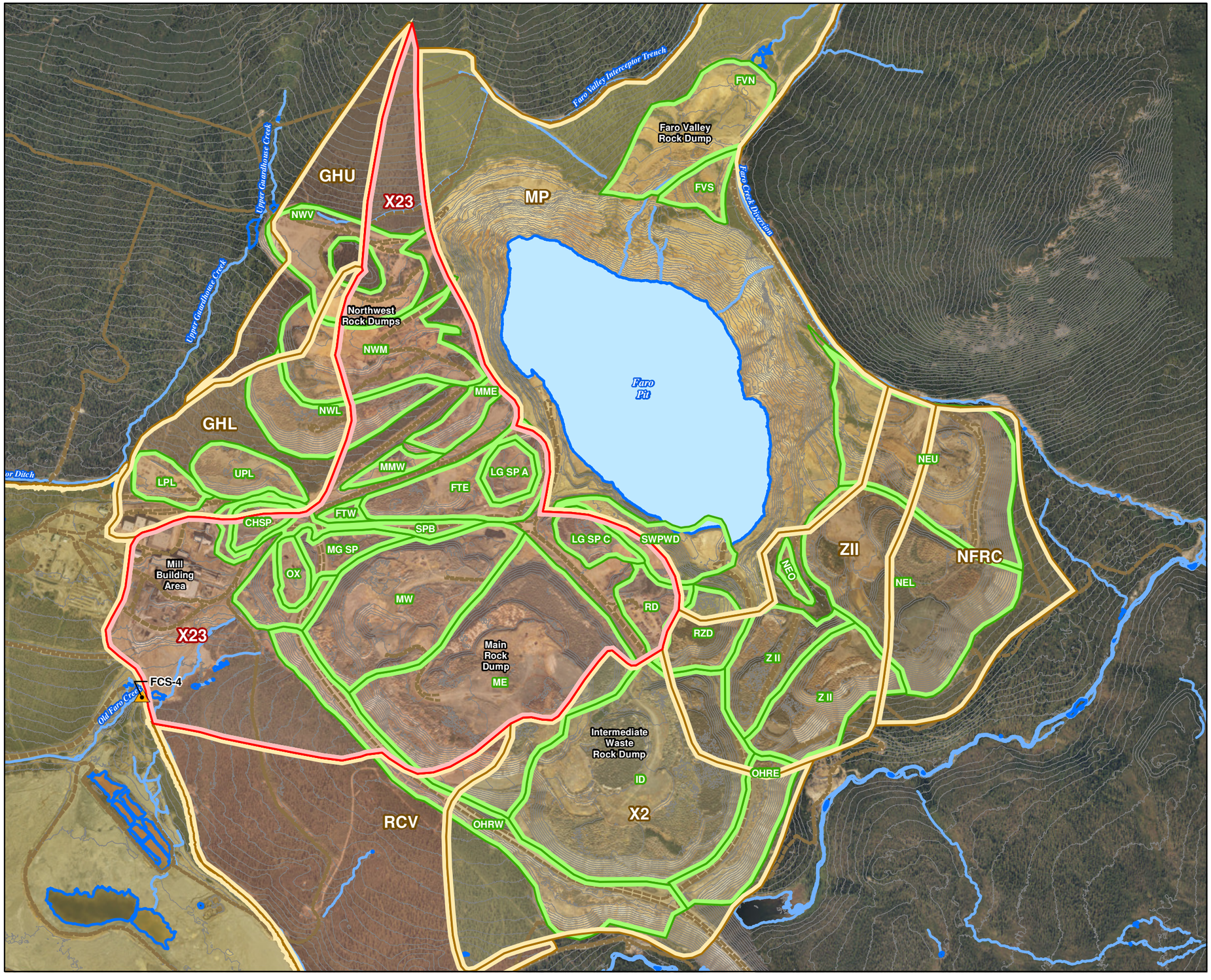

VICINITY MAP

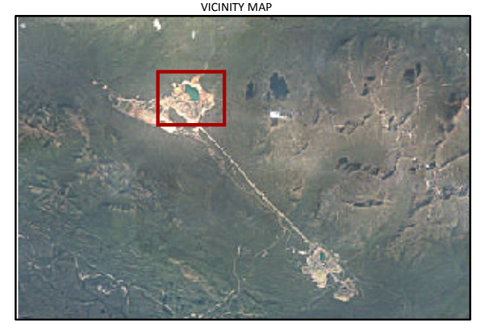

LEGEND

- Flow Monitoring Location
- Elevation Contours
- Roads Unpaved
- Stream
- Lake, Pool, or Pond
- Faro Site Waterbody (Faro Pit)
- Waste Water Catchement (WWC)
- Waste Rock Dump Area (WRD)
- Waste Rock Dump Geochemical Model Boundary (X23)

Notes:

1. Aerial photography acquired by Peregrine Aerial Surveyors Inc. and Eagle Mapping in August 2012.
2. Orthophotography prepared by Critigen Canada Corp.

N

0 130 260 390 520

Metres

Created by:
CRITIGEN

FIGURE 4-3

Waste Rock Dump Reactive Mixing Model Domain

Faro Mine Remediation Project

CH2MHILL

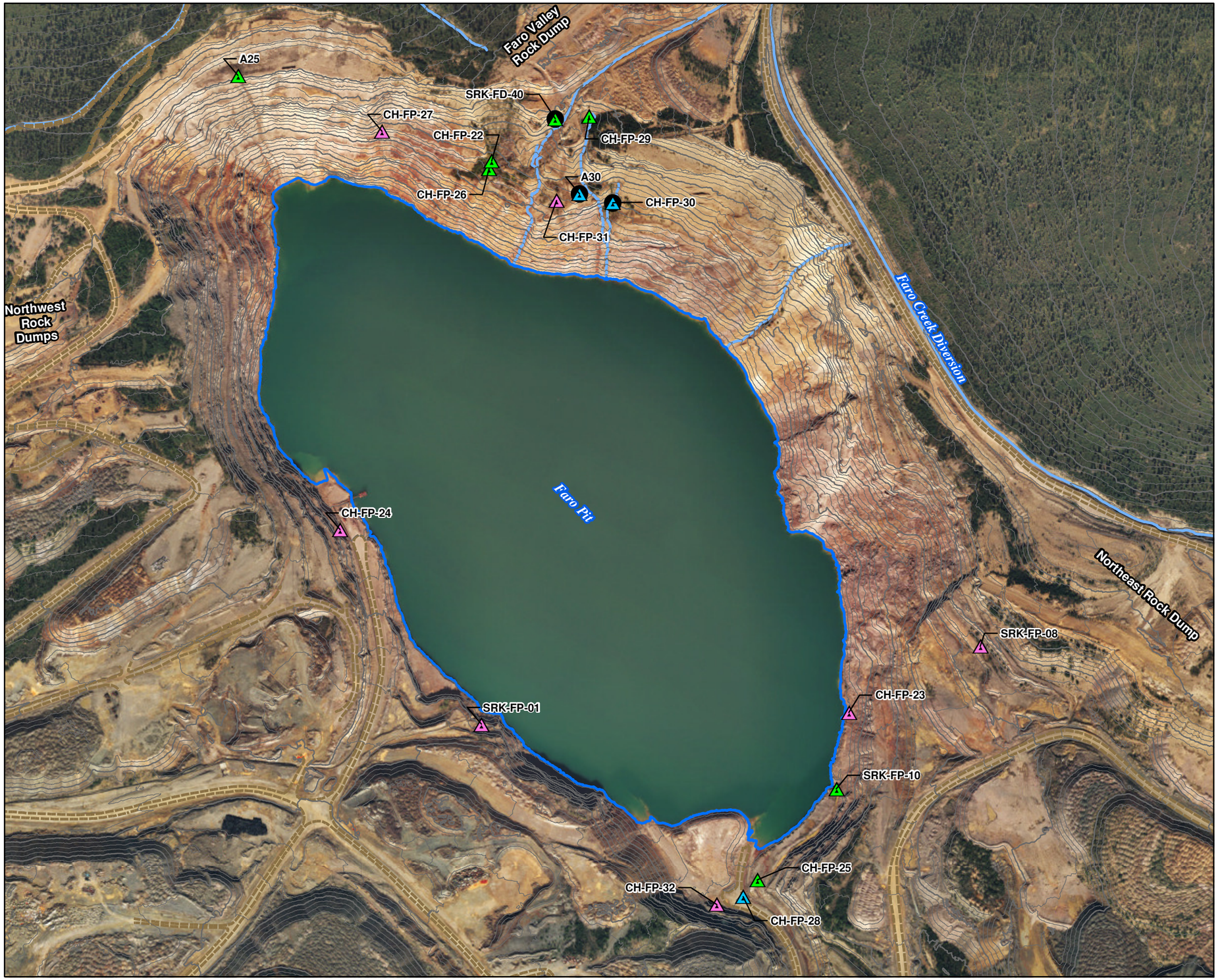

VICINITY MAP

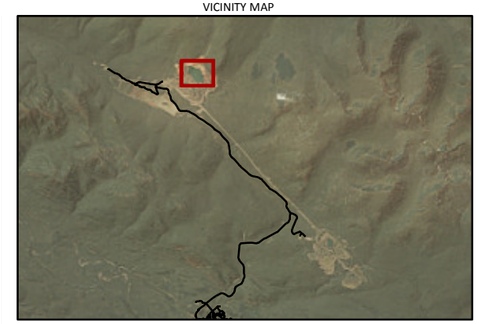

LEGEND

- Seep Sample Location (Spring 2012)
- Seep Sample Location (Fall 2012)
- Seep Sample Location (Spring and Fall 2012)
- Seep Locations Used to Calculate Faro Creek Diversion Leakage Composition
- Elevation Contours
- Roads Unpaved
- Stream
- Lake, Pool, or Pond

Notes:

1. Aerial photography acquired by Peregrine Aerial Surveyors Inc. and Eagle Mapping in August 2012.
2. Orthophotography prepared by Critigen Canada Corp.
3. 5-metre contour interval shown based on October 2011 LiDAR.
4. Seep sample locations shown are based on hand held GPS coordinates.

N

0 75 150 225 300

Metres

Created by: CRITIGEN

FIGURE 4-4

Seep Locations Used for Background Conditions

Faro Mine Remediation Project

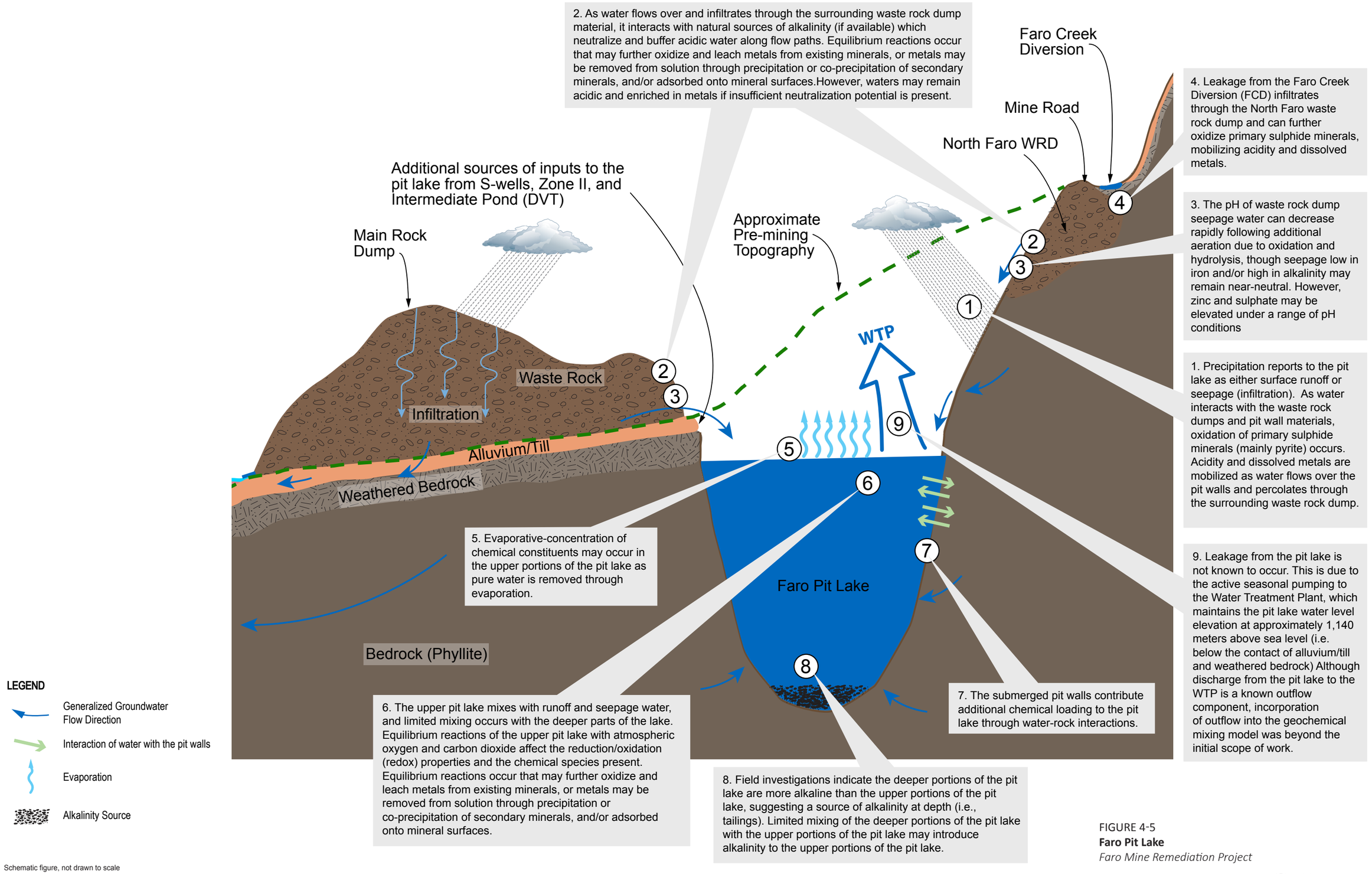

Schematic figure, not drawn to scale

FIGURE 4-5
Faro Pit Lake
Faro Mine Remediation Project

1. As precipitation falls on and infiltrates the waste rock dump, oxidation of primary sulphide minerals (mainly pyrite) occurrs. Acid and dissolved metals are mobilized as water percolates through the waste rock dump.

2. As water migrates through the waste rock dump, it interacts with natural sources of alkalinity (if available) which neutralize and buffer acidic water along flow paths. Equilibrium reactions occur to further dissolve and oxidize minerals, and metals may be removed from solution through precipitation or co-precipitation into mineral structures, and/or adsorbed onto mineral surfaces. However, waters may remain acidic and enriched in metals if insufficient neutralization potential is present.

3. Dissolved metals and mineral acidity are transported through the waste rock dumps to the underlying alluvial material where the water either travels along the paleo-surface topography or infiltrates the alluvium. Water following the paleo-surface emerges at the toe of the waste rock dumps as surface water seeps (4), whereas water infiltrating the underlying alluvium migrates away from the waste rock dumps as groundwater.

4. The pH of surface water seeps can decrease rapidly following additional aeration due to oxidation and hydrolysis (i.e., X23 seepage), though seepages low in iron and/or high in alkalinity may remain near-neutral. However, zinc and suphate may be elevated under a range of pH conditions.

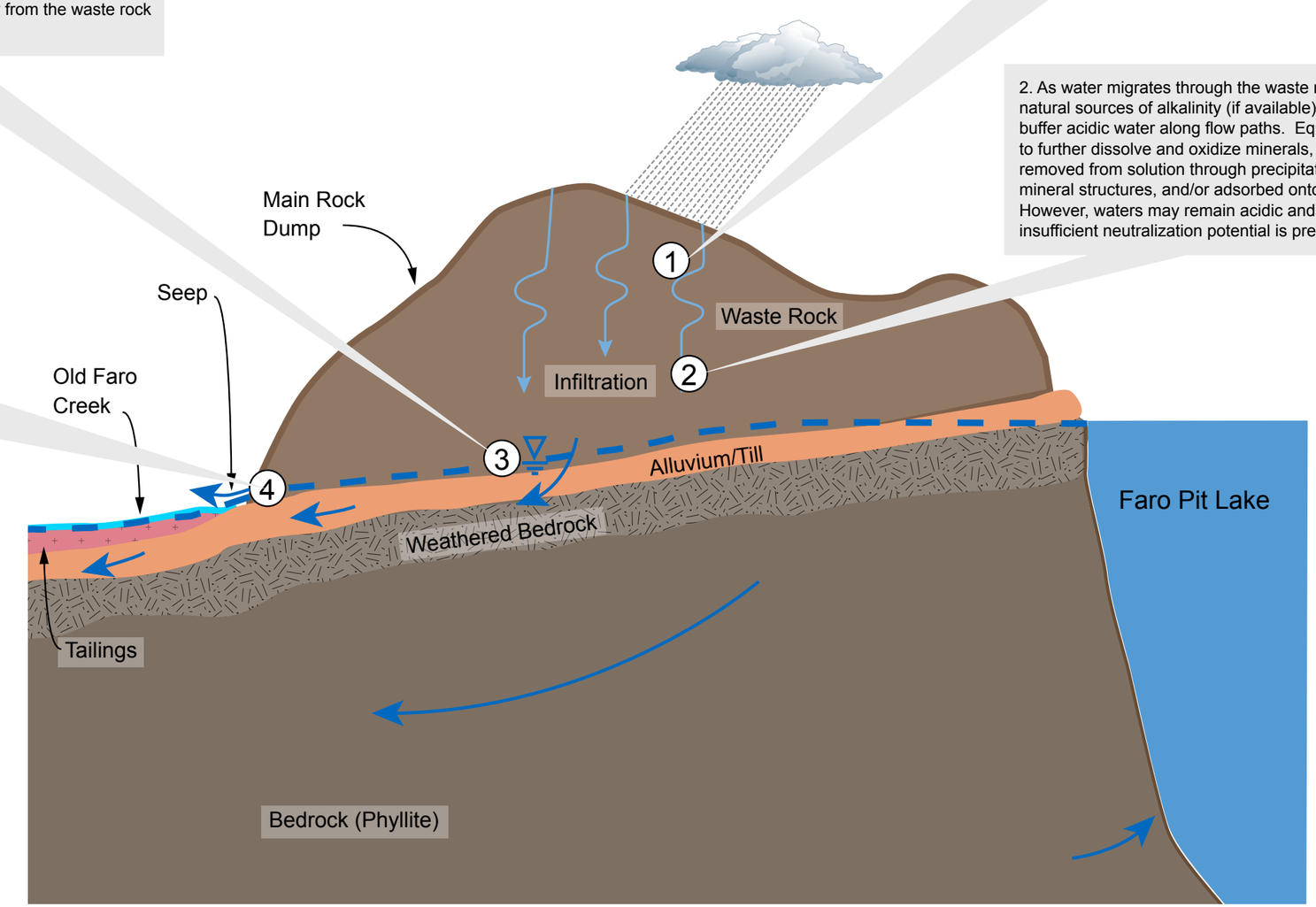

LEGEND

Water Table

Generalized Groundwater Flow Direction

0 500m

Vertical Exaggeration: 4.4x

FIGURE 4-6
Waste Rock Dump Geochemical Inputs
Faro Mine Remediation Project

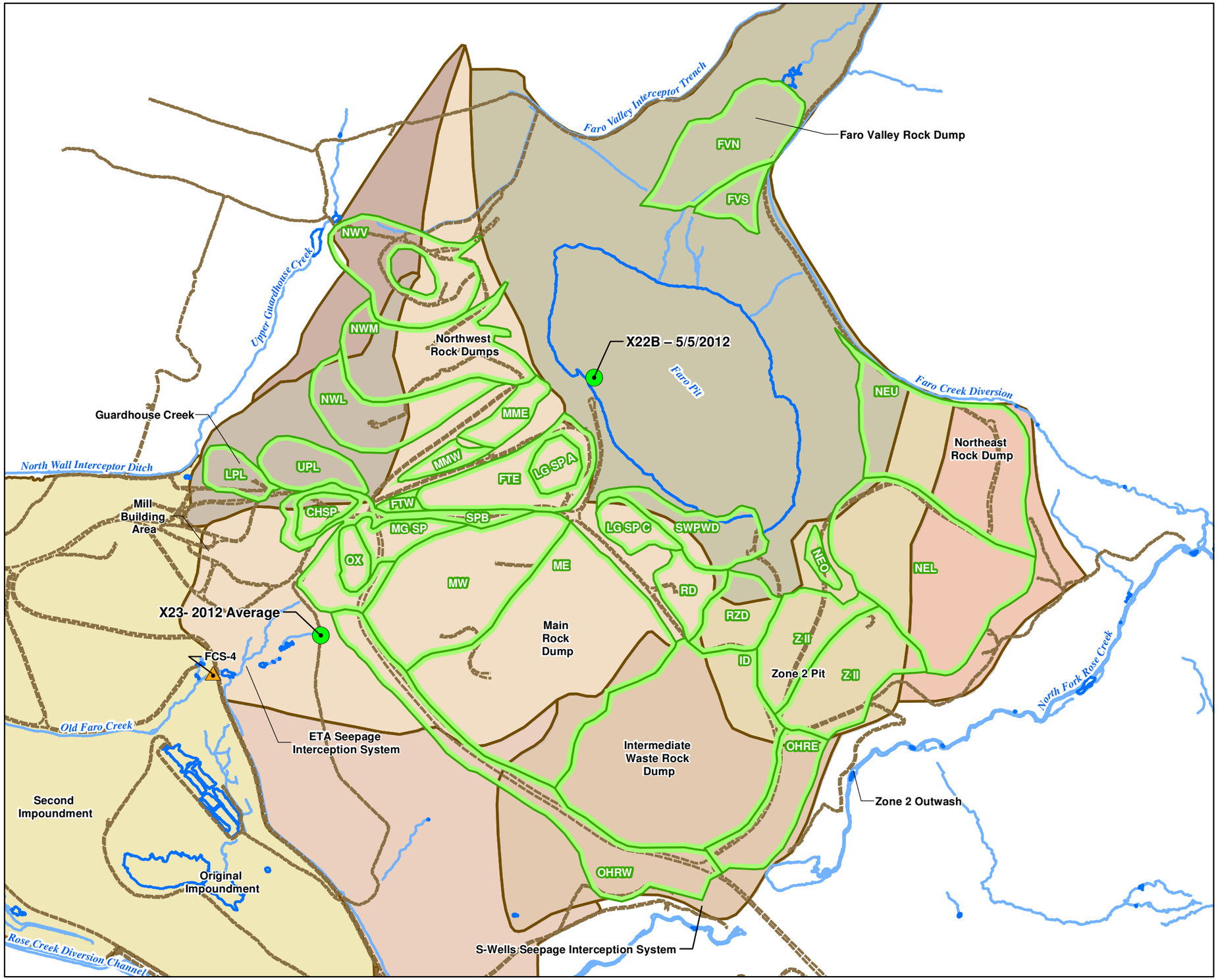

VICINITY MAP

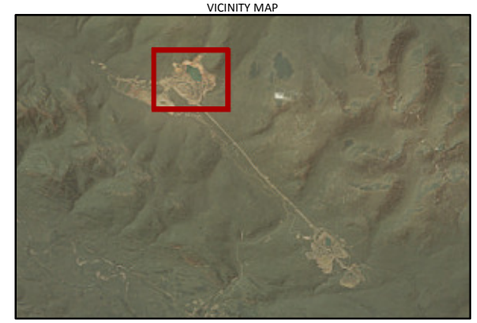

LEGEND

- Calibration Target
- Flow Monitoring Location
- Roads Unpaved
- Stream
- Lake, Pool, or Pond
- Waste Rock Dump Area (WRD)
- Waste Water Catchement (WWC)

Notes:

1. Aerial photography acquired by Peregrine Aerial Surveyors Inc. and Eagle Mapping in August 2012.
2. Seep sample locations shown are based on hand held GPS coordinates.

N

0 175 350 525 700

Metres

Created by: CRITIGEN

FIGURE 4-7

Reactive Mixing Model Calibration Targets

Faro Mine Remediation Project

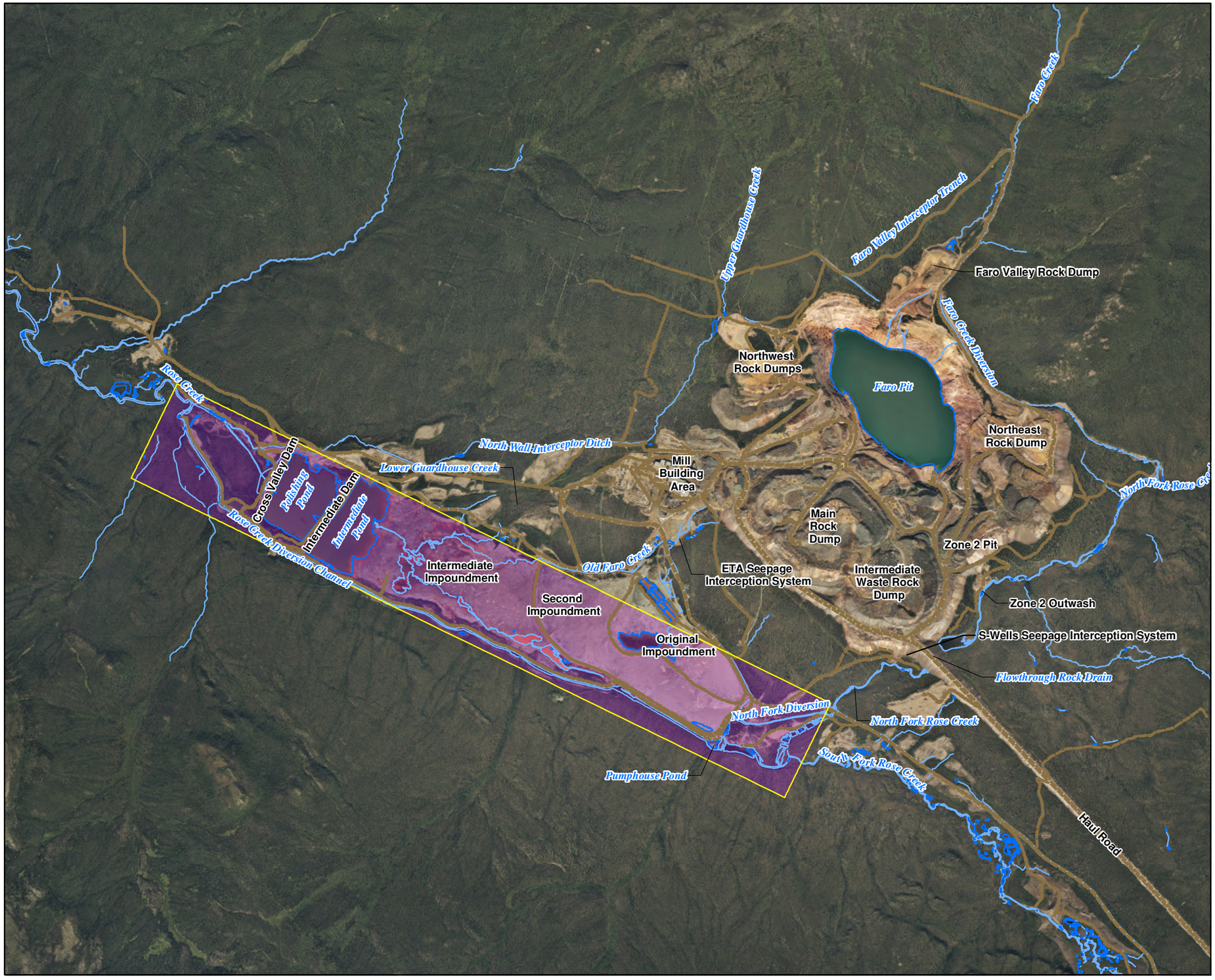

VICINITY MAP

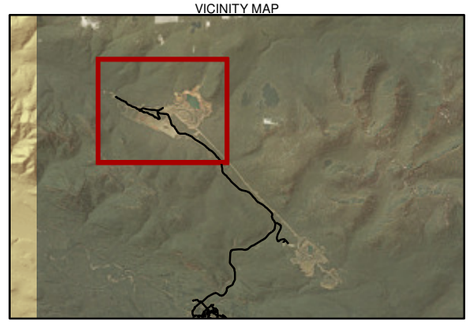

LEGEND

- Roads Unpaved
- Stream
- Lake, Pond, or Pool
- Model Domain

Notes:
1. Aerial photography acquired by Peregrine Aerial Surveyors Inc. and Eagle Mapping in August 2012.
2. Orthophotography prepared by Critigen Canada Corp.

N

0 280 560 840 1,120
Metres

Created by:
CRITIGEN

FIGURE 4-8
Tailings Area Reactive Transport Model Domain
Faro Mine Remediation Project

CH2MHILL

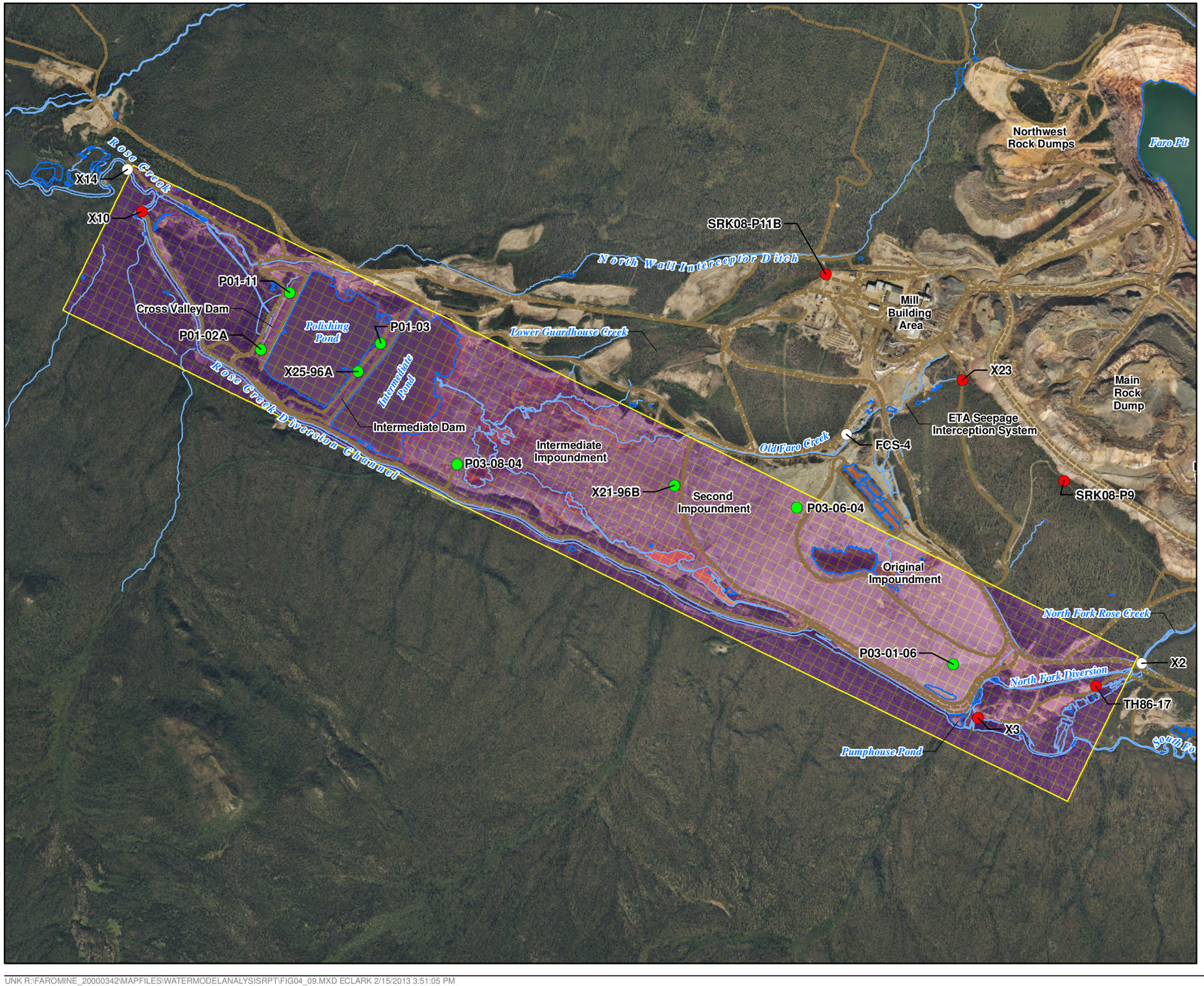

VICINITY MAP

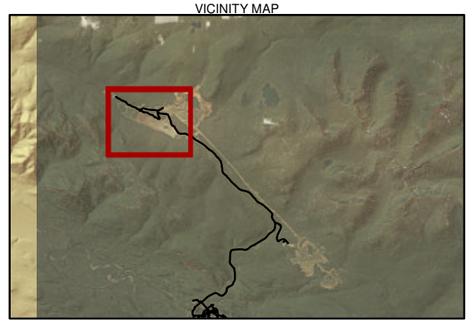

LEGEND

- General Reference Well Location
- PHAST Chemistry Flux Well Location
- PHAST Calibration Target Well Location
- Roads Unpaved
- Stream
- Lake, Pond, or Pool
- PHAST Model Grid

Notes:

1. Aerial photography acquired by Peregrine Aerial Surveyors Inc. and Eagle Mapping in August 2012.
2. Orthophotography prepared by Critigen Canada Corp.

N

0 180 360 540 720

Metres

Created by:
CRITIGEN

FIGURE 4-9
PHAST Model Grid
Faro Mine Remediation Project

CH2MHILL

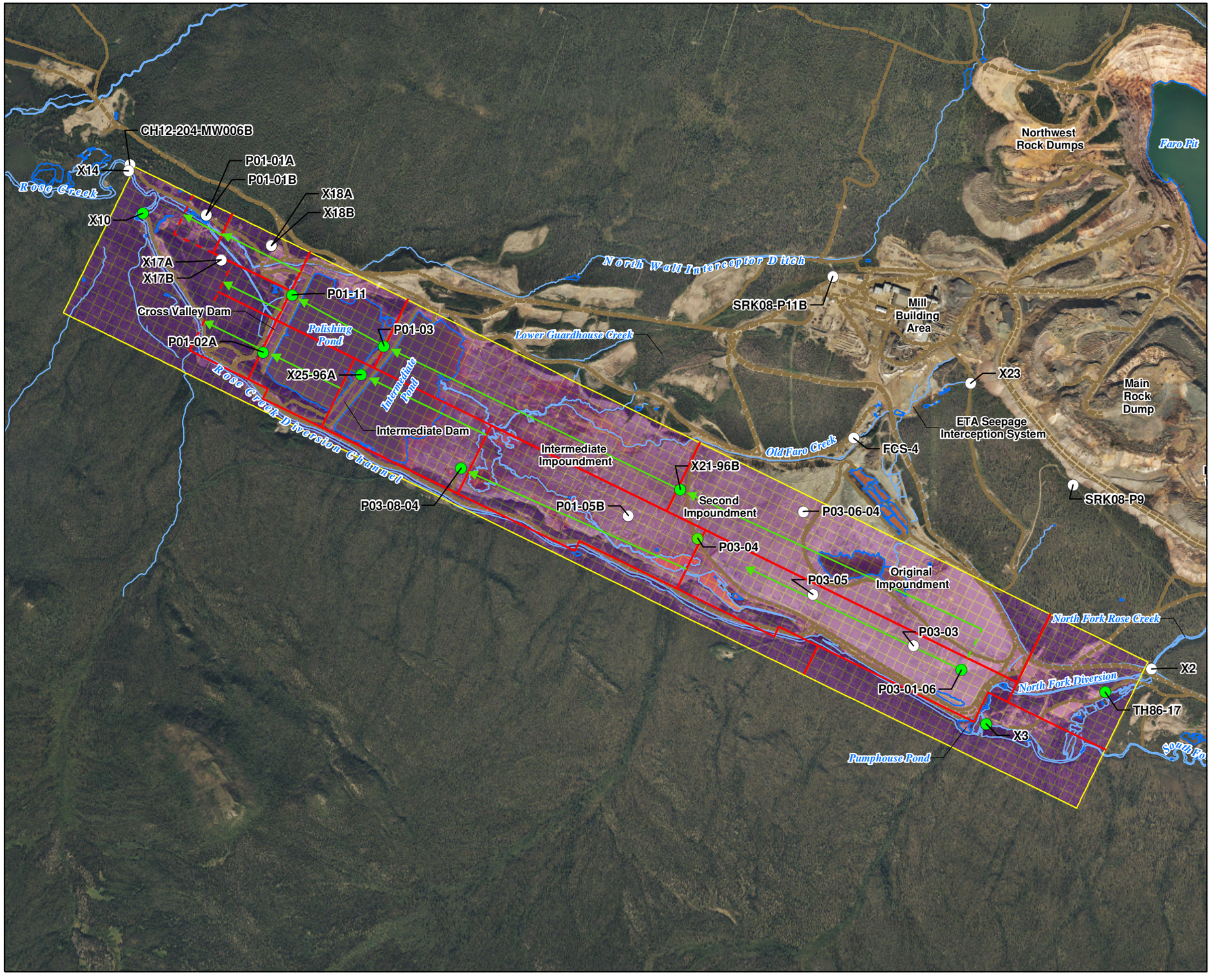

VICINITY MAP

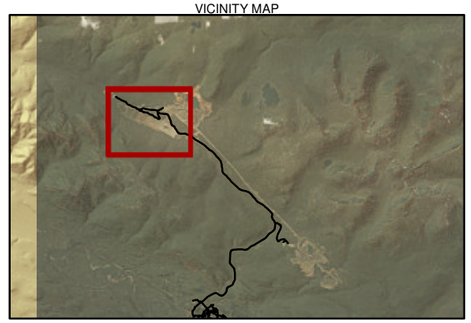

LEGEND

- General Reference Well Location
- PHAST Initial Condition Well Location
- Roads Unpaved
- Stream
- Lake, Pond, or Pool
- Boundary of Initial Chemical Conditions Zones Assigned to Model (based on the chemistry of the representative well in each zone)
- X10 Water Chemistry Boundary
- Transition from Upgradient to Downgradient Water Chemistry
- PHAST Model Grid

Notes:
1. Aerial photography acquired by Peregrine Aerial Surveyors Inc. and Eagle Mapping in August 2012.
2. Orthophotography prepared by Critigen Canada Corp.

N

0 180 360 540 720
Metres

Created by:
CRITIGEN

FIGURE 4-10
PHAST Model Initial Chemical Conditions
Faro Mine Remediation Project

CH2MHILL

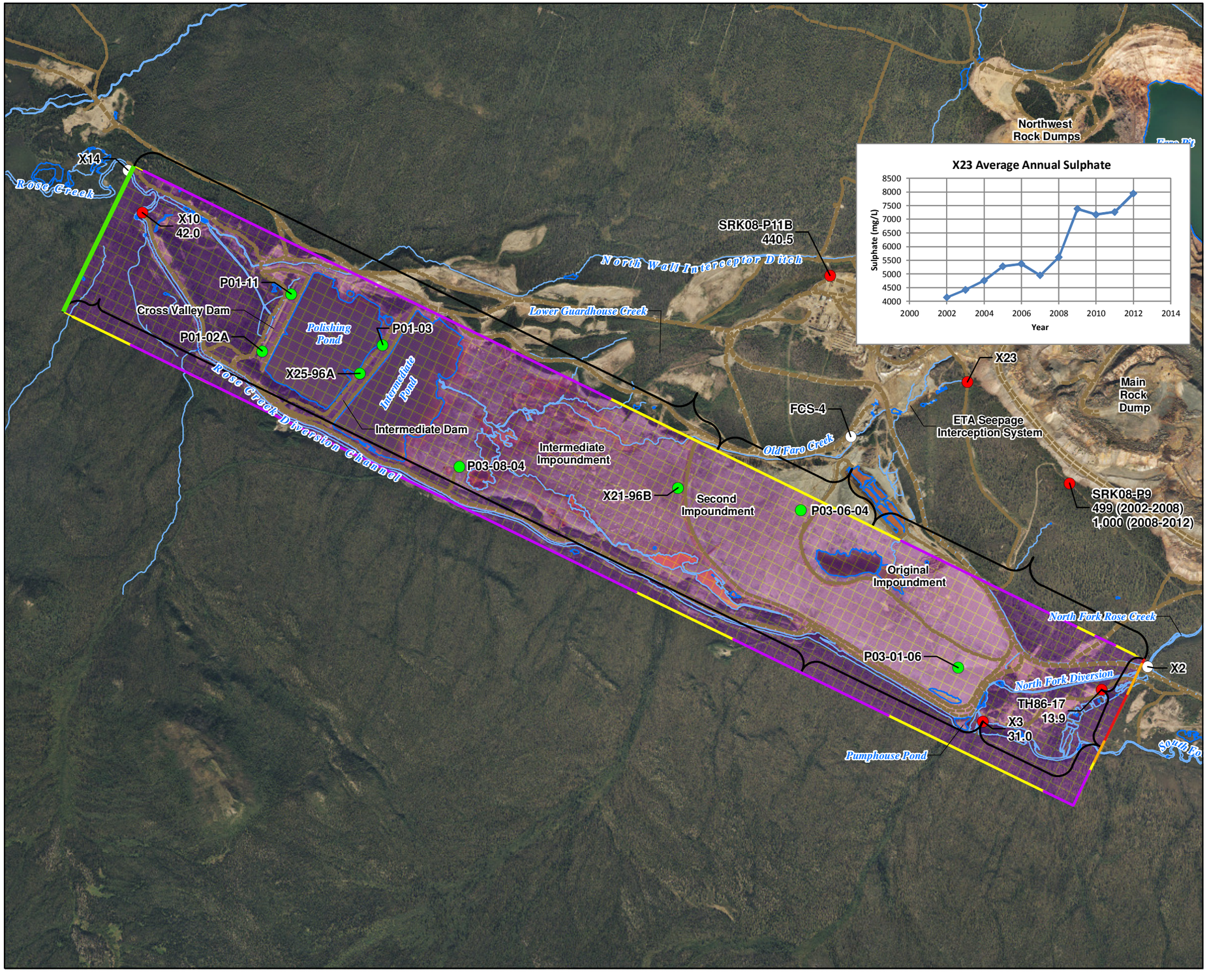

VICINITY MAP

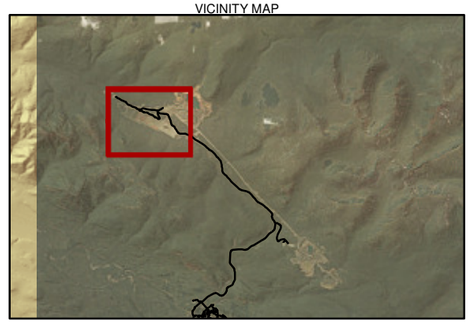

LEGEND

- General Reference Well Location
- PHAST Chemistry Flux Well Location
- PHAST Calibration Target Well Location
- Roads Unpaved
- Stream
- Lake, Pond, or Pool
- Constant Head: 1,013.0 m CGVD28
- PHAST Model Grid
  440.5 Sulphate Concentration of Assigned Solution (mg/L)

Specified Flux (m/day)

- 0 to 0.01
- 0.01 to 0.05
- 0.05 to 0.10
- 0.10 to 0.18

Notes:

1. Aerial photography acquired by Peregrine Aerial Surveyors Inc. and Eagle Mapping in August 2012.
2. Orthophotography prepared by Critigen Canada Corp.

N

0 180 360 540 720

Metres

Created by:
CRITIGEN

FIGURE 4-11
PHAST Model Lateral Boundary Conditions
Faro Mine Remediation Project

CH2MHILL

VICINITY MAP

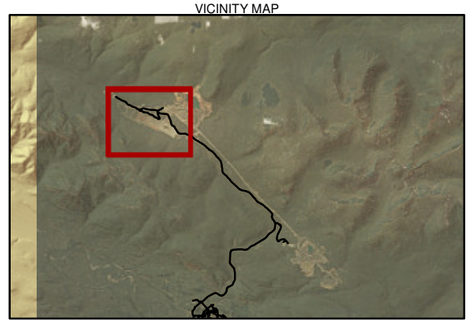

LEGEND

- General Reference Well Location
- PHAST Chemistry Flux Well Location
- PHAST Target Well Location
- Roads Unpaved
- Stream
- Lake, Pond, or Pool
- PHAST Model Grid
- Tailings Infiltration Zone based on SRK (2005)

Notes:

1. -c = Coarse Tailings
2. -f = Fine Tailings
3. Infiltration zone names and boundaries based on SRK (2005).
4. Aerial Photography Acquired by Peregrine Aerial Surveyors Inc. and Eagle Mapping in August 2012.
5. Orthophotography prepared by Critigen Canada Corp.

N

0 180 360 540 720

Metres

Created by:
CRITIGEN

FIGURE 4-12

PHAST Model Infiltration Boundary Zones

Faro Mine Remediation Project

CH2MHILL

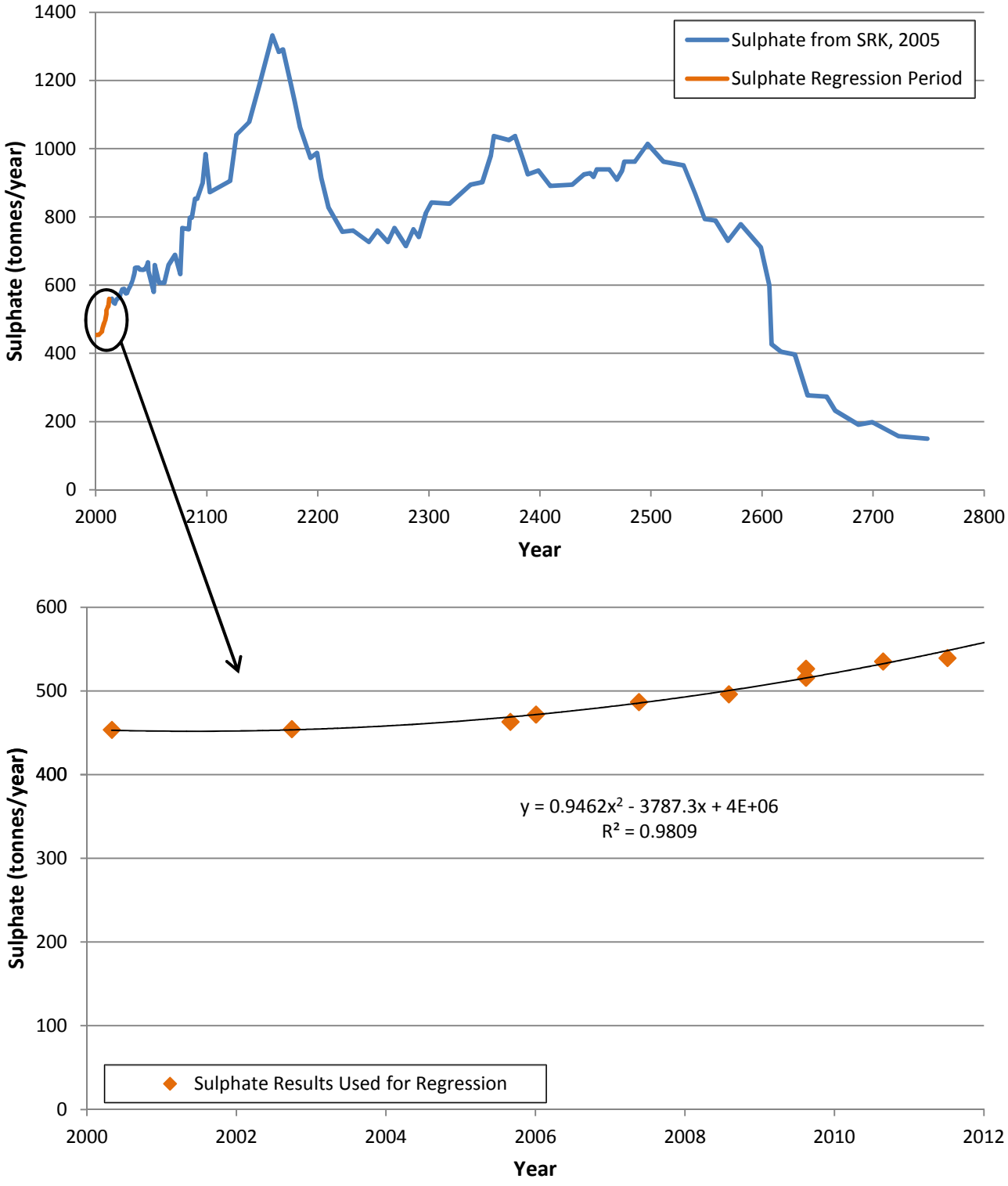

FIGURE 4-13
Projected Sulphate Loading to RCCA via Infiltration Through Tailings
Faro Mine Remediation Project

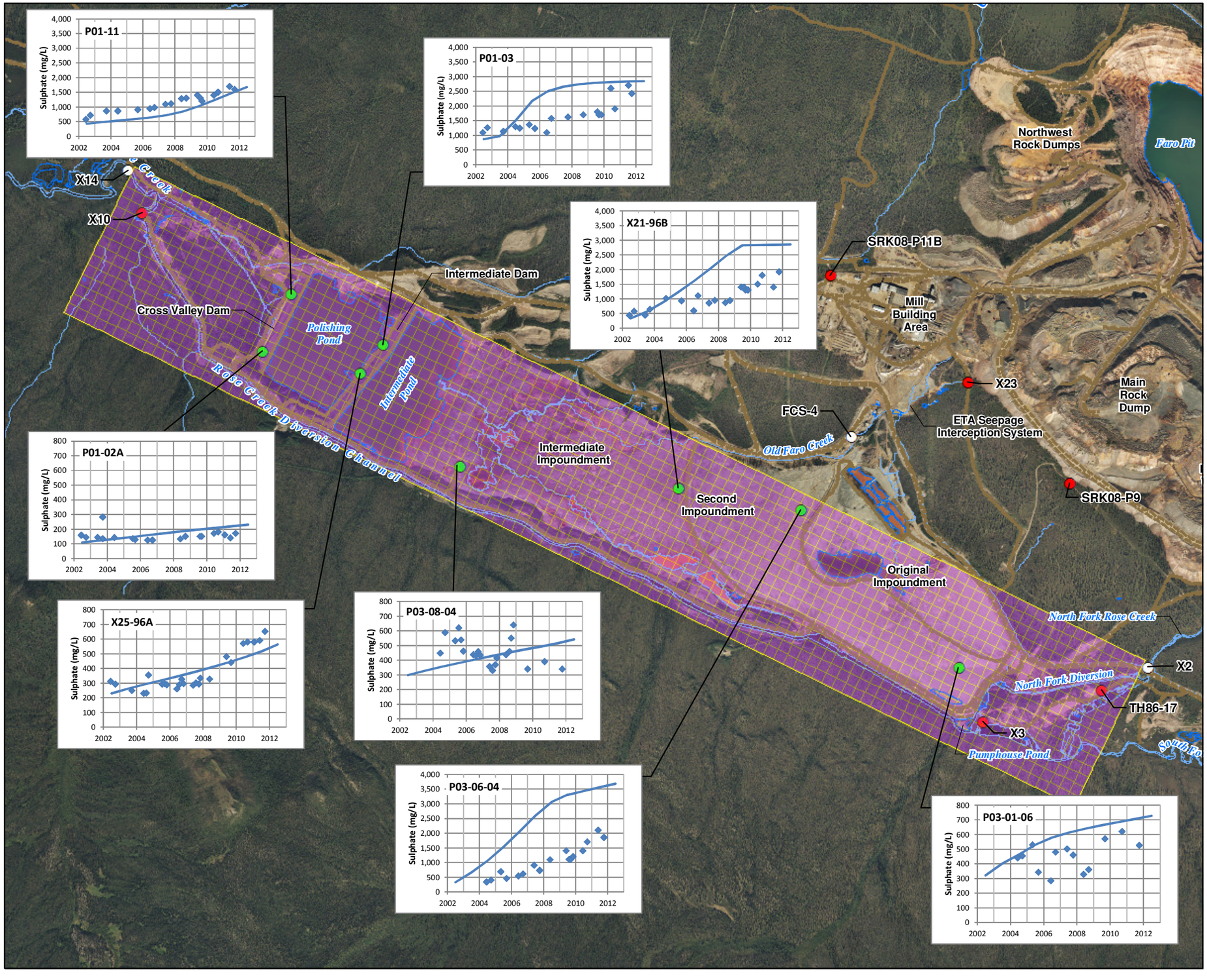

VICINITY MAP

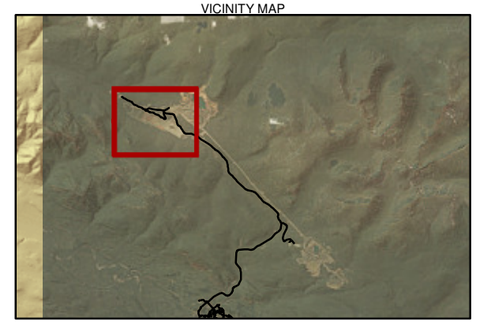

LEGEND

- General Reference Well Location
- PHAST Chemistry Flux Well Location
- PHAST Calibration Target Well Location
- Roads Unpaved
- Stream
- Lake, Pond, or Pool
- PHAST Model Grid

Graph Legend

- Actual Concentration
- PHAST Simulated Concentrations

Notes:

1. Aerial photography acquired by Peregrine Aerial Surveyors Inc. and Eagle Mapping in August 2012.
2. Orthophotography prepared by Critigen Canada Corp.

N

0 180 360 540 720

Metres

Created by: CRITIGEN

FIGURE 4-14a

PHAST Model Calibration Results - Sulphate

Faro Mine Remediation Project

CH2MHILL

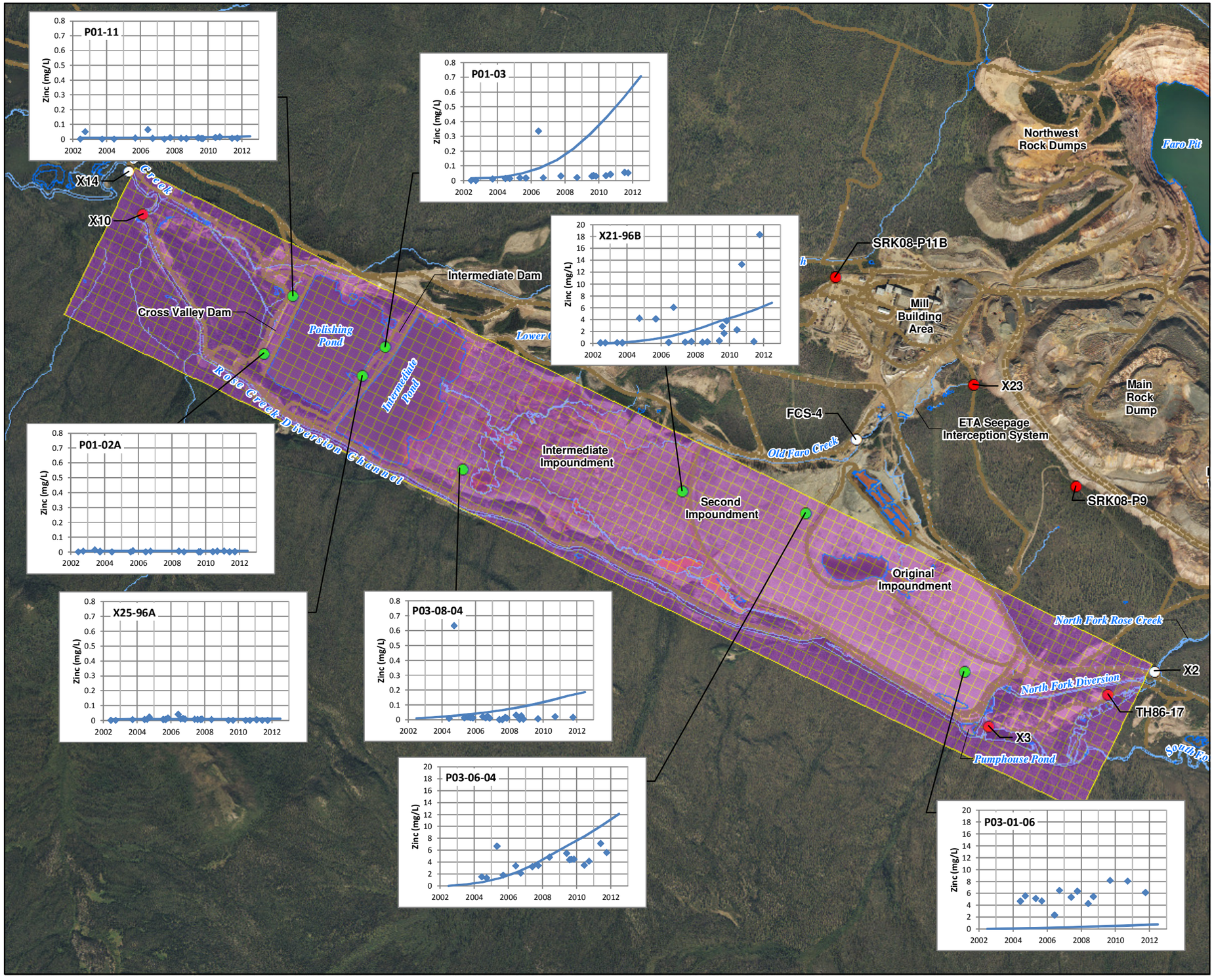

VICINITY MAP

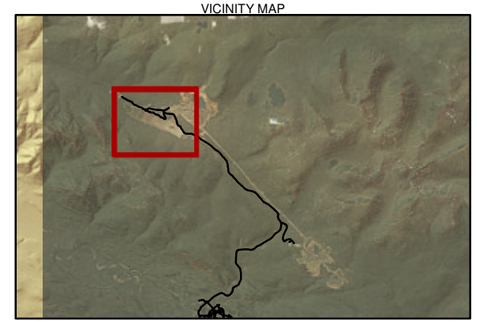

LEGEND

- General Reference Well Location
- PHAST Chemistry Flux Well Location
- PHAST Calibration Target Well Location
- Roads Unpaved
- Stream
- Lake, Pond, or Pool
- PHAST Model Grid

Graph Legend

- Actual Concentration
- PHAST Simulated Concentrations

Notes:

1. Aerial photography acquired by Peregrine Aerial Surveyors Inc. and Eagle Mapping in August 2012.
2. Orthophotography prepared by Critigen Canada Corp.

N

0 180 360 540 720

Metres

Created by:
CRITIGEN

FIGURE 4-14b
PHAST Model Calibration Results - Zinc
Faro Mine Remediation Project

CH2MHILL

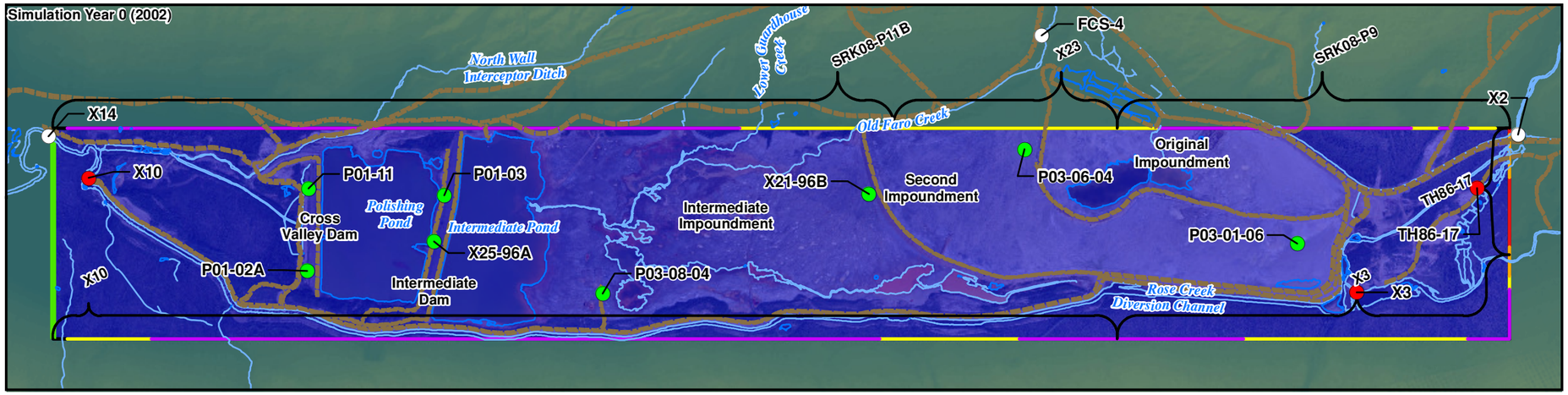

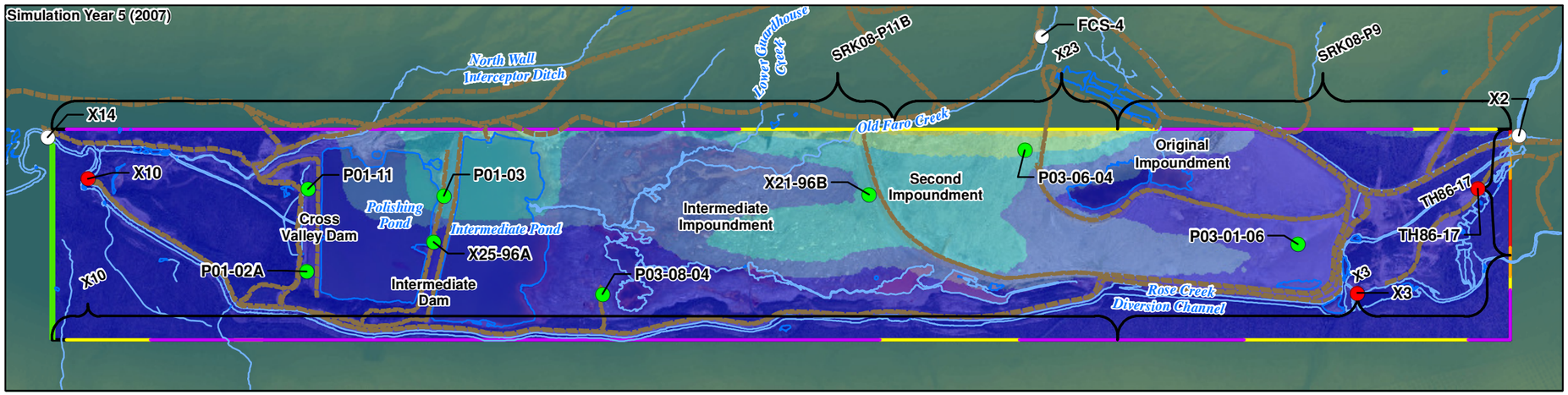

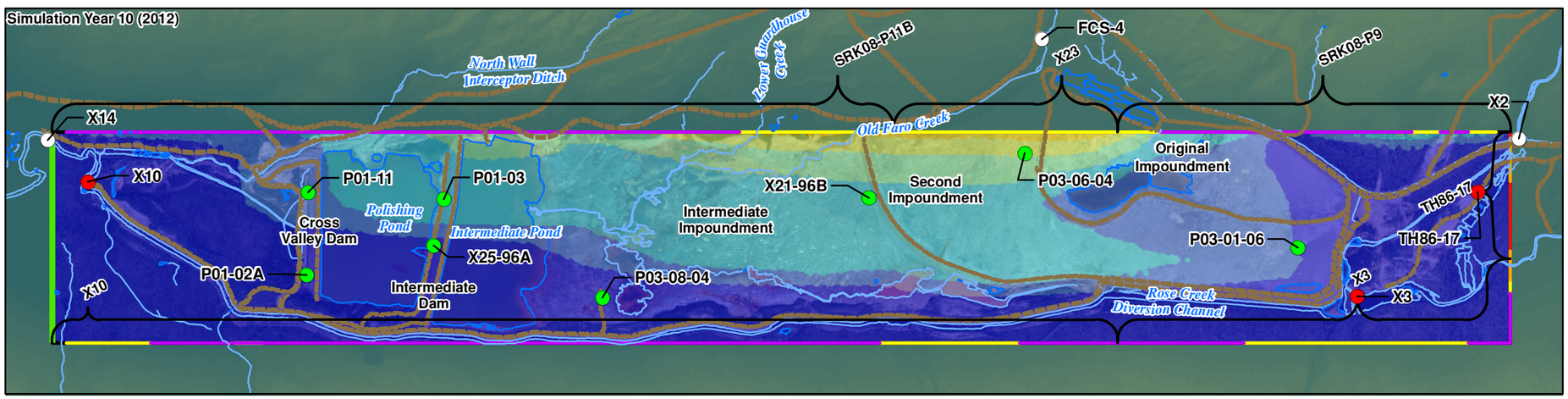

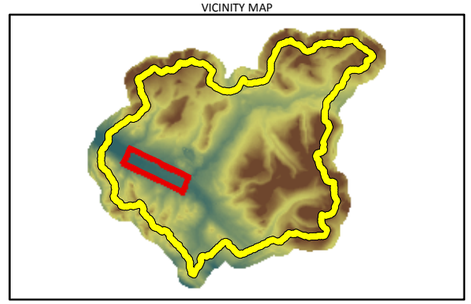

LEGEND

- General Reference Well Location
- PHAST Chemistry Flux Well Location
- PHAST Calibration Target Well Location
- Roads Unpaved
- Stream
- Lake, Pond, or Pool
- Constant Head: 1,013.0 m CGVD28

Specified Flux (m/day)

- 0 to 0.01
- 0.01 to 0.05
- 0.05 to 0.10
- 0.10 to 0.18
- PHAST Model Domain Boundary

Sulphate Concentration (mg/L)

- 0 to 1,000
- 1,000 to 2,000
- 2,000 to 3,000
- 3,000 to 4,000
- 4,000 to 5,000
- 5,000 to 6,000
- 6,000 to 7,000
- 7,000 to 7,645

Notes:

1. Aerial photography acquired by Peregrine Aerial Surveyors Inc. and Eagle Mapping in August 2012.
2. Orthophotography prepared by Critigen Canada Corp.

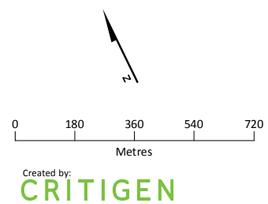

FIGURE 4-15

Modelled Sulphate Concentrations at Selected Times During the Calibration Period

Faro Mine Remediation Project

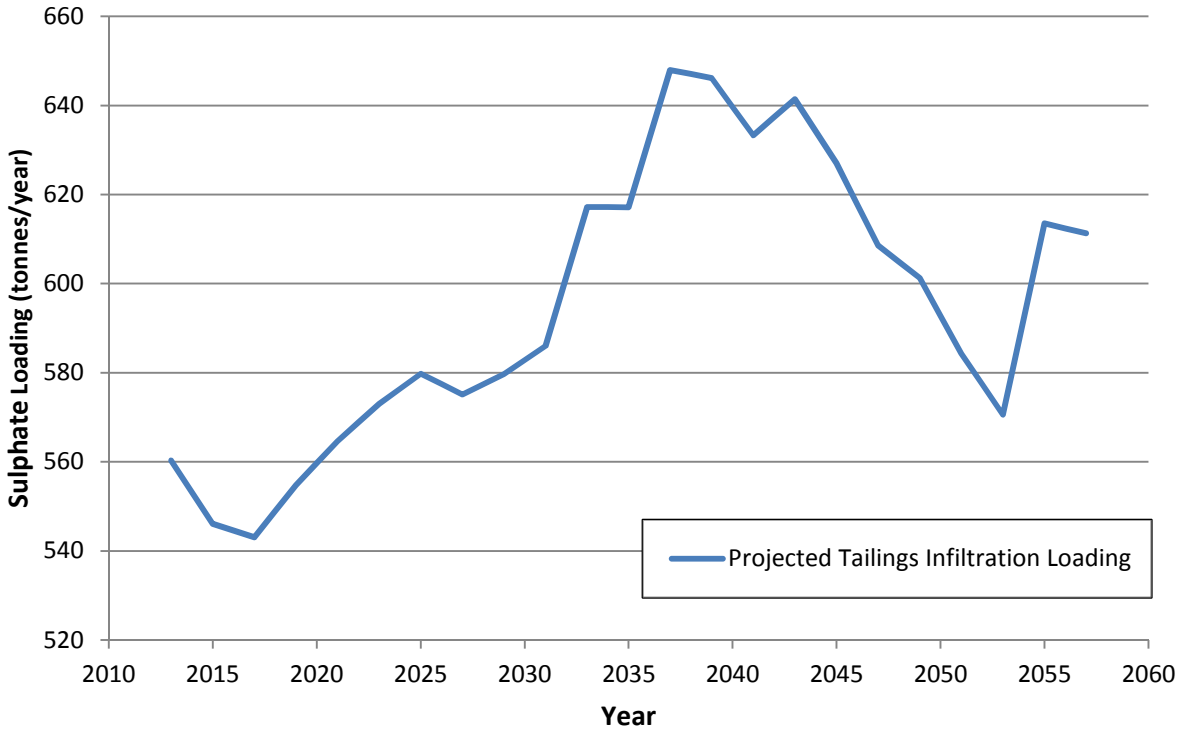

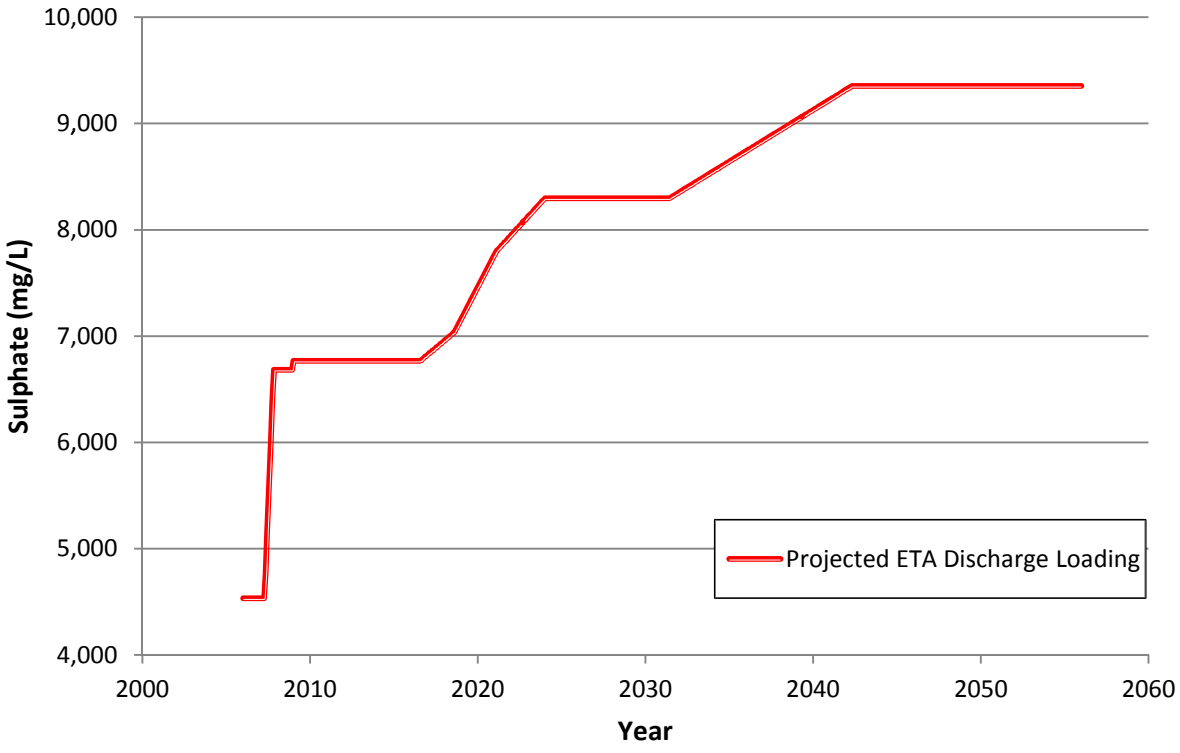

FIGURE 4-16
Projected Sulphate Loading from ETA and Tailings Infiltration
Faro Mine Remediation Project

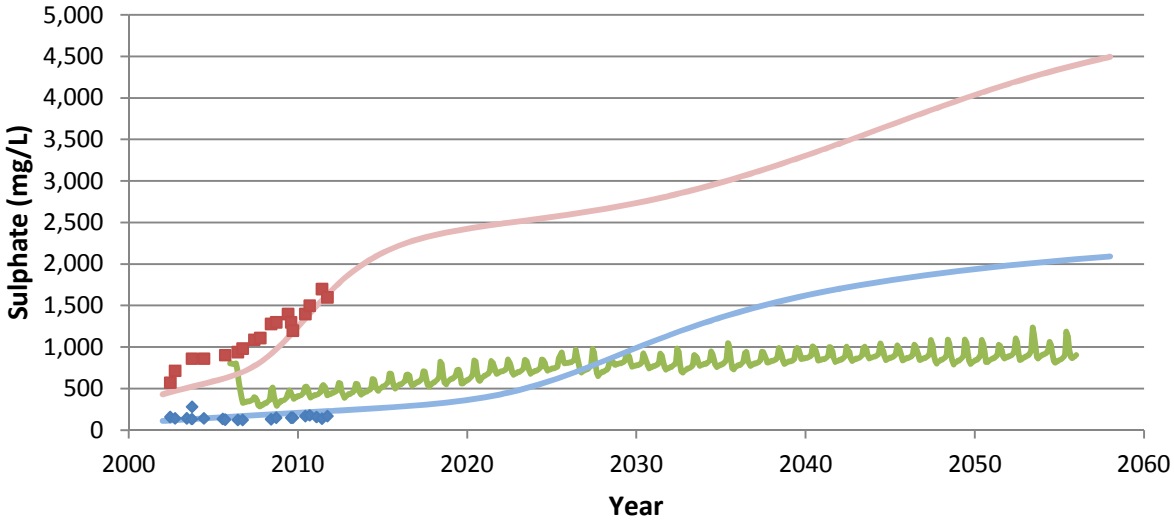

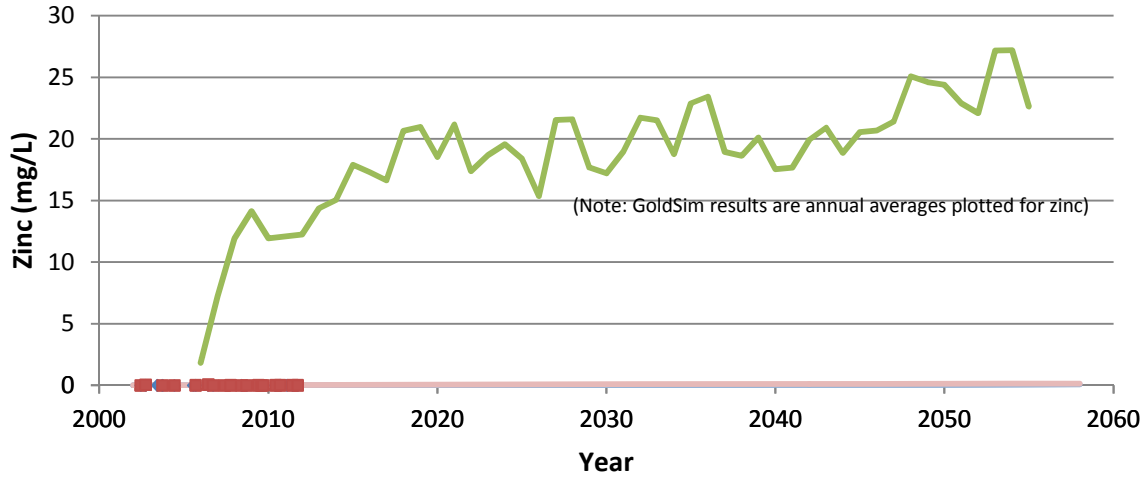

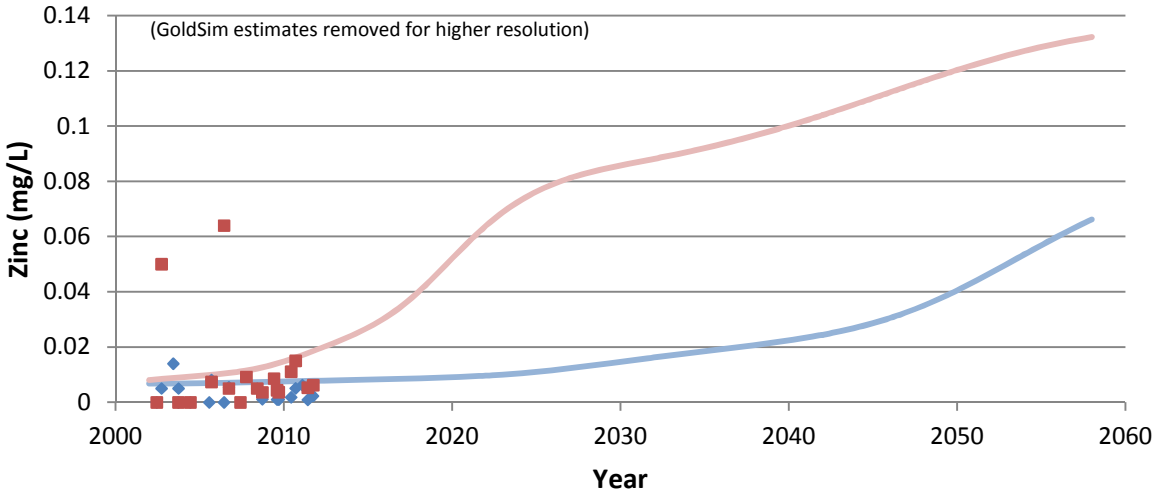

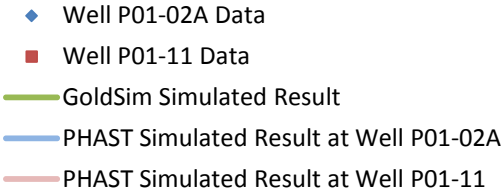

FIGURE 4-17a
PHAST Model Prediction of Future Conditions - CVD
Faro Mine Remediation Project

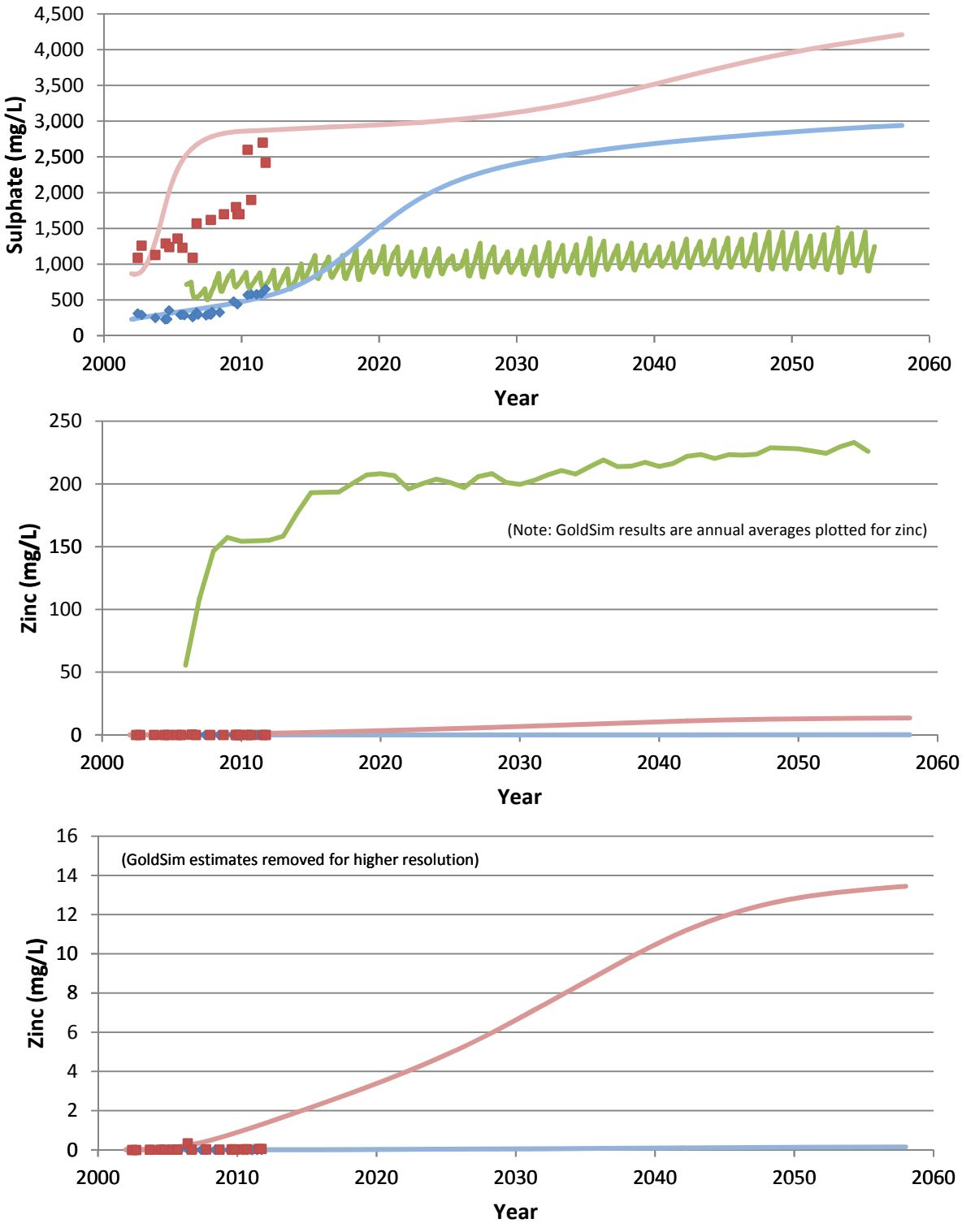

FIGURE 4-17b
PHAST Model Prediction of Future Conditions - Intermediate Dam
Faro Mine Remediation Project

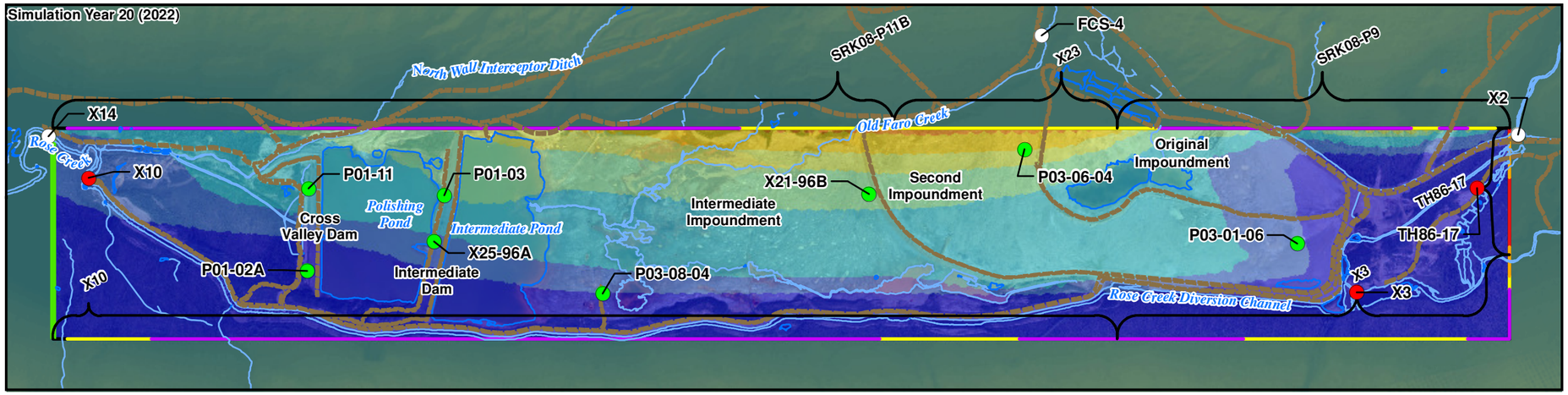

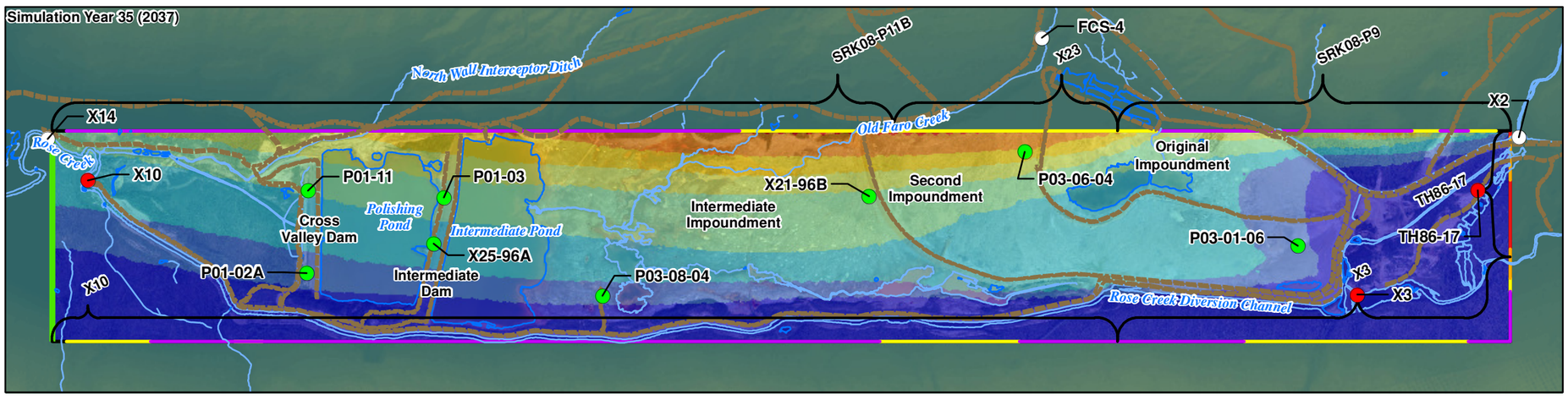

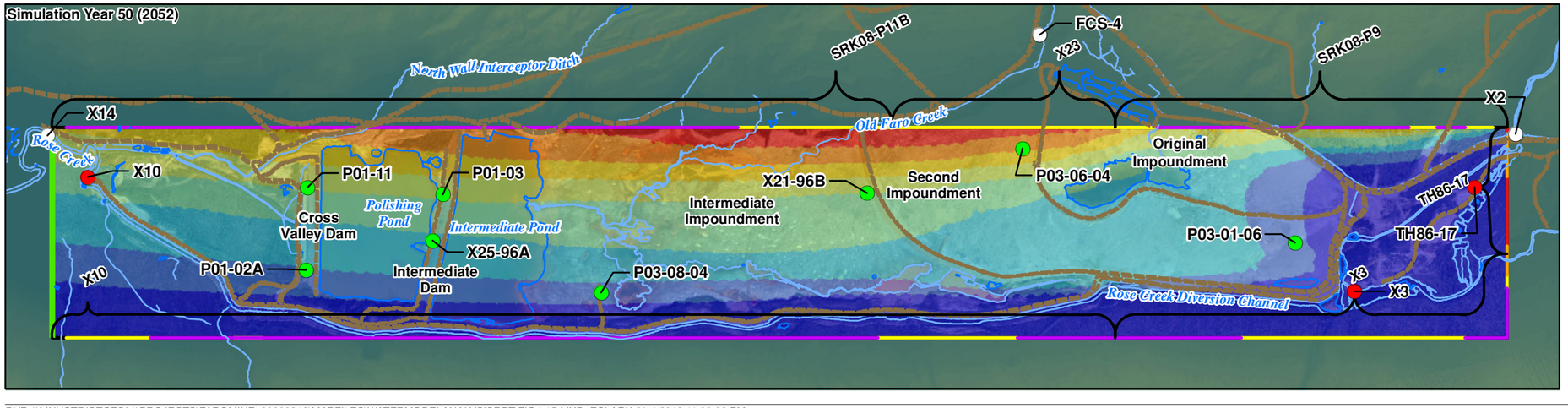

VICINITY MAP

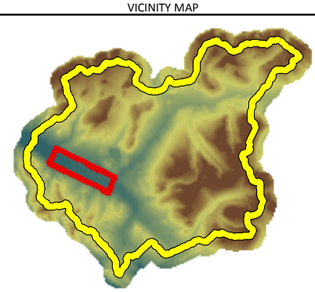

LEGEND

- General Reference Well Location
- PHAST Chemistry Flux Well Location
- PHAST Calibration Target Well Location
- Roads Unpaved
- Stream
- Lake, Pond, or Pool
- Constant Head: 1,013.0 m CGVD28

Specified Flux (m/day)

- 0 to 0.01
- 0.01 to 0.05
- 0.05 to 0.10
- 0.10 to 0.18
- PHAST Model Domain Boundary

Sulphate Concentration (mg/L)

- 0 to 1,000
- 1,000 to 2,000
- 2,000 to 3,000
- 3,000 to 4,000
- 4,000 to 5,000
- 5,000 to 6,000
- 6,000 to 7,000
- 7,000 to 7,645

Notes:

1. Aerial photography acquired by Peregrine Aerial Surveyors Inc. and Eagle Mapping in August 2012.
2. Orthophotography prepared by Critigen Canada Corp.

Created by: CRITIGEN

FIGURE 4-18
Forecast Sulphate Concentrations at Selected Times After the Calibration Period
Faro Mine Remediation Project

CH2MHILL

SECTION 5

Recommendations for Future Modelling

This report documents the development, calibration, and application of computer models that were constructed to support the ongoing development, refinement, and implementation of the FMRP. These computer models are subdivided into three classifications: SW flow models, GW flow models, and geochemical models. For each of these types of models, this report documents objectives, approach, data sources, constructions, calibrations, applications, and recommendations.

The level of complexity varies among these computer models, reflecting the availability of data to define the particular aspects of the CSM that each computer model attempts to simulate. As such, these computer models were developed to the extent practical given the site data, time, and resources available for this effort during FY12. As with any computer model aimed at approximating conditions and processes of interest of a physical system, the computer models described herein will never be "final." This is because site conditions will continue to evolve and respond to changes associated with the dynamic natural environment and site engineering activities. As a result, information presented herein should be considered a work in progress. Improvements to these computer models can and should continue as additional site characterization, monitoring, and operational data become available; as knowledge of the FMC evolves; and as necessitated by the FMRP. CH2M HILL fully intends these models to provide a foundation for future enhancements. The following sections describe recommended model enhancements and applications, as well as supporting field work. These recommendations necessarily focus on near-term project needs, but these tools also represent longer-term investments for the FMRP that can provide critical information to inform decision-makers throughout its evolution.

5.1 Future Surface Water Flow Modelling

Recommendations for future SW modeling generally consist of two categories: (1) an expanded data collection program for use in subsequent calibration of the hydrological model, and (2) additional model runs to assess changes in the flow regime of the FMC system because of proposed closure activities and climate change. The following sections provide more detailed recommendations for these two areas.

5.1.1 Field Monitoring Program Recommendations

A hydrological model of the FMC has been developed based on available FMC physical data, as well as available flow and meteorological data. Meteorological data collected at the Faro Airport and, to a lesser extent, from monitoring stations located at the FMC, were used to prepare input precipitation and air temperature data sets. The model was calibrated at key locations throughout the system based on available continuous flow monitoring data. As noted, model input data gaps were filled based on available FMC and regional data. Based on review of available flow and meteorological data and analysis of model results, a list of additional data and future modelling scenarios has been developed.

As noted in Sections 2.3 and 2.4, inconsistencies and data gaps associated with data collected at the two onsite meteorological stations resulted in the need to rely more heavily on data collected by Environment Canada at the Faro Airport. In particular, the lack of total precipitation data (i.e., rain and snow) at the FMC stations resulted in the FMWT having to estimate total precipitation using data collected at the Faro Airport Station and inferred correlation functions. CH2M HILL recommends a review of the instrumentation's installation and operation at the FMC meteorological stations, as well as a defined quality assurance/quality control process to analyze and interpret the collected data.

Data collected at continuous flow monitoring stations were used to calibrate the hydrological model. For the Rose Creek model, Station R7 (NFRC, upstream of FCD) and Station X14 (Rose Creek, downstream of FMC) were calibrated. Limited continuous data (i.e., 1 year) for Station X2 (NFRC, upstream from the Mine Access Road) were also used. For the Vangorda Creek Model, data from Station V1 (Vangorda Creek upstream from the Vangorda Mine Area and Blind Creek Road) and Station V8 (Lower Vangorda Creek near Faro) were used. To provide a more catchment-specific calibration, the existing flow monitoring station network should be expanded. For example,

continuous flow data for the South Fork of Rose Creek, upstream of the confluence with the NFRC, would allow for catchment-specific calibration of the upstream area. Additional flow monitoring along the RCDC, NFRC, and FCD would also allow for the analysis of GW contributions and further refinement of the model. Similarly, monitoring flows along Vangorda Creek between Stations V1 and V8 would allow for more catchment-specific calibration of the model.

In addition to continuous monitoring, expanding the current spot measurement field program would also be beneficial to identify variations in flow regime throughout the FMC. This would also provide useful information for subsequent model calibration and analysis.

Finally, collecting additional snow and air temperature data in headwater catchments would allow for the refinement of assumptions related to site-specific effects of elevation on these parameters.

A condition assessment and geomorphic assessment program is recommended for future efforts to provide additional site characteristics for sensitive stream and diversion reaches. The condition assessment and geomorphic assessment will be a rapid geomorphic assessment that will support a more detailed modelling analysis of particular streams and diversion reaches. In particular, this assessment information can assist in the modification of final calibrated values for the canopy, surface, and soil loss parameters.

The rapid geomorphic assessments will evaluate channel stability, health, and function. This assessment is intended to be completed for all of the identified channels to some degree. The actual effort for each channel section will be scoped and prioritized based, on background review and priority of channel in the design process for channel rehabilitation/upgrades. The assessments will identify the channel reaches that would be most prone to erosion/sedimentation based on overall visual observations of channel stability and configuration, as well as the type of bed and bank materials present.

5.1.2 Hydrological Modelling

The FMC SW flow models' further development will be facilitated by the collection of additional site data. This model development will provide more detailed stream and diversion reach-specific model components, which will be used for design purposes. The following enhancements to the FMC hydrological models will be proposed to enable design efforts:

- Detailed definition of base flow conditions on a catchment-specific basis based on additional flow monitoring data and integration with work prepared by the FWMT
- Further sub-discretization of catchment areas to better represent more localized drainage and conveyance elements
- Catchment-specific calibration using flow data collected at new flow monitoring sites
- Input of historical (i.e., pre-2000) air temperature and precipitation data from the Faro Airport Station based on the methodology detailed in this report, to simulate historical flow conditions at the FMC
- Preparation of a modified air temperature and precipitation input data set to simulate potential impacts, based on various climate change scenarios

The development and further refinement of the FMC SW models is a requirement for the successful development of designs for the various diversions/stream upgrades at the FMC.

5.2 Future Groundwater Flow Modelling

Two separate GW flow models were developed during this modelling effort. One focuses on the RCAA Subarea; the other focuses on the NFRC Subarea. The RCAA Subarea model is intended primarily to support the design and installation of the CVD SIS and to evaluate the nature of the interaction between Rose Creek and the underlying aquifer. The NFRC Subarea model is intended to support the further investigation, design, and construction of a SIS in the Zone 2 Outwash area, as well as to improve the understanding of how the NFRC and the aquifer system in the area interact. This model will be used to assess the effectiveness of the existing S-Wells SIS and to explore

potential modifications to the system to improve its effectiveness. The recommendations for future GW modelling work in both focus areas are presented herein.

5.2.1 RCAA Subarea Modelling Recommendations

Recommendations for future RCAA Subarea modelling include the following:

- Investigate the benefits of including low-permeability slurry walls into the CVD design in terms of reducing extraction flow rates and treatment requirements. These slurry wall systems may include:
    1. A slurry wall constructed across the axis of the valley downgradient from the CVD SIS and keyed into bedrock on the north and south sides of the valley.
    2. A slurry wall system constructed parallel with, and adjacent to, the RCDC to minimize the quantity of clean water leaking from the channel and entering the future CVD SIS.
- Investigate alternative construction approaches to developing the CVD SIS. Options include constructing a large-scale trench (approximately 10-m wide) across the axis of the valley with a sump extending along its length, instead of installing multiple GW extraction wells. This trench would need to be combined with a low-permeability slurry wall system, as previously described.
- Use transient GW-level and boundary condition data to develop a transient version of the RCAA Subarea model. The development of this version of the model could use the simulated transient stream stage projections obtained from the SW flow model of the FMC. A transient GW model would provide estimates of how GW levels, flow directions and rates, and stream-aquifer interaction change over time. The model could also be used to evaluate how the degree of hydraulic capture provided by the CVD SIS varies seasonally in response to changing hydrologic conditions.

It is anticipated that additional field work will be conducted during the 2013 field season at the CVD area, including several seismic profiles to map the bedrock topography in the area. These data should be used to refine the currently assumed competent and weathered bedrock surfaces in the model, and the model should be recalibrated based on the new conceptualization of the system, if necessary. The potential SIS designs should then be evaluated using the refined model.

5.2.2 NFRC Subarea Modelling Recommendations

Recommendations for Future NFRC Subarea modelling include the following:

- Use the groundwater flow model to identify regions within the Faro WRDs that contribute GW flow to areas of interest within the NFRC drainage, such as the S-Wells area and the Zone 2 Outwash area. This evaluation would assess which WRD sources flow toward, and are eventually captured by, existing or proposed SIS systems and which ones do not.
- Coordinate with the geochemical team to compare the simulated hydraulic capture extent of the proposed SIS system at Zone 2 Outwash with the WRD areas that are predicted to significantly increase in source loading in the future.
- Develop a Zone 2 SIS design that will effectively capture the highest projected WRD load sources in the future. This information will inform decision-makers about future actions that may be necessary to maintain effective capture of GW contamination over time.
- Compare WRD source loading with the current simulated hydraulic capture zone generated by the operation of the S-Wells SIS. Determine whether system modifications are necessary to increase effectiveness and minimize mass loading to the NFRC.
- Design S-Wells system modifications, as necessary, to intercept currently contaminated GW. Evaluate future modifications that may be required based on projected WRD loading. Use the refined model to improve understanding of how SW and GW in the NFRC drainage interact and to determine the degree of influence that currently operating/future SISs have on NFRC flows.

- Use the refined model to improve understanding of the hydrogeology and how SW and GW interact in the Northeast WRD and Guardhouse Creek areas. Use the model to evaluate which WRD sources appear to contribute flow to areas where current monitoring wells are showing significant increases in zinc concentrations.
- Use the GW flow model to develop an SIS design that can intercept contaminated GW in the Northeast WRD area, if warranted.
- Use transient GW-level and boundary condition data to develop a transient version of the NFRC Subarea model. The development of this version of the model could use the simulated transient stream stage projections obtained from the SW model of the site. A transient GW model would provide estimates of how GW levels, flow directions, and flow rates change seasonally. The model could also be used to investigate the transient nature of stream-aquifer interaction along the NFRC during key periods such as peak freshet flows and other episodic events.
- Use the NFRC model to evaluate the potential benefits provided by lining and/or re-routing portions of the NFRC to minimize contaminated groundwater discharge into the stream channel. Evaluate the potential benefit of installing a low-permeability cut-off wall beneath the NFRC channel upstream of the WRDs to force clean GW up into the creek channel.

Additional field investigation activities are planned in the NFRC area. As additional information is collected regarding FMC aquifer properties, bedrock topography, and SW-GW interaction, these data should be used to refine the GW flow model of the area.

5.3 Future Geochemical Modelling

The main focus of the geochemical modelling activities during FY12 was to evaluate the geochemical loading component of the existing GoldSim model and make improvements, where appropriate. Reactive transport and reactive mixing models were used to evaluate the GoldSim model. These models account for known geochemical processes that occur between source and receiving areas and are designed to improve the predictive capabilities of the GoldSim model. To the extent feasible, the GoldSim model geochemical parameters were kept intact during the reactive geochemical model calibrations to observed data. In some cases, the geochemical calibrations were not satisfactory, suggesting that some of the GoldSim model assumptions and parameters may require adjustment. This was especially evident in the WRD model for the X23 catchment. Further study is recommended to explore these issues. Data gaps in key areas of the RCTA should also be filled by installing additional monitoring wells. The following additional work is recommended:

- In light of the conclusions of the WRD model study (Section 4.4.2.4), the following tasks are recommended:
  - Revision of assigned infiltrating water chemistry for each WRD. Water types used in the GoldSim model were selected on the basis of sound field and laboratory testing, but the water types themselves represent averages of highly variable and geographically widespread seepage samples. There are sufficient data to justify a more direct geochemical assessment of present and future water quality emerging from these WRDs by building on the tools introduced in the mixing (PHREEQC) and transport (PHAST) models. Judicious use of available seep, mineralogical, and acid-base accounting data in modeling WRD seepage generation and evolution is recommended to produce a stronger geochemical tool for prediction of critically important element concentrations.
  - Continued review and revision, as necessary, of assigned neutralization potential depletion rates. These values, assigned to each WRD, are the key to predicting the timing and nature of future water quality changes. Refinement of these rates, in conjunction with the water chemistry adjustments of the previous bullet, will increase confidence in the model's forecasting ability.
  - Refine the WRD mixing model using the tools described above to produce a calibrated, predictive tool for all catchments that will feed directly into the Faro Pit Lake and Tailings models.

- More detailed examination of Faro Pit Lake chemical distribution, including profiling and assessment of the potential for mixing and turnover at depth. There are currently only summer depth profiles; therefore, no assessment of seasonal variation in lake properties, which are key to understanding the lake's continuous behavior and potential for turnover.
- Continued monitoring of deepest tailings pore water at as many locations in the RCTA as possible.
- Installation of new nested wells in the unmonitored northwestern area of the tailings and immediately upgradient from this area. This will improve model flux and loading estimates to the critical area on the north side of CVD and further downgradient. Collection of a series of core samples from aquifer solids beneath and downgradient of the RCTA. The cores may be analyzed for reactive iron oxide/hydroxides via a series of selective extractions. This will improve estimates of adsorption capacity of the RCAA, which will improve confidence in predicting subsurface trace metal mobility into the future.
- Upgrade the PHAST model using newly gathered groundwater and core data, along with improved estimates of hydraulic inputs from the groundwater flow model.
- Currently in the GoldSim model, surface water runoff geochemistry is assigned an arbitrary concentration equal to 10 percent of the assigned seepage geochemistry for a given individual WRD; however, there are no field data supporting this assumption. Field observations during summer dry spells, where secondary effervescent salts are observed throughout the site, are likely to generate higher concentration runoff than is currently predicted. A surface water sampling program is recommended to monitor the first runoff during the freshet and following storm events during the summer and fall months.

SECTION 6

Works Cited

Access Mining Consultants. 1996. *Geology and exploration potential of the Anvil District, Yukon.*

AECOM Canada Ltd (AECOM). 2009. *Faro Mine Complex Closure and Reclamation–Project Proposal, Current Environmental Conditions Supporting Document*. Prepared for Faro Project Management Team. March.

Allison, J.D. and T.L. Allison. 2005. *Partition Coefficients for Metals in Surface Water, Soil, and Waste*. U.S. EPA Document EPA/600/R-05/074.

Al-Suwaiyan, M. "Discussion of "Use of Weighted Least-Squares Method in Evaluation of the Relationship Between Dispersivity and Field Scale," by M. Xu and Y. Eckstein." *Ground Water* 34.4 (1996): 578.

BGC Engineering Inc. (BGC). 2006. *Final Report. Task 22D North Fork Rock Drain*. September.

Bond. 1999. Data accessed from Yukon Government GIS FTP site: http://ygsftp.gov.yk.ca/standardized_geodatabases_ArcGIS_9.

CH2M HILL Canada Limited (CH2M HILL). In preparation. *Fiscal Year 2012 Site-wide Water Quality Modelling Report, Faro Mine Remediation Project.* Draft.

CH2M HILL Canada Limited (CH2M HILL). 2013a. *Waste Rock Dump Monitoring Data Report*. Prepared for the Government of Yukon.

CH2M HILL Canada Limited (CH2M HILL). 2013b. *CVD Interception System Investigation Data Technical Memorandum.*

CH2M HILL Canada Limited (CH2M HILL). 2012. *Conceptual Site Model, Faro Mine Remediation Project.* Draft. Prepared for the Government of Yukon. August.

Chow, Ven Te. 1964. *Handbook of Applied Hydrology.* New York: McGraw-Hill.

Clement, T.P. 1997. *A Modular Computer Code for Simulating Reactive Transport in 3-Dimensional Groundwater Systems. Pacific* Northwest National Laboratory. PNNL-11720.

Critigen. 2013. *Geospatial Data Products Created from the 2011 LiDAR and the 2012 Low and High Altitude Stereo Imagery for the Faro Mine Project Area*. Prepared for CH2M HILL Canada Limited. February.

Curragh Resources Inc. 1987. *Development of the Zone 2 Waste Dump.* December.

Denison Environmental Services (DES). 2012a. *2011 Annual Environmental Monitoring and Activities Report. Faro Mine Complex – Faro, YT.* Prepared for Yukon Government. February.

Denison Environmental Services (DES). 2012b. *emLine*. Available online at: http://emline.denisonenvironmental.com/emline/Login/Login.aspx?ReturnUrl=%2femline%2fdefault.aspx. Accessed July 28, 2012.

Denison Environmental Services (DES). 2011. *2010 Annual Environmental Monitoring and Activities Report. Faro Mine Complex – Faro, YT.* Prepared for Yukon Government. March.

Denison Environmental Services (DES). 2010a. *North Fork of Rose Creek (NFRC) Low Flow Loading Studies: NF2-X2.* November 22. Memorandum within DES's monthly report: *Monthly Environmental Monitoring Report: Special Projects Monitoring: October 2010* (submitted November 30, 2010).

Denison Environmental Services (DES). 2010b. *North Fork of Rose Creek (NFRC) Low Flow Loading Studies: R7-R10.* November 22. Memorandum within DES's monthly report: *Monthly Environmental Monitoring Report: Special Projects Monitoring: October 2010* (submitted November 30, 2010).

Doherty, J. 2010. *Addendum to the PEST Manual*. September. 5th Edition. Brisbane, Australia: Watermark Numerical Computing.

Doherty, J. 2004. *PEST Model-Independent Parameter Estimation User Manual*. 5th Edition. Brisbane, Australia: Watermark Numerical Computing.

Dzombak, D.A., and Morel, F.M.M. 1990. *Surface Complexation modelling, Hydrous Ferric Oxide*. New York: John Wiley. 393 p.

Environmental Solutions, Inc. (ESI). *2012 Groundwater Vistas*. Available at: http://www.groundwatermodels.com/ESI_Software.php.

Freeze, R. and J. Cherry. 1979. *Groundwater.* Prentice-Hall, Inc., Englewood Cliffs, New Jersey 07632. 604 p.

Gartner Lee Limited (GLL). 2008. *Anvil Range Mine Complex 2007 Annual Environmental Report Water Licence QZ03-059.* Prepared for Deloitte and Touche Inc. February.

Gartner Lee Limited (GLL). 2007. *Anvil Range Mine Complex 2006 Annual Environmental Report Water Licence QZ03-059.* Prepared for Deloitte and Touche Inc. February.

Golder Associates. 1991. *Intermediate Dam Raising and Cross Valley Dam Toe Drain, Cross section and Detailed Plan.* August.

Golder Associates. 1980a. *1980 Embankment Dam Raising.* April.

Golder Associates. 1980b. *Final Design Recommendations for the Down Valley Tailings Disposal Project, Volume 1, 2 and 3.* June.

Golder Associates. 1980c. *Construction Report, Cyprus Anvil Mining Corporation, 1980 Raising of the Tailings Dam, Faro, Yukon Territory, Appendix II*.

Golder, Brawner and Associates. 1979. *1978 Dyke Raising for the Tailings Retention Facility, Faro, Yukon Territory, Figure 2 Tailings Dam, 1978 Construction.* April.

Golder, Brawner and Associates. 1975. *Cyprus Anvil Mining Corporation, Tailings Containment Construction, Construction Carried out to end of 1975.* September.

Golder Associates. 1973. *Report to Cyprus Anvil Mining Corporation Limited on the Tailings Containment Facility*. October.

Gomm Environmental Engineering and Consulting (GEEC). 2010. *Faro Mine Complex Closure and Reclamation. Site Wide Water Quality Model. Draft 1.* Prepared for Yukon Government, Assessment and Abandoned Mines. April.

Government of Yukon (YG). 2012. *Faro Mine Remediation Project Phase 2B Work Plan FY2013-2017*. Prepared for Faro Management Board. December.

Harbaugh, A.W. 2005. *MODFLOW-2005, the U. S. Geological Survey Modular Ground-water Model -- the Ground-Water Flow Process.* U.S. Geological Survey Techniques and Methods 6 A16.

Harbaugh, A.W., E.R. Banta, M.C. Hill, and M.G. McDonald. 2000. *MODFLOW-2000, the U. S. Geological Survey Modular Ground-water Model -- User Guide to Modularization Concepts and the Ground-Water Flow Process.* U.S. Geological Survey Open-File Report 00-92, 121 p.

Hill, M.C., E.R. Banta, A.W. Harbaugh, and E.R. Anderman. 2000. *MODFLOW-2000, the U. S. Geological Survey Modular Ground-water Model -- User Guide to the Observation, Sensitivity, and Parameter-Estimation Processes and Three Post-processing Programs.* U. S. Geological Survey Open-File Report 00-184, 210 p.

HydroGeoLogic, Inc. (HGL) 2011. *MODHMS/MODFLOW-SURFACT. A Comprehensive MODFLOW-Based Hydrologic Modeling System.* http://www.hglsoftware.com/Modhms.cfm. Reston, Virginia.

Janowicz, J.R., N.R Hedstrom and R.J. Granger. 2008. *Investigation of Anvil Range Mining Corporation (Faro) Waste Dump Water Balance – Vangorda Trial Covers Water Balance*. Prepared for SRK Consulting Inc. on behalf of Deloitte and Touche Inc.

Janowicz, J.R., N.R Hedstrom and R.J. Granger. 2006. *Investigation of Anvil Range Mining Corporation (Faro) Waste Dump Water Balance – Final Water Balance*. Prepared for SRK Consulting Inc. on behalf of Deloitte and Touche Inc.

Laberge Environmental Services (Laberge). 2012a. *Draft Report, Faro Pit Lake Hydrographic Survey.* October.

Laberge Environmental Services (Laberge). 2012b. *Draft Field Summary – Faro Pit Lake Sampling*. September.

Laberge Environmental Services (Laberge). 2007. *Memorandum. Re: Data From Recording Hydrometric Sites.* November.

Laberge Environmental Services (Laberge). 2005a. *Memorandum Re: Preliminary Observations Continuous Recording Sites*. May.

Laberge Environmental Services (Laberge). 2005b. *Memorandum: Maintenance of Weirs Below the Cross Valley Dam*. September.

Laberge Environmental Services (Laberge). 2005c. *Memorandum, Hydrometric Measurements 2005.* February.

Lewkowicz, A.G. and P.P. Bonnavenbure. 2009. *Influence of topography on mountain permafrost distribution through variable air and ground surface lapse rates, Yukon Territory, Canada.* Geophysical Research Abstracts (11).

McDonald, M.G., and A.W. Harbaugh. 1988. *"A Modular Three-Dimensional Finite-Difference Groundwater Flow Model. "* U.S. Geological Survey Techniques for Water-Resources Investigation. Book 6, Chapter A1.

Parkhurst, D.L., and C.A.J. Appelo. 1999. *User's guide to PHREEQC (Version 2), a computer program for speciation, batch-reaction, one-dimensional transport, and inverse geochemical calculations*. U.S. Geological Survey Water-Resources Investigations Report 99-4259, 326 p. Code available at: http://wwwbrr.cr.usgs.gov/projects/GWC_coupled/phreeqc/index.html.

Parkhurst, D.L., Christenson, Scott, and Breit, G.N. 1996. "Ground-water-quality assessment of the Central Oklahoma Aquifer--Geochemical and geohydrologic investigations." U. S. Geological Survey Water-Supply Paper 2357-C, 101 p.

Parkhurst, D.L., K.L. Kipp, P. Engesgaard, and S.R. Charlton. 2010. *PHAST (Version 2) – A Program for Simulating Ground-Water Flow, Solute Transport, and Multicomponent Geochemical Reactions*. USGS Techniques and Methods 6–A35. Code available at: http://wwwbrr.cr.usgs.gov/projects/GWC_coupled/phast/.

Pollock, D.W. 1994. *User's Guide for MODPATH/MODPATH-PLOT, Version 3: A particle tracking post-processing package for MODFLOW, the U.S. Geological Survey finite-difference ground-water flow model.* U.S. Geological Survey Open-File Report 94-464. September.

Robertson GeoConsultants Inc. (RGC). 2012. 2011 *S-Cluster SIS Performance Review, Anvil Range Mining Complex, YT REV A.* September.

Robertson GeoConsultants Inc. (RGC). 2011. *DRAFT – Tracing Contaminant Sources to Groundwater and Surface Water in the Rose Creek Valley, Anvil Range Mining Complex (ARMC), Yukon Territory REV0*. RGC Project No. 118020. July 4.

Robertson GeoConsultants Inc. (RGC). 2010. 2009 *Performance Review of ETA SIS, Faro Mine Complex, Yukon Territory*. Prepared for the Government of Yukon. March 1.

Robertson GeoConsultants Inc. (RGC). 2006a. *Design of Groundwater Interception System for Rose Creek Tailings Storage Facility, Faro Mine, Yukon Territory*. Prepared for Deloitte & Touche Inc. on behalf of Faro Mine Closure Planning Office. October.

Robertson GeoConsultants Inc. (RGC). 2006b. *Water & Load Balance Study for Rose Creek Tailings Storage Facility, Faro Mine, Yukon Territory*. Report No. 118001/1. March.

Robertson Geoconsultants Inc. (RGC). 1996. *Anvil Range Mining Complex – Integrated Comprehensive Abandonment Plan*. Prepared for Anvil Range Mining Corporation. November.

Scenarios Network for Alaska and Arctic Planning. 2011*. Yukon Water Availability Analysis*. Prepared for The Northern Climate Exchange, Yukon College. July.

Scharffenberg, William /USACE. 2011. Email to Daniel Murrer/CH2M HILL. March 31.

SRK Consulting Engineers and Scientists (SRK). 2011. *Faro Groundwater Investigation 2010: As-built Report: Vangorda & Zone II Pumping Wells*. Prepared for April.

SRK Consulting Engineers and Scientists (SRK). 2010a. *2009 Modifications to the Seepage Interception and Pumping System at the S-wells Area, Faro Mine Complex, Yukon*. March.

SRK Consulting Engineers and Scientists (SRK). 2010b. *Faro Mine Complex Final Closure and Remediation Plan Project Description – Draft 4.* Prepared for Indian and Northern Affairs Canada and Yukon Government. November.

SRK Consulting Engineers and Scientists (SRK). 2009a. *Faro Mine Complex 2008 S-Cluster Groundwater Investigation and Option Assessment.* Prepared for Deloitte and Touche Inc. on behalf of Faro Mine Closure Planning Office. February.

SRK Consulting Engineers and Scientists (SRK). 2009b. *Faro Mine Complex Design and Installation of a Seepage Interception and Pumping System at the S-wells Area.* Prepared for Deloitte and Touche Inc. on behalf of Faro Mine Closure Planning Office. July.

SRK Consulting Engineers and Scientists (SRK). 2009c. *Faro Mine Complex: Future Water Quality Prediction*. 2007/08 Task 17b – FINAL. February.

SRK Consulting Engineers and Scientists (SRK). 2008. *Anvil Range Mining Complex 2007 Waste Rock and Seepage Monitoring Report.* Prepared for Deloitte and Touche Inc. on behalf of Faro Project Management Team.

SRK Consulting Engineers and Scientists (SRK). 2007. *Anvil Range Mining Complex Continued Seepage Investigation Zone 2 Pit Outwash Area.* January.

SRK Consulting Engineers and Scientists (SRK). 2006a. *Anvil Range Mining Complex: Dump Water Quality Prediction Revisions, 2005/2006 Task 19b.* Memorandum prepared for Deloitte and Touche Inc. November.

SRK Consulting Engineers and Scientists (SRK). 2006b. *Anvil Range Mining Complex 2005 Seepage Investigation at the Emergency Tailings Area*. November.

SRK Consulting Engineers and Scientists (SRK). 2006c. *Anvil Mining Complex: Rose Creek Tailings Deposit Assessment of Zinc Attenuation*. 2005/06 Task 22h(ii). July.

SRK Consulting Engineers and Scientists (SRK). 2005. *Faro Tailings Source Term Calculations*. June 14.

SRK Consulting Engineers and Scientists (SRK). 2004a. *Water Quality Estimates for Anvil Range Waste Rock.* Prepared for Deloitte and Touche Inc. November.

SRK Consulting Engineers and Scientists (SRK). 2004b. *Anvil Range Pit Lakes Assessment of Post Closure Conditions, Draft*. Prepared for Xx. January.

SRK Consulting Engineers and Scientists (SRK). 1991. *Down Valley Tailings Impoundment Decommissioning Plan*. Report 60636. April.

Turner, K. 1985. *"Water Loss from Forest and Range Lands in California."* Presented at the Chaparral Ecosystems Research: Meeting and Field Conference, University of California, Santa Barbara, California, May 16-17.

United States Army Corps of Engineers (USACE). Hydrologic Engineering Center. 2010. *Hydrologic Modelling System HEC-HMS User's Manual Version 3.5.* August.

Xu, M. and Y. Eckstein. 1995. Use of weighted least-squares method in evaluation of the relationship between dispersivity and field scale. *Ground Water* 33(6): 905-908.

Wels, Christoph. 2013. Robertson GeoConsultants, Inc. Personal Communication. January.

Zachara, J.M., Cowan, C.E., Resch, C.T. 1993. Metal cation/anion adsorption on calcium carbonate: implications to metal ion concentrations in groundwater. In *Metals in Groundwater*, H.E. Allen, E.M. Perdue, and D.S. Brown (eds). Lewis Publishers, 437 pp.

Zachara, J.M., Cowan, C.E., Resch, C.T. 1991. Sorption of divalent metals on calcite. *Geochim. Cosmochim. Acta* 55, 1549–1562.

Zheng, C. 2010. *MT3DMS v5. 3 Supplemental User's Guide.* Technical Report to the U. S. Army Engineer Research and Development Center, Department of Geological Sciences, University of Alabama. 51 pp.

Zheng, C. and P. Wang. 1999*. MT3DMS, A Modular Three-dimensional Multi-species Transport Model for Simulation of Advection, Dispersion and Chemical Reactions of Contaminants in Groundwater Systems: Documentation and User's Guide.* U. S. Army Engineer Research and Development Center Contract Report SERDP-99-1, Vicksburg, Mississippi. 202 pp.

Zheng, C. 1990. *MT3D, A Modular Three-dimensional Transport Model for Simulation of Advection, Dispersion and Chemical Reactions of Contaminants in Groundwater Systems.* Report to the U. S. Environmental Protection Agency, 170 pp.

Appendix A
HEC-HMS Surface Water Modelling Results

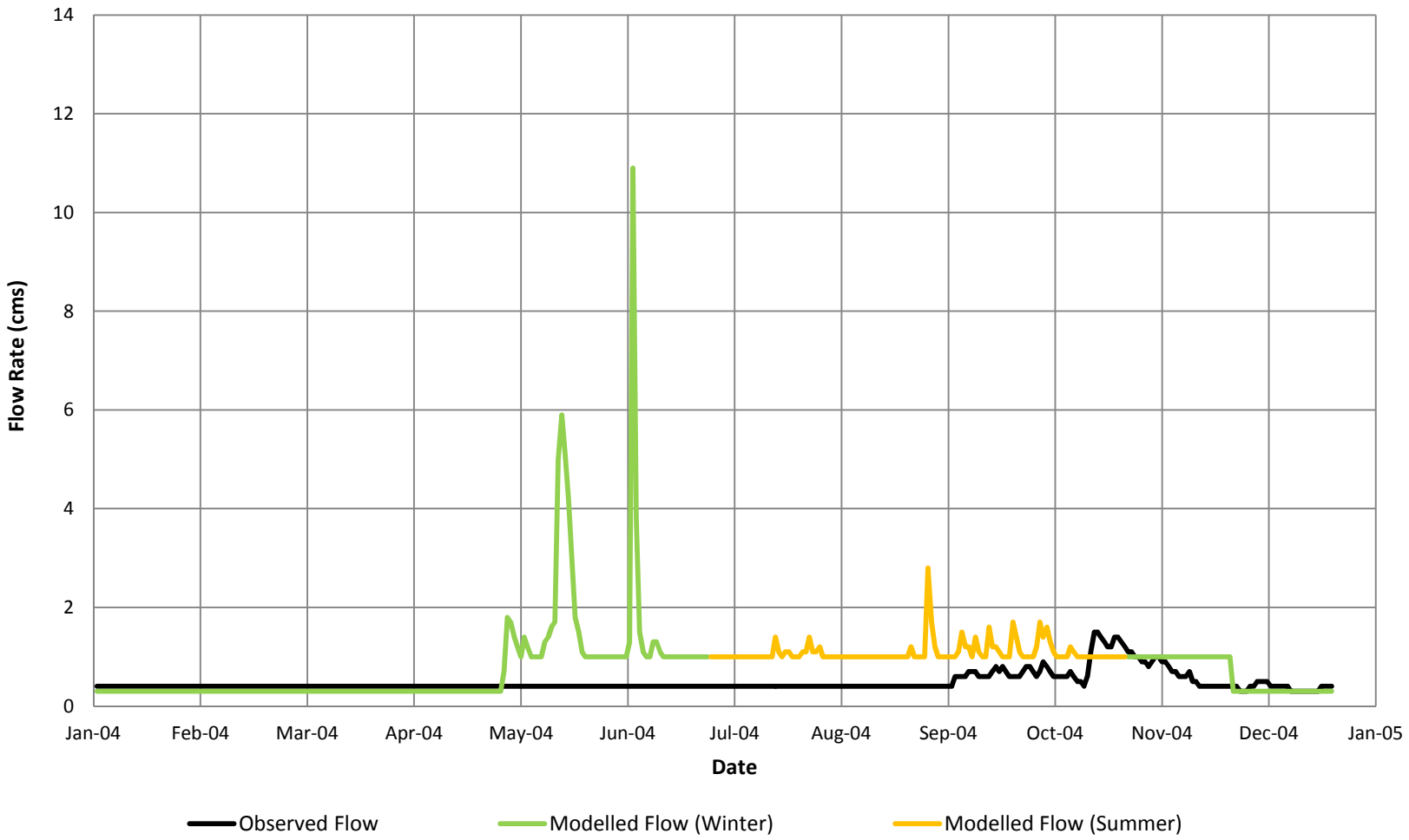

FIGURE A-1
Modelled vs. Observed Flow at Station R7, 2004
Faro Mine Remediation Project

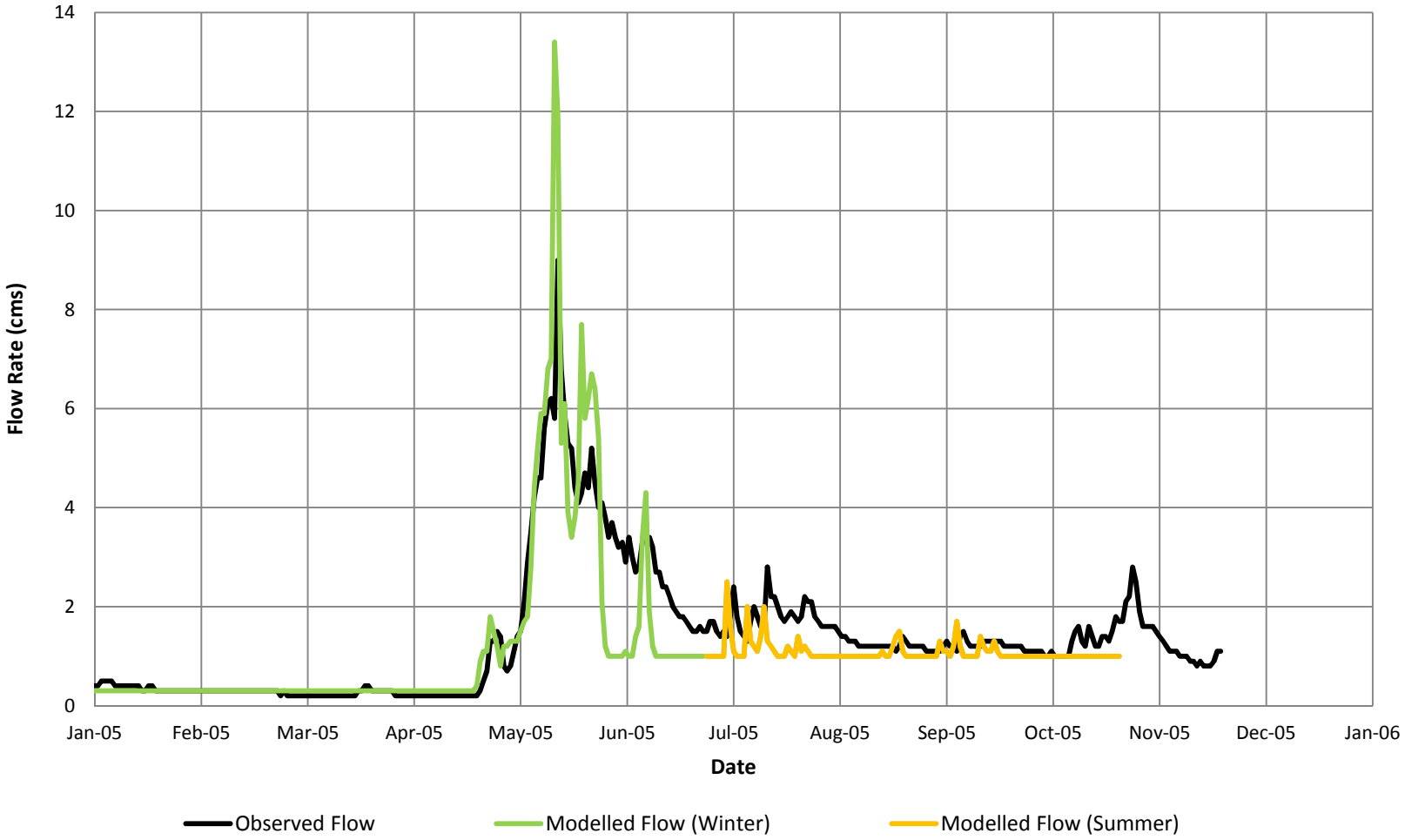

FIGURE A-2
Modelled vs. Observed Flow at Station R7, 2005
Faro Mine Remediation Project

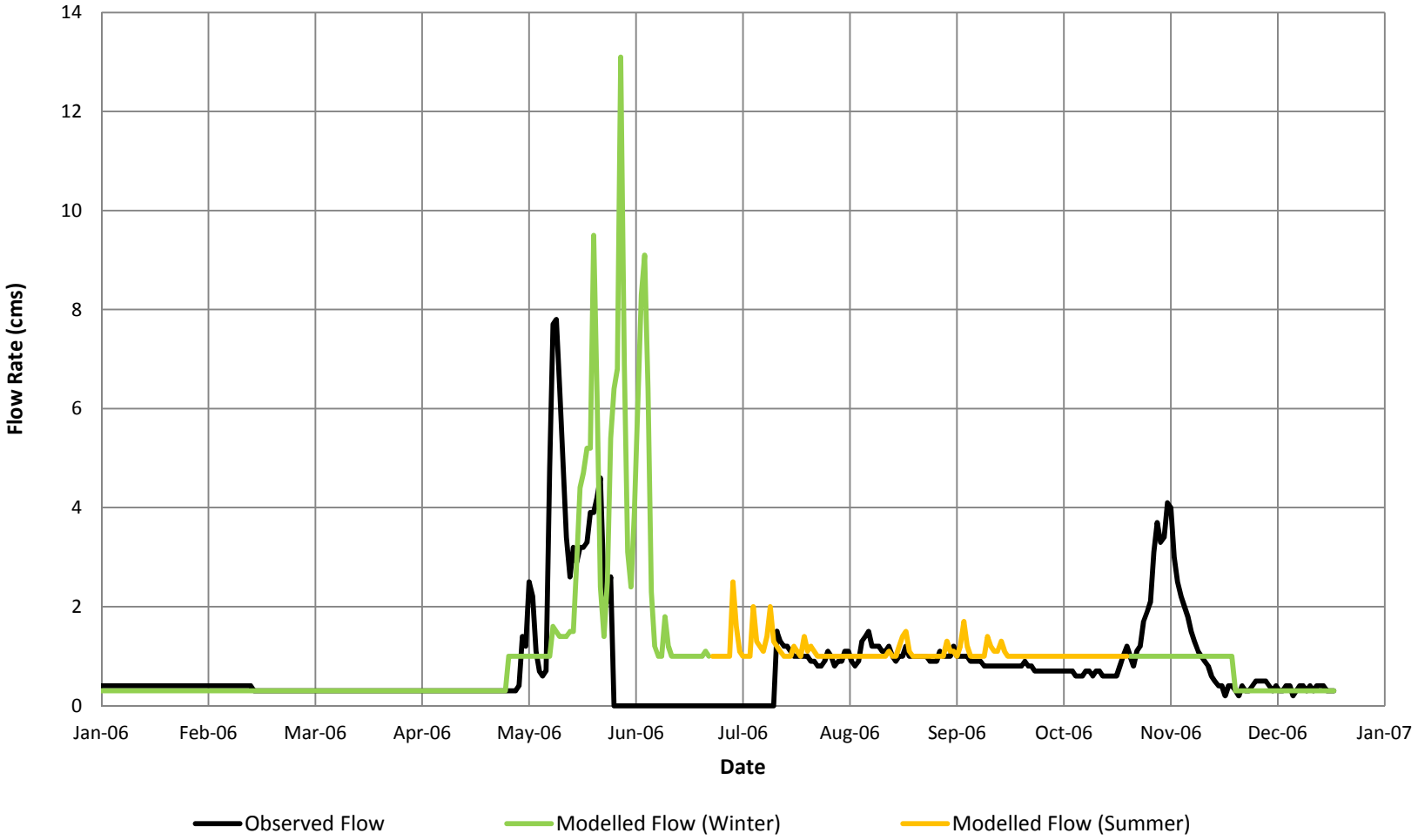

FIGURE A-3
Modelled vs. Observed Flow at Station R7, 2006
Faro Mine Remediation Project

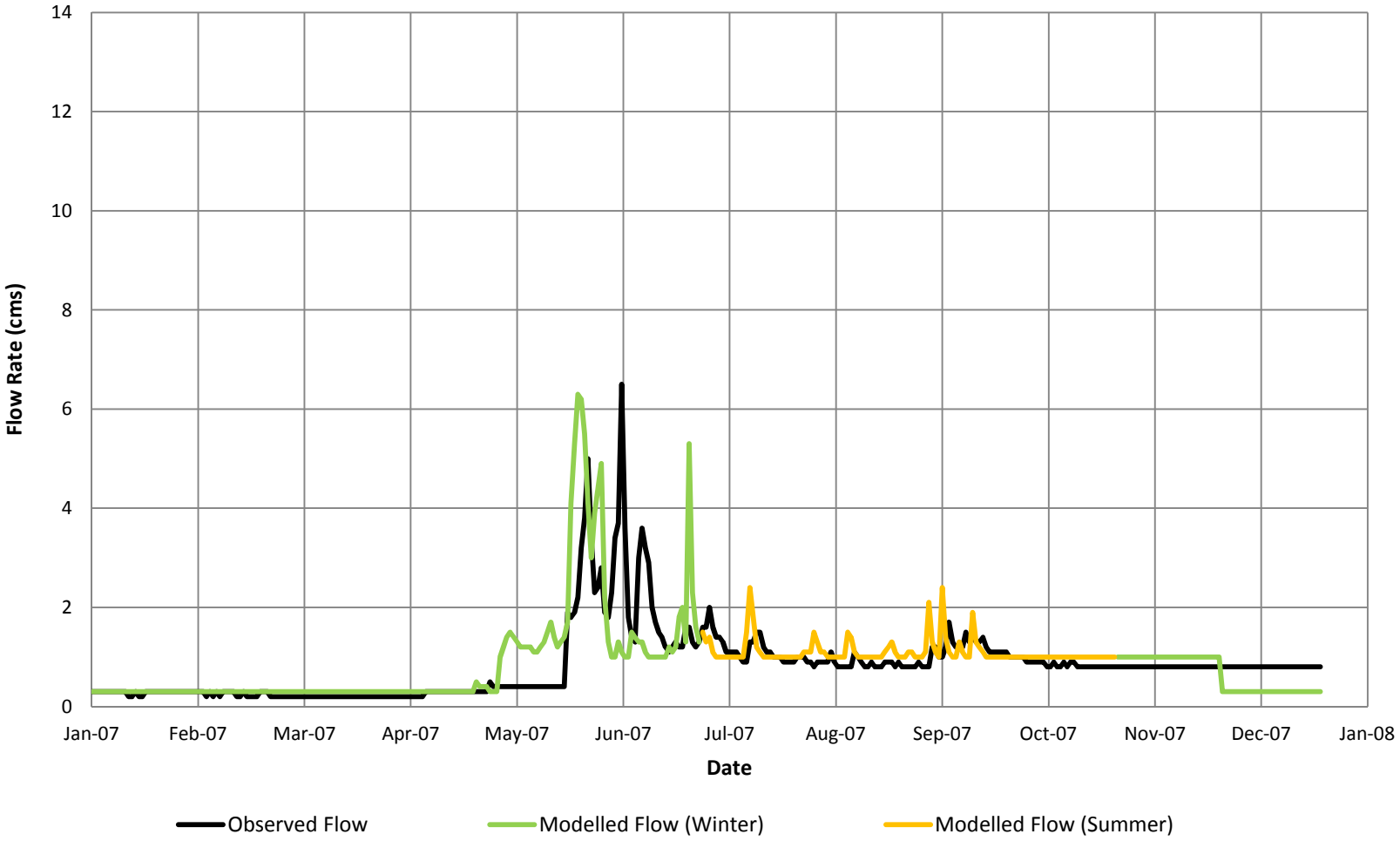

FIGURE A-4
Modelled vs. Observed Flow at Station R7, 2007
Faro Mine Remediation Project

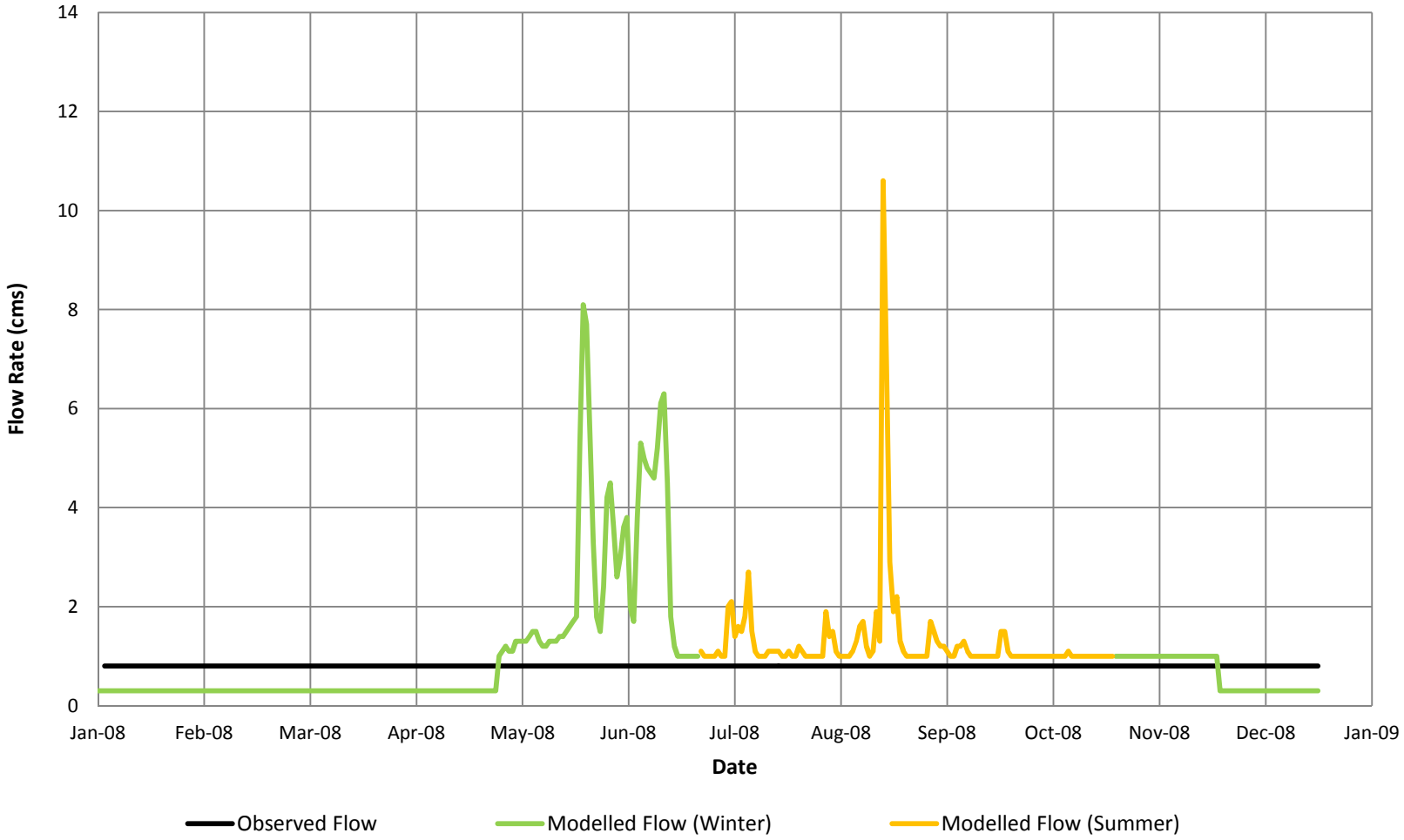

FIGURE A-5
Modelled vs. Observed Flow at Station R7, 2008
Faro Mine Remediation Project

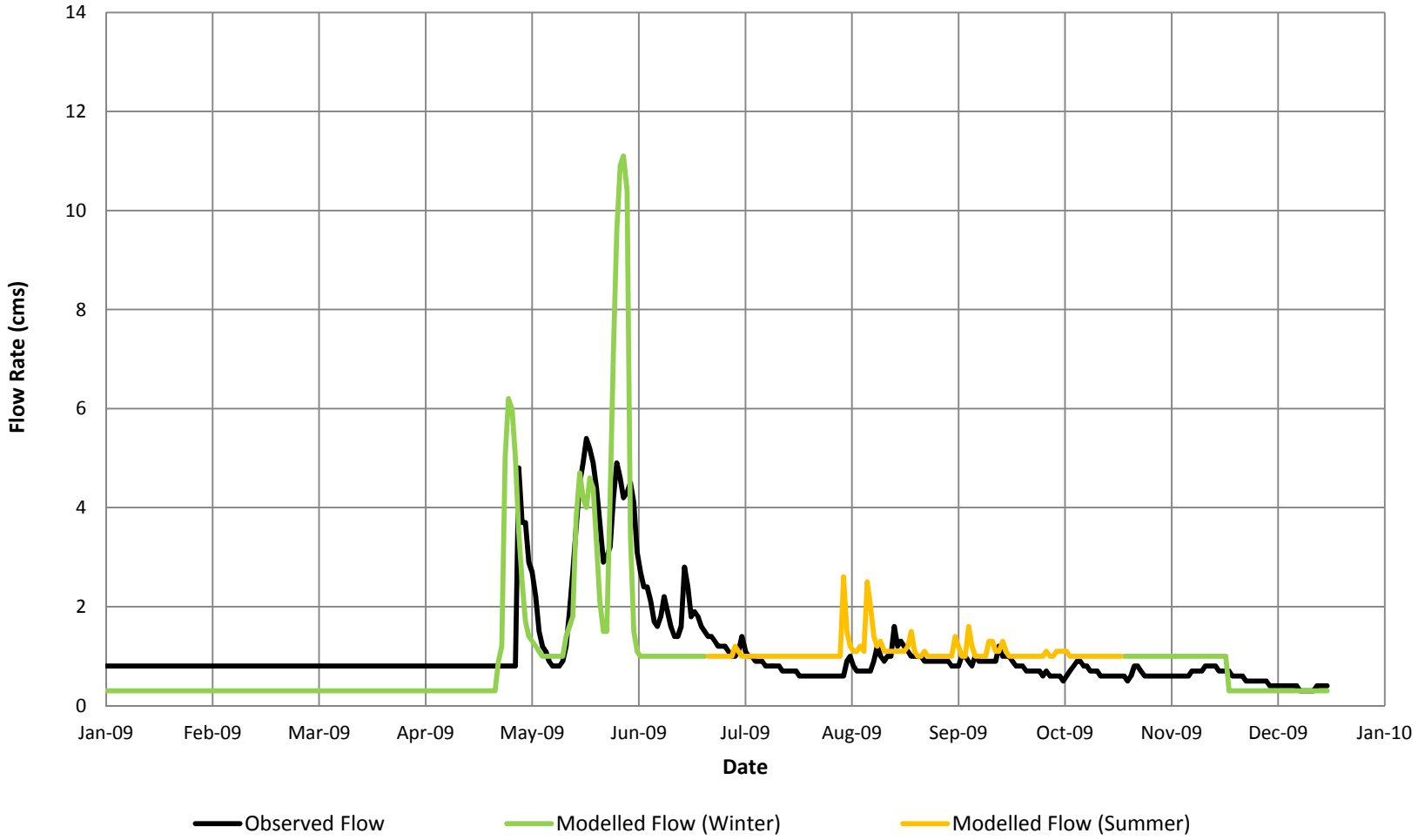

FIGURE A-6
Modelled vs. Observed Flow at Station R7, 2009
Faro Mine Remediation Project

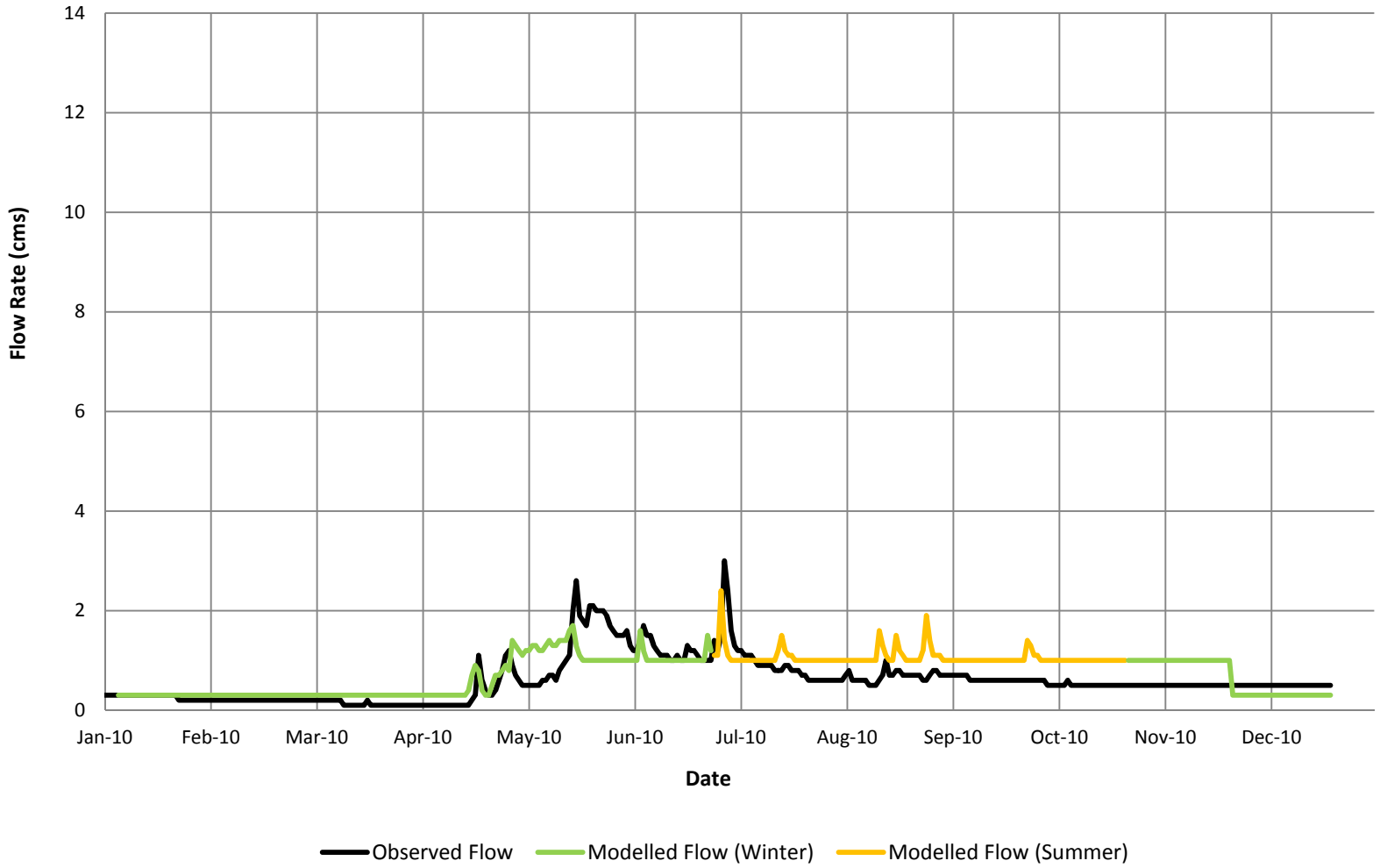

FIGURE A-7
Modelled vs. Observed Flow at Station R7, 2010
Faro Mine Remediation Project

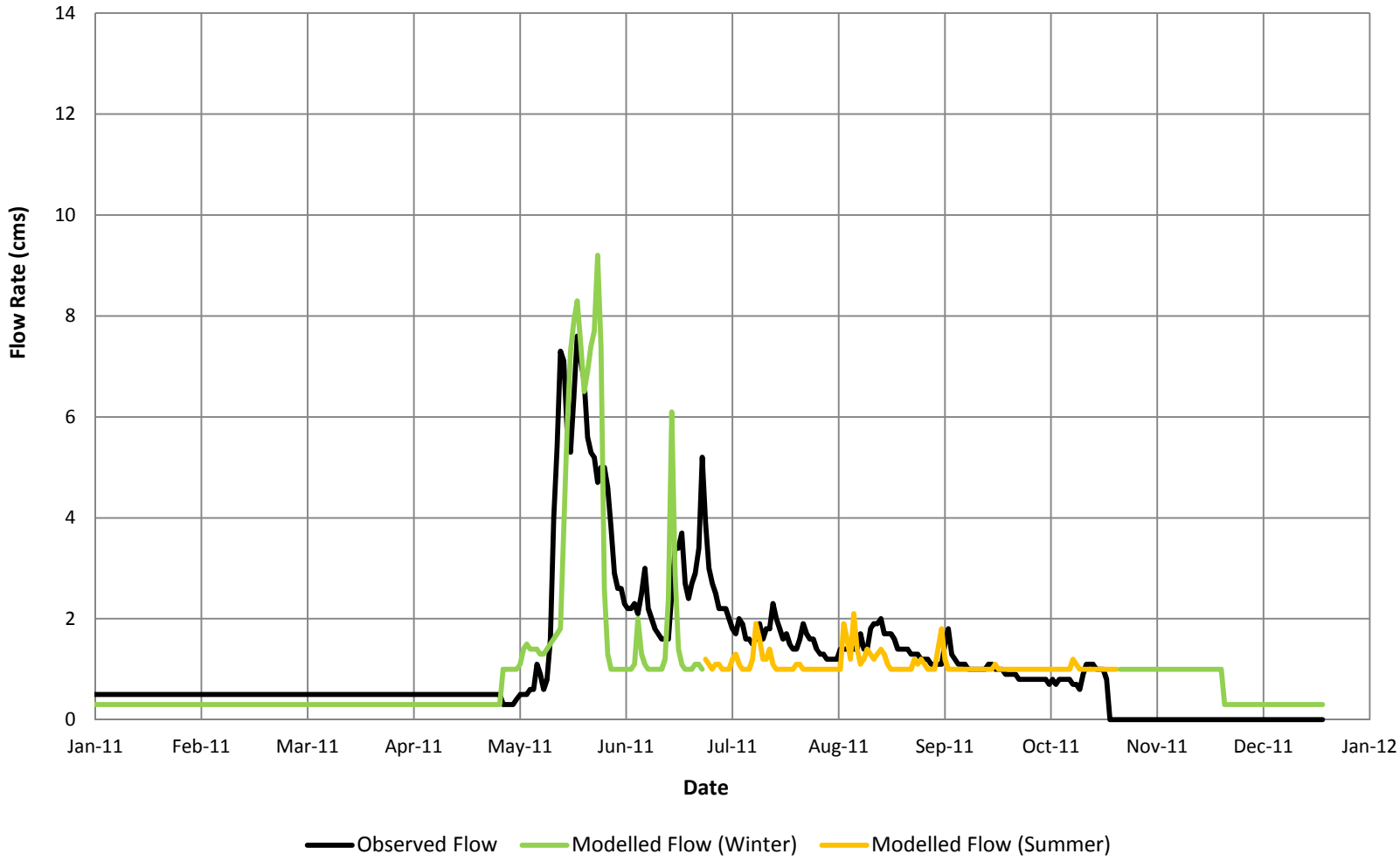

FIGURE A-8
Modelled vs. Observed Flow at Station R7, 2011
Faro Mine Remediation Project

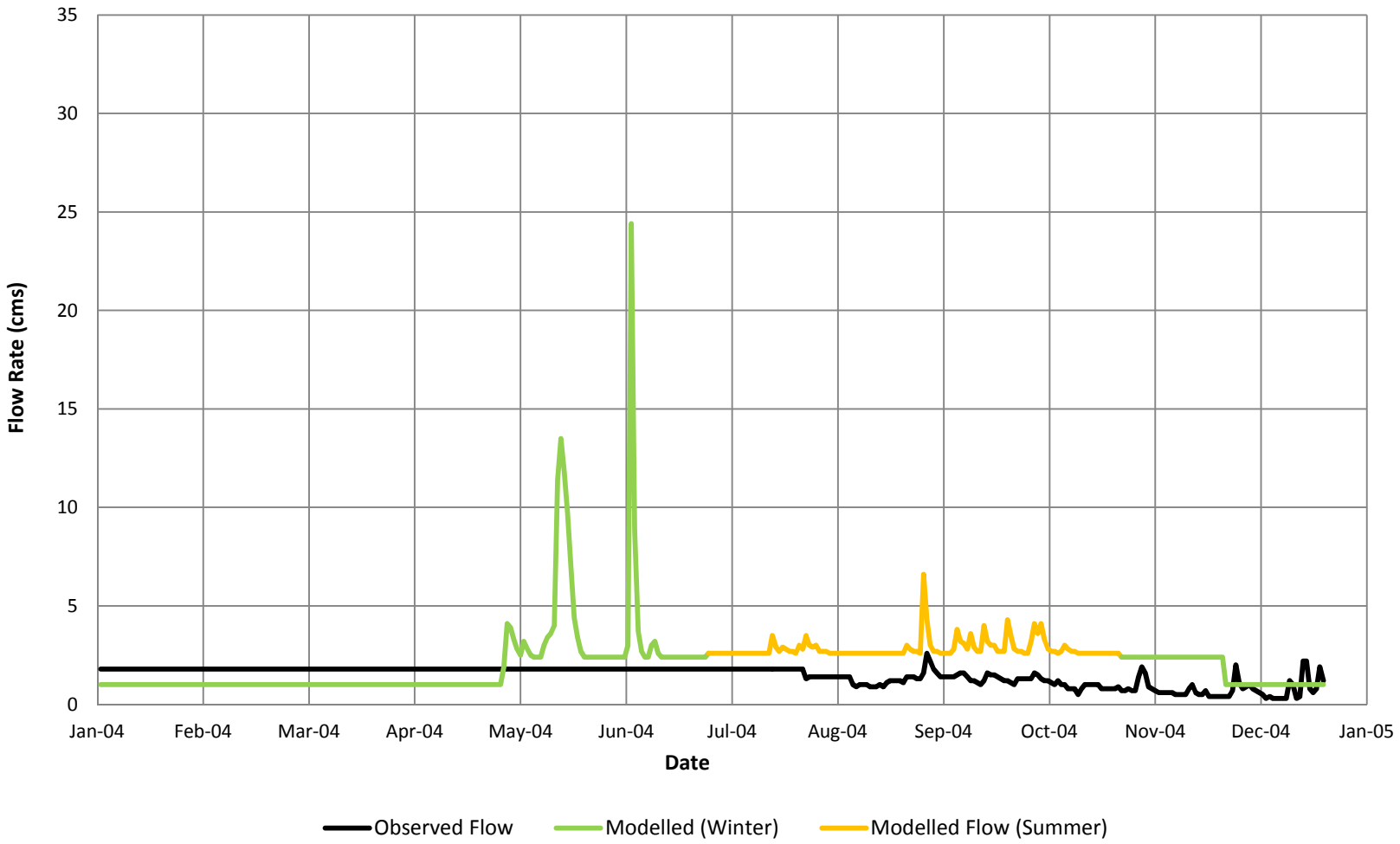

FIGURE A-9
Modelled vs. Observed Flow at Station X14, 2004
Faro Mine Remediation Project

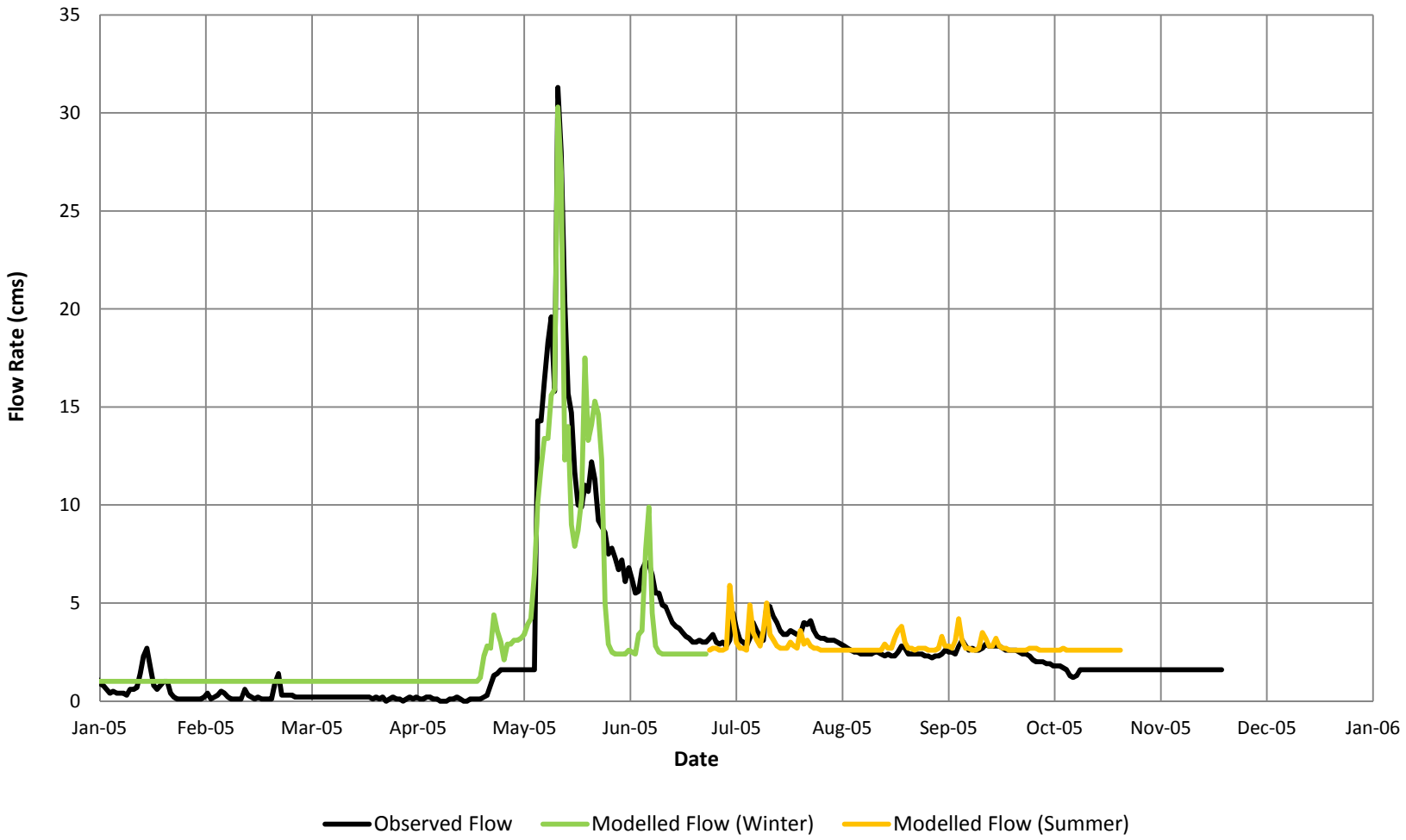

FIGURE A-10
Modelled vs. Observed Flow at Station X14, 2005
Faro Mine Remediation Project

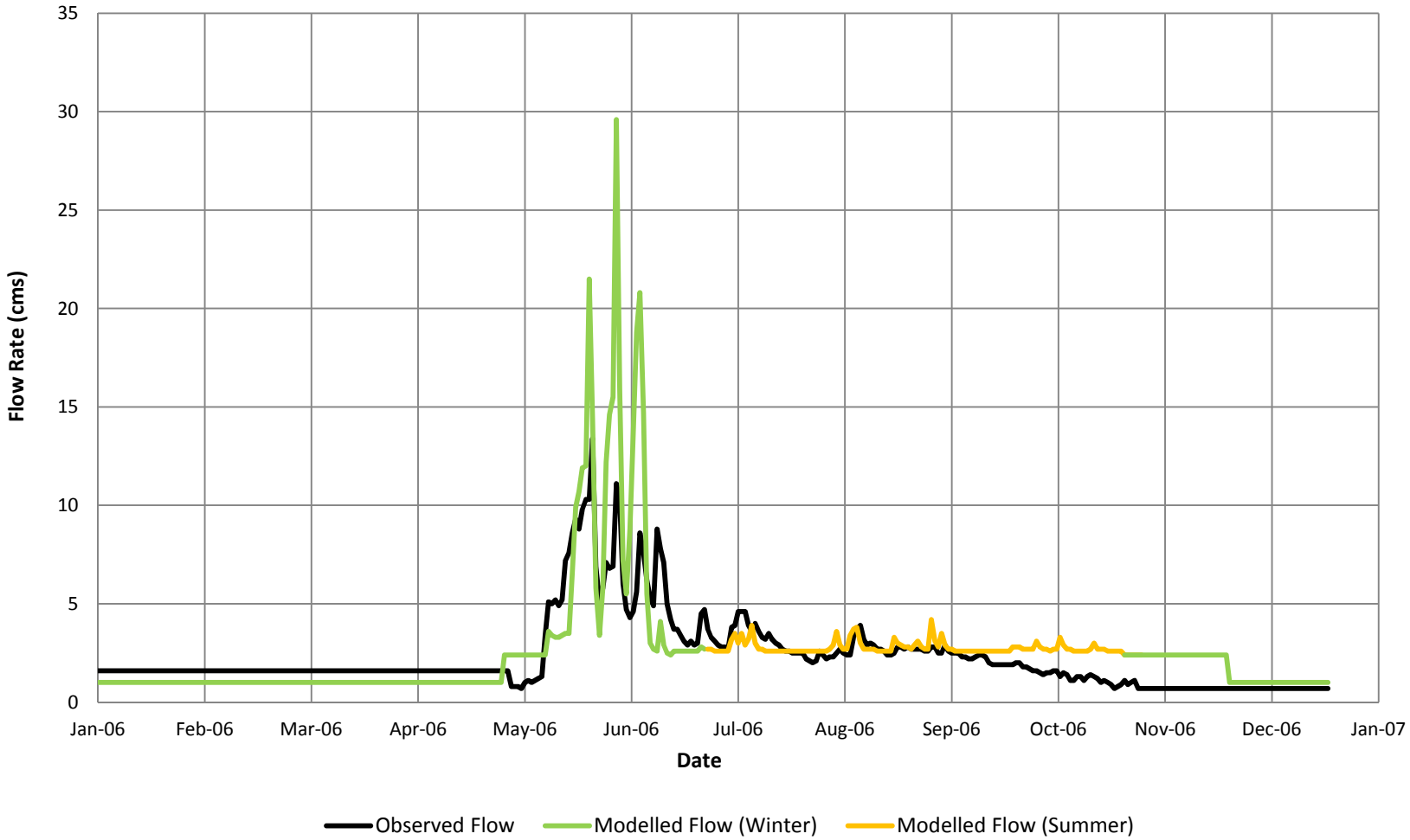

FIGURE A-11
Modelled vs. Observed Flow at Station X14, 2006
Faro Mine Remediation Project

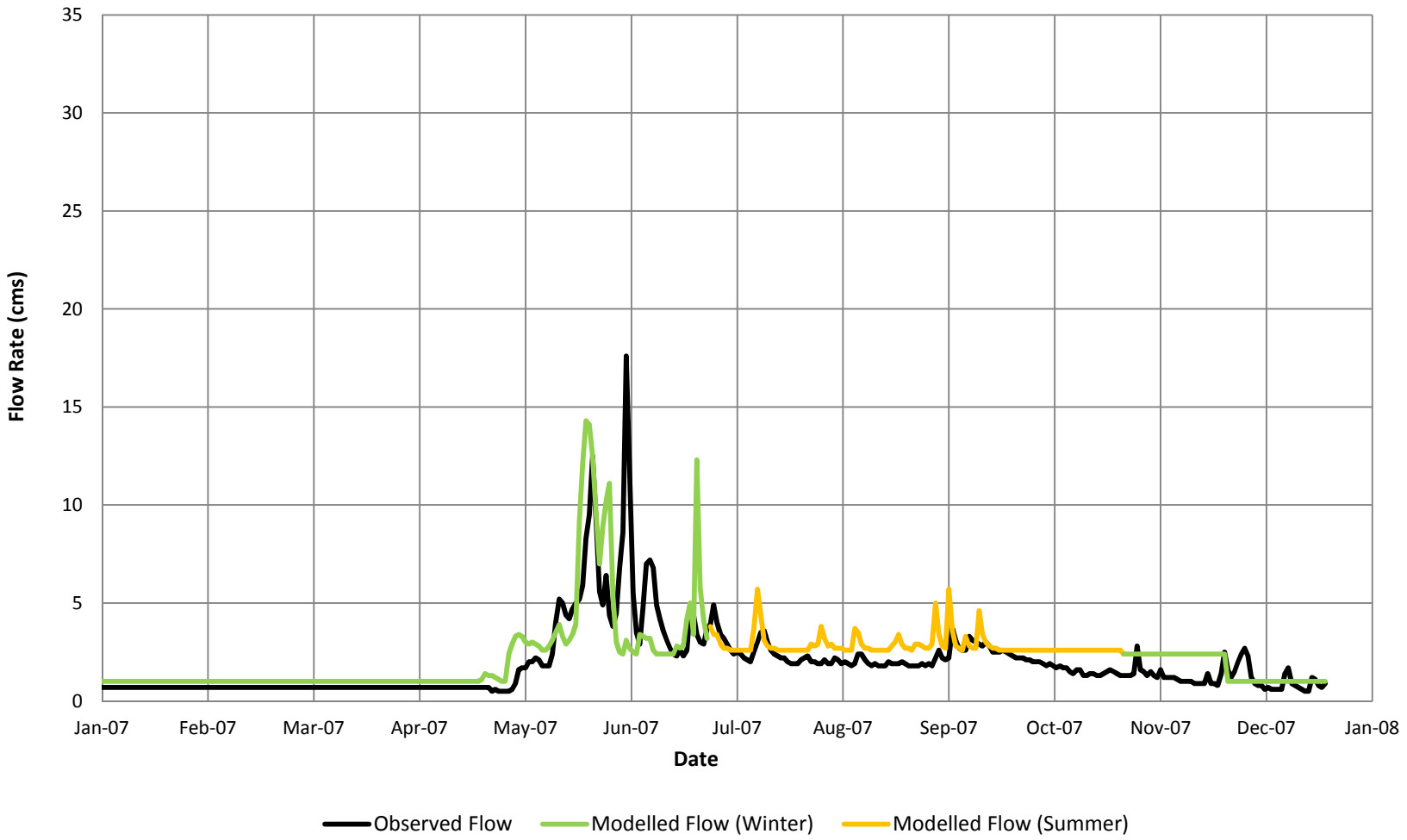

FIGURE A-12
Modelled vs. Observed Flow at Station X14, 2007
Faro Mine Remediation Project

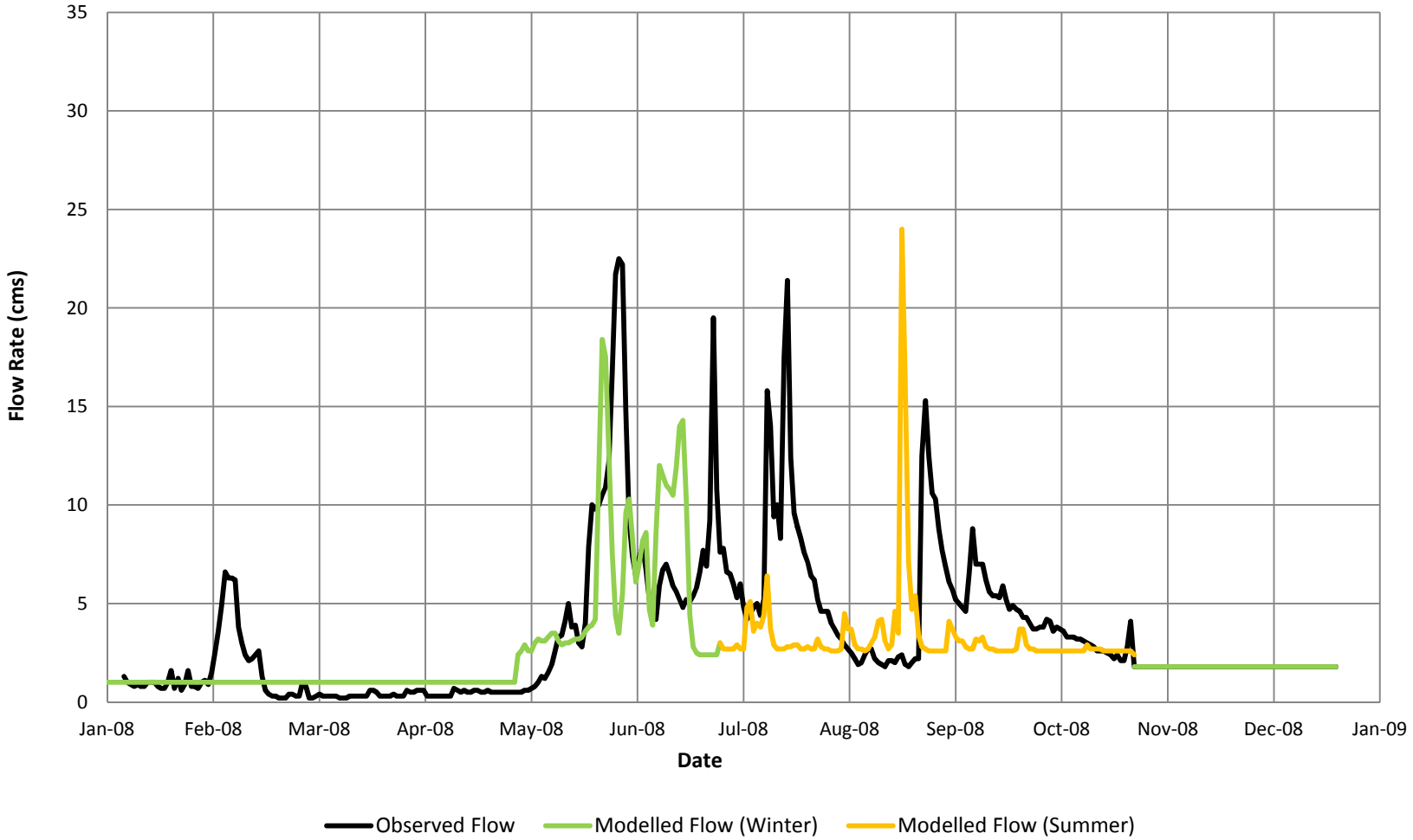

FIGURE A-13
Modelled vs. Observed Flow at Station X14, 2008
Faro Mine Remediation Project

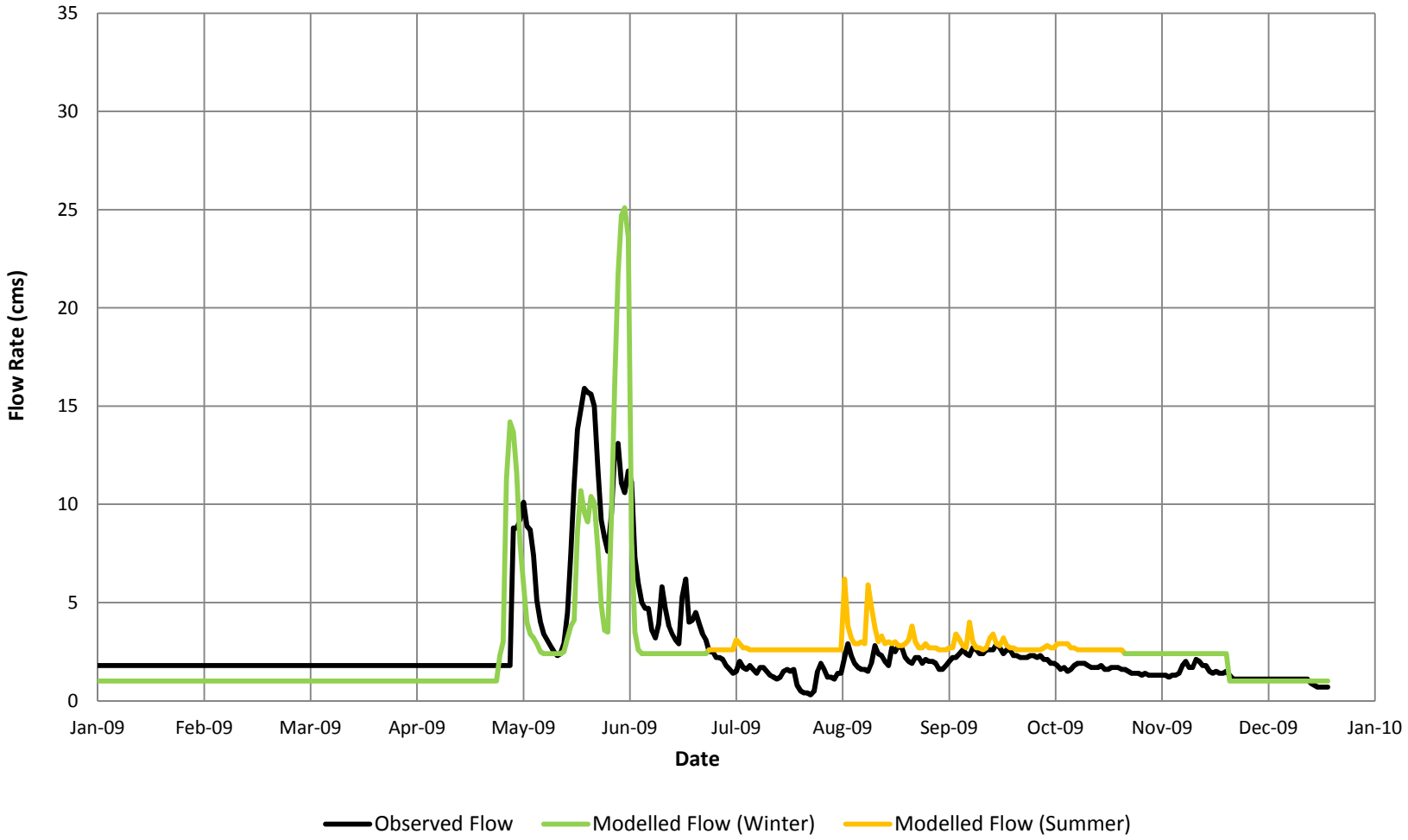

FIGURE A-14
Modelled vs. Observed Flow at Station X14, 2009
Faro Mine Remediation Project

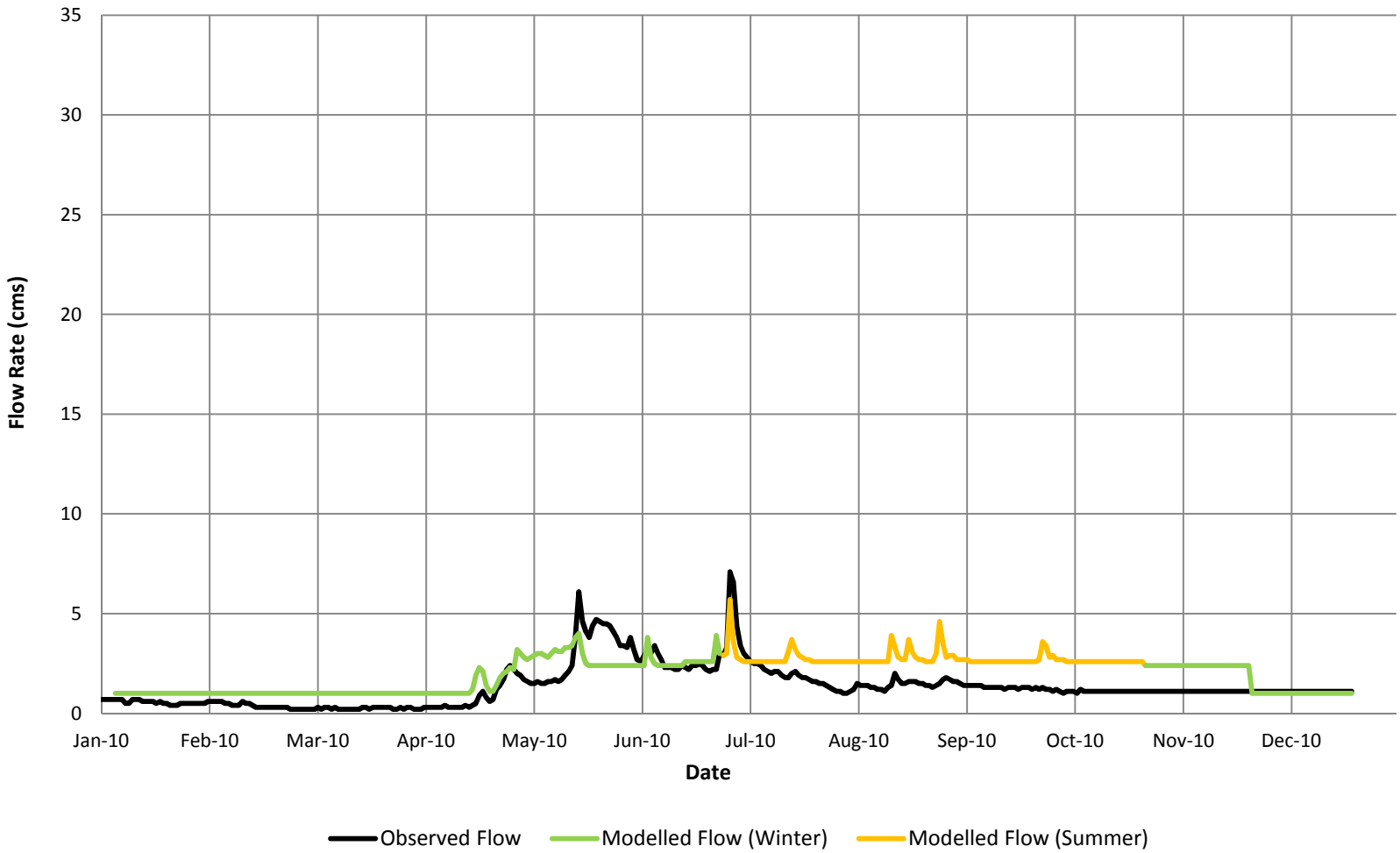

FIGURE A-15
Modelled vs. Observed Flow at Station X14, 2010
Faro Mine Remediation Project

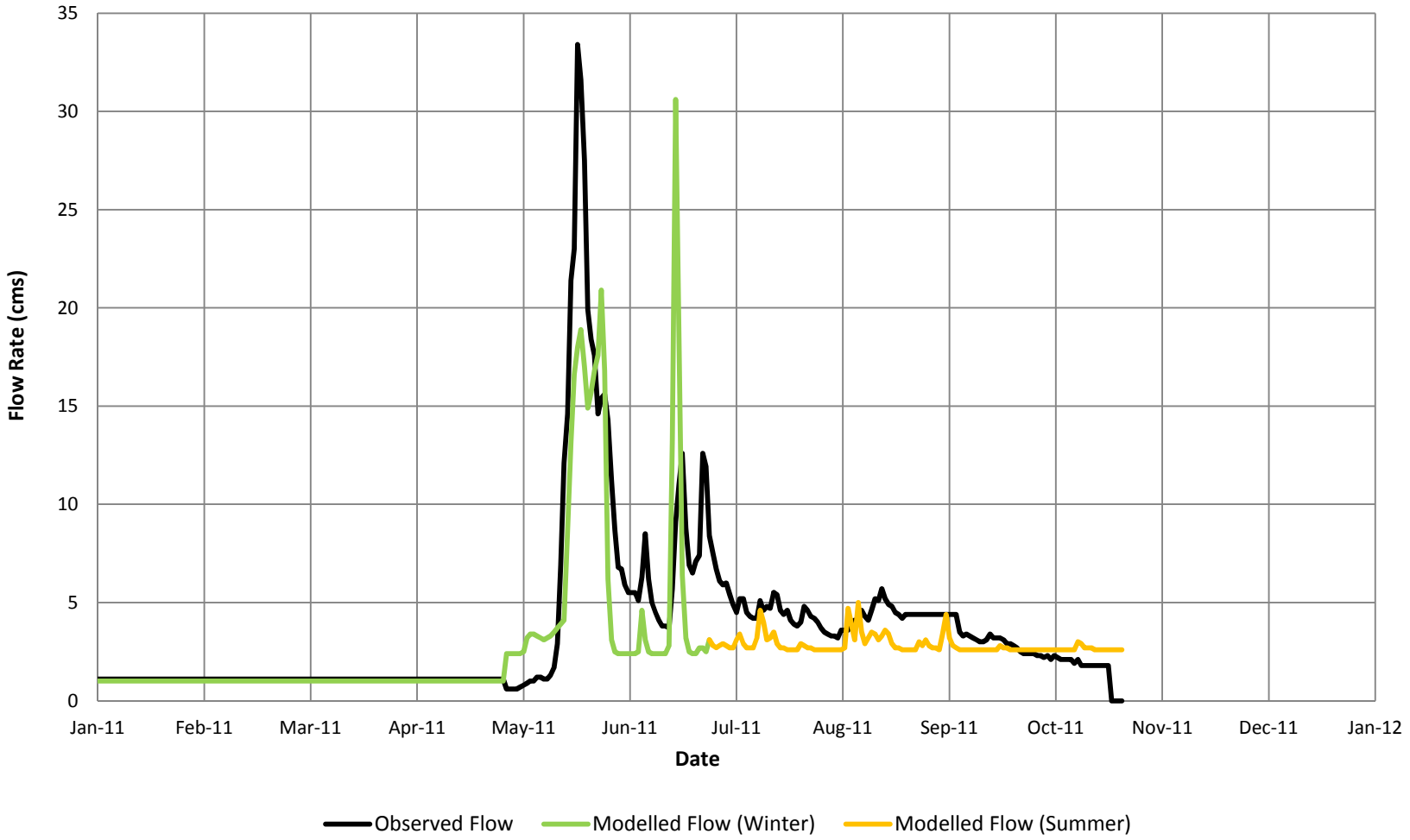

FIGURE A-16
Modelled vs. Observed Flow at Station X14, 2011
Faro Mine Remediation Project

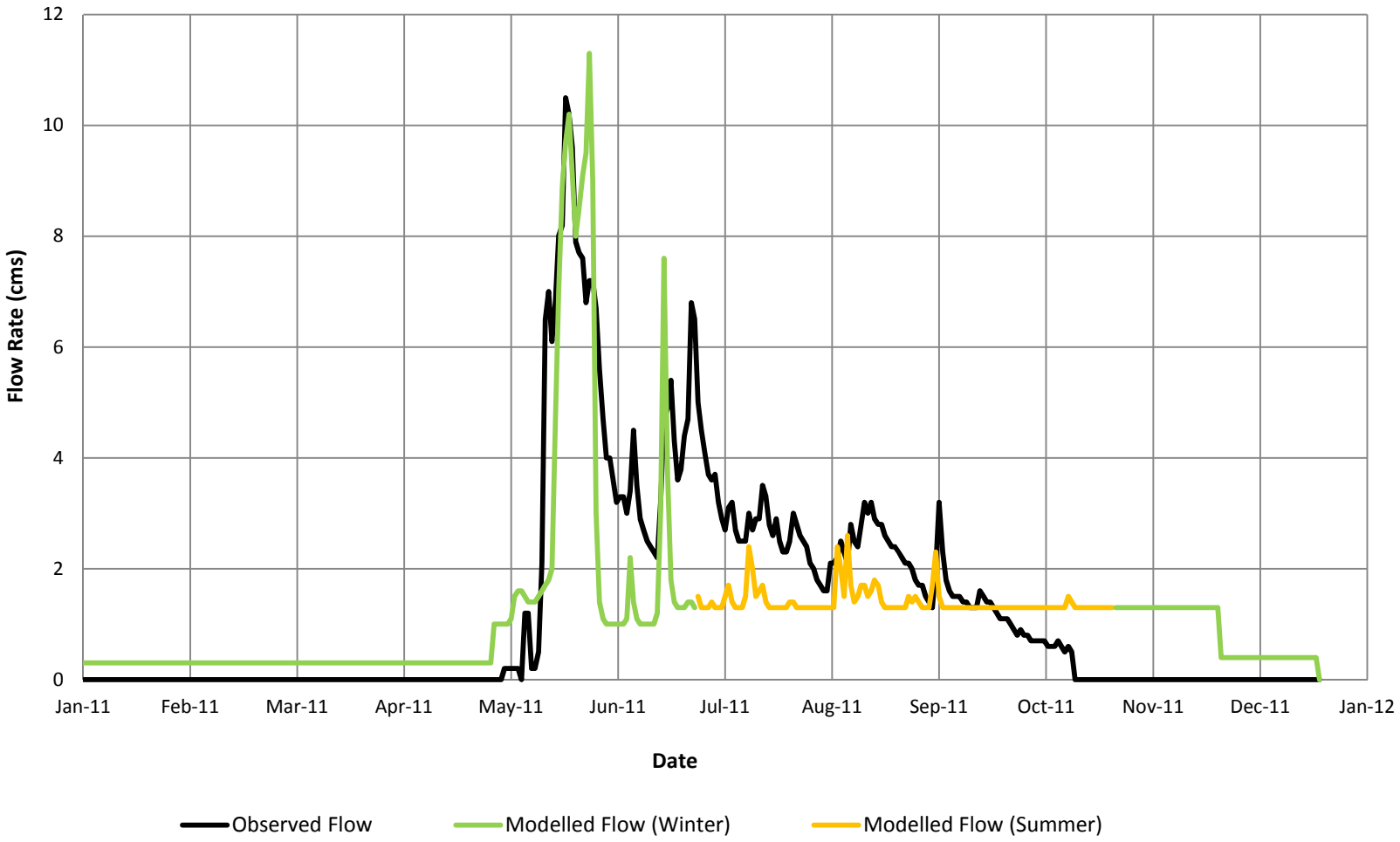

FIGURE A-17
Modelled vs. Observed Flow at Station X2, 2011
Faro Mine Remediation Project

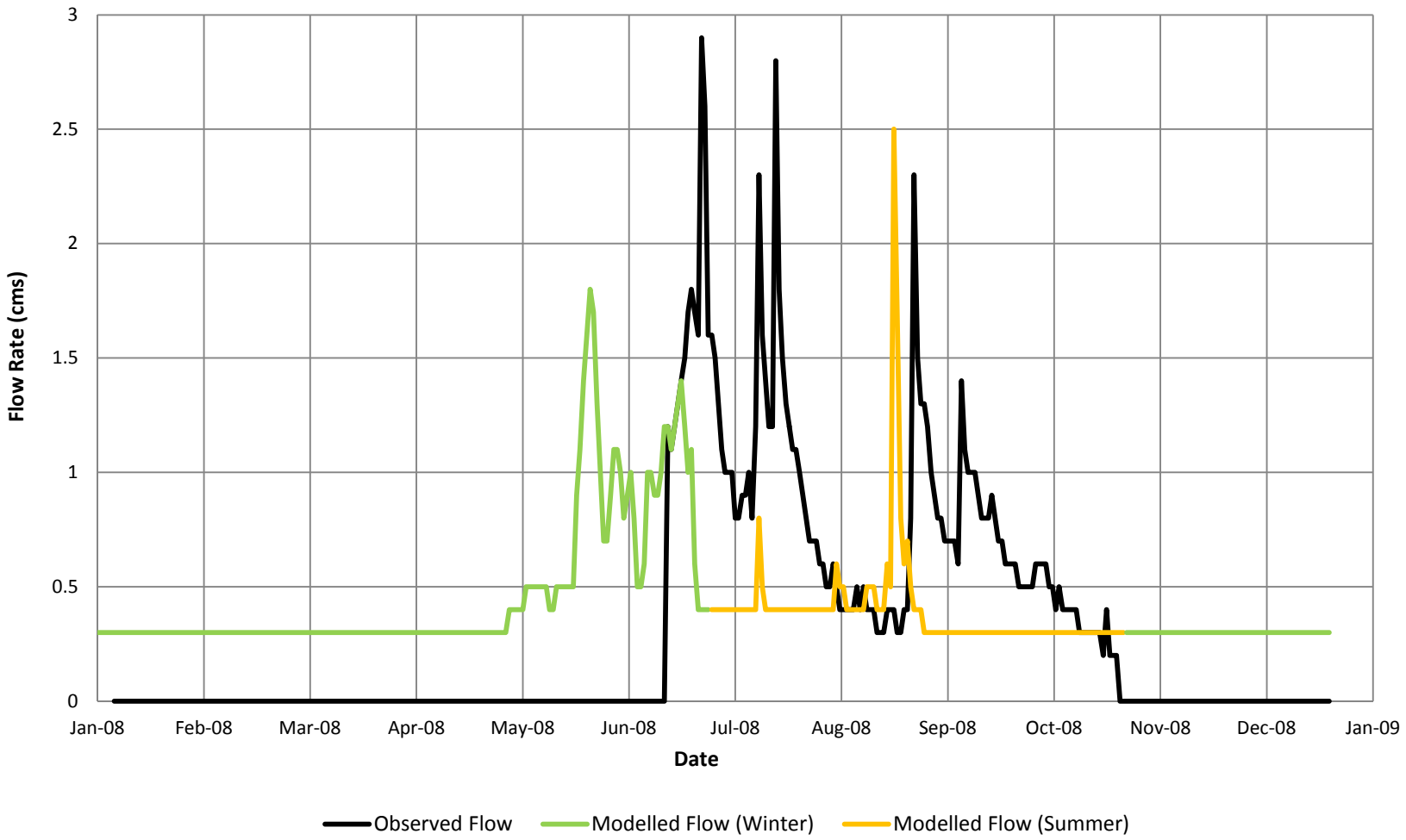

FIGURE A-18
Modelled vs. Observed Flow at Station V1, 2008
Faro Mine Remediation Project

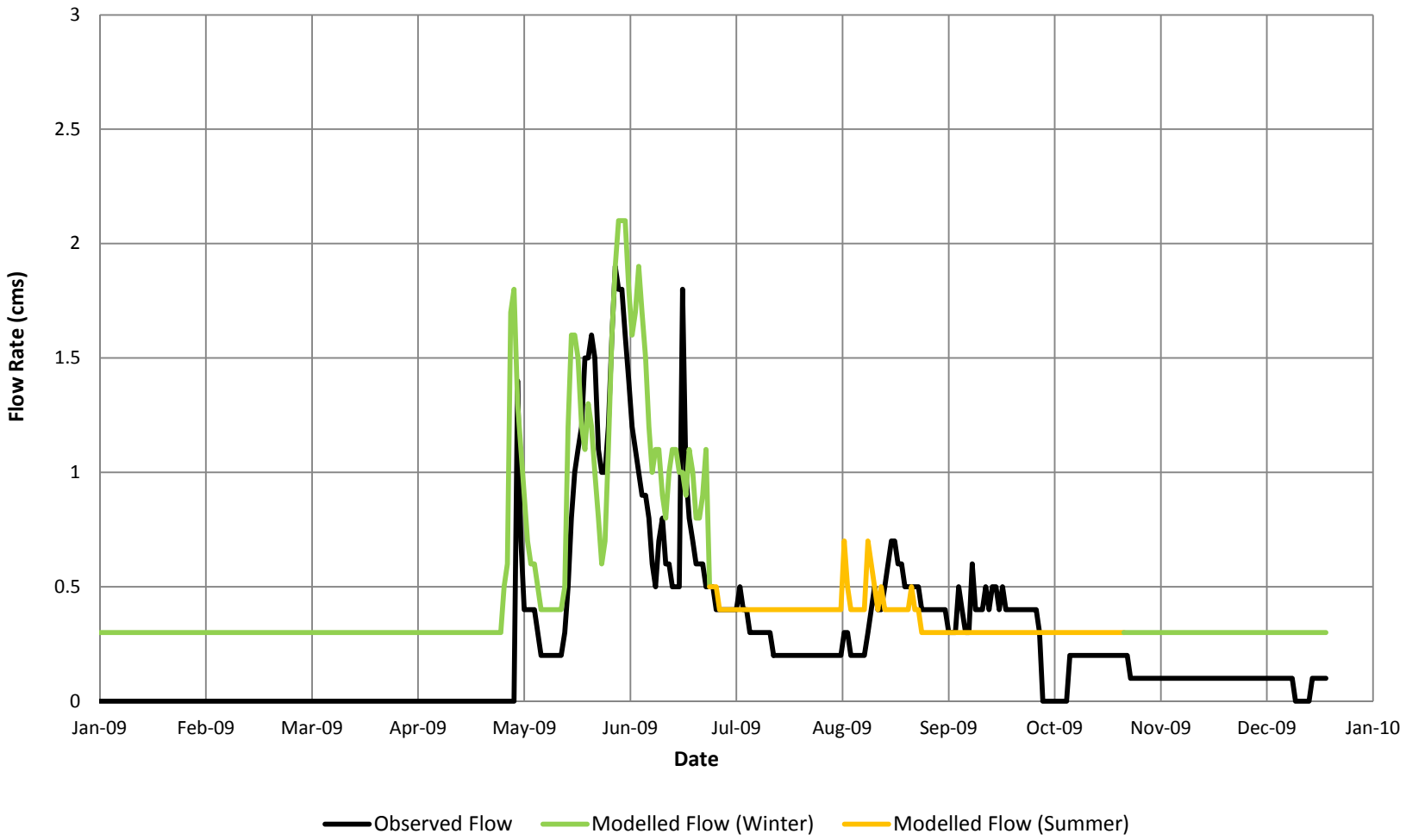

FIGURE A-19
Modelled vs. Observed Flow at Station V1, 2009
Faro Mine Remediation Project

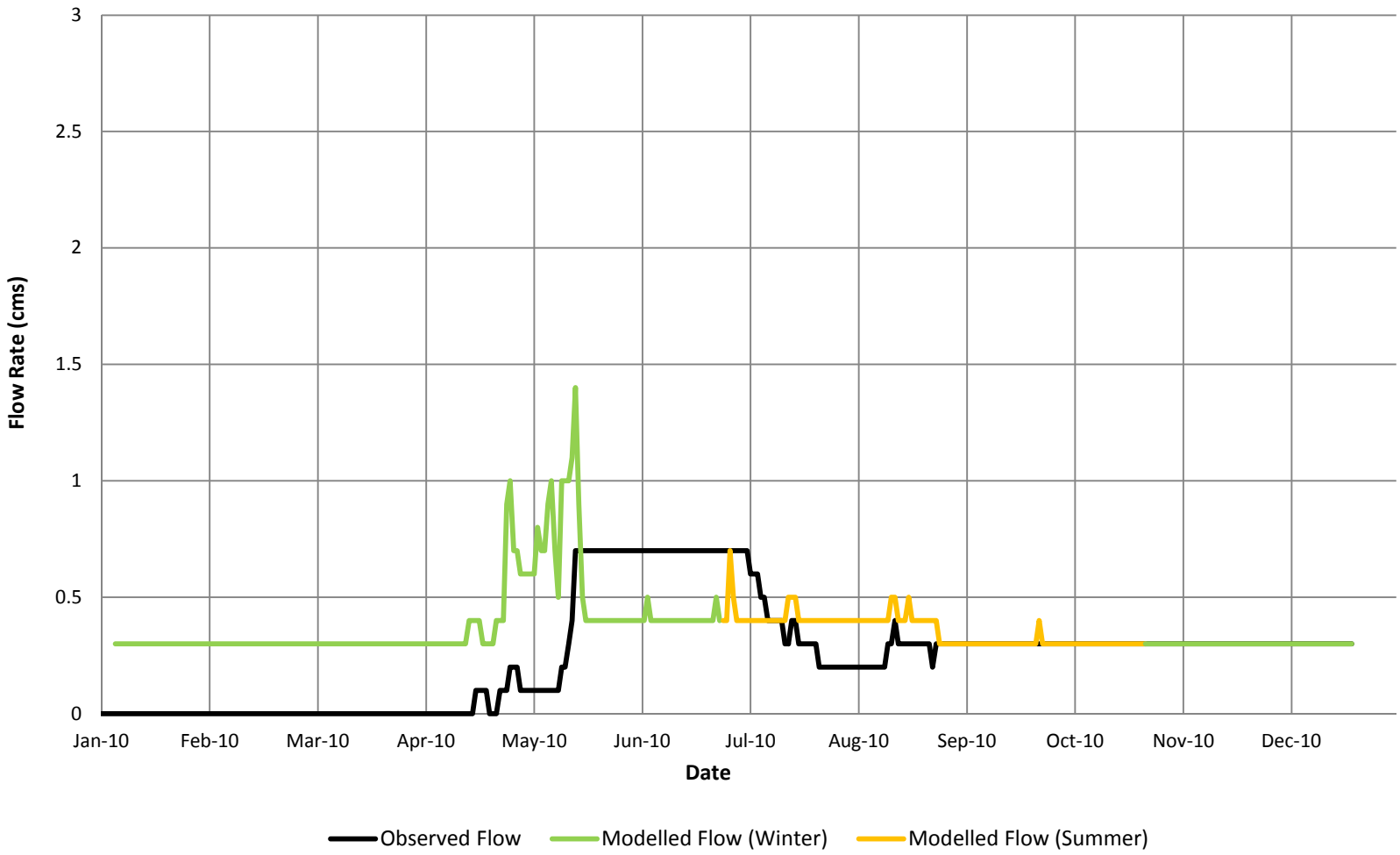

FIGURE A-20
Modelled vs. Observed Flow at Station V1, 2010
Faro Mine Remediation Project

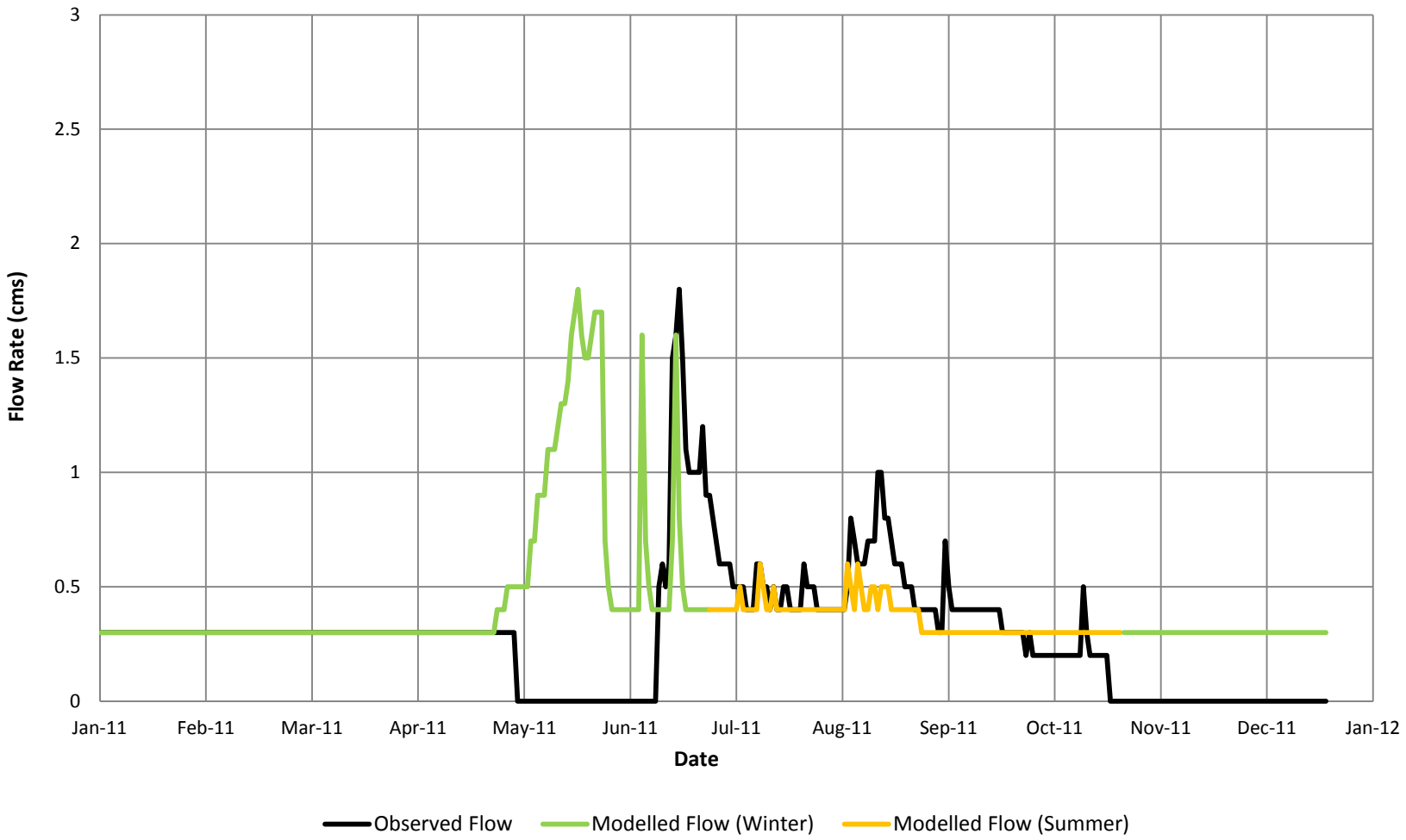

FIGURE A-21
Modelled vs. Observed Flow at Station V1, 2011
Faro Mine Remediation Project

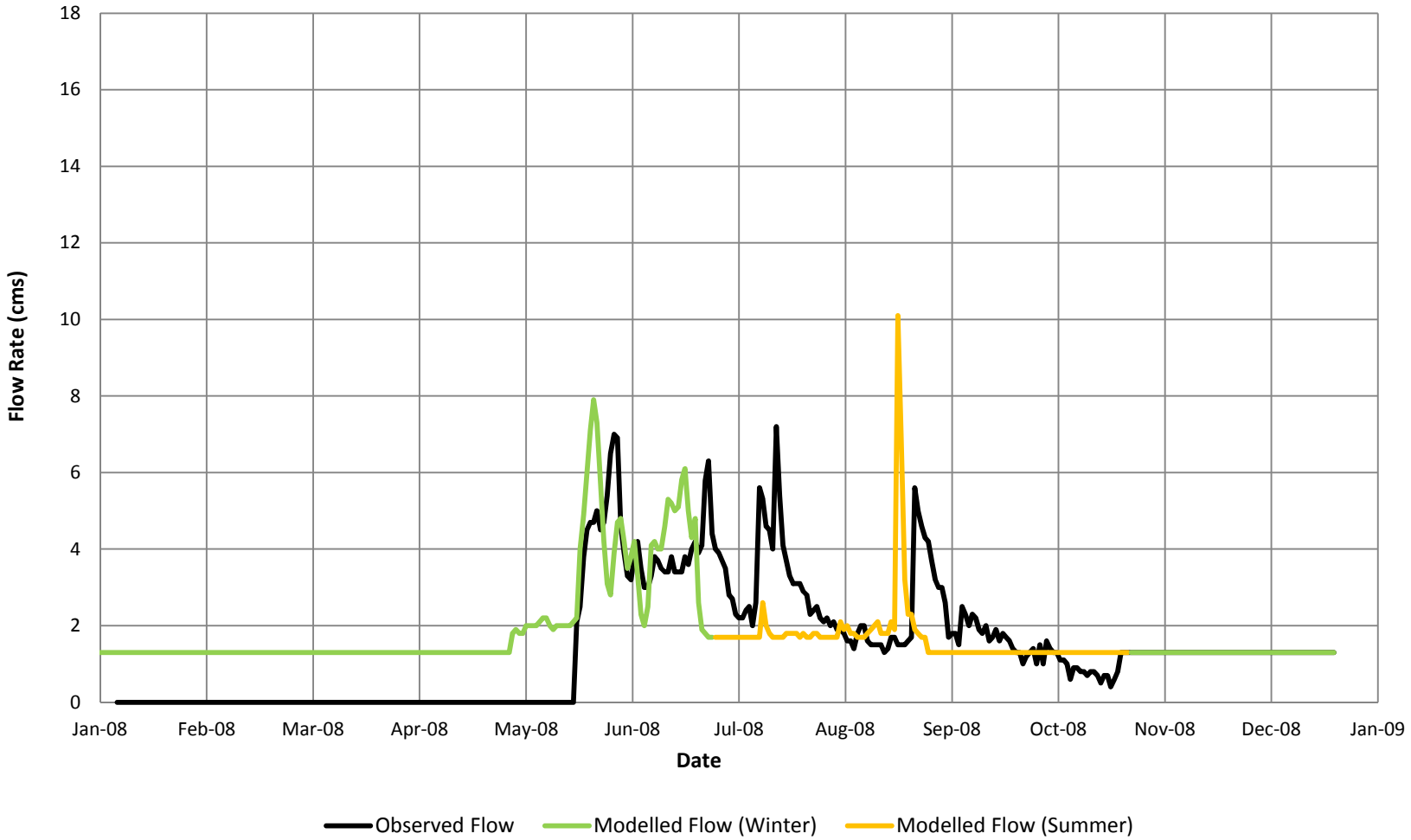

FIGURE A-22
Modelled vs. Observed Flow at Station V8, 2008
Faro Mine Remediation Project

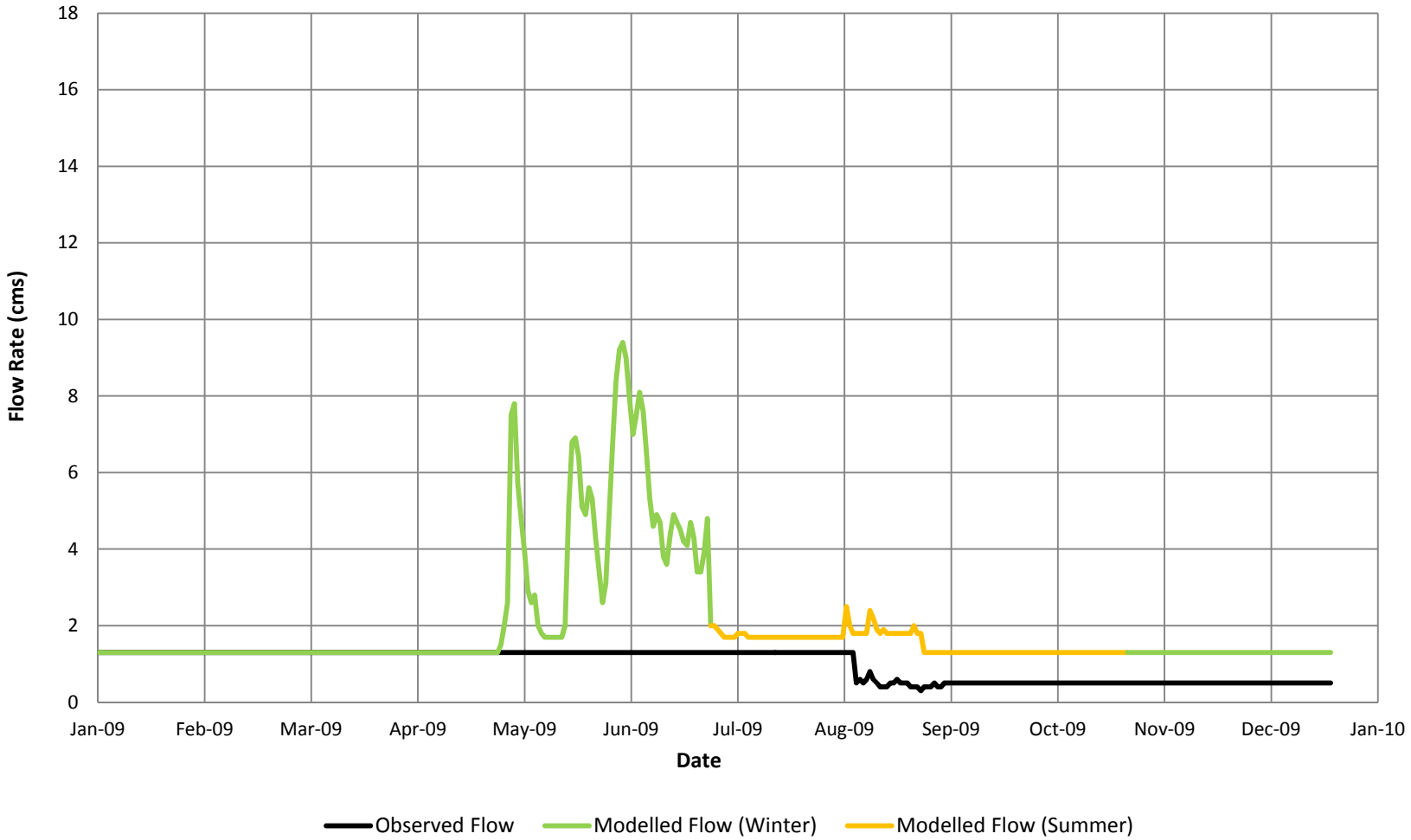

FIGURE A-23
Modelled vs. Observed Flow at Station V8, 2009
Faro Mine Remediation Project

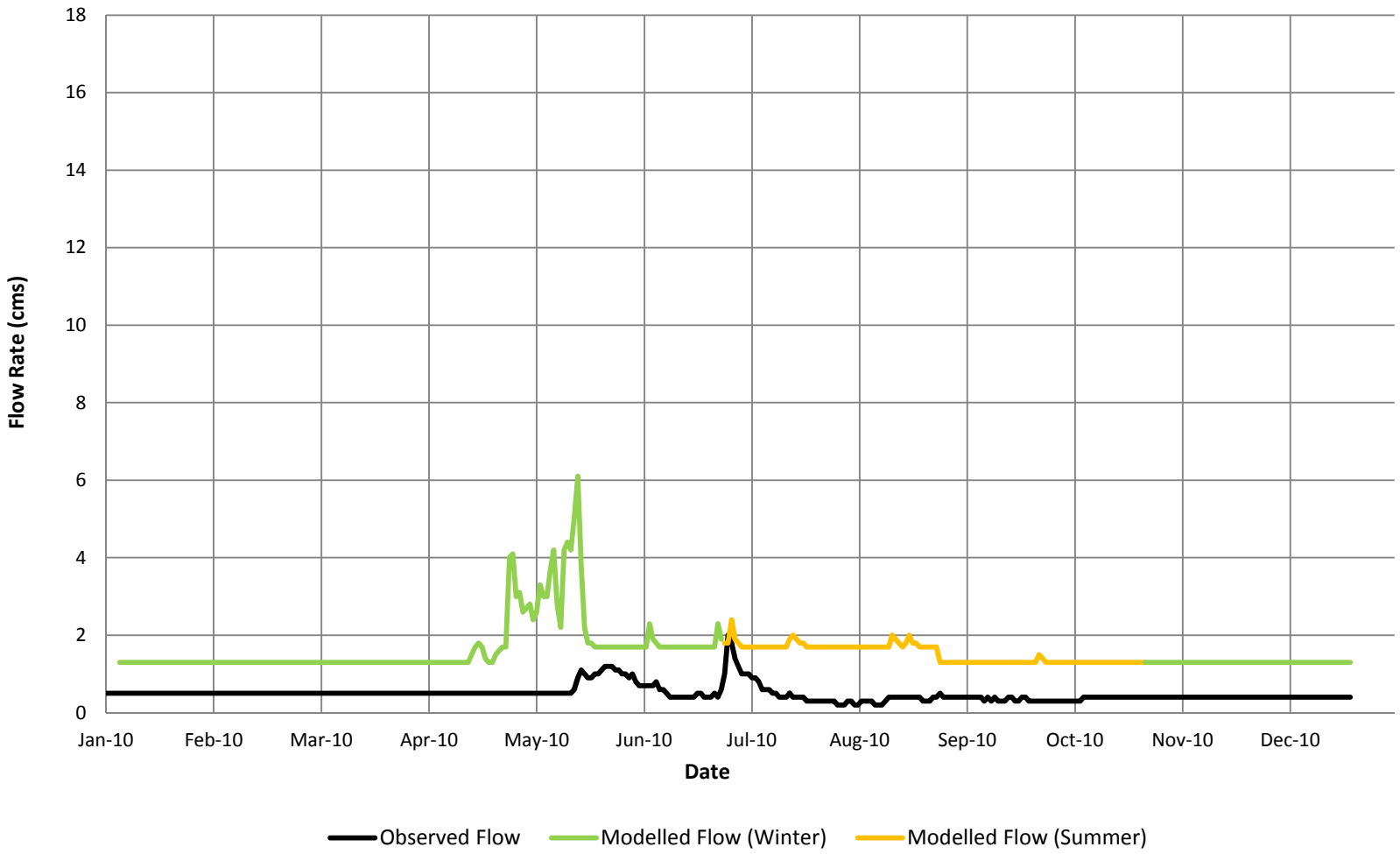

FIGURE A-24
Modelled vs. Observed Flow at Station V8, 2010
Faro Mine Remediation Project

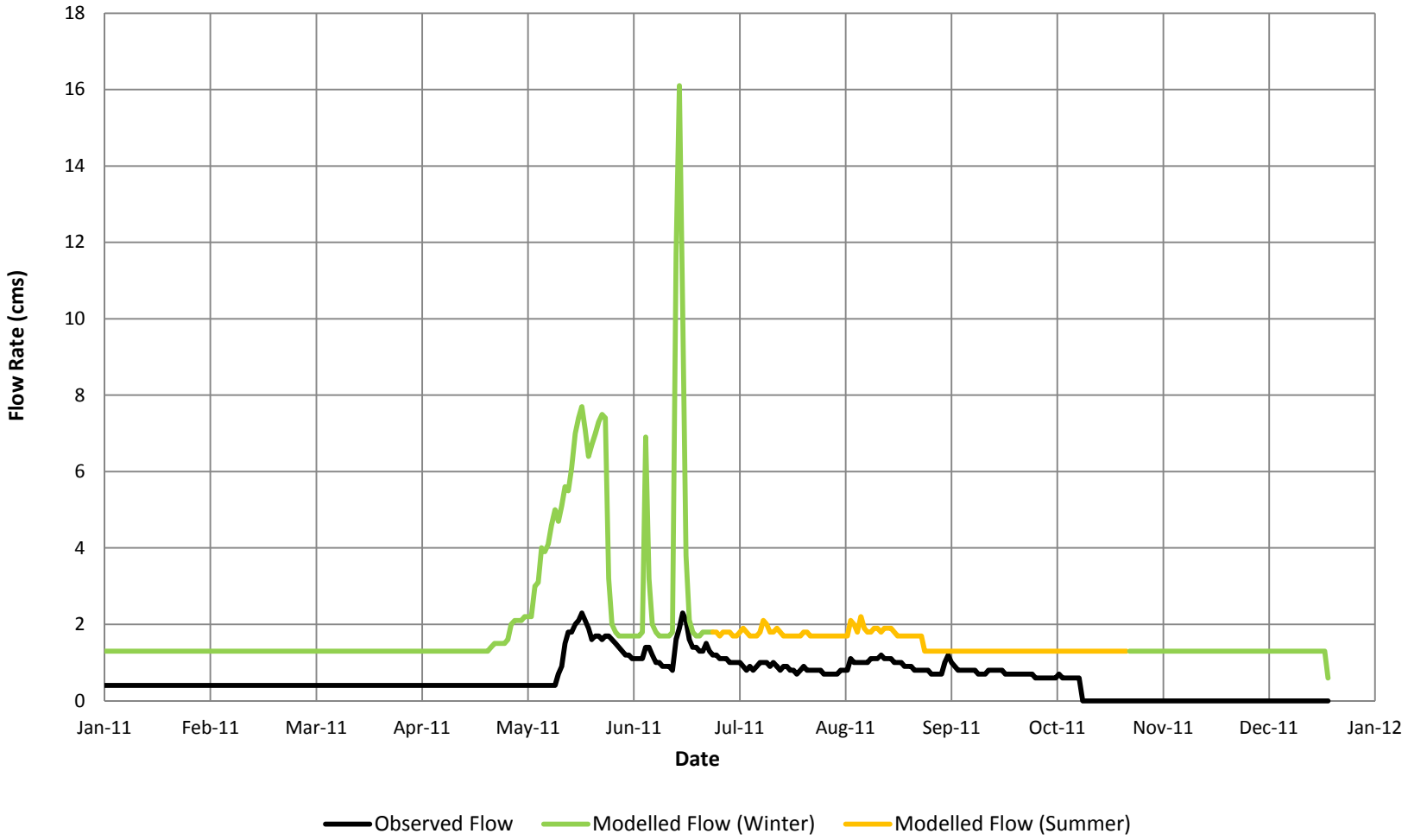

FIGURE A-25
Modelled vs. Observed Flow at Station V8, 2011
Faro Mine Remediation Project

Appendix B
2012 Cross Valley Dam Aquifer Test Simulation Results

APPENDIX B

2012 Cross Valley Dam Aquifer Test Simulation Results

Introduction

This appendix describes the calibration of the Rose Creek Alluvial Aquifer (RCAA) Subarea groundwater (GW) flow model (RCAA Subarea model) using selected drawdown data collected during the 2012 Cross Valley Dam (CVD) aquifer testing program. A more complete discussion of the 2012 aquifer tests can be found in the *Cross Valley Dam Interception System Investigation Data Report* (CH2M HILL, 2013), which describes the field investigation activities performed during summer 2012 as part of the CVD subsurface interception system (SIS) investigation. This appendix only discusses data that were relevant to the calibration of the RCAA Subarea model.

The 2012 CVD investigation was partially designed to provide geologic and hydraulic data to support the design of a SIS capable of collecting contaminated GW moving through the RCAA downstream from the CVD. This portion of the investigation addresses data gaps identified in the *Field Sampling Plan* (FSP) (CH2M HILL Canada Limited [CH2M HILL], 2012a), which found insufficient detail available to characterize the aquifer properties of both the alluvial and weathered bedrock aquifers along the proposed CVD SIS alignment, including areas on the northeast and southwest margins of the Rose Creek Valley. The objective of this portion of the field investigation was to obtain geologic and GW flow data to support side-wide engineering design decisions associated with the proposed CVD SIS.

Methods

After preliminary calibration of the RCAA Subarea model was achieved with steady-state head targets (as described in the main text), the model was modified to simulate selected portions of the 2012 aquifer tests, as follows:

- Eight-hour constant rate aquifer test using wells CH12-204-MW001B, CH12-204-MW002B, and CH12-204-MW004B along the proposed CVD SIS alignment, as shown on Figure B-1)
- Four-hour constant-rate aquifer tests using Rose Creek wells CH12-204-MW005B and CH12-204-MW006B
- Four-day aquifer test using wells CH12-204-MW001A, CH12-204-MW004A, RGC-PW1 and RGC-PW2 along the proposed SIS alignment

Table B-1 summarizes the pumping rates and stress period details for the aquifer test calibration simulation. Average pumping rates for each test are listed at the bottom of Table B-1.

Pressure transducers (in-situ model 500) were deployed in pumping and monitoring wells for continual GW level data collection. Recording intervals varied from 15 seconds to 15 minutes depending on the specific data needs of the deployment. GW levels were monitored in an additional 23 wells as frequently as practical. Pumping wells and observations wells are listed in Table B-2 and are shown on Figure B-1. As noted in Table B-2 and Figure B-1, not all data collected were used to help calibrate the RCAA Subarea model. The GW level data that were used were ultimately converted to drawdown values and imported into the RCAA Subarea model as drawdown targets.

The initial version of the RCAA Subarea model was adjusted for aquifer test calibration in the vicinity of the pumping and observation wells such that model layering and hydraulic conductivity zones better corresponded to changes in lithology and well screen elevations. Any additional hydraulic conductivity zones added to the model were kept as localized zones, only extending within the influence of the specific aquifer tests. Calibration of the RCAA Subarea model using both selected drawdowns from aquifer testing and the steady-state heads proceeded in an iterative fashion until the goodness of fit to both types of calibration targets was deemed adequate.

The primary parameters that were adjusted during calibration were the horizontal and vertical hydraulic conductivities, extents of hydraulic conductivity zones, and GW storage.

Results

Background Water Levels

Water level elevations monitored at downgradient background wells X16A and X16B indicated that water levels declined by about 0.06 metres (m) from September 22, 2012 through October 3, 2012, about 0.01 m per day. Water levels then rose about 0.02 m from October 3, 2012 through October 7, 2012. The X16 well nest is adjacent to Rose Creek and is believed to be beyond the influence of any of the aquifer tests.

Water level elevations monitored at upgradient wells at the base of the Intermediate Dam (P01-04A, P01-04B, X25-96A, X25-96B) indicated that groundwater levels steadily rose about 0.3 m between September 23, 2012 and October 7, 2012, about 0.02 m per day.

These background water level changes were assumed to be insignificant to the aquifer testing program, and no de-convolution or normalizing of aquifer test drawdown data was performed.

Drawdown in Observation Wells

Figures B-2 through B-7 show observed and modelled drawdown data from the RCAA aquifer testing simulation. In several cases, multiple wells were co-located within one model cell, and this was considered when evaluating the quality of the calibration (e.g., P05-01-01 and P05-01-02). In most wells, the calibration was considered good to very good. The poorest calibration was at well P01-02B, which experienced very steep drawdown when CH12-204-MW004B was pumping.

Hydraulic conductivity values at observation and pumping wells are summarized in Table B-3. Values in the alluvium (Model Layers 1 through 3) ranged from 3.5×10^{-3} to 5.8×10^{-2} centimetres per second and were generally two to three orders of magnitude lower in Model Layers 4 and 5 (i.e., bedrock layers). These results are comparable to those from Robertson GeoConsultants Inc (RCG) (2006).

A specific yield value of 0.01 resulted from the calibration effort. Calibrated specific storage values includes 1×10^{-3} per metre (m^{-1}) in Model Layer 1; 2×10^{-4} m^{-1} in Model Layers 2 and 3; and 2×10^{-5} m^{-1} in Model Layers 4, 5, and 6. RGC (2006) reported a specific yield of 0.1, with comparable specific storage values using earlier versions of the MODFLOW code.

Works Cited

CH2M HILL Canada Limited (CH2M HILL). 2012a. *Subtask 07.01.04.22 – 204.2. Construct Cross Valley Dam Interception System*. Activity Code 204.2; HCSS Bid Item 20420. 2012 Field Sampling Plan. Prepared for Government of Yukon.

CH2M HILL 2013. *Geochemical Data Technical Memo*. Prepared for Government of Yukon. February.

Robertson Geoconsultants Inc. (RGC). 2006. *Draft – Design of Groundwater Interception System for Rose Creek Tailings Storage Facility, Faro Mine, Yukon Territory*. Prepared for: Deloitte & Touche. July.

Tables

TABLE B-1

Aquifer Test Calibration Model Pumping Rates and Stress Periods

Faro Mine Remediation Project

		Pumping Rates (L/S)												
Date-Time	Event	CH12-204-MW001A	CH12-204-MW004A	RGC-PW2	RGC-PW1	CH12-204-MW001B	CH12-204-MW002B	CH12-204-MW004B	CH12-204-MW005B	CH12-204-MW006B	Total Pumping Rate	Stress period	Stress Period Duration (hours)	Cumulative Time (days)
9/26/2012 0:00	Start model										0	1	60.1	2.5
9/28/2012 12:04	MW004B Starts Pumping							570			570	2	0.1	2.5
9/28/2012 12:11	MW04B Rate Change							307			307	3	0.2	2.5
9/28/2012 12:23	MW04B Rate Change							284			284	4	0.8	2.6
9/28/2012 13:12	MW04B Rate Change							264			264	5	1.8	2.6
9/28/2012 15:01	MW04B Rate Change							391			391	6	0.6	2.7
9/28/2012 15:37	MW04B Rate Change							456			456	7	0.2	2.7
9/28/2012 15:51	MW04B Rate Change							376			376	8	2.0	2.7
9/28/2012 17:48	MW04B Stops Pumping										0	9	21.5	3.6
9/29/2012 15:16	MW001 Starts pumping	2929									2929	10	0.2	3.6
9/29/2012 15:28	MW001 Rate Change	7896									7896	11	1.4	3.7
9/29/2012 16:49	MW001 Rate Change	7083									7083	12	2.5	3.8
9/29/2012 19:17	MW001 Rate Change	6408									6408	13	2.3	3.9
9/29/2012 21:36	MW001 Rate Change	6154									6154	14	3.2	4.0
9/30/2012 0:50	MW001 Rate Change	5968									5968	15	3.8	4.2
9/30/2012 4:35	MW001 Rate Change	5827									5827	16	3.6	4.3
9/30/2012 8:11	MW001 Rate Change	5916									5916	17	5.0	4.5
9/30/2012 13:10	MW004A Starts Pumping	5916	2378								8294	18	6.8	4.8
9/30/2012 19:56	MW004A Rate Change	5916	3170								9086	19	16.3	5.5
10/1/2012 12:14	PW2 Starts Pumping	5916	3170	3001							12087	20	0.9	5.5
10/1/2012 13:06	PW2 Rate Change	5916	3170	7931							17018	21	8.1	5.9
10/1/2012 21:11	MW001 Rate Change	5865	3170	7931							16966	22	12.7	6.4
10/2/2012 9:53	PW1 Starts Pumping	5865	3170	7931	2005						18971	23	0.4	6.4
10/2/2012 10:19	PW1 Rate Change	5865	3170	7931	3182						20148	24	0.2	6.4
10/2/2012 10:30	PW1 Rate Change	5865	3170	7931	4083						21049	25	0.3	6.5
10/2/2012 10:51	PW1 Rate Change	5865	3170	7931	6176						23142	26	0.1	6.5
10/2/2012 10:57	PW1 Rate Change	5865	3170	7931	4858						21824	27	2.1	6.5
10/2/2012 13:06	MW004A Rate Change	5865	4121	7931	4858						22775	28	2.4	6.6
10/2/2012 15:27	PW2 Rate Change	5865	4121	9922	4858						24766	29	2.9	6.8
10/2/2012 18:21	PW1 Rate Change	5865	4121	9922	5906						25813	30	1.3	6.8
10/2/2012 19:37	PW1 Rate Change	5865	4121	9922	4692						24599	31	3.6	7.0
10/2/2012 23:15	MW001 Rate Change	5769	4121	9922	4692						24504	32	12.8	7.5
10/3/2012 12:00	Shallow DVD Test Ends										0	33	69.1	10.4
10/6/2012 9:05	MW02B Starts Pumping						245				245	34	1.5	10.4
10/6/2012 10:37	MW02B Rate Change						398				398	35	1.8	10.5
10/6/2012 12:28	MW005B Start Pumping						398		1284		1682	36	4.1	10.7
10/6/2012 16:35	MW005B Stop Pumping						398				398	37	0.4	10.7
10/6/2012 17:00	MW02B Stops Pumping										0	38	18.0	11.5
10/7/2012 10:58	MW001B Starts Pumping					239					239	39	1.7	11.5
10/7/2012 12:41	MW006B Start Pumping					239				309	548	40	4.0	11.7
10/7/2012 16:42	MW006B Stop Pumping					239					239	41	0.8	11.7
10/7/2012 17:31	MW001B Stops Pumping										0	42	30.5	13.0
10/9/2012 0:00	Stop Model													
	Average Pumping Rate (L/s):	5924	3434	8165	4531	239	360	378	1284	309				

TABLE B-2

Wells Monitored During 2012 Cross-Valley Dam Aquifer Testing

Faro Mine Remediation Project

Well ID	Data Collection Method	Used For Model Calibration	Pumping Well?
CH12-204-MW001A	Transducer	Yes	Yes
CH12-204-MW001B	Transducer	Yes	Yes
CH12-204-MW002B	Transducer	Yes	Yes
CH12-204-MW003B	Transducer	Yes	No
CH12-204-MW004A	Transducer	Yes	Yes
CH12-204-MW004B	Transducer	Yes	Yes
CH12-204-MW005A	Transducer	Yes	No
CH12-204-MW005B	Transducer	Yes	Yes
CH12-204-MW006A	Transducer	Yes	No
CH12-204-MW006B	Transducer	Yes	Yes
MW1	Transducer	Yes	Yes
MW2	Transducer	Yes	Yes
P01-02A	Transducer	Yes	No
P01-02B	Transducer	Yes	No
P01-11	Transducer	Yes	No
P03-09-1	Hand	Yes	No
P03-09-2	Hand	Yes	No
P03-09-3	Hand	Yes	No
P03-09-4	Hand	Yes	No
P03-09-5	Hand	Yes	No
P03-09-6	Hand	Yes	No
P03-09-7	Hand	Yes	No
P03-09-8	Hand	Yes	No
P03-09-9	Hand	Yes	No
P05-01-1	Hand	Yes	No
P05-01-2	Hand	Yes	No
P05-01-3	Hand	Yes	No
P05-01-4	Hand	Yes	No
P05-01-5	Hand	Yes	No
P05-01-6	Hand	Yes	No
P05-02	Transducer	Yes	No
P05-03	Transducer	Yes	No
RGC-PW1	Transducer	Yes	Yes
RGC-PW2	Transducer	Yes	Yes
P01-01A	Hand	No	No
P01-01B	Hand	No	No
P01-04A	Hand	No	No
P01-04B	Hand	No	No
X16A	Transducer	No	No
X16B	Transducer	No	No
X17A	Transducer	No	No
X17B	Transducer	No	No
X18A	Hand	No	No
X18B	Hand	No	No
X25-96A	Hand	No	No
X25-96B	Hand	No	No

TABLE B-3

Model Results: Hydrogeologic Conductivity at Observation and Pumping Wells

Faro Mine Remediation Project

	Horizontal Hydraulic Conductivity at Well (cm/s)				
Well ID	**Layer 1**	**Layer 2**	**Layer 3**	**Layer 4**	**Layer 5**
CH12-204-MW001A	5.8E-03	1.2E-02			
CH12-204-MW001B				1.2E-04	
CH12-204-MW002B				1.2E-04	
CH12-204-MW003B					1.2E-04
CH12-204-MW004A			5.8E-03		
CH12-204-MW004B				1.2E-04	
CH12-204-MW005A	5.8E-02				
CH12-204-MW005B		3.5E-02			
CH12-204-MW006A	5.8E-03				
CH12-204-MW006B		3.5E-03			
MW1		3.5E-02			
MW2	5.8E-02	5.8E-02			
P01-02A		3.5E-02			
P01-02B				5.8E-02	
P01-11		3.5E-02			
P03-09-1				8.1E-05	
P03-09-2			5.8E-02		
P03-09-3			5.8E-02		
P03-09-4			5.8E-02		
P03-09-5		5.8E-02			
P03-09-6		5.8E-02			
P03-09-7		5.8E-02			
P03-09-8		5.8E-02			
P03-09-9	5.8E-02				
P05-01-1			5.8E-03		
P05-01-2			5.8E-03		
P05-01-3		3.5E-02			
P05-01-4		3.5E-02			
P05-01-5	5.8E-03				
P05-01-6	5.8E-03				
P05-02	5.8E-02				
P05-03		5.8E-02			
RGC-PW1	5.8E-02	3.5E-02	5.8E-03		
RGC-PW2	5.8E-03	5.8E-02			

Figures

VICINITY MAP

LEGEND

- Weirs
- Pumping Well

DataType

- Hand
- Transducer
- Roads Unpaved
- Stream
- Lake, Pond, or Pool

Notes:

1. Aerial photography acquired by Peregrine Aerial Surveyors Inc. and Eagle Mapping in August 2012.
2. Orthophotography prepared by Critigen Canada Corp.
3. Yellow label indicates well was used in model.

N

0 50 100 150 200

Metres

Created by: CRITIGEN

FIGURE B-1

Aquifer Test

Faro Mine Remediation Project

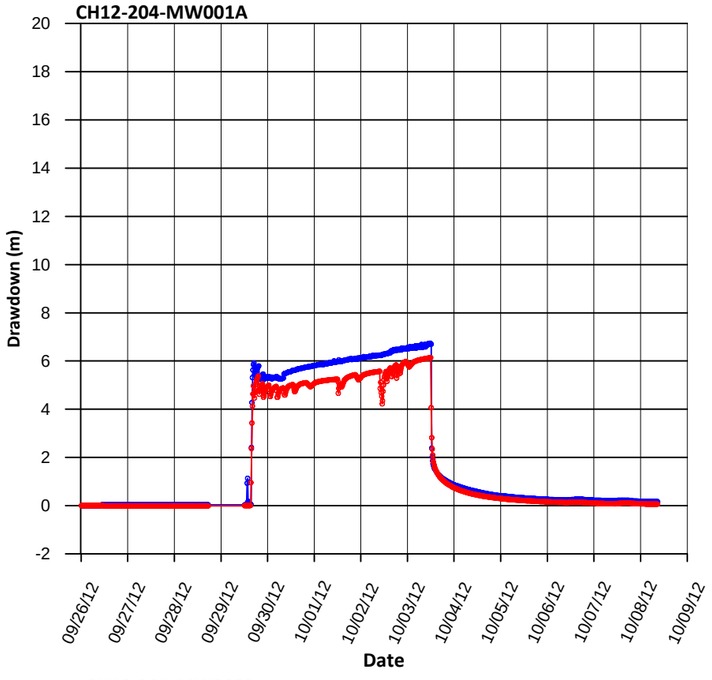

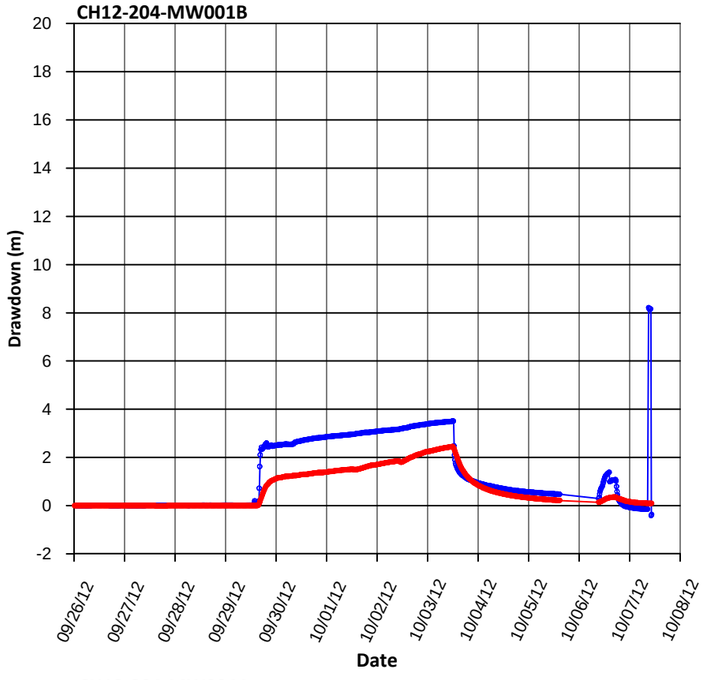

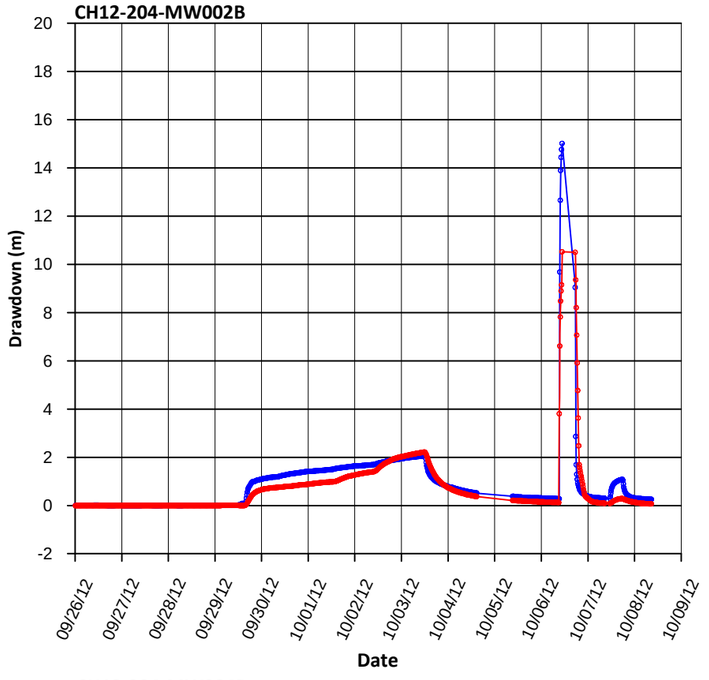

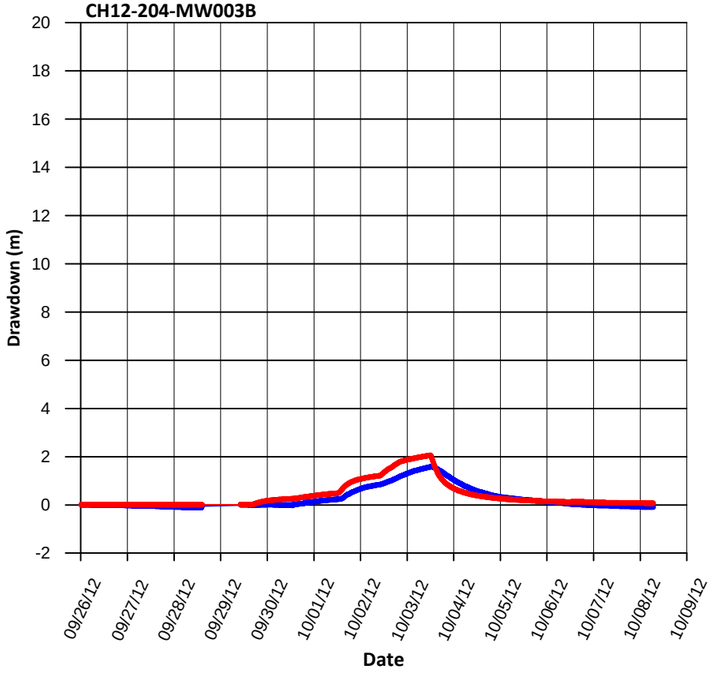

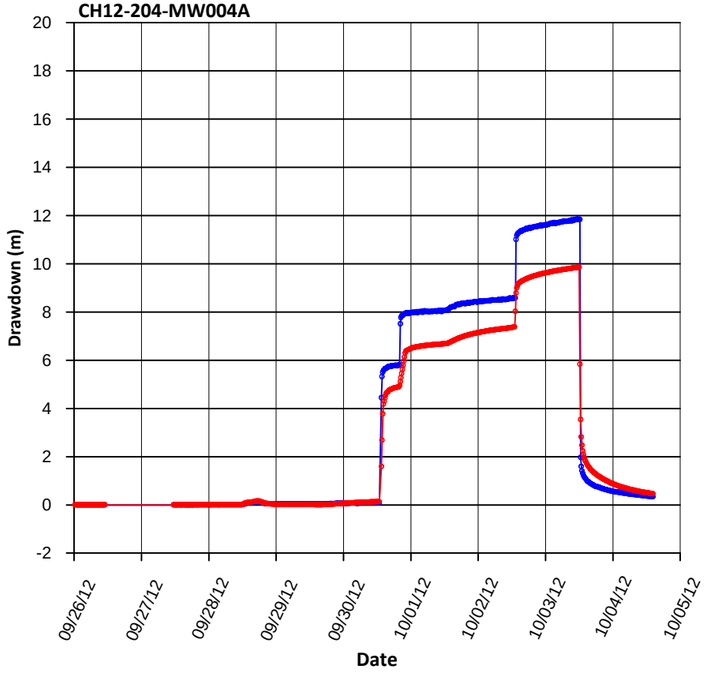

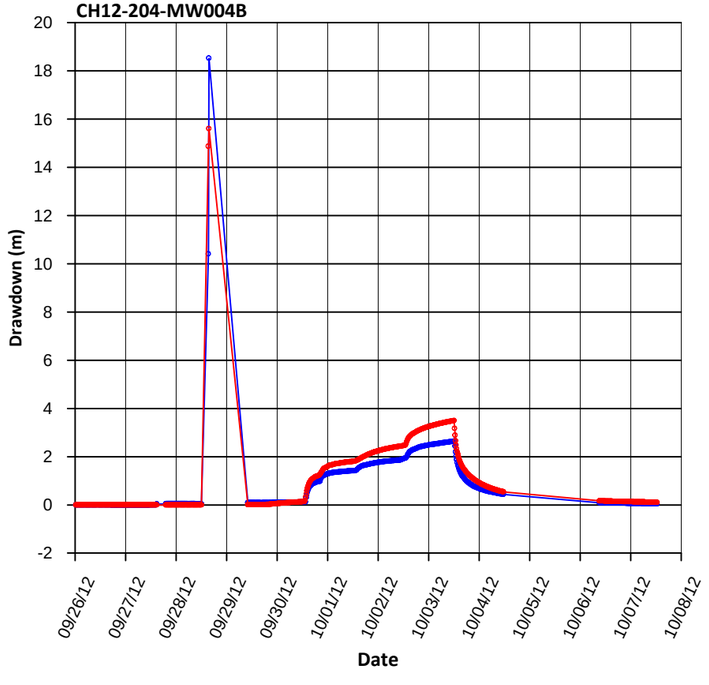

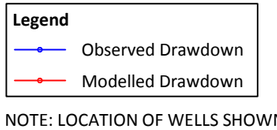

NOTE: LOCATION OF WELLS SHOWN ON FIGURE B-1.

FIGURE B-2
Modelled and Observed Drawdown
Faro Mine Remediation Project

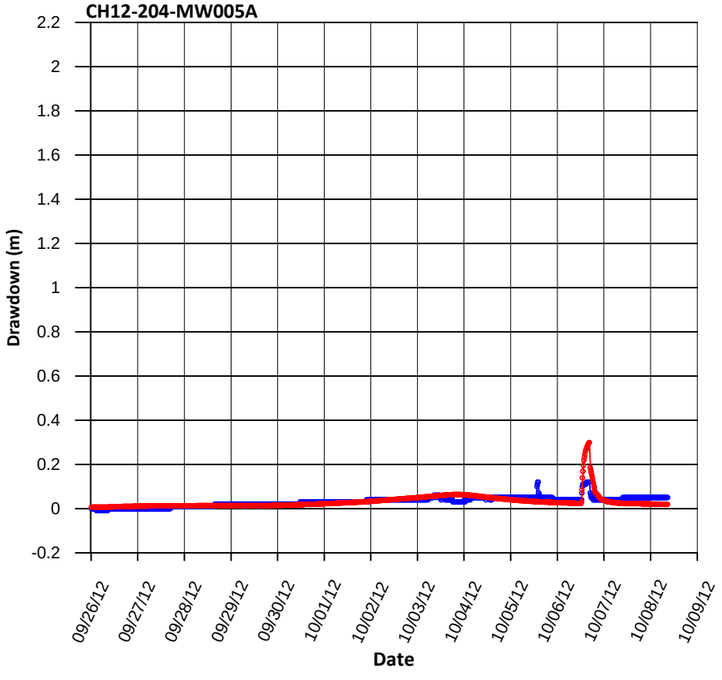

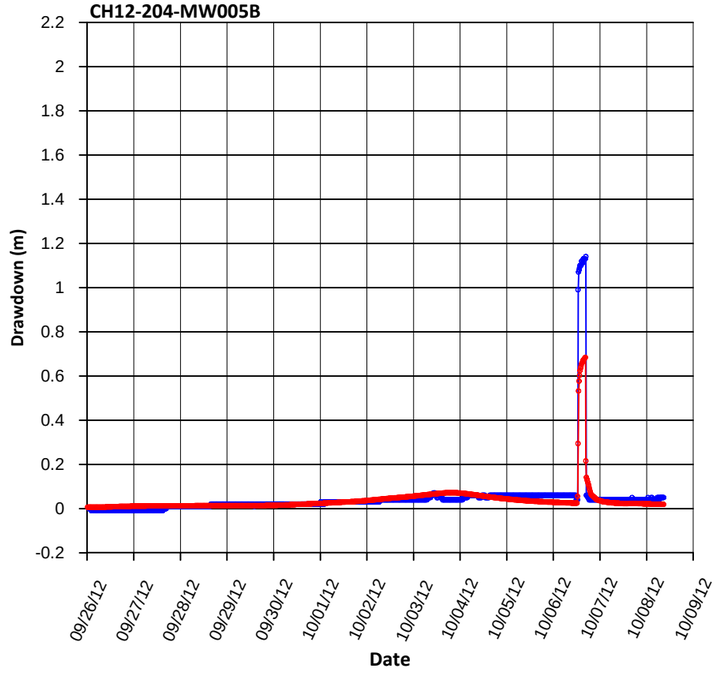

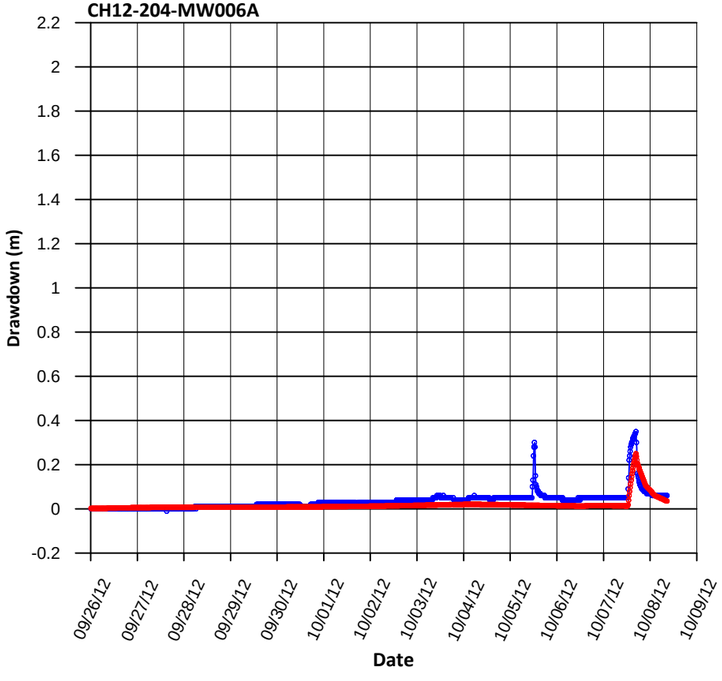

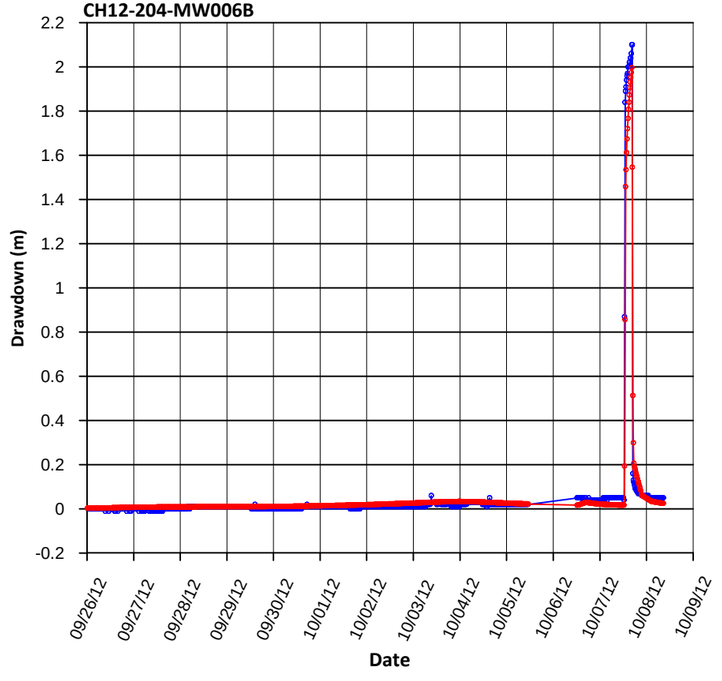

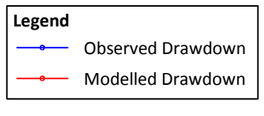

NOTE: LOCATION OF WELLS SHOWN ON FIGURE B-1.

FIGURE B-3
Modelled and Observed Drawdown
Faro Mine Remediation Project

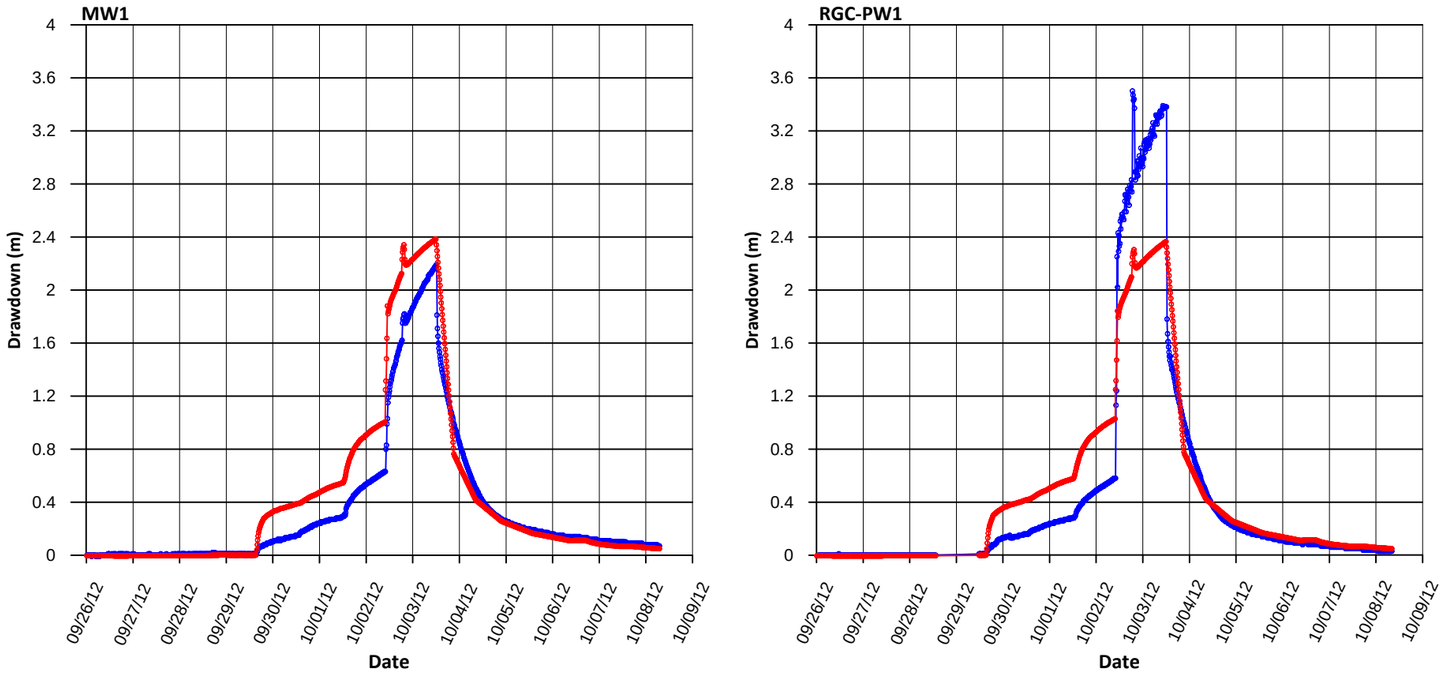

NOTE: LOCATION OF WELLS SHOWN ON FIGURE B-1.

FIGURE B-4
Modelled and Observed Drawdown
Faro Mine Remediation Project

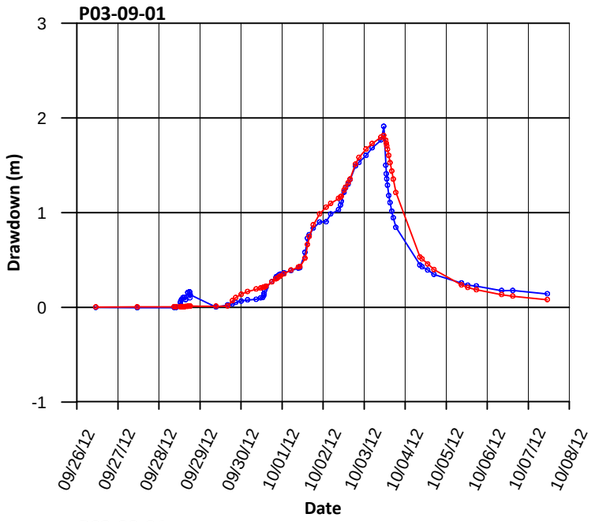

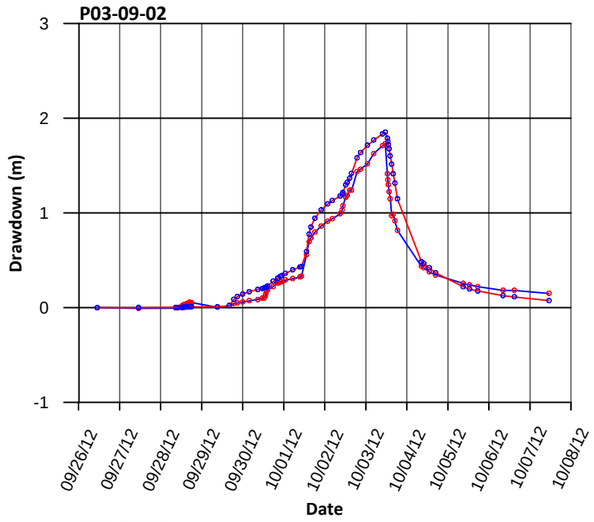

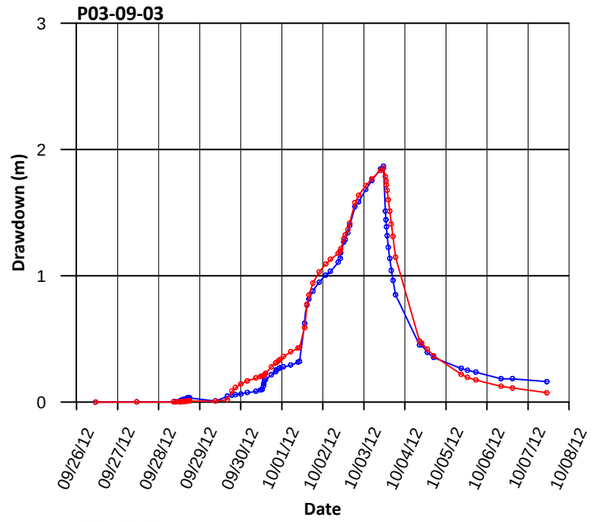

Legend
- Observed Drawdown
- Modelled Drawdown

NOTE: LOCATION OF WELLS SHOWN ON FIGURE B-1.

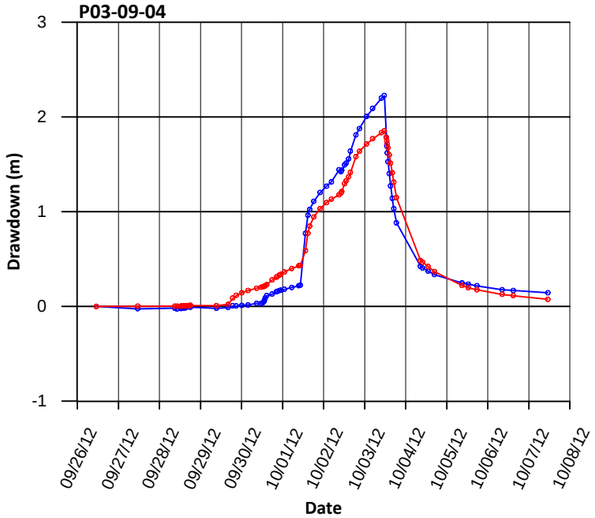

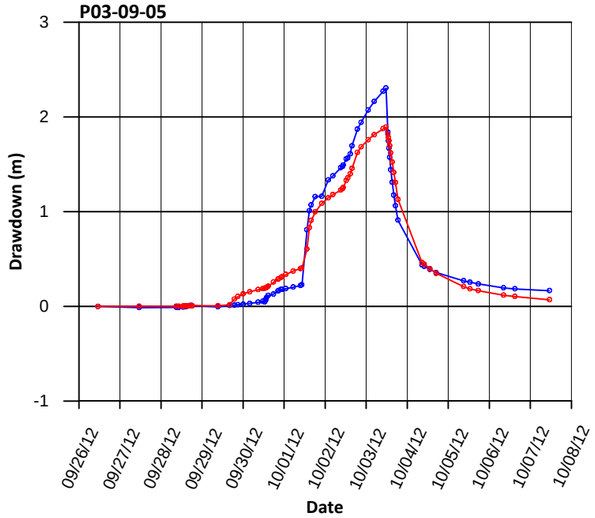

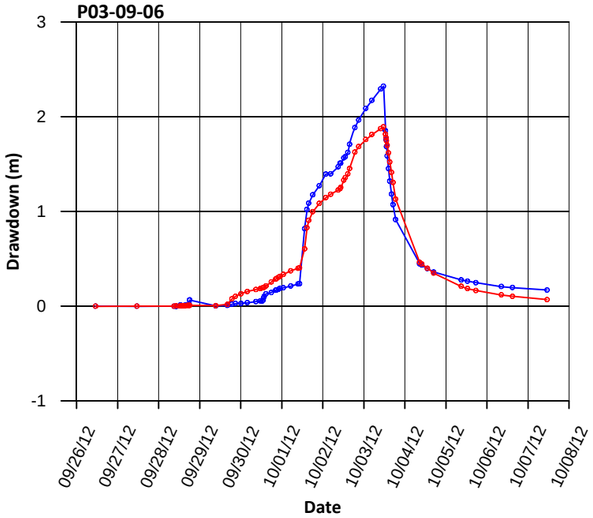

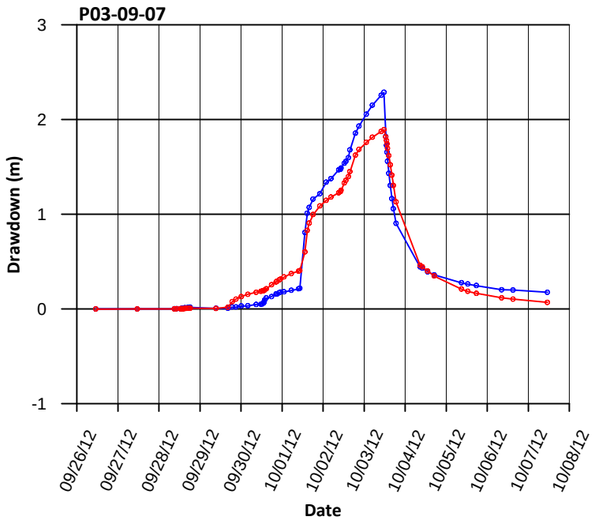

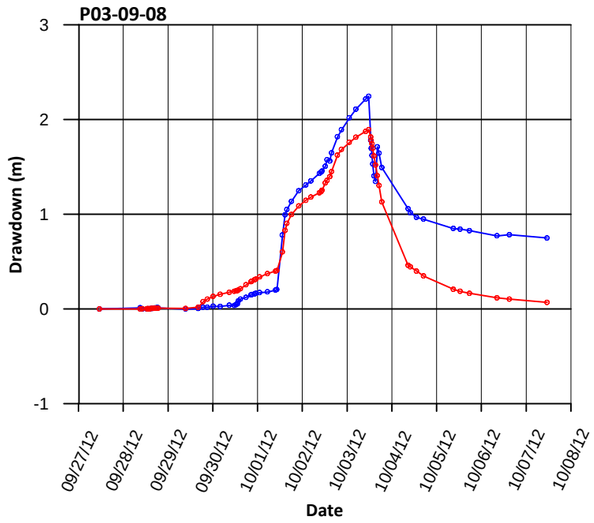

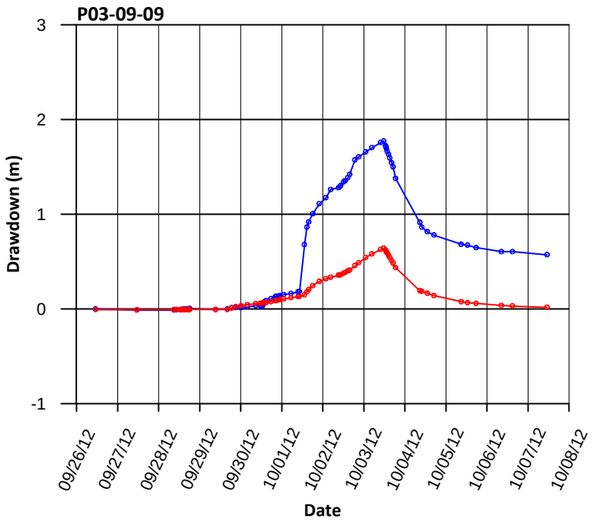

FIGURE B-5
Modelled and Observed Drawdown
Faro Mine Remediation Project

FIGB-05.grf

CH2MHILL

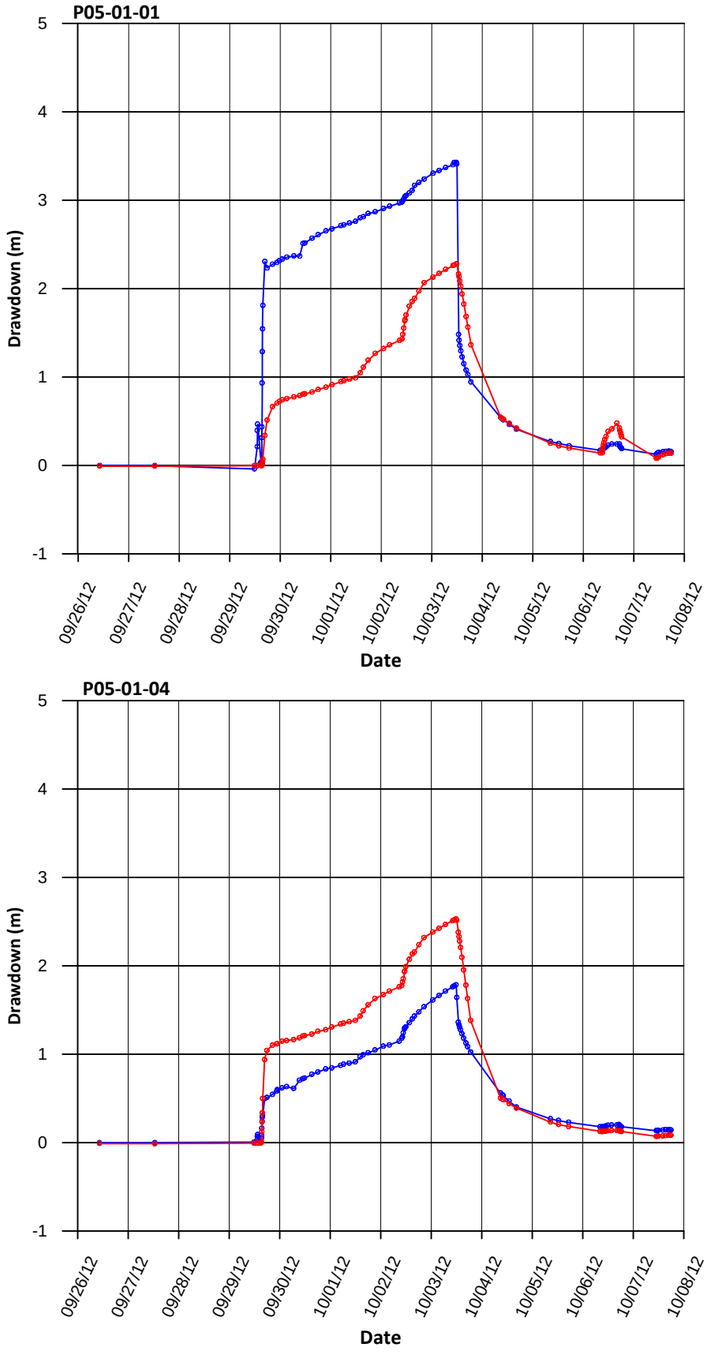

NOTE: LOCATION OF WELLS SHOWN ON FIGURE B-1.

FIGURE B-6
Modelled and Observed Drawdown
Faro Mine Remediation Project

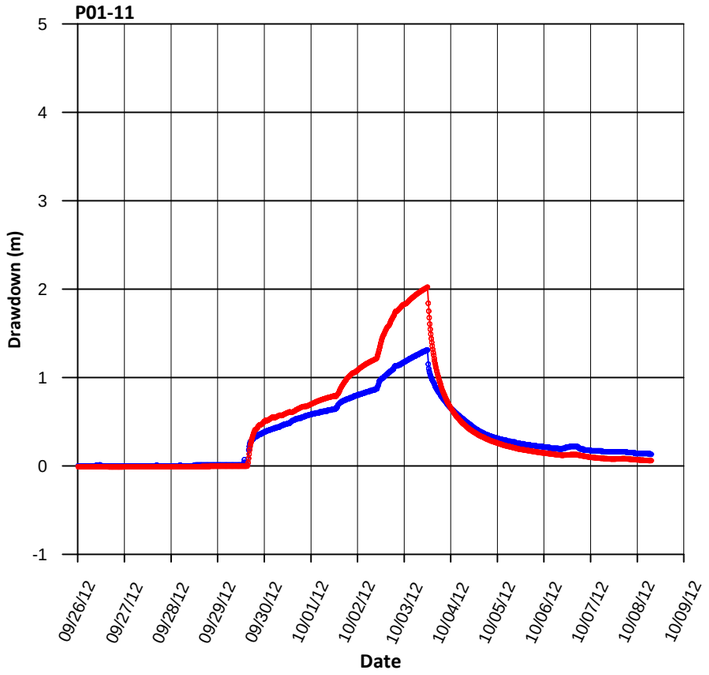

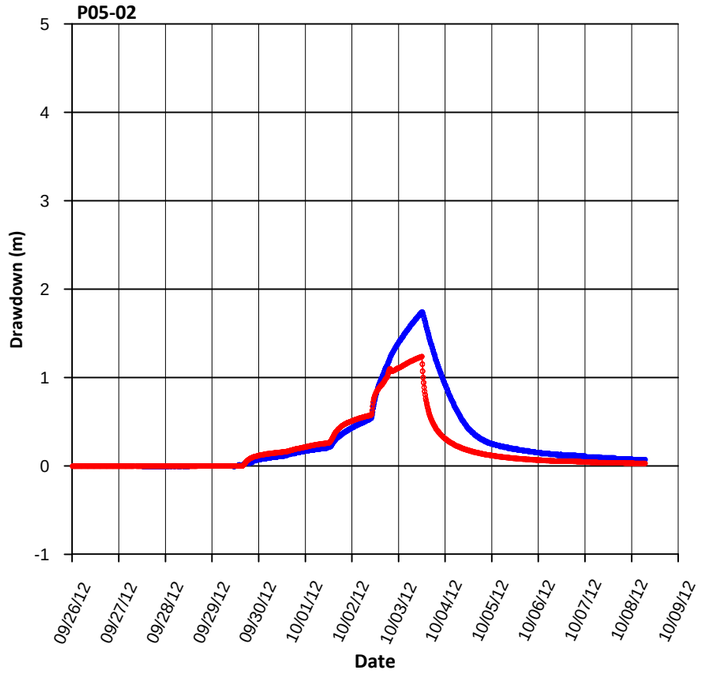

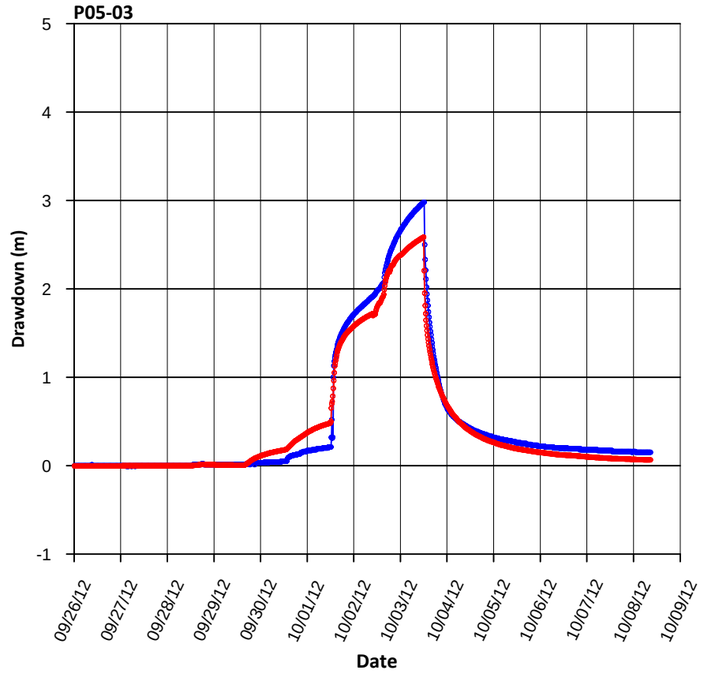

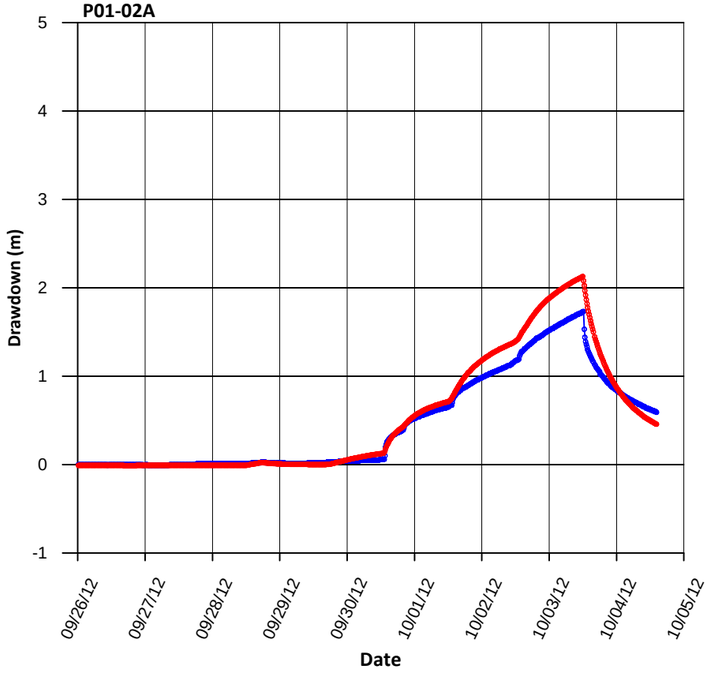

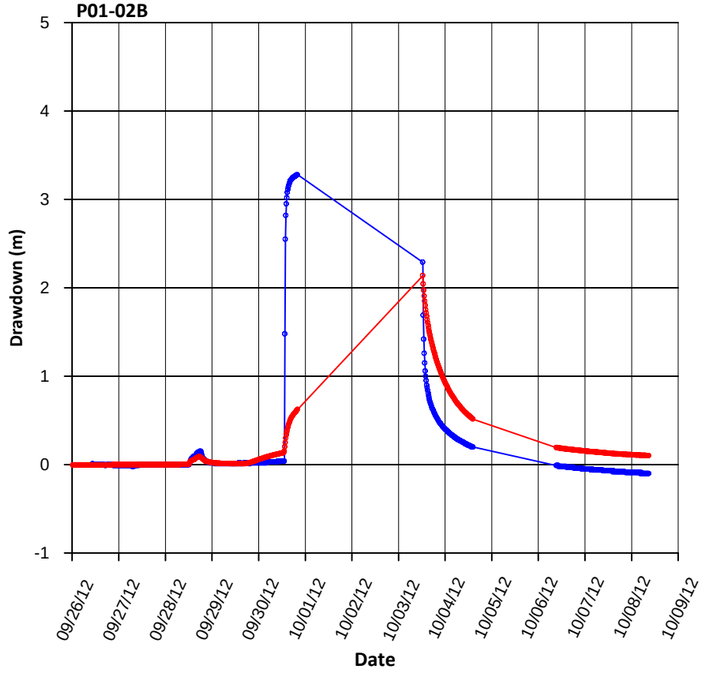

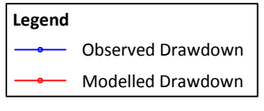

NOTE: LOCATION OF WELLS SHOWN ON FIGURE B-1.

FIGURE B-7
Modelled and Observed Drawdown
Faro Mine Remediation Project